

**CARBON AND NITROGEN REMOVAL IN
MUNICIPAL AND INDUSTRIAL WASTEWATER
USING MEMBRANE BIOREACTORS**

**Ph.D. Thesis by
M.Murat SARIOĞLU, M.Sc.**

Department : Environmental Engineering

Programme: Environmental Engineering

DECEMBER 2007

FOREWORD

It was a great pleasure and privilege to work with my supervisor Prof.Dr.Derin Orhon who supported me with his fruitful and satisfactory discussion sessions in the preparation of this work as he also did for my Master's thesis. Under his supervision and thanks to his vast expertise, it became possible for me to find the answers to the problems I have faced very quickly and continue on to the next step.

I would also like to thank all my professors, colleagues and researchers who are the staff at the Istanbul Technical University , Environmental Engineering Department. I appreciate their kind cooperation and valuable input to this work. I especially want to thank Prof.Dr. Nazik Artan for her precious ideas on biological modelling, Assoc.Prof.Erdem Görgün , Assis.Prof. Güçlü İnel for his utmost support in every aspect of this thesis, Assis.Prof. Özlem Karahan for her support in respirometric analysis and Assist.Prof.Nevin Yağcı for her support in IC and last but not least for all their valuable cooperation and help in the preparation of this study. My special thanks to Assoc.Prof.Emine Ubay Çokgör for her support in using the laboratory facilities. I would like to acknowledge Prof.Dr.Mehmet Karpuzcu from Gebze Institute of Technology for his valuable support in using the laboratory facilities of his institute during the final stages of the study.

I would like to acknowledge the Scientific and Technical Research Council of Turkey (TÜBİTAK) for the financial support in making this project possible. On top of all; very special thanks to my company MASS Treatment Systems Ind.and Trade Co.,Inc and their owners Sedat Soybay and Dr.Mithat Akkaya who have also financially and technically supported me and the project until the end. I would also like to acknowledge them for being open to innovative ideas and new technologies.

I would like to thank Christoher Bye, Imre Takacs and Mark Fairlamb from Envirosim Assoc.Ltd team for their help and support in using BioWin for advanced biological modelling purposes in MBR. On the other hand, I would like to acknowledge the help and support of Spencer Snowling and Oliver Schraa from Hydromantis Inc, for pyhsical modelling of MBRs with GPS-X.

Last but not least; very special thanks to Ersin Yamen and Dincer Öner from the Waste Management Inc. for their precious support in operating the plant continuously even due to too many difficulites faced during the entire study. They indeed deserve the credit.

I dedicate this thesis to my family and on top of all to my wife for her continuous support and encouragement in bringing this study to a conclusion.

To my wife and father.....

August, 2007

M.Murat SARIOĞLU

CONTENTS

	<u>Page</u>
ABBREVIATIONS	vii
LIST OF TABLES	ix
LIST OF FIGURES	xi
LIST OF SYMBOLS	xv
SUMMARY	xx
ÖZET	xxv
1. INTRODUCTION	1
1.1. Significance of the Study	1
1.2. Objectives	4
1.3. Scope of the Thesis	5
2. EXPERIENCE WITH MEMBRANE PROCESSES and MEMBRANE BIOREACTORS	8
2.1. Membrane Definition and Basics	10
2.2. Membrane Structure and Categorization	11
2.3. Membrane Configuration	16
2.4. Commercial Submerged Membrane Technologies	21
2.5. Mechanistic Explanation of Filtration Through Membranes	23
2.5.1. Flux	23
2.5.2. Type of filtration	24
2.5.3. Transmembrane pressure difference(Δp_{TM})-the driving force	26
2.5.4. Hydraulic permeability (H_p)	31
2.5.5. Crossflow velocity (V_{CF})	31
2.5.6. Concentration polarization	32
2.5.7. Concept of fouling	33
2.5.8. Avoiding fouling	36
2.5.9. Critical flux	36
2.6. Mass Transfer Theory in Membrane Filtration Processes	37

	<u>Page</u>
2.6.1. Membrane controlled mass transfer	38
2.6.2. Cake layer controlled mass transfer	38
2.6.2.1. The reknown resistance model	38
2.6.2.2. The concentration polarization model	39
2.7. The Membrane Coupled Activated Sludge Process- Membrane Bioreactor (MBR)	41
2.7.1. Historical background of MBRs	44
2.8. Aerobic MBR's for Domestic Sewage Treatment- Performance and Operational Aspects	45
2.8.1. Biological and solids removal performance	46
2.8.1.1. Carbon and solids removal performance	46
2.8.1.2. Nutrient removal performance	48
2.8.1.3. Virus and bacterial elimination performance	54
2.8.1.4. Physical (hydraulic) performance and fouling	57
2.9. Microbial Population Diversity in Membrane Bioreactors	61
2.10. Proposed Biological and Hydraulic Models for Membrane Bioreactors – A Review of Previous Studies	66
3. MATERIALS and METHODS	70
3.1. MBR Selection	70
3.2. System Description	72
3.2.1. Membrane and module specifications	72
3.2.2. Pilot membrane bioreactor plant specifications	75
3.3. Experimental Program and Testing Procedures	80
3.4. Measurement and Analysis Procedure	82
3.4.1. Data acquisition	82
3.4.2. Analytical methods	82
3.5. Application of FISH (Fluorescence in situ Hybridization) Technique	86
3.6. Tools used for Modelling	88
4. MODELLING OF MEMBRANE BIOREACTORS	99
4.1. Wastewater Characterization	100
4.1.1. Organic material	100
4.1.2. Influent solids characterization	105
4.1.3. Nitrogenous material	107
4.2. Measurement Techniques for Wastewater Characterization	110
4.3. Process Kinetics for Carbon Removal	113
4.3.1. Fate of carbonaceous particulate components	113

	<u>Page</u>
4.3.2. Fate of carbonaceous soluble components	120
4.4. Process Kinetics for Nitrification	124
4.4.1. Growth of autotrophs	124
4.4.2. Decay of autotrophs	126
4.4.3. Ammonification of organic nitrogen	127
4.5. Process Kinetics for Denitrification	127
4.5.1. Growth of denitrifiers	128
4.5.2. Anoxic hydrolysis of slowly biodegradable substrate	129
4.5.3. Decay of denitrifiers	130
4.5.4. Switching functions	130
4.6. Model Development for Carbon and Nitrogen Removal in MBR	133
4.7. A New Proposed Model for Membrane Bioreactor Activated Sludge Systems	135
4.8. Modelling of Carbon Removal, Nitrification and Denitrification in MBR with the New Adopted Model	141
4.8.1. Solids balance	141
4.8.2. Stoichiometric assessment of sludge production in MBR	148
4.8.3. Nitrification stoichiometry	150
4.8.4. Denitrification stoichiometry	152
4.8.5. Oxygen utilization	156
4.9. Dynamic Modelling of Membrane Bioreactors with the New Adopted Process Matrix using a Computer Simulator	158
4.9.1. Configuration of the MBR pilot plant in the simulator	159
4.9.2. Data collection	162
4.9.3. Calibration protocol	162
4.9.4. Sensitivity analysis	167
4.10. Dynamic Physical Modelling of Membrane Bioreactors using a Computer Simulator	171
4.10.1. Configuration of the MBR Pilot Plant in the simulator	177
5. EXPERIMENTAL RESULTS AND EVALUATION	179
5.1. Influent Wastewater Characterization	179
5.2. Solids Balance	184
5.3. Organics Removal	189
5.4. Oxygen Utilization	191
5.5. Nitrogen Removal	192
5.5.1. Nitrification	192

	<u>Page</u>
5.5.2. Denitrification	196
5.6. Calibration Results	211
5.7. Operation of the MBR without the Anoxic Tank- Results of Run III	212
5.8. Physical Modelling Results	222
5.9. Microbiological Findings	231
6. DISCUSSION AND CONCLUSIONS	237
6.1. Evaluation of Results	237
6.1.1. Biological Modelling and Validation	237
6.1.2. Physical Modelling	242
6.1.3. Microbiological Findings	245
6.2. Conclusions and Recommendations	246
REFERENCES	248
ANNEX	257
CURRICULUM VITAE	262

ABBREVIATIONS

AbwV	: The German Wastewater Ordinance
AS	: Air sparging
ASM1	: Activated sludge model No:1
ASM2	: Activated sludge model No:2
ASM3	: Activated sludge model No:3
ATV DWVK131	: German Standards for wastewater treatment plant design
BAP	: Biomass associated products
BCOD	: Biodegradable COD
BF	: Backflushing
BOD	: Biological oxygen demand
CFSTR	: Completely stirred tank reactor
CMBR	: Conventionally operated MBR
COD	: Chemical oxygen demand
DO	: Dissolved oxygen
EPA	: Environmental protection agency
EPS	: Extracellular polymeric substances
F/M	: Food to microorganism ratio
FBDA	: Fine bubble diffused aeration
FISH	: Fluorescence <i>in situ</i> hybridization
HRT	: Hydraulic residence time
IAWPRC	: International Association on water Pollution research and Control
ISS	: Inorganic suspended solids
IWA	: International Water Association
MBR	: Membrane bioreactor
MF	: Microfiltration
MLSS	: Mixed liquor suspended solids
MLVSS	: Mixed liquor volatile suspended solids
NF	: Nanofiltration
NON	: Non-enhanced filtration
NTU	: Normal turbidity unit
ORP	: Oxidation reduction potential
PFR	: Plug flow tank reactor
RO	: Reverse osmosis
SBMBR	: Sequencing batch membrane bioreactor
SEM	: Scanning electron microscope
SMP	: Soluble microbial products
SNdN	: Simultaneous nitrification and denitrification
SRT	: Sludge retention time
STOWA	: Dutch foundation for applied water research
TKN	: Total kjeldahl nitrogen
TMP	: Transmembrane pressure
TN	: Total nitrogen
TSS	: Total suspended solids

UAP : Utilization associated products
UF : Ultrafiltration
WERF : Water environment research federation

LIST OF TABLES

	<u>Page</u>
Table 2.1: Dense and porous membranes for water and wastewater treatment	12
Table 2.2: Membrane materials by type.....	14
Table 2.3: Phase inversion polymeric membrane materials.....	15
Table 2.4: Membrane configurations	22
Table 2.5: Driving forces applied to membrane processes	29
Table 2.6: Microbiological quality requirements for bathing waters (EC Bathing Water Guideline dated 8.12.1975;76/160 EWG).....	55
Table 2.7: Disinfection performance of various MBRs (Stephenson et al., 2000)	56
Table 2.8: Hydraulic performance of various membrane bioreactors with submerged hollow fiber and flat sheet modules	60
Table 3.1: Specification of the Kubota submerged membrane unit.....	73
Table 3.2: Specifications of the pilot scale membrane bioreactor	75
Table 3.3: List of the experimental periods.....	80
Table 3.4: List of crucial operating parameters for all experimental periods	81
Table 3.5: Data acquisition campaign during experimental testing	82
Table 3.6: Analysis methods	85
Table 3.7: Client list of BioWin	91
Table 3.8: Some of the technical papers referencing BioWin.....	92
Table 3.9: Client list of GPS-X	96
Table 3.10: Some of the technical papers referencing GPS-X.....	96
Table 4.1: COD fractions in domestic sewage.....	104
Table 4.2: Typical nitrogen fractions for domestic sewage	109
Table 4.3: Nitrogenous material in Istanbul domestic sewage.....	110
Table 4.4: Equations used in wastewater characterization using physical-chemical methods (ASM1).....	112
Table 4.5: Equations for nitrogen fractionation	113
Table 4.6: Process kinetics and stoichiometry for carbon oxidation,nitrification and denitrification,ASM1 (Henze et al., 1987).....	132
Table 4.7: Process kinetics and stoichiometry for carbon oxidation,nitrification and denitrification in membrane bioreactors	136
Table 4.8: Half saturation constants used in ASM1, ASM2, ASM2d and ASM3	139
Table 4.9: Summary of the calibrated ASM1 parameters to the new adopted process matrix for MBR.....	166
Table 4.10: Model parameter sensitivity table	169
Table 4.11: Influent and operational parameters sensitivity table	170
Table 4.12: MBR model modes	172
Table 4.13: MBR setup parameters in GPS-X	178
Table 5.1: Influent COD concentration of raw sewage (average).....	181
Table 5.2: Influent COD fractions of raw sewage (average)	181

	<u>Page</u>
Table 5.3: Influent nitrogen concentration and fractions	182
Table 5.4: Average influent solids concentration.....	183
Table 5.5: Influent wastewater characterization (Run I).....	184
Table 5.6: Calibrated half saturation constants for MBR (Run I).....	197
Table 5.7: Influent wastewater characterization (Run II)	205
Table 5.8: Calibrated half saturation constants for MBR (Run II).....	209
Table 5.9: Summary of calibrated model parameter for MBR	211
Table 5.10: Influent wastewater characterization (Run III)	213
Table 5.11: Calibrated half saturation constants for MBR (Run III)	219
Table 5.12: Summary of calibrated physical model parameters for flatsheet membranes	230
Table 5.13: Average count of cells per field of view (Pala, 2006)	232
Table 5.14: Relative abundances of phylogenetically defined groups of microorganisms in the eubacterial community (Pala, 2006).....	232
Table A1: Batch experiment results	257

LIST OF FIGURES

	<u>Page</u>
Figure 2.1: Schematic representation of various membrane structures.....	13
Figure 2.2: The filtration spectrum for different membrane separation processes.....	16
Figure 2.3: Tubular MF(microfiltration module).....	18
Figure 2.4: Schematic of spirally wound membrane.....	18
Figure 2.5: Flat sheet membrane structure and a single module.....	19
Figure 2.6: (a) 3 μm non-woven membrane surface (b) 5 μm non-woven membrane surface.....	20
Figure 2.7: Hollow fiber membrane module.....	20
Figure 2.8: 0.4 μm woven membrane surface structure.....	21
Figure 2.9: (a) Zenon and (b) Kubota membrane modules.....	23
Figure 2.10: Schematic presentation of dead-end and crossflow filtration.....	25
Figure 2.11: Definition of operational parameters in crossflow filtration.....	26
Figure 2.12: Schematic illustration of pressure distribution across the membrane and the cake layer.....	30
Figure 2.13: Relationship between transmembrane pressure and permeate flux in crossflow microfiltration.....	31
Figure 2.14: Schematic representation of concentration polarization.....	33
Figure 2.15: Effect of EPS concentration on membrane fouling resistance.....	36
Figure 2.16: Schematic representation of MBR with (a) external membrane filtration (b) internal submerged membrane filtration.....	43
Figure 2.17: Nitrogen removal in intermittent MBR (Ujang et al., 2002).....	50
Figure 2.18: Structure of support aerated biofilm in a membrane bioreactor (Timberlake et al.,1988).....	52
Figure 2.19: Relationship between the permeate volume and time (a) flat sheet membranes, (b) hollow fiber membranes (operational sequence) (Günder,2001).....	58
Figure 2.20: Relationship between transmembrane pressure and flux at 10°C (Günder, 2001).....	59
Figure 2.21: Clusters of <i>Nitrospira</i> spp. (2-a), clusters of <i>Nitrospira</i> spp. (2-b), genus <i>Paracoccus</i> cells (2-c,2-d), (Sofia et al.,2004).....	63
Figure 2.22: (a) Mixed liquor size distributions for membrane bioreactors and conventional activated sludge plants at 30 day sludge age, (b) Example photographs of biomass for the membrane bioreactor and conventional activated sludge plant at a 30 day sludge age (Smith et al., 2003).....	64
Figure 2.23: Phase-contrast micrographs of activated sludge flocs from the (a) conventional activated sludge with a secondary clarifier (b) from the membrane bioreactor (Manser et al., 2005).....	65

	<u>Page</u>
Figure 2.24: Confocal laser scanning microscopic sections through an activated sludge floc, stained with gene probes. Green: general probe for all bacteria; Yellow: specific probe for a group of ammonia-oxidizing bacteria.....	65
Figure 2.25: Different environments in a membrane aerated biofilm (Semmens and Shanahan,2005).....	68
Figure 3.1: Schematic representation of permeate extraction in the pilot plant.....	72
Figure 3.2: Schematics of (a) membrane panel (b)submerged membrane unit.....	73
Figure 3.3: Pictures of the (a) submerged membrane module, (b) flatsheet membrane panel.....	74
Figure 3.4: Pictures of the pilot plant.....	76
Figure 3.5: Schematic setup of the pilot plant.....	77
Figure 3.6: Daily variation of (a) Influent COD and (b) Influent TSS,VSS.....	84
Figure 3.7: Phylogenetic tree inferred from comparison of 16S rRNA sequences. (Target organisms for probes Nso190, Nso1225, Nsm156, Nsv443,NEU, NIT3, and Nb1000) (Mobarry et al., 1996).....	88
Figure 4.1: Categorization of COD components in raw sewage.....	103
Figure 4.2: Quantified COD components in raw sewage , $C_{Tin}=400\text{mg/l}$	104
Figure 4.3: Influent wastewater characterization for nitrogenous material.....	109
Figure 4.4: Schematic illustration of death-regeneration model (basis of ASM1) under (a) Aerobic (b) Anoxic conditions (Henze et al., 1987).....	119
Figure 4.5: Schematic illustration of endogenous decay model (basis of for this research) under (a) Aerobic (b) Anoxic conditions.....	119
Figure 4.6: Schematic illustration for conversion of organic nitrogen to ammonia. 127	
Figure 4.7: Oxygen profile inside (a) Large flocs (b) small flocs.....	138
Figure 4.8: Schematic process diagram for carbon and nitrogen removal in submerged membrane bioreactor.....	141
Figure 4.9: Methodology followed for using the process simulator (Dold et al., 2003).....	158
Figure 4.10: Plant layout implemented in BioWin 2.2® Software.....	160
Figure 4.11: Model builder unit in BioWin for implementing the new adopted MBR process matrix.....	161
Figure 4.12: Calibration methodology of the new adopted process matrix for MBR (Insel et al., 2006).....	165
Figure 4.13: Membrane bioreactor model structures.....	171
Figure 4.14: GPS-X membrane bioreactor objects.....	172
Figure 4.15: Physical membrane properties.....	174
Figure 4.16: Plant layout implemented in GPS-X® software.....	177
Figure 5.1: Fitted BOD curve for the set of measured BOD ₅ data points.....	180
Figure 5.2: Influent total, particulate and soluble COD.....	182
Figure 5.3: InfluentTKN and ammonia nitrogen profiles.....	183
Figure 5.4: Influent TSS,VSS and ISS Profiles.....	184
Figure 5.5: Solids Balance (a) MBR reactor, (b) in Anoxic reactor.....	185
Figure 5.6: Fate of particulate components (a) MBR reactor, (b) in Anoxic reactor.....	186
Figure 5.7: Variation of active biomass concentration with respect to changing dissolved oxygen concentration.....	188

	<u>Page</u>
Figure 5.8: Variation of active biomass concentration with respect to changing temperature.....	189
Figure 5.9: Influent COD and simulated/calculated effluent COD concentration profiles.....	190
Figure 5.10: Simulated effluent COD fractions.....	190
Figure 5.11: MBR air supply rate vs recorded DO.....	191
Figure 5.12: Airflowrate vs. measured and simulated DO in MBR unit.....	192
Figure 5.13: Nitrification performance of the pilot membrane bioreactor with respect to dissolved oxygen.....	195
Figure 5.14: Nitrification performance of the pilot membrane bioreactor with respect to temperature.....	195
Figure 5.15: Nitrate removal performance (a) overall longterm results, (b) magnified results for low DO conditions (c) magnified results for high DO conditions (d) influent TKN and effluent S_{NO} results with respect to ORP values.....	199
Figure 5.16: Dynamic simulation results and experimental data for S_{NH} and S_{NO}	200
Figure 5.17: Total nitrogen removal efficiency vs. DO and influent COD/TKN ratio.....	201
Figure 5.18: Simulated and calculated effluent ammonia (S_{NH}) and nitrate (S_{NO}) concentrations.....	202
Figure 5.19: Comparison of total effluent nitrogen level with respect to stoichiometric and model results for varying dissolved oxygen.....	204
Figure 5.20: Comparison of total effluent nitrogen level with respect to , stoichiometric and model results for varying temperature.....	204
Figure 5.21: Ammonia (S_{NH}) profile for Run II.....	206
Figure 5.22: Nitrate (S_{NO}) profile for Run II.....	207
Figure 5.23: Efficiencies nitrification, denitrification and total nitrogen.....	208
Figure 5.24: Variation of K_{OA} and K_{OH} with respect to MLSS.....	209
Figure 5.25: Measured and calculated nitrification rates as a function of oxygen concentration under excess substrate conditions (Manser et al., 2005).....	210
Figure 5.26: BioWin® 2.2 modelling setup for Run III.....	212
Figure 5.27: Solids balance of MBR in Run III in terms of (a) VSS,TSS (b) all the particulate components.....	214
Figure 5.28: Influent, effluent COD and removal efficiencies.....	214
Figure 5.29: Oxygen modelling results.....	215
Figure 5.30: (a) Oxygen transfer rates, (b) Oxygen transfer efficiencies.....	216
Figure 5.31: Ammonia nitrogen profile with respect to dissolved oxygen and temperature.....	217
Figure 5.32: Nitrate profile.....	218
Figure 5.33: N_{OX} vs S_{NO} with respect to dissolved oxygen and COD/TKN ratio....	219
Figure 5.34: Oxidized S_{NH} and denitrified S_{NO}	220
Figure 5.35: Nitrification and denitrification efficiencies.....	221
Figure 5.36: Phenomena limiting flux performance in membrane filtration (Wintgens et al., 2003).....	223
Figure 5.37: Variation of longterm TMP and flux values.....	224
Figure 5.38: Longterm simulated vs measured flux values.....	224

	<u>Page</u>
Figure 5.39: Longterm simulated vs measured hydraulic permeability values.....	225
Figure 5.40: Temperature effect on the hydraulic permeability.....	226
Figure 5.41: Longterm simulated vs measured TMP results with the effect of temperature.....	226
Figure 5.42: Simulated cake resistance.....	228
Figure 5.43: Intrinsic membrane resistance.....	228
Figure 5.44: Fouling resistance of the membrane bioreactor.....	229
Figure 5.45: Total membrane resistance of the membrane bioreactor.....	229
Figure 5.46: Superposed resistance parameters.....	230
Figure 5.47: Relative abundance of filamentous morphotypes (Pala, 2006).....	234
Figure 5.48: Relative abundance of the microbial population (Pala, 2006).....	235
Figure 5.49: Cells detected with EUBMIX probe (a) Hybridized cells (b) DAPI-stained cells (Pala, 2006).....	235
Figure 5.50: Cells detected with ALF968 probe (a) Hybridized cells (b) DAPI-stained cells (Pala, 2006).....	235
Figure 5.51: Cells detected with NB1000 probe (a) Hybridized cells (b) DAPI-stained cells (Pala, 2006).....	236
Figure 5.52: Cells detected with BET42a probe (a) Hybridized cells (b) DAPI-stained cells (Pala, 2006).....	236
Figure 5.53: Cells detected with GAM42a probe (a) Hybridized cells (b) DAPI-stained cells (Pala, 2006).....	236
Figure A1: Change of active biomass with respect to time.....	258
Figure A2: Comparison of the experimental results with the calculation results.....	259
Figure A3: Results of the respirometric analysis.....	260
Figure A4: Determination of the decay rate coefficient (b_H) with OUR values.....	260

LIST OF SYMBOLS

κ	: Boltzmann constant
σ	: Cake layer thickness
β	: Correction coefficient
μ	: Fluid viscosity
α	: Fraction of biodegradable COD converted to soluble residual
α	: Proportional constant
δ	: Thickness of cake layer
μ_A	: Specific autotrophic growth rate
μ_{Amax}	: Maximum autotrophic growth rate
ϵ_c	: Cake porosity
η_D	: Anoxic correction factor for decay
α_D	: Fraction of influent biodegradable substrate converted to soluble
η_g	: Anoxic correction factor for growth
θ_H	: Hydraulic residence time
μ_H	: Specific heterotrophic growth rate
μ_{HD}	: Specific growth rate of denitrifiers
μ_{HDmax}	: Maximum growth rate of denitrifiers (heterotrophic)
μ_{Hmax}	: Maximum heterotrophic growth rate
θ_{HT}	: Total hydraulic residence time
η_{HYD}	: Anoxic correction factor for hydrolysis
$\delta_{i,j}$: Relative change in state
ρ_L	: density of the feed solution
ϵ_m	: Membrane porosity
ρ_p	: Density of a particle
α_R	: Growth associated soluble inert product formation fraction for the
$\gamma_{UAP,A}$: Fraction of biodegradable organic substrate converted to soluble
$\gamma_{UAP,H}$: Fraction of biodegradable organic substrate converted to soluble
θ_X	: Total sludge age
θ_{XA}	: Aerobic sludge age
A_M	: Membrane area
A_S	: Specific surface of a cake layer particle
b_A	: Autotrophic decay rate coefficient (endogenous decay approach)
$b_{BAP,A}$: Decay coefficient for the formation of biomass associated products
$b_{BAP,H}$: Decay coefficient for the formation of biomass associated products
b_H	: Heterotrophic decay rate coefficient (endogenous decay approach)
$b_{H(d-r)}$: Heterotrophic decay coefficient (death –regeneration approach)
	Biodegradable COD
BOD_{eff}	: Effluent BOD
C_{Iin}	: Influent total nonbiodegradable COD
C_{NDin}	: Influent total biodegradable organic nitrogen
C_S	: Biodegradable COD

C_{Sin}	: Influent total biodegradable COD
C_{Tin}	: Influent total COD
C_{TKNin}	: Influent total kjeldahl nitrogen
d	: Diameter of tubes
D_B	: Brownian diffusion coefficient
D-R	: Death regeneration model
d_p	: Diameter of particle
f_A	: Fraction of autotrophic active excess biomass to total active excess
f_{CV}	: Fraction of influent particulate COD to the influent VSS
f_{DNA}	: Oxygen switch function for autotrophs
f_{DNH}	: Oxygen switch function for heterotrophs
f_{ES}	: Fraction of endogenous biomass
f_{ES}	: Inert soluble fraction of heterotrophic active biomass
f_{EX}	: Inert particulate fraction of heterotrophic active biomass
f_I	: Total nonbiodegradable fraction of influent COD
f_{PS}	: Fraction of endogenous particulate matter converted into soluble
f_R	: Recirculation ratio fraction
f_S	: total biodegradable fraction of influent COD
f_{SI}	: Fraction of total COD which is soluble nonbiodegradable
f_{SNI}	: N content of influent nonbiodegradable COD
f_{SNP}	: Fraction of soluble microbial products that is nonbiodegradable
f_{SS}	: Fraction of soluble COD which is soluble biodegradable
f_{XH}	: Heterotrophic biomass fraction in the influent
f_{XI}	: Fraction of total COD which is particulate nonbiodegradable
f_{XNI}	: N content of influent nonbiodegradable COD
f_{XP}	: inert fraction of particulate organic matter
f_{XS}	: Fraction of total COD which is particulate biodegradable
g	: gravitational constant
H_p	: Hydraulic permeability
i	: Number of parameters
i_N	: Fixed nitrogen fraction
i_{NSF}	: Nitrogen fraction associated with hydrolyzable COD
i_{NSI}	: Nitrogen fraction associated with soluble inert COD
i_{NSS}	: Nitrogen fraction associated with readily biodegradable COD
i_{NXI}	: Nitrogen fraction associated with inert particulate COD
i_{NXS}	: Nitrogen fraction associated with slowly biodegradable COD
i_{XB}	: Nitrogen content of active biomass
i_{XI}	: Nitrogen content of inert biomass
i_{XP}	: Nitrogen content of endogenous biomass
J	: Flux
j	: m number of states
K	: Constant for membrane pores
k	: Kozeny constant
k_f	: Deposition rate
k_h	: Maximum specific hydrolysis rate
K_{MP}	: Maximum specific utilization rate for slowly biodegradable substrate
K_{NH}	: Ammonia half saturation constant
K_{NO}	: Nitrate half saturation constant
K_O	: Oxygen half saturation constant
K_{OA}	: Oxygen half saturation constant for autotrophs

K_{OH}	: Oxygen half saturation constant for heterotrophs
k_R	: Ammonification rate constant
K_S	: Half saturation constant for heterotrophic growth
K_{SMP}	: Half saturation constant for soluble microbial products
K_{SP}	: Half saturation constant for hydrolysis of slowly biodegradable COD
K_X	: Half saturation constant for hydrolysis of slowly biodegradable
L	: Hydraulic dimension
l_c	: Cake thickness
l_m	: Membrane thickness
M_d	: Amount of deposits
m_p	: Total dried mass of a cake layer
M_{XHT}	: Total mass of heterotrophic active biomass
N_{DP}	: Overall denitrification potential
N_{DPanox}	: Denitrification potential of the anoxic reactor
N_{Dpmbr}	: Denitrification potential of the MBR reactor
N_{OX}	: Available oxidizable nitrogen
N_X	: Nitrogen that is incorporated into biomass
OR_A	: Oxygen requirement of autotrophs
OR_H	: Oxygen requirement of heterotrophs
OR_T	: Total oxygen requirement
OUR_A	: Oxygen uptake rate of autotrophs
OUR_H	: Oxygen uptake rate of heterotrophs
P	: Pressure
P_{TM}	: Transmembrane pressure
P_{XA}	: Autotrophic excess sludge production
P_{XH}	: Heterotrophic excess sludge production
P_{XISS}	: Excess sludge production associated with inorganic suspended solids
P_{XP}	: Excess sludge production associated with endogenous inert COD
P_{XS}	: Excess sludge production associated with particulate slowly
P_{XT}	: Total excess sludge production
q_A	: Specific substrate utilization rate
Q_C	: Concentrate flow
Q_F	: Feed flow
Q_{in}	: Inlet flow
Q_P	: Permeate flow
Q_W	: Excess sludge flow
R	: Recirculation ratio
R_C	: Cake layer resistance
r_c	: Specific cake resistance
R_F	: Fouling resistance
R_m	: Intrinsic membrane resistance
R_{NDanox}	: Nitrate requirement for anoxic reactor
R_{NDmbr}	: Nitrate requirement for MBR reactor
r_p	: Radius of rejected material
R_T	: Total resistance
S_C	: Cake surface area to volume ratio
S_{Iin}	: Influent soluble inert COD
S_m	: Pore surface area to volume ratio
S_{ND}	: Soluble organic nitrogen
S_{NDin}	: Influent soluble biodegradable organic nitrogen

S_{NE}	: Effluent nitrogen
S_{NH}	: Ammonia nitrogen concentration
S_{NHin}	: Influent ammonia nitrogen
S_{Nin}	: Influent nonbiodegradable soluble organic nitrogen
S_{NO}	: Nitrate nitrogen
S_{NOE}	: Effluent nitrate nitrogen concentration
S_{NOin}	: Influent nitrate nitrogen concentration
S_{NP}	: Soluble nonbiodegradable nitrogenous products
S_O	: Dissolved oxygen concentration
S_S	: Readily biodegradable COD
S_{Sin}	: Influent readily biodegradable COD
S_{SMP}	: Soluble microbial products
S_{Teff}	: Total effluent COD
T	: Temperature
t	: time
$TKN_{eff,sol}$: Effluent soluble TKN
$TKN_{in,part}$: Influent particulate TKN
$TKN_{in,sol}$: Influent soluble TKN
TSS_{in}	: Influent total suspended solids
U	: Crossflow velocity (2)
V_{anox}	: Anoxic reactor volume
V_{CF}	: Crossflow velocity (1)
V_D	: Anoxic reactor volume
V_{mbr}	: MBR reactor volume
V_P	: Permeate volume
VSS_{in}	: Influent volatile suspended solids
V_T	: Total volume
X_A	: Autorrophic active biomass
X_A	: Autotrophic active biomass
X_{Aanox}	: Anoxic tank autotrophic active biomass concentration
X_{Ambr}	: MBR tank autotrophic active biomass concentration
X_H	: Heterotrophic active biomass
X_H	: Heterotrophic active biomass concentration
X_{Hanox}	: Anoxic tank heterotrophic active biomass concentration
X_{HD}	: Denitrifying active biomass
X_{Hin}	: Heterotrophic active biomass in the influent
X_{Hmbr}	: MBR tank heterotrophic active biomass concentration
X_I	: Inert biomass concentration
X_{Iin}	: Influent particulate inert COD
X_{ISS}	: Inorganic suspended solids concentration
X_{ISSin}	: Influent inorganic suspended solids
X_{Nin}	: Influent nonbiodegradable particulate organic nitrogen
X_P	: Endogenous biomass concentration
X_S	: Slowly biodegradable COD
X_{SC}	: Slowly biodegradable COD of colloidal nature
X_{Sin}	: Influent slowly biodegradable COD
X_{SP}	: Slowly biodegradable COD of particulate nature
X_{TISS}	: Total inorganic suspended solids concentration
X_{VASS}	: Volatile active suspended solids concentration
X_{VSS}	: Volatile suspended solids concentration

Y_A : Autotrophic yield coefficient
 Y_H : Heterotrophic yield coefficient
 Y_{HD} : Denitrifying bacteria yield coefficient
 Y_{SMP} : Yield coefficient for soluble microbial products

CARBON AND NITROGEN REMOVAL IN MUNICIPAL AND INDUSTRIAL WASTEWATER USING MEMBRANE BIOREACTORS

SUMMARY

The coupling of a membrane to a bioreactor is called the membrane coupled activated sludge process which is known as the membrane bioreactor process (MBR). The permeate from the membrane is free from solids and macro collidal material. Complete retention of all suspended material is achieved including bacteria and viruses. Sludge age and HRT are completely independent, removing some of the acknowledged operational limitations of the conventional activated sludge process. The membrane effectively nullifies problems of filamentous growth and degassing sludges. Therefore MBRs can be operated at low hydraulic residence times and long sludge ages without washout of biomass which is common in activated sludge. Mixed liquor concentrations of up to 30,000 mg/lit can be easily maintained. The combination of high biomass concentrations and complete retention of solids allow the process to be operated at low organic loading rates. The lower loading rates also reduce excess sludge production down to below half that commonly encountered in activated sludge. These circumstances are believed to enhance the microbial community and floc morphology to result in a rather different bacterial culture which in turn promotes the development of specialized microorganisms such as nitrifiers which are able to nitrify higher influent nitrogen loads under adverse conditions.

Membranes used for membrane coupled activated sludge process are usually in the microfiltration or ultrafiltration range which have a cutoff size of 0.1 μ m-0.4 μ m. Membranes are either submerged within the activated sludge reactor or configured externally as a sidestream filtration process. External sidestream configurations require high pressure to permeate the activated sludge through the membranes whereas submerged membrane modules even offer the opportunity of gravity filtration without even using a low pressure suction pump. During the internal submerged arrangement the required crossflow is produced through ascending air bubbles. The air bubbles necessary for scouring of the cake layer off the membrane surface also provide oxygen for the biological reactions. Membrane bioreactors provide superb treatment efficiency in terms of organic and nutrient removal. Although the organic removal efficiency of membrane bioreactors is very well known; nitrogen removal and especially simultaneous nitrification and denitrification capacity of membrane bioreactors still remains to explored. Simultaneous nitrification and denitrification brings the advantage of high nitrogen removal efficiencies due to increased denitrification potential. However lack of knowledge still remains for the source of increased denitrification potential. A better understanding of the biological reactions occurring in a membrane bioreactor will provide an optimized design and energy consumption which in turn will promote the faster commercialization of the membrane bioreactors.

Apart from the biological aspects, membrane bioreactors involve physical operational restraints which attracted more attention in the past researches and studies. Obviously, fouling remains to be the main obstacle in the way of membrane bioreactor technology spreading and commercializing worldwide much faster. Many operational and physical aspects have been identified as the cause of irreversible fouling however past operational experience indicate that these aspects to be membrane specific as the cause of fouling for one type of membrane cannot be solely attributed to another type. Therefore recent researches and studies have been focused on the ways and techniques for minimizing fouling and reducing the time period necessary for chemical regeneration of the membranes.

This study focuses on two initiatives and objectives: *i.) To identify the true potential of membrane bioreactors for nitrogen removal with simultaneous nitrification and denitrification thereby deriving the denitrification potential of the system with respect to available carbon and dissolved oxygen (for longterm conditions) ii.) To minimize and to avoid irreversible fouling to a maximum time extent by implementing a different operational mode from the ones conducted in previous studies.*

For the above mentioned objectives, a pilot scale membrane bioreactor based on microfiltration technology was setup at a domestic sewage treatment plant. The plant was fed with municipal wastewater. Flatsheet membranes with a cutoff size of 0.4 μm were used. The inflow to the pilot scale membrane bioreactor was set at 4m³/day however the plant had the capacity for a throughput of 6 m³/d. Total membrane area was 8 m² and the operating flux was constant at 0.5 m³/m²-day (20.8 lt/h-m²). The membrane module was supplied from Kubota Inc., Japan. The system setup for nitrogen removal was based on predenitrification where the content of the MBR tank was recirculated back to the anoxic tank with capacity up to 6 times the inflow. Coarse bubble aeration was used to supply oxygen for the microorganisms to carry out the biological reactions where it also simultenaously provided the necessary scouring effect on the membrane surface.

System was biologically modelled for all runs using BioWin 2.2 software from EnviroSim Associates Ltd. whilst physical modelling was done by GPS-X from Hydromantis Inc. Longterm simulations were conducted both for the biological and the physical model. Physical-chemical methods were used to determine the influent readily biodegradable COD(S_S) and the influent inert COD(S_I), where afterwards this was coupled with a BOD analysis campaign which included the measurement of BOD as a function of time to determine the biodegradable fraction (S_S+X_S) of the influent total COD.

The activated sludge model No.1 (ASM1) was used as the basis for the model developed. ASM1, based on death-regeneration approach was modified to endogenous decay model where the overall decrease in the VSS concentration is explained by means of an endogenous decay coefficient b_H , in which some portion (f_{EX}) is converted to particulate inert organic products (X_P). It can be postulated that the bacteria in MBRs consume nitrate extensively as the electron acceptor during the decay process where this consumption increases with decreasing dissolved oxygen levels in the reactor. Processwise explanation of this mechanism was done by adding two more processes to the original matrix of ASM1 which includes the anoxic decay

of autotrophs and heterotrophs bound to an electron acceptor (S_{NO}). The soluble product formation was also added to the matrix to account for the inert soluble products (S_{SMP}) formed during decay.

The model developed characterized the measured effluent COD efficiently. The average organic removal efficiency was 95% in terms of COD removal reaching up to a max of 99% independent from the influent loading where BOD in the effluent was not detectable. The effluent total COD only consisted of inert soluble fraction (S_I) and inert soluble microbial products (S_{SMP}). The S_{SMP} accounted to less than 10 mg/lit in average throughout the study where S_S was completely consumed.

The COD/TKN ratio exhibits high variation in the range of 5-20. Under low DO (from day 50 to 100 days) the system yielded high and stable nitrogen removal performance in spite of oscillating COD/TKN ratio in the influent. The system exhibited nearly full TN removal under low DO set-points. The effect of increase in DO level in the reactor had a negative effect on system performance with respect to TN removal. For instance, increase in DO level from 0.3 to 1.8 mg/L caused a gradual decrease in TN removal performance from 100% to 70%. The impact of COD/TKN level is much more pronounced under high DO levels in MBR reactor. At high DO levels, (>1.5 mg/lit) the ammonia concentrations observed in the MBR tank was below 1 mg/lit, whilst the nitrate levels in the same tank was in the range of 8-16 mg/lit. Considering that the average influent TKN and ammonia concentrations were 45-60 mg/lit and 30-45 mg/lit respectively, the level of denitrification in the MBR tank which is oxic was observed to be approximately 20-30 mg/lit. This corresponds to a nitrate removal rate of nearly 50-60% in the MBR tank itself. The level of denitrification is related to the denitrification potential, N_{DP} within the MBR reactor which is solely dependant on available COD. However in membrane bioreactors, it can be stated that the level of oxygen inside the MBR also plays an important role in defining denitrification potential.

The influent COD and ammonia concentrations for Run II and Run III were well over the values taken into account for the pilot design. As this was the case, there was residual oxygen of 1.5-3 mg/lit in the bulk liquid throughout the study where it should have been expected to be much lower with values less than 1 mg/lit due to air feed deficiency and oxygen uptake by the bacteria. This clearly explains and verifies the fact that major portion of the supplied oxygen is unable to pass into the floc due to mass transfer limitation which is explained by increased half saturation constant of oxygen.

The high concentration in the bulk liquid and the population diversity results in a size distribution of flocs where in MBR it is assumed to be larger in the size of 50-110 μ m. It is stipulated that a substantial anoxic mass fraction exists in the center of the biomass flocs resulting in an oxygen diffusion limitation into the flocs. The level of $SNdN$ occurring in the membrane bioreactor suggests that this level of diffusion limitation is so high that it is even causing the anoxic fraction of biomass inside the floc to be dominant during high DO levels. It can be concluded that during high DO levels this fraction of biomass shifts from being anoxic to aerobic decreasing the level of $SNdN$. The oxygen diffusion limitation from the bulk liquid into the flocs can be explained by assigning specific values to half saturation constants in the corresponding switching functions namely $K_{OH}=1$ mg/lit, $K_{OA}=1.25$ mg/lit, $K_{NH}=2$

mg/l and $K_{NO}=2$ mg/l which are much higher than the values adopted to previous models. The system nitrified with dissolved oxygen concentrations as low as 0.5 mg/l where it partially nitrified with dissolved oxygen concentrations down to 0.3 mg/l. It can be concluded that the factors and parameters triggering SNdN in MBR can be listed as *i.) dissolved oxygen concentration, ii.) floc size, iii.) MLSS concentration of the bulk liquid* which the latter two severely affects diffusion limitation of oxygen from the bulk liquid into the floc. MLSS concentration of the bulk liquid is interrelated with the sludge age of the system which is thought to have a direct effect on the culture and morphology of the bacteria in a membrane bioreactor system and thus SNdN.

A stepwise long term dynamic calibration methodology was developed by initial introduction of three iterative steps in the order of VSS, TSS, NH_4^+-N , O_2 and $NO_3^- - N$ profiles respectively. The calibration parameters were chosen from the processes that had a considerable impact on the solids balance and simultaneous nitrification-denitrification. Detailed model sensitivity was conducted both for the stoichiometric and kinetic parameters as well as influent operational parameters. The results of the sensitivity analysis revealed high sensitivity of the model to oxygen half saturation constants of heterotrophs and autotrophs. The simultaneous nitrification and denitrification was also very sensitive to the η_D factor which governed the degree of denitrification occurring during anoxic decay of heterotrophs and autotrophs.

The level of SNdN occurring in the aerated MBR reactor fluctuates according to the oxygen level within the bulk liquid where low DO levels in the range of 0.3-0.6 mg/l increases the denitrification potential dramatically triggering up to more than 30 mg/l of nitrate uptake within the MBR, whilst DO levels in the range of 1.5-3.5 mg/l reduces the nitrate uptake to levels in between 10-20 mg/l. It can be concluded that a minimum of 10-15 mg/l of nitrate will be removed simultaneously in a MBR with DO levels in the range of 1.5-2.5 mg/l. In light of the stoichiometry of denitrification, it can be also concluded that anoxic decay of heterotrophs and autotrophs significantly contribute to the SNdN occurring in the MBR verifying that these systems are decay dominant. There exists a balance point between the level of nitrification and denitrification with respect to the level of oxygen in the MBR reactor, when if controlled, effluent TN limits less than 15 mg/l can easily be achieved by operating a MBR continuously at DO levels in the range of 0.3-0.8 mg/l and V_D/V_T ratios as low as 0.10. Effluent TN regulations of 10-15 mg/l can be achieved with MBRs operated without an anoxic tank for domestic sewage provided that MLSS, dissolved oxygen levels and SNdN performance are kept under control through instrumental observation and automation.

Recommended MLSS concentrations for MBRs operated without an anoxic tank to reach the desired effluent TN regulations must be in the range of 15,000-20,000mg/l. Two factors are governing when giving this range, *i.) the MLSS levels and hence sludge age that will not inhibit nitrification through mass transfer limitation and provide sufficient ammonia oxidation, ii.) the MLSS levels hence sludge age that will provide the necessary mass transfer limitation for enhanced SNdN for nitrate reduction without the need for a dedicated volume for denitrification.*

The pilot scale membrane bioreactor system was operated in a different membrane operational mode when compared to previous studies and the recommendation of the supplier. The permeate was filtered through the membranes by gravity. Activated sludge was filtered through the membranes for a continuous 12 h period where afterwards a 10min relaxation with high air scouring for the removal of the cake layer were the basis of the operational mode. According to the field and modelling results it can be concluded that the system was successfully operated with the adopted operational sequence without any fouling for 310 days (Run I) of continuous operation. This is linked to the type of aeration system (coarse bubble) used to create the necessary crossflow velocity to remove the cake layer from the membrane surface. The in series resistance model was dynamically calibrated by adjusting the physical characteristics of the membranes to fit the recorded data. It is obvious that temperature has a detrimental effect on the transmembrane pressure and hydraulic permeability. However since the in series resistance model does not incorporate the affect of temperature, the model calibration for the fluctuation of temperature was done by adjusting the maximum fouling resistance and the fouling rate constant parameters to fit the TMP and hydraulic permeability data. The physical model was successfully calibrated to mimic the recorded data. It can be concluded that the type of aeration to create the crossflow velocity for air scouring has the most influential affect in the removal of the cake layer from the surface of the membrane and hence a positive affect in avoiding/delaying the irreversible fouling. It can be further concluded that; a very well and efficient operating primary treatment is a must upstream of the membrane bioreactor system. 0.75-1 mm screening along with grit and grease removal will have a positive affect in the reduction of the irreversible fouling casued by inorganic solids and grease.

Different populations in natural and engineered systems can be determined using the FISH technique without cultivation from the natural environment, hence quantitative data can be obtained as a result of homogenization. Quantification of nitrifying bacteria in the pilot membrane bioreactor was achieved as part of the research. It was found that the relative abundance of the nitrifying bacteria in the total bacterial population was 13%. Previous researches have reported lower relative abundance values due to the very high sludge ages of the membrane bioreactors studied. Quantitative and qualitative analysis of the filamentous bacterial community present in a membrane bioreactor system is a must for a better understanding of the fouling mechanism in this technology. Furthermore, the operational conditions of membrane bioreactor systems in relation to the maintenance of high amount of nitrifying microorganisms is also a crucial matter that must be investigated for the occurrence of robust nitrification regardless of the environmental factors.

EVSEL VE ENDÜSTRİYEL ATIKSU ARITIMINDA MEMBRAN BİYOREAKTÖR İLE KARBON VE NÜTRİYENT GİDERİMİ

ÖZET

Membranların aktif çamur prosesi ile birleşimine membranlı aktif çamur prosesi veya diğer bilinen adıyla membran biyoreaktör denilmektedir (MBR). Membran biyoreaktörler içindeki veya dışındaki membran modüllerden süzülen çıkış suyunda hiçbir katı ve veya makro kolloidal madde bulunmamaktadır. Reaktör içinde askıdaki tüm katı ve kolloidal maddeler bakteri ve virüsler dahil olmak üzere membranda tutulmaktadır. MBR'ların işletimi çamur yaşı ve bekletme süresinden bağımsız olduğundan dolayı konvansiyonel sistemlerde görülen işletme zorluklarını ortadan kaldırmaktadır. MBR prosesi, filamentli bakteri büyümesi ve yüzen çamur problemlerini de engellemektedir. Dolayısıyla MBR'ler, konvansiyonel aktif çamur proseslerinde görüldüğü gibi çamurun üst akımla kaybına neden olmadan düşük hidrolik bekletme sürelerinde ve yüksek çamur yaşlarında tasarlanıp işletilebilmektedir. Askıda 30,000 mg/lt biyokütle konsantrasyonlarına kadar bu sistemleri işletmek mümkündür. Yüksek biyokütle konsantrasyonu ve %100 katı madde tutulması sayesinde MBR'ler çok düşük organik yükleme hızları altında işletilebilir. Çok yüksek çamur yaşları sayesinde elde edilen düşük organik madde yüklemeleri, konvansiyonel aktif çamur sistemlerinde gözlemlenen çamur oluşumun neredeyse yarısı kadarı membran biyoreaktör sistemlerinde gözlemlenmektedir. Bu tür işletmesel koşulların, reaktör içindeki bakteriyel popülasyonu flok morfolojisi ve mikrobiyel kültür açısından değiştirdiğine ve bu sayede özellikle nitrifikasyon bakterilerinin konvansiyonel sistemlere nazaran daha değişik yapıda olmasına ve beraberinde daha yüksek azot yüklerini daha olumsuz çevresel koşullarda dahi oksitleyebildiğine inanılmaktadır.

Membranlı aktif çamur proseslerinde kullanılan membranlar, genellikle mikrofiltrasyon ve ultrafiltrasyon aralığında olup 0.1µm ila 0.4µm gözenek açıklıklarına sahiptir. Membranlar reaktör içinde batık şekilde teşkil edilebildikleri gibi reaktör dışında yan akımlı filtrasyon prosesi olarak da kurulabilmektedir. Reaktör dışında ayrı düzenekle konuşlandırılan membranlardan aktif çamur süzme işlemi yüksek basınçlara ihtiyaç duyarken; batık teşkil edilen membranlar filtrasyon için çok düşük basınçlı emiş pompası gereksiniminin ötesinde cazibe ile filtrasyona bile imkan tanımaktadır. MBR'ler, organik ve nütriyent giderimi açısından çok yüksek verimler sağlayabilmektedir. MBR'lerin organik madde giderim verimleri çok iyi bilinmesine rağmen; azot giderimi ve özellikle simültane nitrifikasyon ve denitrifikasyon kapasitesi bu teknoloji için hala keşfedilmesi gereken bir konudur. Simültane nitrifikasyon ve denitrifikasyon (SNdN), denitrifikasyon potansiyelinin artmasından dolayı yüksek azot giderim verimi açısından avantaj sağlamaktadır. Ancak denitrifikasyon potansiyelinin artmasındaki neden hala bilgi yetersizliği olarak karşımızda yer almaktadır. MBR içinde gerçekleşen biyolojik reaksiyonların

daha iyi anlaşılması, hem optimize tasarım ve enerji kullanımını hem de bu sistemlerin daha hızlı bir şekilde yaygınlaşmasına imkan tanıyacaktır.

MBR'ler, biyolojik proseslerin yanında işletme açısından kısıtlayıcı olan fiziksel özellikleri ile de ön plan çıkmış ve bu konuda geçmişte pek çok araştırma ve çalışma yapılmıştır. Membran gözeneklerinin zaman içinde tıkanmasının, MBR'lerin kullanımı ve yaygınlaşmasında en önemli engel olduğu aşikardır. Pekçok işletme ve fiziksel bazlı olgu geri döndürülemez tıkanma için tanımlanmış olmasına rağmen işletmesel tecrübeler bu olguların membran spesifik olduğu ve bir membran tipinde yaşanan tıkanma sebebinin diğer bir membran tipi için geçerli olamayacağını göstermiştir. Bu nedenle son yıllarda yapılan araştırma ve çalışmalar tıkanmanın minimize edilmesi ve kimyasal rejenarasyon için geçerli olan periyodun kısaltılması için gerekli olan teknikler üzerine yoğunlaşmıştır.

Bu çalışma iki önemli amaç ve bulgu üzerine odaklanmıştır: i.) *MBR'lerin SNdN ile gerçek azot giderim potansiyelinin belirlenmesi ve böylelikle kullanılabilir karbon ve oksijeni içeren sistem denitrifikasyon potansiyelinin belirlenmesi (uzun dönem şartları) ii.) Geri döndürülemez tıkanmanın minimize edilmesi ve önlenmesi için daha önceki yapılan çalışmalarda kullanılan işletme tekniğinden farklı bir tekniğin uygulanması.*

Yukarıda anlatılan amaçlar için evsel bir atıksu arıtma tesisi girişinde mikrofiltrasyon teknolojisi bazlı pilot ölçekli bir MBR sistemi kurulmuştur. Tesis gerçek evsel atıksu ile beslenmiştir. Sistemde gözenek açıklığı 0.4µm olan plaka tip membranlar kullanılmıştır. Tesisin kapasitesi maksimum 6m³/gün olmasına rağmen çalışmada giriş debisi günlük ortalama ve sabit 4m³/gün olarak tespit edilmiştir. Toplam membran alanı 8m² ve işletme akışı sabit 0.5m³/m²-gün (20.8 lt/m²-h) olarak tespit edilmiştir. Membran modülü Japonya orijinli Kubota firmasında temin edilmiştir. Sistem kurulumu önde denitrifikasyonlu azot giderimine yönelik olarak tasarlanmış ve bu konfigürasyon membran tankı muhteviyatının giriş debisinin maksimum 6 katı oranında anoksik tanka geri devrettirilmesine imkan vermektedir. Biyolojik reaksiyonlar için ihtiyaç olan oksijen, kaba habbecikli havalandırma sistemi ile tedarik edilirken söz konusu havalandırma sistemi aynı zamanda membran yüzeyindeki kek film tabakasının temizlenmesi için gerekli olan havayı da tedarik etmiştir. Sistemin EnviroSim Associates Ltd firması tarafından geliştirilen BioWin 2.2 programı ile biyolojik olarak her çalışma periyodu için modellenmesi yapılmıştır. Sistemin uzun dönemli çalışma periyodu için fiziksel modellenmesi Hydromantis Inc. firmasına ait olan GPS-X programı ile gerçekleştirilmiştir. Giriş kolay ayrışabilir KOİ (S_S) ve giriş inert KOİ (S_I) fraksiyonları fiziksel-kimyasal metodlar kullanılarak gerçekleştirilmiştir. Bu yöntemle gerçekleştirilen giriş KOİ fraksiyonasyonu, BOİ analiz kampanyası ile birleştirilmiş ve bu çerçevede zamana karşı BOİ ölçümleri yapılarak giriş ham atıksuyunun biyolojik ayrışabilir fraksiyonunun (S_S+X_S) giriş toplam KOİ'sine oranı belirlenmiştir.

Model geliştirilmesinde aktif çamur model No.1 (ASM1) baz olarak kullanılmıştır. Ölüm -yenilenme mekanizmasının esas olduğu ASM1, UAKM konsantrasyonundaki toplam azalmanın içsel ölüm katsayısı, b_H ile ifade edildiği ve ölen biyokütlenin belli bir fraksiyonunun (f_{EX}) partiküler inert organik madde (X_P) oluşumuna sebebiyet verdiği içsel solunum yaklaşımının esas olduğu hale dönüştürülmüştür. MBR'lerde bakterilerin ölüm fazı sırasında elektron alıcısı olarak nitratı aşırı derecede kullandığı

ve bu tüketimin reaktör içinde azalan çözünmüş oksijen (ÇO) konsantrasyonları ile arttığı birincil yaklaşım olarak getirilebilir. Bu yaklaşımın proses ve modelleme açısından açıklaması, orjinal ASM1 proses matrisine iki yeni proses olan ototrof ve heterotrofların anoksik ortamda nitratı elektron alıcısı olarak kullanıp öldükleri mekanizmanın eklenmesi ile yapılabilir. Ölüm sırasında gerçekleşen çözünmüş inert organik madde (S_{SMP}) oluşumu da orjinal ASM1 proses matrisine eklenmiştir.

Geliştirilen model, ölçülen çıkış KOİ'sini verimli bir şekilde karakterize etmiştir. KOİ cinsinden ortalama organik madde giderim verimi %95 olurken giriş kirlilik yüklerinden bağımsız maksimum %99 oranında KOİ giderim verimi saptanmıştır. Çıkış numunlerinde yapılan BOİ analizlerinde BOİ gözlenmemiştir. Çıkış KOİ'si sadece giriş kökenli inert çözünmüş KOİ (S_I) ve çözünmüş inert organik maddeleri (S_{SMP}) muhteva etmekteydi. Çözünmüş inert organik maddeler (S_{SMP}) I. periyod boyunca ortalama 10mg/l'tnin altında gözlenirken kolay ayrışabilir KOİ bileşeninin (S_S) sistem içinde tamamıyla tüketildiği saptanmıştır.

Giriş KOİ/TKN oranı oldukça yüksek salınım göstererek 5-20 aralığında değişim göstermiştir. Sistem girişindeki bu salınım ve düşük KOİ/TKN oranına rağmen; tesis düşük ÇO konsantrasyonlarında (50. ila 100. işletim günleri arasında) yüksek ve stabil azot giderim performansı göstermiştir. Sistemde düşük ÇO set değerlerinde neredeyse tam toplam azot giderimi gözlemlenmiştir. MBR içindeki ÇO konsantrasyonundaki artış toplam azot giderimi açısından sistem performansını olumsuz yönde etkilemiştir. Örnek olarak, ÇO konsantrasyonunda 0.3 mg/l'den 1.8 mg/l'tye kadar gözlenen artış neredeyse %100 olan toplam azot giderim performansının %70'e düşmesine sebep olmuştur. Düşük KOİ/TKN oranlarının etkileri membran biyoreaktör içinde gözlenen yüksek ÇO konsantrasyonlarında daha da ortaya çıkmaktadır. Yüksek ÇO konsantrasyonlarında (>1.5mg/l) membran tankında ölçülen amonyum azotu değerleri 1mg/l'tnin altında olurken aynı tankta ölçülen nitrat azotu değerleri 8-16 mg/l aralığındaydı. Giriş ortalama TKN ve amonyum azotu değerlerinin sırasıyla 45-60 mg/l't ve 30-45 mg/l't aralığında olduğu dikkate alınırsa; aerobik koşullar altında olan membran tankında gözlenen denitrifikasyon düzeyi yaklaşık olarak 20-30 mg/l't nitrat giderimine tekabül etmektedir. Bu MBR'ler içinde yaklaşık olarak %50-60 nitrat giderimi anlamına gelmektedir. Denitrifikasyon düzeyi, MBR içindeki denitrifikasyon potansiyeli N_{DP} 'ye bağlıdır ki bu da tamamen kullanılabilir KOİ miktarı ile doğrudan ilişkilidir. Ancak MBR sistemlerinde, membran tankı içindeki ÇO konsantrasyonunun denitrifikasyon potansiyeli üzerinde önemli bir etkisinin olduğundan söz edilebilir.

II. ve III. çalışmalardaki giriş KOİ ve amonyak azotu konsantrasyonları pilot tesisin dizaynı için esas alınan değerlerin çok üstündedir. Hal bu iken, çalışma boyunca reaktör içinde rezidü 1.5-3 mg/l't ÇO konsantrasyonları gözlemlenmiştir ki, düşük hava beslemesi ve bakterinin oksijen tüketim hızından dolayı bu değerlerin 1 mg/l't ve/veya altında olması gerekir idi. Bu durum, beslenen oksijenin önemli bir bölümünün kütle transfer kısıtlaması dolayısıyla hücre duvarından flok içine geçemediğini açıkça göstermekte ve doğrulamaktadır. Bu durum hem heterotroflar hem ototroflar için tanımlanan yüksek oksijen yarı doygunluk sabitleri ile açıklanmaktadır.

Membran tank içindeki yüksek biyokütle konsantrasyonu ve popülasyon çeşitliliği, flok büyüklüğü ve yapısının dağılımını beraberinde getirmektedir ki; MBR

sistemlerindeki flokların konvansiyonel sistemlere göre 50-110 µm aralığında olmak üzere daha büyük olduğu tahmin edilmektedir. Biyolojik flokların merkezinde önemli ölçüde anoksik biyokütle fraksiyonunun olduğu bilinmekte ve bu da flok içine oksijen difüzyonunu kısıtlamaktadır. MBR içinde gözlemlenen SNdN düzeyi bu difüzyon limitasyonunun yüksek ÇO konsantrasyonlarında bile etkili olduğunu göstermektedir. Yüksek ÇO konsantrasyonlarında biyokütle içindeki bu fraksiyonun anoksikten aerobik koşullara kaydığı ve oluşan SNdN düzeyini azalttığı sonucuna varılabilir. Membran tank içinde oksijenin flok içine olan difüzyon limitasyonu, siviç fonksiyonlarında yer alan yarı doygunluk sabitlerine spesifik değerlerin verilmesiyle açıklanabilir ki bunlar $K_{OH}=1$ mg/lt, $K_{OA}=1.25$ mg/lt, $K_{NH}=2$ mg/lt ve $K_{NO}=2$ mg/lt olmak üzere önceki aktif çamur modellerine göre oldukça yüksektir. Sistemde 0.5 mg/lt gibi düşük ÇO konsantrasyonlarında bile nitrifikasyon gözlemlenmiş, 0.3 mg/lt daha düşük ÇO konsantrasyonlarında ise kısmi nitrifikasyon olmuştur. MBR sistemlerinde SNdN'a sebep olan faktörler ve parametreler şöyle sıralanabilir; i.) ÇO konsantrasyonu, ii.) Flok büyüklüğü ve yapısı, iii.) Sistem içindeki biyokütle konsantrasyonu ki; son iki faktörün oksijenin membran tank içindeki ortamdan flok içine olan difüzyonunu çok ciddi şekilde etkilemektedir. Reaktör içindeki yüksek biyokütle konsantrasyonu çamur yaşı ile doğrudan ilişkilidir ki, flok morfolojisi ve kültürünün konvansiyonel sistemlerden farklılık arz etmesinde ve dolayısıyla SNdN'nun beklenenden çok fazla olmasında çamur yaşının önemli bir etkisi vardır.

UAKM, AKM, NH_4^+-N , O_2 ve $NO_3^- -N$ parametre profillerinin sırası itibarıyla adımsal uzun dönemli kalibrasyon metodolojisi geliştirilerek sistem kalibrasyonu üçlü iteratif adım ile yapılmıştır. Kalibrasyon parametreleri katı madde balansı ve SNdN üzerinde etkili olan proseslerden seçilmiştir. Kalibre edilen model için detaylı hassasiyet analizi stokiometrik, kinetik parametreler ile giriş ve operasyonel koşullar için yapılmıştır. Hassasiyet analizinin sonuçları modelin heterotrof ve ototrofların oksijen yarı doygunluk sabitleri üzerine oldukça hassas olduğunu göstermiştir. SNdN'nun de heterotrof ve ototrofların anoksik ortamda ölümleri sırasında gerçekleşen ve denitrifikasyonu regüle η_D faktörüne karşı oldukça hassas olduğu tespit edilmiştir.

MBR sisteminde gerçekleşen SNdN düzeyi membran tank içindeki ÇO konsantrasyonuna bağlı olarak değişkenlik göstermektedir ki 0.3-0.6 mg/lt aralığındaki oksijen konsantrasyon değerleri denitrifikasyon potansiyelini ciddi şekilde artırarak 30 mg/lt'ye varan değerlerde nitrat alımına neden olmaktadır. Öte yandan 1.5-3.5 mg/lt aralığındaki oksijen değerleri ise nitrat alımını 10-20 mg/lt düzeylerine düşürmektedir. Sonuç olarak söylenebilir ki; MBR sistemlerinde SNdN yoluyla ve 1.5-2.5 mg/lt ÇO aralıklarında minimum 10-15 mg/lt nitrat alımı gerçekleşebilecektir. Denitrifikasyon stokiometrisi ışığında, heterotrofların ve ototrofların anoksik olarak ölümlerinin SNdN üzerinde ciddi bir etkisi olduğu saptanmıştır ki bu da MBR sistemlerinin ağırlıklı olarak içsel solunum fazında çalıştığı tezini doğrulamaktadır. Membran tank içindeki ÇO konsantrasyonu ile gerçekleşen SNdN arasında bir denge vardır ki, kontrol edilebildiği takdirde, membran biyoreaktör sistemlerini 0.3-0.8 mg/lt gibi düşük ÇO aralığında sürekli çalıştırarak V_D/V_T oranı da 0.10'a kadar düşük önde denitrifikasyon sistemlerinde 15 mg/lt çıkış toplam azot limiti sağlanabilecektir. Deşarj standardı olarak tanımlanabilecek 10-15 mg/lt toplam azot konsantrasyonu, evsel atıksu için çalıştırılan membran biyoreaktör sistemlerinde anoksik tank olmadan AKM konsantrasyonu ve ÇO otomasyonu altında kontrol edilecek SNdN ile sağlanabilir.

Anoksik tank olmadan tasarlanacak ve işletilecek MBR sistemlerinde çıkış toplam azot limitlerinin sağlanabilmesi için tavsiye edilen AKM konsantrasyon aralığı 15,000 ila 20,000 mg/l arasındadır. Bu aralığın tanımlanmasında iki önemli faktör ön plana çıkmaktadır, i.) *AKM konsantrasyonunun ve dolayısıyla çamur yaşının nitrifikasyonu kütle transfer kısıtlaması sonucu inhibe etmeyeceği ve yeterli amonyak oksidasyonu sağlayabileceği değerler*, ii.) *AKM konsantrasyonunun ve dolayısıyla çamur yaşının kütle transfer kısıtlaması ile ve denitrifikasyon için bir anoksik tank olmadan gelişmiş S_ND_N'u tetikleyeceği değerler*.

Pilot ölçekli MBR daha önce yapılmış olan çalışmalardakinin aksine değişik bir işletme mantığı ile çalıştırılmıştır. Aktif çamur plaka tip membranlardan cazibe ile filtre edilmiştir. Aktif çamur, membranlardan sürekli olarak 12 saat boyunca süzülüş ve bu sürenin sonunda dinlendirme olarak adlandırılan adımda 10 dak boyunca membran yüzeyi yüksek hava ile yıkanarak kek tabakasının oluşması önlenmeye çalışılmıştır ki bu döngü uygulanan işletme mantığının temelini oluşturmaktadır. İşletme verilerine göre; adapte edilen bu değişik işletme mantığı çerçevesinde sistemde sorunsuz olarak 310 gün (Periyod I) boyunca sürekli olarak işletilmiştir. Bu değişik çalışma modundaki sorunsuz işletmenin, kullanılan kaba habbecikli havalandırma sisteminin membran yüzeyinden kek tabakasını sıyırmasındaki verimliliği ile ilişkilendirilmiştir. Rezistans modeli, dinamik olarak fiziksel parametrelerin değiştirilip ölçüm sonuçları ile uyumlu hale getirilmesi yöntemine göre dinamik olarak kalibre edilmiştir. Sıcaklığın transmembran basıncı ve hidrolik geçirgenlik üzerinde çok önemli bir etkisinin olduğu açıktır. Ancak rezistans modeli, sıcaklığın etkisini dikkate alamadığından, sıcaklık ile ilgili gözlemlenen salınımlar, maksimum tıkanma rezistansı ve tıkanma hızı parametrelerinin değiştirilerek transmembran basıncı ve hidrolik geçirgenlik profilleri ile uyumlu hale getirilmesi ile kalibre edilebilmiştir. Fiziksel model sonuçları ölçüm sonuçları ile örtüşecek şekilde başarı ile kalibre edilmiştir. Membran yüzeyinden kek film tabakasının temizlenmesinde kullanılan havalandırma sisteminin bu işlem için çok önemli bir etkisinin olduğu ve dolayısıyla tıkanmanın önüne geçilmesi ve/veya geciktirilmesinde çok önemli bir faktör olduğu tespit edilmiştir. Membran biyoreaktör sistemleri için sorunsuz ve verimli çalışan bir ön arıtmanın kurulması zaruridir. 0.75-1 mm aralığında ızgara sistemini müteakip yapılacak bir kum ve yağ tutucu havuzu, membranların inorganik yağ ve katı maddeler sonucunda oluşabilecek tıkanmaları engelleyebilecektir.

Bu çalışmada nitrifikasyon bakterilerinin kantitatif tespiti yapılmıştır. Nitrifikasyon bakterilerinin baskınlığı toplam bakteri popülasyonu içerisinde %13 olarak tespit edilmiştir. Bu sonuç, daha MBR çalışmalarında yapılan relatif basınçlı çalışmalarına göre daha yüksektir ki bunun nedeni söz konusu çalışmaların daha yüksek çamur yaşlarında yapılması ile ilişkilendirilmiştir. Membranların tıkanma mekanizmasının daha iyi anlaşılabilmesi ve aydınlatılabilmesi için filamentli bakteriler üzerinde kantitatif ve kalitatif çalışmaların yapılması gerekmektedir. Bunun ötesinde, nitrifikasyon bakterilerinin varlığı ve performansı ile membran biyoreaktörlerin işletme koşulları ilişkilendirilerek ilave çalışmalar yapılması MBR'lerde çevresel faktörlerden etkilenmeyen nitrifikasyon prosesinin daha iyi anlaşılabilmesini sağlayacaktır.

1 INTRODUCTION

1.1 Significance of the Study

Global population increase in the world is resulting in a growing challenge for the protection of natural resources. This is forcing the governments to set more stringent regulations on the level of wastewater treatment which is discharged to ambient water. Furthermore two critical criterias are coming forward in wastewater treatment technologies; i.) technology that requires minimum amount of land area, ii.) technology that produces the least amount of sludge. In most countries, the value of available land is increasing every year and due to macro economical trends the governments as well as private sector are willing to invest in housing, industrialization,..etc type of projects in valuable lands. However when it comes to building wastewater treatment plants, minimum land area with the most awkward place is granted to contractors and municipalities. Mostly, it is very challenging to fit a layout for wastewater treatment plants in the granted areas with conventional treatment technologies. Due to these reasons, the research and development for full scale implementation of new technologies that require the least amount of area has increased over the past 5-10 years. Handling and disposal of the sludge arising from wastewater treatment plants whether it is chemical and/or biological is also another global growing problem. The problems and nuisance in handling and disposal of sludge increases with increasing amounts. Therefore technologies that produce the least amount of sludge are favored and will be favored in the future. The combination of these two criterias will be the governing factors in the shaping trend of new technologies for the future.

Biological treatment of domestic sewage for carbon and nutrient removal is still considered to be the most advantageous technique applied all over the world. Modifications of biological treatment techniques are still being applied for optimization purposes. However these modifications are more or less the same in a

conventional biological scheme as most of them concentrate specifically on nitrogen and phosphorus removal. The amount of sludge production and footprint are nearly the same.

The development of membranes and the combination of membrane technology with bioreactors have led to a new focus on wastewater treatment. The application of membranes contribute to very compact wastewater treatment systems with an excellent effluent quality. Membrane bioreactor processes are well suited for applications that require small footprint reactors. The production of sludge is also very much less compared to conventional biological schemes.

Up to this date MBR systems have mostly been used to treat industrial wastewater, domestic wastewater and specific municipal wastewater where a small footprint, water reuse or stringent discharge standards were required. It is expected that MBR systems will increase in capacity and broaden in application area due to future more stringent regulations and water reuse initiatives. Full scale commercial applications of MBR technology dated back to 1991. In the early 1990s, MBR installations were mostly constructed in external configurations where the membrane modules were outside the bioreactor and biomass was recirculated through a filtration loop. This limited wider application in treatment of municipal wastewater because of high power consumption. After the mid 1990s with the development of submerged membrane modules, MBR applications in municipal wastewater extended widely. In the past 10 years, MBR technology has gained considerable increase both in municipal and industrial wastewater treatment.

For municipal wastewater treatment, MBR technology becomes economically attractive when a compact technology is required because of lack of space in urban areas or when high effluent quality is required for water reuse or as pretreatment for nanofiltration or reverse osmosis processes. The continued push towards stricter discharge standards increased requirement for water reuse and greater than before urbanization along with land limitations will further promote the use of MBRs for even larger municipal applications. The challenges will center on scale-up ease of operation, simplified membrane cleaning and replacement strategies and peak flow management. In addition to municipal wastewater treatment MBR technology is already gaining interest in industrial wastewater treatment which are highly concentrated and low in flow. Specific areas of application for industrial use include

wastewater from food processing industries, pharmaceutical industries, organic chemical industries and landfill leachates.

MBR technology is also used for the removal of nitrate from drinking water. MBR systems have many advantages over traditional biological denitrification. One of the major advantage is that almost all of the microorganisms as well as some dissolved organic matter can be rejected by the membrane processes which replaces many post and tertiary treatment processes in conventional biological schemes. Many studies have shown that both the organic and nitrogen removal capacity of the MBR technology is considerably higher than conventional biological treatment processes. The high treatment capability of this technology even becomes more interesting when the operational factors such as temperature, dissolved oxygen...etc are taken into account.

The research and commercial application of the membrane bioreactor technology are advancing rapidly around the world both for municipal and industrial wastewater treatment. The primary research focus is on fouling, nutrient removal capability, chemical cleaning, microbial characterization/morphology and optimization of operational performance and energy consumption. In recent years, more publications and research have been conducted on the fouling aspects of the membranes and how to minimize it. Although more research is being conducted on MBRs, published information to date has been in the form of lab or pilot scale studies investigating primarily basic treatment efficiencies for short term operation periods. Full scale studies spanning long term operation have been limited and should be given more attention in the future.

MBR technology is facing some research and development challenges and this increases the significance of future research on this technology. Among these challenges, membrane fouling is one of the most serious problems that is delaying the faster commercialization of MBR technology where on the other hand a better understanding of the nutrient removal capability and especially simultaneous nitrification and denitrification will lead to optimized, cost effective systems with energy savings.

1.2 Objectives

The general objectives of the activated sludge research is to understand and master the biological processes and interactions in full scale activated sludge systems. This requires intensive and extensive research of biological processes occurring in bench or pilot scale systems of the same technology to be investigated. This also applies for physical characteristics and behaviour of the systems including membranes. This study focuses on the following major goals;

- i. Detailed assessment of the nitrogen removal capability of MBR through simultaneous nitrification and denitrification with the affect of dissolved oxygen and temperature and mechanistic explanation of the interactions with a developed activated sludge model
- ii. Detailed assessment of the nitrification capability of the MBR with very high solids retention time against low dissolved oxygen levels and temperature and mechanistic explanation of the interactions with a developed activated sludge model
- iii. The physical behaviour of the membranes towards a different operational mode to minimize the time elapsed for fouling and to increase the time period required for chemical regeneration.
- iv. Better understanding of the microbial culture and morphology in membrane bioreactor systems.

For the purpose of mechanistic explanation of the organics and nitrogen removal capability of MBR through simultaenous nitrification and denitrification a new model will be developed by incorporating new processes and parameters to the original activated sludge model No.1 (ASM1). The model will also be altered from the death regeneration approach to the endogenous decay due to the approach of the MBR systems being decay dominant. The developed model will be longterm dynamically calibrated against the measured data by an adopted calibration methodology. The other objective of the study on biological modelling of membrane bioreactor systems is to investigate the sensitivity of the developed model. Special attention will be given to the effect of dissolved oxygen and temprature on biological processes and especially on nitrification and denitrification. A reknown software will be used for the biological modelling purposes.

It is also the intention of this study to thoroughly investigate the physical characteristics of the membranes and fouling against a different adopted operational mode. For this purpose the setup and the adopted operational mode will be modelled in another software program using the in series resistance model. One of the major bottlenecks in calibration of the in series resistance model is the difficulty in incorporating the affect of temperature. Modelwise it is not possible to include this affect into the model. Some of the previous researches explained this affect empirically. The intention of this study is to explain the temperature affect through calibration of the membrane and cake parameters to fit the measured transmembrane pressure and hydraulic permeability data. This includes the division of certain operational periods into segments for the calibration methodology. The major goal in physical model calibration is to prove that flatsheet membrane bioreactors can also be operated with the new adopted operational mode rather than the one used in previous researches and full scale plants. The factors that enable this operational mode and the reasons will also be discussed.

Furthermore, microbiological investigations using the FISH technique will also be conducted. This is also important in understanding the biological conversions and reactions in MBR systems. It is obvious that the high sludge age will have an affect on the bacterial population. The affect of the existence of filamentous bacteria in membrane bioreactor systems is also an important parameter in this research.

1.3 Scope of the Thesis

This thesis is composed of 6 chapters including discussions and conclusions. The general scope and content of each chapter is summarized as follows:

Chapter 1: Introduction

In this chapter, the past and future significance of membrane bioreactor systems is described and the important aspects of pursuing this study is explained in detail. A brief historical background on the development of MBR technology is given to focus on the increasing importance of this technology. The objectives, goals and targets of the research is given.

Chapter 2: Experience with Membrane Processes and Membrane Bioreactors

The fundamentals of membrane processes and the physical characteristics of different type of membranes along with the modules that are used in membrane bioreactor technology are explained in detail. The basic theory of flux, fouling and transmembrane pressure are described to transfer the basics of membrane filtration. Previous biological modelling attempts both for carbon and nitrogen removal are discussed with specific emphasis on nutrient removal. The performance of MBRs from previous researches and studies as well as full scale applications are discussed.

Chapter 3: Materials and Methods

The pilot plant setup, the characteristics of the membrane module, the process flow diagram, system description and specifications and the P&ID are explained in detail. The instruments used to record field data are also described in detail. Experimental program & testing procedure along with measurement and analysis procedure are described. The softwares that will be used in biological and physical modelling and calibration of the pilot scale membrane bioreactor are presented in detail with their references.

Chapter 4: Modelling of Membrane Bioreactors

In this chapter, the basis of wastewater characterization and the processes to be used in the modelling of the pilot scale membrane bioreactor system are described in detail. The basics and description of the in series resistance model is presented with the formulation that is used in the software. The development of the new adopted biological model for the MBR process and the explanations are given in detail along with the new process matrix to be used in the longterm dynamic modelling calibration for the pilot scale membrane reactor. The dynamic calibration methodology and the sensitivity analysis results for pseudo-steady state analysis of the adopted are given. Mass balance driven stoichiometric equations for the design of membrane bioreactor systems are also presented. The configuration of the pilot scale membrane bioreactor for biological and physical modelling are explained in detail for the two different softwares.

Chapter 5: Experimental Results and Evaluation

The biological and physical modelling results of the longterm dynamic simulations are discussed in detail. Specific emphasis is given to the results and affect of temperature and dissolved oxygen on simultaneous nitrification and denitrification. Short term magnified results with respect to changing dissolved oxygen and temperature on both nitrification and denitrification are evaluated. The temperature affect on transmembrane pressure is illustrated by calibration of the physical membrane parameters. The results of the FISH studies are illustrated.

Chapter 6: Discussion and Conclusions

Concluding remarks along with recommendations on the design of membrane bioreactors systems are discussed. The areas for further research and development are pointed out. The recommendations on the physical operational aspects of flatsheet membrane bioreactors and the ways of minimizing fouling are discussed. The future need for the research on filamentous growth kinetics and the possible effect on the level of simultaneous nitrification and denitrification are evaluated.

2 EXPERIENCE WITH MEMBRANE PROCESSES and MEMBRANE BIOREACTORS

Bioreactors used for the treatment of domestic and industrial wastewater are considered in two major categories where the governing factor is the way how the microorganisms grow in them;

- i. Suspended in the liquid where the treatment is taking place,
- ii. Attached to an inert material or a solid support

In suspended growth cultures the microorganisms are kept in suspension by mixing or aeration and solids-liquid separation takes place by a physical unit operation like sedimentation where the biomass is removed from the treated effluent. Unlike suspended growth systems, attached growth cultures grow as a biofilm forming on a solid support. Media sloughing is encountered where the microorganisms detach from the support and a physical solids-liquid separation is also necessary for attached growth systems prior to being discharged to the receiving body.

Suspended growth reactors can be sub-categorized in two types of tanks;

1. Completely stirred tank reactor (CFSTR),
2. Plug flow tank reactor (PFR)

Completely stirred tanks have constant volume and the content of the reactor is mixed so that the concentration of the constituents are uniform throughout the tank and equal to the outlet concentration of the reactor. The uniform conditions keep the microorganisms in a steady physiological state. The mixing is homogenous and instantaneous so that the constituents fed to the tank is evenly dispersed throughout the reactor.

This uniformity of concentration makes analysis of the completely mixed reactors comparatively simple. Completely mixed reactors are commonly used for aerobic or anaerobic treatment of low to high strength domestic and industrial wastes.

In plugflow reactors, the bulk liquid move through the reactor in the same order that they enter without any backmixing. No mixing is assumed to occur in the longitudinal path of the fluid. These type of reactors cause the biomass to go through cycles of physiological change that can have strong impact on the microbial community. A concentration gradient is formed along the longitudinal path of the reactor in a tendency to decrease towards the outlet of the plug flow tank. The concentration gradient is also valid for the oxygen being introduced into the tank if no external adjustment like tapered aeration is taking place. Ideal plug flow reactors are difficult to establish in practice due to the fact that mixing in the direction of flow can not be prevented, therefore plug flow conditions are approximated by a number of completely stirred tanks connected in series. Concentrations of substrates are highest at the entrance. This tends to increase the oxygenation rates quite high, therefore sufficient oxygen must be supplied to these points to avoid substrate and deficient oxygen inhibition. If the design of the system is done taking these into account, the plugflow reactors will then offer a high degree of removal for the contaminants especially ammonium and trace organics.

There are three types of attached growth reactors;

1. Packed towers or beds,
2. Rotating discs,
3. Fluidized beds

Attached growth reactors are also considered as “biofilm reactors” where the microorganisms are attached to the surface of the media in which the biofilm is established. The electron donor, electron acceptor and all the other nutrients necessary for biochemical reactions are transported through the biofilm by diffusional mechanisms. It is the combined effects of diffusional transport and the biochemical reactions occurring in the biofilm which makes this process quite complicated and complex when compared to suspended growth systems.

The most common and popular biofilm reactor is the packed bed reactor in which the biofilm and microorganisms are attached to a stationary surface like large rocks or plastic media. Trickling filters and biological towers are examples to such packed bed reactors. Packed beds are usually operated in downflow scheme.

Rotating biological contactors is another form of biofilm reactors. The plastic media or the disk itself is attached to a rotating shaft where it is rotated continuously. The portion of the rotating disc in contact with the air, absorbs oxygen from the atmosphere where as; in the submerged portion the biochemical reactions take place and the contaminants are oxidized. The wastewater enters the reactor from one side and leaves from the other side travelling in a perpendicular route with respect to the rotating discs.

In fluidized bed reactors, the microorganism are kept in suspension with the attachment to the biofilm carriers by the upward flow rate of the fluid to be treated. The biofilm carrier used for this purpose can be granular activated carbon, plastic solids, diatomaceous earth or any other kind of small solid particles that are resistant to abrasive environment. The upward velocity of the fluid must be sufficient to maintain that the carriers are kept in suspension. This mainly depends on the density of the particles relative to that of the water, amount of biomass attached and the shape and size of the carrier. One major disadvantage of the fluidized bed reactors is the control of fluidization. The upward flow movement must be enough for fluidization however must not be so high to avoid any carrier washout from the reactor.

Following the discovery of the activated sludge process by Ardenn and Lockett (1914), various types of bioreactors have been extensively used in the treatment of domestic and industrial wastes. Still the conventional process schemes coupled with both suspended and attached growth reactors offer the most reliable and cost effective solutions for pollution control. However the invention of “*membranes*” and the new findings enabling them to be coupled with suspended or attached growth bioreactors opens a new era in the field of wastewater treatment for the many decades that lie ahead of us.

2.1 Membrane Definition and Basics

Membranes are natural or artificial, two dimensional objects that separate fluids with different compositions from each other (Stauder, 1992). The transport of components through the membranes is therefore, selective. This can be defined by the general term, permeation. A membrane can be defined as a material through which one type of substance can pass more readily than others, thus presenting the basis of a

separation process. The membrane acts to reject the pollutants which can be both suspended or dissolved and thus allow the treated water to flow through it.

Consequently, membranes can be considered as a physical barrier in which all parts of the suspended solids that are larger than the cutoff size of the membrane are retained. In conventional activated sludge systems where the final clarifiers are used for physical separation, only the part of the sludge that form floc and settles can be retained. Therefore it can be stated that the physical separation process using membranes is independent of the sludge settling quality of the activated sludge.

2.2 Membrane Structure and Categorization

The range of available membranes is very diverse. They vary widely both in chemical composition and physical structure. Commercial membranes in the market can be categorized in two different aspects:

- Mechanism of separation,
- Material composition

Membrane materials can be either *dense* or *porous*. The type of separation mechanism being achieved is directly related to the membrane structure being either dense or porous. Separation by dense membranes relies to some extent on physicochemical interactions between the permeating components and the membrane material and it can be stated that it has the highest selectivity in terms of the separation process. Reverse osmosis and hyperfiltration are the two most important processes for separation with dense material and thus able to separate ions from water. On the other hand, porous materials achieve separation mechanically by sieving or in other words size exclusion where the rejected components may be either dissolved or suspended depending on its relative size relative to that of the pore. Separation with porous membrane materials is close to conventional filtration processes by nature due to separation being achieved by a driving force which is exerted either mechanically or hydrostatically. Table 2.1 illustrates a profound categorization of the membranes with respect to the separation process (Stephenson et al., 2000).

Table 2.1: Dense and porous membranes for water and wastewater treatment

Dense	Porous
<i>Membrane Separation Processes</i>	
<p><i>Reverse Osmosis (RO)</i> Separation achieved by virtue of differing solubility and diffusion rates of water and solutes in water</p> <p><i>Electrodialysis</i> Separation achieved by virtue of differing ionic size, charge and charge density of solute ions using ion exchange membranes</p> <p><i>Pervaporation</i> Same mechanism as RO but with the (volatile) solute partially vaporised in the membrane by partially vacuumating the permeate.</p> <p><i>Nanofiltration (NF)</i> Formerly called the leaky reverse osmosis. Separation achieved through combination of charge rejection, solubility –diffusion and sieving through micropores (<2 nm)</p>	<p><i>Ultrafiltration (UF)</i> Separation by sieving through mesopores (2-50 nm)</p> <p><i>Microfiltration (MF)</i> Separation of suspended solids from water by sieving through macropores (>50nm)</p> <p><i>Gas Transfer (GT)</i> Gas transferred under a partial pressure gradient into or out of water in molecular form.</p>
<i>Membrane Materials</i>	
Limited to polymeric materials	Both polymeric and inorganic materials available

Membranes are also categorised according to the material composition which is either organic(polymeric) or inorganic(ceramic or metallic) or on the basis of their physical structure in other words their morphology. The membrane morphology is dependent on the exact nature of the material and/or the way it is processed. The predominant type of membranes used today are organic polymer which is also the type used in membrane bioreactors. This membrane material can be adopted to most requirements by easy modifications in the chemical composition.

Different membrane structures can be created through different processing methods for the organic type of membranes. The classification can be made according to the

homogeneity of the pore structure along the membrane cross section as; symmetric, asymmetric and composite membranes. These types are represented in Figure 2.1. (Ripperger, 1992).

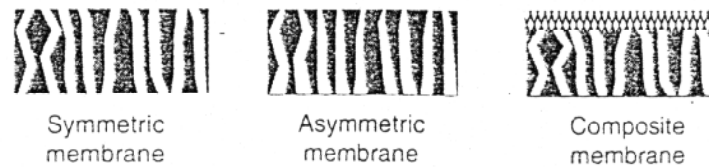


Figure 2.1: Schematic representation of various membrane structures

Symmetric membranes have a homogenous pore diameter and/or pore cross section across the thickness of the membrane. For asymmetric membranes, the pore structure is distributed unevenly via the cross section of the membrane. The small pores turn to the suspension to be filtered and enlarge to the permeate side. Composite membranes consist of at least two layers, which differ in structure. In most cases, the upper layer takes on the separation process and the lower layer the supporting function.

The surface structure of a membrane decisively influences its selectivity and permeability. The inner construction determines the mechanical behaviour, in particular, the compressive strength. During membrane production, attempts are made to optimize the surface by selection of suitable materials and process variables with regard to the maximum permeability and sufficient selectivity.

Polymeric microporous membranes are mainly produced by phase inversion. A polymeric solution is cast to produce a thin layer of material. The porous side of the membrane is produced by precipitation of the polymer in water, a process called as gelation. The selective side of the membrane is produced by evaporation of the polymer solvent to produce a skin of much lower permeability resulting in an anisotropic membrane structure. The membranes are categorized by their material type in Table 2.2 (Stephenson et al., 2000).

Table 2.2: Membrane materials by type

<i>Membrane</i>	<i>Manufacturing Procedure</i>	<i>Structure</i>	<i>Applications</i>
Ceramic	Pressing, sintering of fine powders	0.1-10 μ m pores	MF, gas separation, separation of isotopes
Stretched	Stretching of partly crystalline foil	0.1-1 μ m pores	Filtering of aggressive media, sterile filtration, medical technology
Etched polymers	Radiation followed by acid etching	0.5-10 μ m cylindrical pores	Analytical and medical chemistry, sterile filtration
Supported liquid	Formation of liquid film in inert polymer matrix	Liquid filled porous matrix	Gas separations, carrier mediated transport
Symmetric microporous	Phase inversion reaction	0.05-5 μ m pores	Sterile filtration, dialysis, membrane distillation
Integral asymmetric microporous	Phase inversion reaction followed by evaporation	1-10nm pores at membrane surface	UF, NF, gas separation, pervaporation
Composite asymmetric microporous	Application of thin film to microporous membrane	1-5nm pores at membrane surface	UF, NF, gas separation, pervaporation
Ion exchange	Functionalization of polymer material	Matrix of positive and negative charges	ED

The phase inversion process involves dissolving the polymer in a suitable solvent and then casting it in a film, less than 1 mm thick, and then adding another liquid to precipitate the polymer. The membrane skins forms at the interface between the solvent and the second liquid in which the membrane is only sparingly soluble. Careful choice of the solvent and non-solvent liquids, concentration of the polymer, temperature and reaction times can produce the membrane with the desired characteristics. The polymeric membranes produced by phase inversion is given in Table 2.3 according to their base polymer material (Judd and Jefferson, 2003).

Table 2.3: Phase inversion polymeric membrane materials

<i>Polymer^a</i>	<i>Advantages</i>	<i>Disadvantages</i>	<i>Process</i>
CA	Chlorine resistant, inexpensive, more fouling resistant than PA	Susceptible to alkaline hydrolysis at pH>6 Susceptible to biodegradation, limited thermal and chemical stability, limited permselectivity(%95 rejection), slightly lower permeability	RO, NF, UF
PA	More allround stability than CA, more permselectivity than CA	Very limited chlorine tolerance(<0.1 mg/l)	RO, NF
PAN	High resistance to hydrolysis, high resistance to oxidation	Hydrophobic, requires copolymers to make less brittle	UF, RO substr.
PSU, PES	Very good allround stability, mechanically strong	Hydrophobic	UF, RO substr.
PVDF, PTFE	Extremely high chemical stability, high thermal stability	Highly hydrophobic, limited mechanical stability, limited intrinsic permability, expensive	UF, MF
PEI	High chemical stability, very high thermal stability, mechanically strong	Hydrophobic, less solvent resistant than PVDF, poorer alkaline stability than PSU or PAN	UF, RO Substr.
PP	Inexpensive	Hydrophobic	UF, MF

^a CA: Cellulose acetate; PA : Polyamide;

PAN: Polyacrylonitrile; PSU: Polysulphone; PES: Polyethersulphone; PVDF: Polyvinylidene fluoride; PTFE: Polytetrafluoroethane; PEI: Polyetherimide; PP: Polypropylene

Microfiltration is the most widely used separation process in membrane bioreactors due to their ability to achieve high degree of solids-liquid separation and produce a bacteria, virus free permeate. The cutoffs of the porous membranes used for this purpose are normally between 0.1 and 10 μm . However membranes with cutoff sizes between 0.02 and 20 μm are also used in microfiltration depending on the size

of the solids to be separated and the final aim of the membrane process. The particle rejection is mainly based on sieve mechanism and the particles are restrained on the membrane surface due to their size. The filtration spectrum showing the rejection capability of different membrane separation processes can be seen in Figure 2.2. (courtesy of Osmonics, Inc)

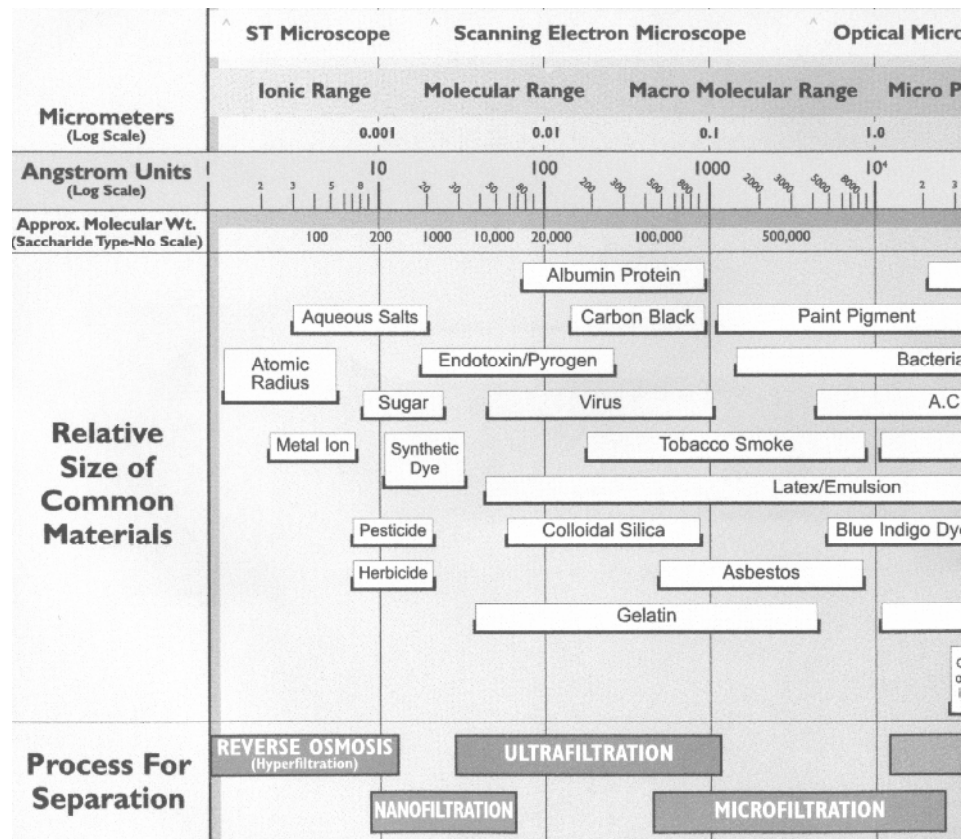


Figure 2.2: The filtration spectrum for different membrane separation processes

2.3 Membrane Configuration

A membrane sheet will only be useful when coupled with a structural base allowing the water to pass through it. The configuration of the membrane, geometry of the base structure, the way it is mounted and oriented in relation to the water flow is very important in the process performance. Other aspects on process performance include the rigidness of the base structure and the method of which the membrane sheet is attached to the surface. The membrane sheets or the hollow fibres housed on to the base structure form a membrane module, which can be defined as the “hydraulic element” that allows the water to pass to the permeate line. Membrane modules are the key elements of membrane bioreactors as the performance is directly related to the module having the following characteristics: (Stephenson et al., 2000).

- i. A high membrane area to module bulk volume ratio,
- ii. A high degree of turbulence for mass transfer promotion on the feed side,
- iii. A low energy expenditure per unit product water volume,
- iv. A low cost per membrane unit area,
- v. A design that facilitates cleaning,
- vi. A design that permits modularisation

Some of the above characteristics are mutually exclusive. For example, promoting turbulence results in an increase in the energy expenditure. Direct mechanical cleaning of the membrane will only be possible on comparatively low area:volume units where the membrane will be accessible. These kind of module designs increase the total cost per unit membrane area. It is not possible to produce a high membrane area to module bulk volume ratio without producing a unit having narrow feed channels, which will adversely affect turbulence promotion. There are mainly three types of module configurations employed for the membrane bioreactors :

- Plated filter cartridges
- Tubular models (non-woven)
- Spiral wound
- Plate modules or more widely used name as flat sheets & frame, (non-woven)
- Hollow fiber or capillary modules (woven)

The plated filter cartridge used extensively in microfiltration has a very low cost and is designed as a disposable unit in the purification or polishing of clean waters. It has a high area to volume ratio and the construction is made in such a way that the loss of filter area at the folds is avoided by using a suitably designed membrane separator. This type of configuration is suitable for both organic polymeric media and porous metal media, the latter having a minimum pore size of 2 μm .

Tubular modules consist of membrane tubings with an internal diameter of approximately 4-24 mm. The tubes are normally not pressure proof so an additional supporting tube is required to handle the transmembrane pressure. The suspension moves through the membrane tubes with a specific velocity and generated the required crossflow. The filtration occurs from the inside outwards and the permeate is collected in outer frame tube. Several single tubular membranes can be combined

in a frame tube to create a multi tubular module. They provide a modest surface area to volume ratio, and thus the highest cost per unit area of all cylindrical membrane geometries, but also provide potentially the greatest turbulence promotion and the best access to the membrane surface. A typical tubular membrane module can be seen in Figure 2.3.(courtesy of *X-Flow*)



Figure 2.3: Tubular MF(microfiltration module)

Commercially available membranes are usually multi channel with mechanical support required for the polymeric tubes.

Spirally wound membranes have the advantage of simple and robust construction whilst providing a reasonable membrane area per unit volume and find use in reverse osmosis and nanofiltration plant. The membrane element comprises two membranes attached to each other forming a rectangular bag sealed on three sides. The membrane element is rolled up to produce a spiral which forms a cylindrical shape, one end of which is presented to the feedwater. The fluid path is equal to the length of the cylinder and spacers are used to maintain separation of membrane leaves both in retentate and in the permeate channels. A typical schematic of the spirally wound membrane can be seen in Figure 2.4. (courtesy *Ionics*)

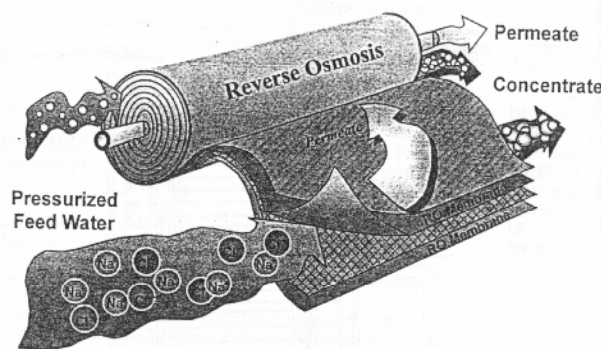


Figure 2.4: Schematic of spirally wound membrane

Plate modules are made up of flat sheet membranes arranged in parallel. Usually the flat sheet membranes are placed 5-8 mm apart from each other where they are located in a casing. The membrane case incorporates multiple cartridges which are connected to a manifold with tubes. The membranes are normally raised on both sides on a support plate with drainage. The membranes are flooded by the suspension and the filtration occurs through a connection tube towards the collector. The plate modules are mostly run on ultrafiltration/microfiltration separation processes which rely on low pressure operation. An example is the Kubota membrane, employed in a membrane bioreactor. This membrane operates at transmembrane pressures as low as 50 mbar and thus does not require robust case construction like a pressure sealed unit. The membrane sheets are ultrasonically welded on a plastic frame. Thickness of the plastic frames are usually 6mm and they have a nominal pore size of 0.4 μm . A flat felt layer either side of the base plate which acts as a spacer between the membrane sheet and the flat support. Flat sheet membranes and the module can be seen in Figure 2.5.(courtesy *Kubota*)

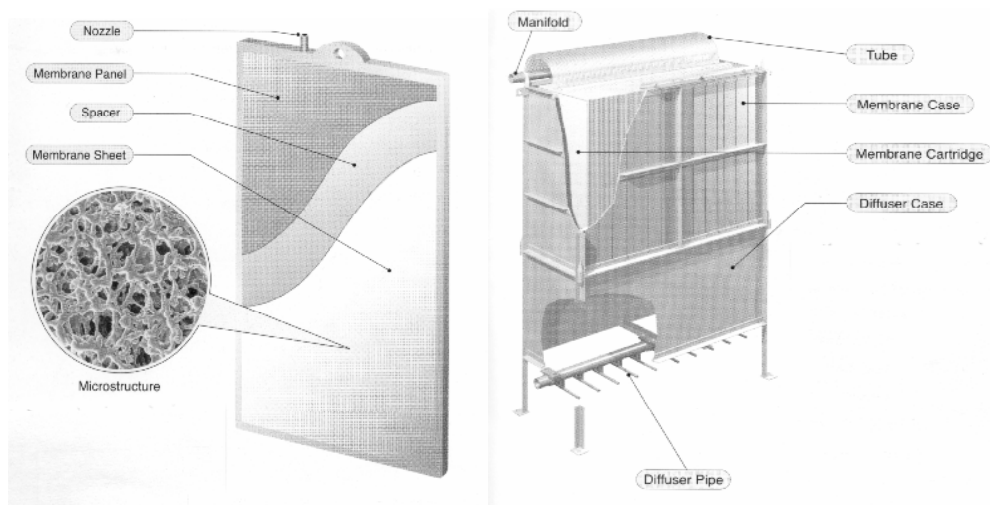


Figure 2.5: Flat sheet membrane structure and a single module

The base section of the module houses the air diffusers and upon which the top sections sit. A cleaning mechanism of the air diffuser is incorporated into the base section. When more than one membrane unit is installed in a membrane bioreactor tank the cleaning valve and the discharge port is common along the installed units. As mentioned previously flat sheet membranes are also referred to as the non-woven membranes. The surface structure of a 3 and 5 μm non-woven membrane photographed by a scanning electron microscope can be seen in Figure 2.6.

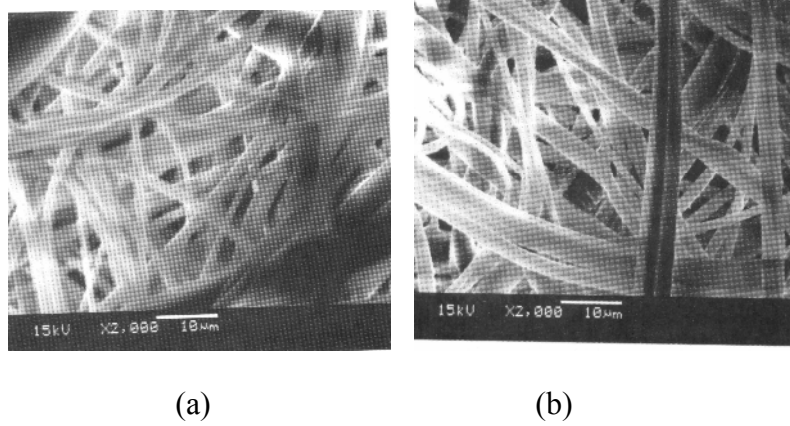


Figure 2.6: (a) 3 μm non-woven membrane surface (b) 5 μm non-woven membrane surface

Hollow fiber modules consist of self supporting membrane tubing with an internal diameter of 0.5 to 4 mm. For capillary modules, even finer membrane tubing with internal diameters of less than 0.5 mm is used. The thin membrane tubing is normally pressure proof and self supporting so additional supporting layers are not needed. In case of microfiltration the filtration occurs from the outside inwards since particles would clog up the thin membrane tubing in the opposite case. To create a module several fibers are combined to a bundle and stuck into permeate collectors at both ends. Hollow fiber membranes provide the highest membrane area per unit volume and are usually operated out to in with reference to water permeation however they require very frequent backwashing which deteriorates the pores on the fibers. As the pores of the membranes become larger and larger over the years there is a risk of bacteria and virus breakthrough after each backpulsing. The hollow fiber membrane module can be seen in Figure 2.7. (courtesy Zenon)



Figure 2.7: Hollow fiber membrane module

The surface structure of a 0.4 μm woven membrane can be seen in Figure 2.8.

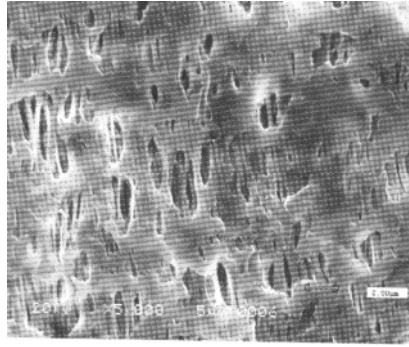


Figure 2.8: 0.4 μ m woven membrane surface structure

The development of membrane materials and module configurations for membrane bioreactors has been governed by the need to suppress membrane fouling and/or decrease the problems associated with it. Various membrane configurations are shown in Table 2.4 (Stephenson et al., 2000).

2.4 Commercial Submerged Membrane Technologies

Although there are a number of reknown membrane bioreactor system suppliers and integrators, they are widely based on either (1) *flat sheet membrane* configuration such as the *Kubota(Japan)*, *MMF(Germany)* products or (2) *the hollow fiber configuration* from *Zenon* (Canada). There is still a continuing debate over which of the two technologies is better for wastewater treatment. The membrane bioreactors that use the flat sheet technology are simple in operation and they run at higher permeabilities. Flat sheet technology offers the advantage of extracting the permeate from the module by hydrostatic pressure without the necessity of having a suction pump. This enables in maintaining a sustainable flux for the duration of the operation before the necessity for a chemical cleaning due to fouling. Flat sheet membranes also do not require any backflushing. Both flat sheet and hollow fiber technologies are able to sustain reasonable operational fluxes by employing relaxation, which means air scouring over the membrane surface for a period of time by closing the permeate valve. However, hollow fiber systems also require backpulsing along with air scouring which employs a complicated relaxation and backflushing protocol.

Table 2.4: Membrane configurations

<i>Configuration</i>	<i>Area/Volume Ratio(m²/m³)</i>	<i>Cost</i>	<i>Turbulence Promotion*</i>	<i>Advantages</i>	<i>Disadvantages</i>	<i>Applications (most important first)</i>
Pleated cartridge	800-1000	Low	Very poor	robust construction, compact design	easily fouled, cannot be cleaned	Dead end MF
Plate and frame (flat sheet)	400-600	Low	Good	can be dismantled for cleaning, very easy to operate	cannot be backflushed	ED, UF, RO
Spiral wound	800-1000	Low	Poor	low energy cost, robust and compact	not easily cleaned , cannot be backflushed	RO, UF
Tubular	20-30	Very high	Very good	easily mechanically cleaned, tolerate high TSS	high capital and membrane replacement cost	Cross flow filtration, high TSS waters
Capillary tube	600-1200	Low	Good	displays characteristics between tubular and hollow fiber	displays characteristics between tubular and hollow fiber	UF
Hollow Fiber	5000-40000	High	Very poor	tolerates high colloidal levels	Sensitive to pressure, shocks, very frequent backpulsing	MF, RO

*: for mass transfer promotion on the feed side

The major aim of the membrane manufacturers is to eliminate or avoid fouling as much as possible by employing different techniques for scouring or backflushing.

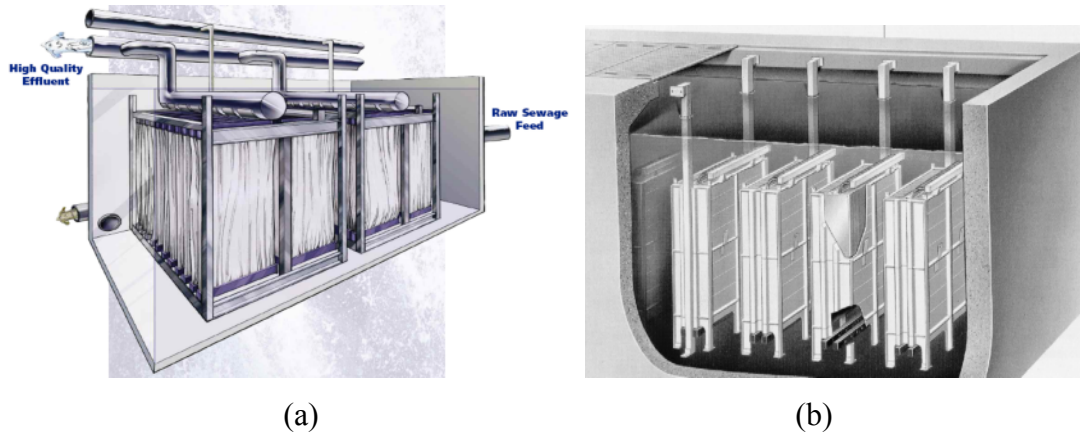


Figure 2.9: (a) Zenon and (b) Kubota membrane modules

Both hollow fiber and flat sheet membranes employ the principles of microfiltration. for the selection of particles that are bigger than the cutoff of the membranes. In microfiltration particle rejection is based on a sieve mechanism (Günder, 2000). The particles are restrained primarily due to their geometrical measurement on the surface of the membrane.

2.5 Mechanistic Explanation of Filtration Through Membranes

2.5.1 Flux

Flux can be defined as the amount of flow passing through a unit area of membrane per unit amount of time, which is also called the *permeate flux*. Permeate flux is the decisive factor in determining the hydraulic performance of membrane systems. The key elements of the operation of membrane systems lie in the influence of the following parameters on the permeate flux (Stephenson et al., 2000).

- The membrane resistance
- The operational driving force per unit membrane area
- The hydrodynamic conditions at the membrane:liquid surface
- The fouling and subsequent cleaning of the membrane surface

The flux is determined by the driving force employed, the membrane resistance and the resistance of the interfacial region adjacent to the membrane. The interfacial

region can be defined as the cake layer accumulating on the membrane surface due to the rejected material. The resistance of the membrane is fixed and known from production, however it will change as the membrane surface will get clogged or fouled in a certain period time. The interfacial region resistance which can also be defined as the *cake layer resistance* is both a function of the influent raw wastewater composition and the permeate flux. The accumulation of the rejected materials on the membrane surface is directly proportional to the permeate flux. These materials will then foul the membrane through a number of complex physicochemical mechanism which are still have not been fully explained. With regards to conventional operational techniques of the membranes, the resistance to flow is strictly associated with the membrane itself. The permeate flux for porous membranes can be expressed as :

$$J = \frac{Q_p}{A_M} = \frac{1}{A_M} \cdot \frac{\Delta V_p}{\Delta t} \quad (2.1)$$

where ;

J : flux , lt/m²-h

Q_p : permeate flow (lt/h)

ΔV_p : Permeate volume (lt)

Δt : time (h)

2.5.2 Type of filtration

There are two major filtration mechanisms in membrane systems;

- Dead-end filtration,
- Crossflow filtration

Nearly all the membrane processes have three associated streams: (1) *The feed stream*, (2) *The permeate stream* and (3) *The retentate stream*. Dead-end filtration can simply be defined as the type of filtration where there is no retentate stream which then can be compared with conventional cake filtration. The flow direction of the suspension to be filtered is perpendicular to the membrane surface. All rejected materials remain on the surface of the membrane forms a cake layer.

The thickness of this cake layer increases with time and results in the decrease of flow. In dead-end filtration the cake layer must be removed from the membrane surface by periodic backflushing.

In case of crossflow filtration, the wastewater or the suspension to be filtered flows parallel to the membrane surface. Due to this crossflow velocity, cleaning or in other words scouring effects are generated by shear forces over the membranes surface. These shear forces hinder the formation of a cake layer. It is expected that equilibrium conditions will be formed after a period of time due to the cleaning and deposition effects taking place on the membrane surface which tends to keep the cake thickness constant. This point can be defined as the steady state condition for crossflow filtration. Both dead-end and crossflow filtration have permeate streams. Figure 2.10 schematically illustrates both types of filtration techniques (Günder, 2001).

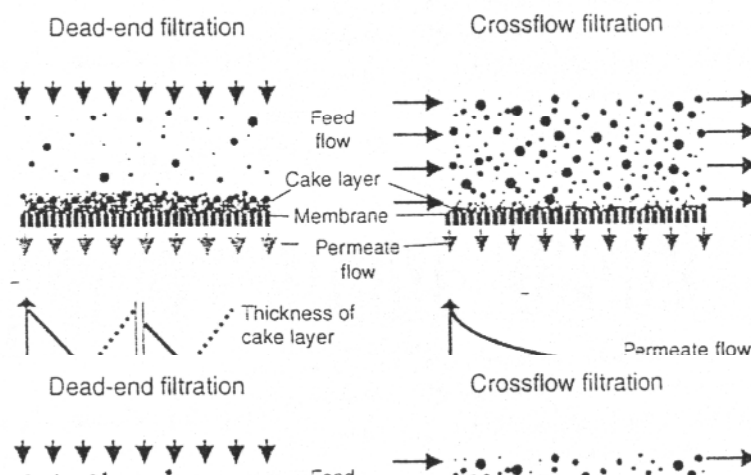


Figure 2.10: Schematic presentation of dead-end and crossflow filtration

Figure 2.11. illustrates the most important definitions and the operating parameters that characterize a crossflow filtration. Q_F , Q_P and Q_C are feed flow, permeate flow and concentrate flow respectively. Membrane surface area is shown as A_M , where the crossflow velocity is shown as V_{CF} . When compared to conventional sand filtration it should be noted that the effluent of microfiltration is always designated as permeate and not filtrate.

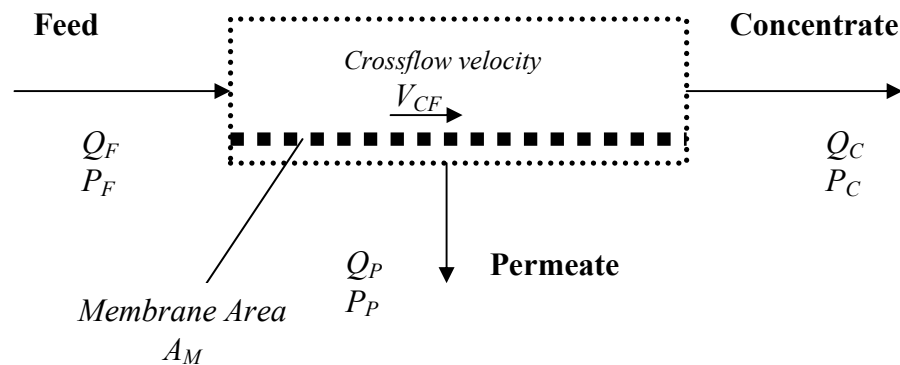


Figure 2.11: Definition of operational parameters in crossflow filtration

2.5.3 Transmembrane pressure difference(Δp_{TM})-the driving force

Filtration or permeation through a membrane requires that some force be applied to drag the suspension across it. This force can be either natural or artificial meaning that the permeate can be either sucked via pump or it can be extracted purely by hydrostatic pressure. Two major transport mechanisms are governing in membrane processes; *convection* and *diffusion*.

Convection results from the movement of the bulk fluid thus any flowing liquid constitutes convective transport. The type of flow produced or the flow regime is dependent upon the flow rate. At high flow rates the flow is described as turbulent, whereas at low flow rates it is defined as laminar. Higher flow rates usually yield greater mass transport and it is always desirable to promote turbulence on the retentate side of the membrane.

Diffusion results from the transport of individual ions, atoms or molecules by thermal motion. The basic law defining diffusive transport states that its rate is dependent upon the concentration gradient coupled with the component Brownian diffusivity, which increases with decreasing size.

Transmembrane pressure difference is the driving force behind crossflow microfiltration. Transmembrane pressure can be defined as the difference between the average or mid static pressure on the suspension side and the dynamic pressure on the permeate side.

$$\Delta p_{TM} = \text{Static Pressure} - \text{Dynamic Pressure} \quad (2.2)$$

Δp_{TM} : Transmembrane pressure (bar, kPa)

Flux and the driving force or in other words the transmembrane pressure are interrelated so one of them can be fixed for design purposes. In general, the flux is fixed and the corresponding driving force is determined for permeation. This kind of operating strategy requires the tracking of the transmembrane pressure over time as will increase due to constant flux. The overall resistance of the membrane and the cake layer are influenced by a number of factors where these play an important role in the design of the membrane processes:

- the concentration of rejected solute (as in RO and UF) or permeated ions (as in ED) near the membrane surface
- the depletion of ions near the membrane surface (as in ED)
- the precipitation of, normally, macromolecular species at the membrane surface (gel layer formation)
- the accumulation of retained solids on the membrane as in the present membrane bioreactor processes employing microfiltration
- the accumulation of foulants especially the extracellular polymeric substances (EPS) on or within the membrane

All of the above mentioned factors have an influence on fouling. Fouling takes place through a number of complex physicochemical and biochemical reactions where all of these, individually or jointly relate to the deposition of solids or foulants on the membrane surface or within the membrane. Fouling can be either temporary which can be removed by backwashing or permanent where fouling can only be overcome by chemical cleaning. The term *clogging* must be distinguished from fouling as clogging relates to the filling of the membrane pores with solids and deposits due to the unsatisfactory hydrodynamics or false operation. Clogging can be removed by backflushing.

The membrane resistance is fixed whilst the cake layer resistance is variable. The membrane resistance only increases with decreasing hydraulic permeability due to the foulant content of the feed water and the solids accumulation on the membrane surface. The cake layer resistance is dependent on the foulants in this region which is also related to the thickness of the cake layer. It can be concluded that the physical and hydraulic performance of the membrane processes largely

depend on (1) *the quality of feed water and the existence of the foulants*, (2) *operating conditions such as flux, TMP, permeability*. Table 2.5. summarizes the driving forces applicable to certain membrane processes (Stephenson et al., 2000).

Table 2.5: Driving forces applied to membrane processes

<i>Membrane Separation Process</i>	<i>Driving force for mass transport</i>	<i>Type of membrane used (pore size)</i>	<i>Contaminant size</i>	<i>Separation achieved</i>
Microfiltration (MF)	Suction or hydrostatic pressure difference, 20-200kPa	Isotropic or anisotropic porous (0.1-2 μm)	0.2-100 μm	Water from suspended solids (used in MBR processes for biomass retention)
Ultrafiltration (UF)	Hydrostatic pressure difference, 50-1000kPa	Anisotropic porous (2-50 nm)	5-500 nm	Water from dissolved solids or colloidal macromolecules
Reverse Osmosis (RO)	Hydrostatic pressure difference, 600-10 ⁴ kPa	Composite homogenous ultrathin layer	0.2-10 nm	Water from low molecular weight components and ions
Extraction/Aeration	Concentration difference/pressure	Composite homogenous ultrathin layer	0.2-10 nm	Volatile species from water/gas into water (as used in the membrane aeration bioreactors and extractive MBR)
Dialysis	Concentration difference	Homogenous	50-5000 nm	Low molecular weight components from macromolecules
Electro-dialysis	Difference in electrical potential	Ion exchange membrane	<0.1 – 0.5 nm	Ions from water

In the case of dead-end filtration process, the resistance increase according to the thickness of the cake formed on the membrane, which is expected to be proportional to the total volume of filtrate passed. For crossflow processes, this deposition continues until the adhesive forces binding the cake to the membrane are balanced by the scouring forces of the liquid permeating through the membrane (Judd and Jefferson, 2003). In relation to the other parameters being equal, steady state conditions for crossflow processes can be attained.

Figure 2.12 illustrates the pressure distribution across the membrane and the cake layer.

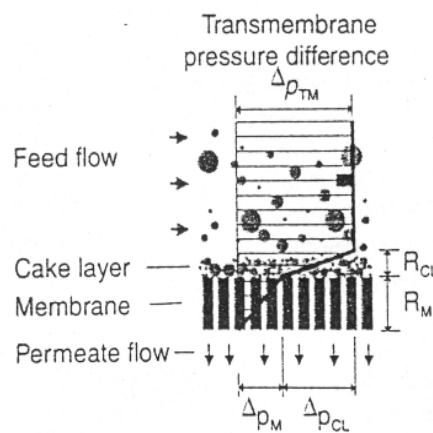


Figure 2.12: Schematic illustration of pressure distribution across the membrane and the cake layer

Ripperger (1993) represented the relationship between transmembrane pressure, permeate flux and crossflow velocity as shown in Figure 2.13. In case of low pressure differences and low fluxes it can be expected that the thickness of the cake layer will be small. The flux will only be dependant on the membrane resistance and proportional to the transmembrane pressure. Under these operating conditions, it can be concluded that the filtration process is *membrane controlled*, in which the flux is determined by the physical characteristics of the membrane like it's porosity and resistance.

During the course of the operation more solids and rejected materials are retained on the surface of the membrane. This increases with increasing transmembrane pressure and corresponding higher flux values. The result will that the cake layer thickness will increase until it reaches an equilibrium with the amount of solids removed by crossflow. At this point the resistance of the cake layer will predominantly effect the

flux such that the flux will become independent of the transmembrane pressure and it will not be possible to increase it further. The mechanism of filtration will then be *cake layer controlled* instead of membrane controlled.

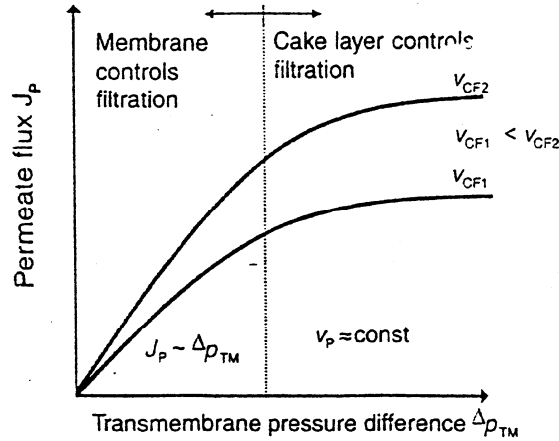


Figure 2.13: Relationship between transmembrane pressure and permeate flux in crossflow microfiltration

2.5.4 Hydraulic permeability (H_P)

Hydraulic permeability defines the relationship between the permeate flow and the transmembrane pressure difference. It is an important measure for the characterization of permeability of the membrane and it is expressed as;

$$H_P = \frac{J_P}{\Delta p_{TM}} \left[\frac{lt}{m^2 \cdot h \cdot bar} \right] \quad (2.3)$$

This parameters is also used to;

- assess the performance of the operating membrane system,
- to establish the effect of cleaning on the membrane, chemical based or time/process based

Hydraulic permeability is a temperature dependant parameter (Günder, 2001).

2.5.5 Crossflow velocity (V_{CF})

Crossflow velocity sustains the necessary scouring for the membrane cake layer formed on the surface of the membrane, thereby forming an equilibrium or steady state conditions with the solids deposited on the membrane and the solids removed by crossflow. This action sets a uniform cake layer thickness and it is the major parameter that distinguishes crossflow filtration from dead-end filtration.

The cleaning effect increases with increasing crossflow velocity and the cake layer thickness decreases with increasing crossflow velocity.

The crossflow velocity directly influences the permeate flow passing through the membrane. As the crossflow increases, it will have more detaching effect on the retained particles on the membrane surface making the cake layer thinner.

2.5.6 Concentration polarization

Concentration polarization is the term used to describe the tendency of the solute to accumulate at the cake layer within a concentration boundary layer or liquid film (Judd and Jefferson, 2003). This layer contains near stagnant liquid, since at the membrane surface itself the liquid velocity must be zero. This implies that the only mode of transport within this layer is diffusion, which is around two orders of magnitude slower than convective transport in the bulk liquid region. Rejected materials build up in this region adjacent to the membrane increasing their concentration over the bulk value at a rate that increases exponentially with increasing flux. The thickness of the boundary layer or in other words the cake layer is determined entirely by the system hydrodynamics. The thickness of the cake layer will decrease with increasing crossflow velocity or increased turbulence.

In pressure driven processes it can be stated that, the greater the flux the greater the build up of solute at the interface; the greater the solute build up, the higher the concentration gradient; the steeper the concentration gradient, the faster the diffusion. At steady state conditions the forces that drive the suspension through the membrane will come in equilibrium with the forces that scour the deposits away from the membrane. Concentration polarization determines this balance. The aim and setup of the membrane process should enable to suppress concentration polarization by *(1) increasing crossflow velocities or increasing turbulence, (2) running at low fluxes, (3) avoiding feed water with high fouling contents*. Figure 2.14 gives a schematic representation of concentration polarization (Stephenson et al., 2000).

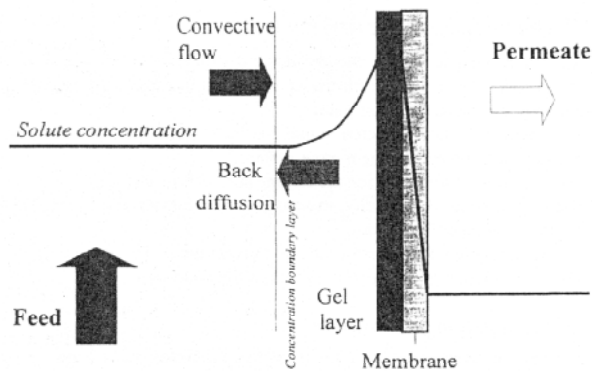


Figure 2.14: Schematic representation of concentration polarization

The relationship between driving force and polarization in pressure driven membrane separation processes can be summarized as follows:

- The flow through a given type of membrane varies with the membrane area and the driving force where the driving force is inversely proportional to the membrane area installed.
- The selective nature of the membrane processes cause the rejected materials to remain on the membrane surface. Crossflow operation restricts the accumulation of the rejected particles onto the membrane surface to some extent.

2.5.7 Concept of fouling

Although fouling is a very complex process interrelated to various physicochemical and biochemical reactions, it can be simply defined as *the decrease of flux over a certain period of time*. Mathematical models developed to represent fouling are given in the proceeding chapters. Concentration polarization has a significant effect on fouling since this increases the concentration of the foulants in the vicinity of the membrane. Fouling can be caused by the membrane itself, the concentrations of foulants within the feed water and their reactions between the membrane and the suspension.

Because of the very complex nature and processes involved, it is not possible to explicitly define membrane fouling. Many researches and modelling attempts have been made to bring a mechanistic explanation to fouling, however there is still not a solidified model explaining the reason and occurrence of fouling which still remain as as further research area in membrane processes.

Fouling can be either reversible which can be removed by scouring or irreversible which can only be removed by chemical cleaning. Fouling can occur on the membrane surface, in the membrane pores and the inner surface of the membrane. The following processes are considered as causes for the fouling process (Ripperger, 1992; Staude, 1992; Flemming, 1995).

- adsorption of macromolecular and/or colloidal matters on the external and inner surface of the membrane,
- adhesion and growth of biofilms on the membrane surface (biofouling) ,
- precipitation of solved matters on the membrane surface (scaling),
- aging of the membrane (polymerization)

Proteins are considered to be the most important substance in membrane fouling. They can cause fouling on many different MF membrane materials, in particular hydrophobic polymers such as polypropylene causing flux declines (Palacek and Zydney, 1994 ; Judd and Till, 2000) ultimately due to irreversible deposition onto and penetration into the bulk membrane material. UF membranes are less prone to fouling by macromolecules they have smaller pores and they are more impenetrable. Hydrophilicity and surface charge play an important role in determining the extent of fouling both in UF and MF membranes. Hydrophobic materials are more prone to deposition leading to irreversible fouling.

Membrane fouling takes place both by *adsorption* and *deposition*. Deposition is the worst form affecting the performance with regards to flux decline. It is postulated that the high shear conditions prevailing at the cake layer promote aggregation of the proteins or produce other changes which result in deposits of widely varying structures and hydraulic behaviour (Kim et al., 1992). It has been proposed by Kelly et al. (1993) that the deposited protein aggregates may serve as nucleation sites for non-aggregated dissolved proteins. The extent of internal to external fouling appears to be governed by the physical characteristics of the membrane such as surface porosity and flux. Mueller and Davis (1996) found high surface porosities to be deleterious to maintaining a high flux in their studies of membrane fouling of different membrane materials of the same nominal pore size. Marshall et al. (1997) found internal fouling to be promoted at lower fluxes.

With specific regard to filtration of activated sludge in membrane processes it is widely recognized that the main foulants are the extra cellular polymeric substances

(EPS) excreted from cells. EPS form an essential part of activated sludge. Among many functions of EPS are; formation of flocs and a protective layer around the cell. Apart from EPS that is bound in microbial flocs, EPS can be found in the water phase as free EPS. Substances in this category originate from break-up of flocs and cell lysis or can be introduced by the influent. The substances can escape the influence of crossflow and enter the boundary layer (cake layer) near the membrane. EPS found in the water phase are quite small compared to bacterial flocs which can be stated that activated sludge flocs are not involved in fouling. According to Chang and Lee (1998), through the separation of the activated sludge into three portions, bulk, cell and EPS fraction it was found that EPS was the major fraction contributing to the total membrane resistance and hence fouling. It can be concluded that with greater amount of EPS found in the activated sludge whether it is in the water phase or in the bacterial flocs, the greater flux reduction will be observed regardless of the physiological state and the membrane material. This implies that under these circumstances the filtration will be cake layer controlled. Chang and Lee (1998) experimentally determined that a 40% reduction in EPS resulted in an equivalent reduction in the resistance of the cake for activated sludge cultivated under nitrogen deficient conditions. Nagaoka (1999) similarly linked hydraulic resistance to EPS levels including empirical parameters for EPS production.

Meng et al. (2006) found that the total EPS including protein and carbohydrate had the strongest influence on the membrane permeability and thus fouling. The increase of the total EPS would cause an increase in the dynamic viscosity of the mixed liquor and cause more polymers and sludge particles accumulating on the membrane surface. Figure 2.15 shows the effect of EPS on membrane fouling resistance (Meng et al., 2006). It can be seen from the figure that protein is the major factor in EPS affecting membrane flux.

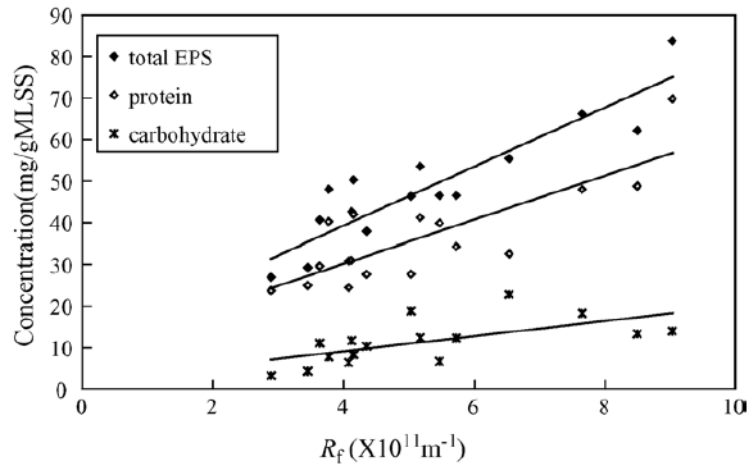


Figure 2.15: Effect of EPS concentration on membrane fouling resistance

2.5.8 Avoiding fouling

Fouling can be suppressed in three ways

- Pre-treatment or in-situ treatment like membrane cleaning to remove foulants,
- Promotion of turbulence or in other words maintaining odd crossflow velocity to limit the thickness of the cake layer,
- Reduction of flux

In biological membrane processes, it is not feasible to remove the foulants by pre-treatment, because this part forms the majority of the pollutants intended to be removed by the membrane process itself. Second option can be achieved by installing or providing highly efficient coarse or fine bubble diffused air system for higher crossflow velocities.

Flux reduction can be employed in membrane processes where the membrane is submerged in the reactor. This limits the degree of turbulence promotion and hence air scouring by crossflow velocity. This operational concept is called the *critical flux*.

2.5.9 Critical flux

Fouling can be considered to be either reversible or irreversible. A long term decrease in flux which is not recovered by simple cleaning techniques is referred to as irreversible fouling and this is often attributable to colloidal deposition onto the membrane. Since mass transport of colloidal material to the membrane surface is directly related to the flux for an membrane separation system, Howell (1995)

postulated that there exists a *critical flux* below which there is no fouling or deposition onto the membrane surface by colloidal particles. Below this threshold value the flux is directly proportional to transmembrane pressure. The critical flux can be considered as a function of the hydraulic conditions tending to increase with increase crossflow along with the nature of the membranes and the foulants existing in the feed water.

Howell (2004) experimentally found that, at moderate flux values in the near-critical flux region, membrane fouling due to a temporary increase in permeate flux can be controlled by increasing the crossflow velocity or the air scouring and concluded that most of the fouling was removed when the permeate flux was reduced back to the sub-critical level. Critical flux is dependant on the biomass in a membrane process incorporating activated sludge but it is not just a simple function of concentration. High biomass concentrations may only be attained at the cost of a change in sludge morphology that may lead to more severe irreversible fouling.

2.6 Mass Transfer Theory in Membrane Filtration Processes

Theory of filtration is basically based on determination of flux under a given pressure in relation to the hydraulic resistance of the membrane and the resistance arising from the cake layer which is also defined as the *simple resistance model*. This approach can be used as vice versa. In this theory, it is vital that the membrane resistance and the cake layer resistance is known. Cake layer resistance can be empirically derived where on the other hand membrane resistance is known for a specific type of membrane. With the knowledge of the two most important parameters, the simple resistance theory can easily be applied to membrane systems in determining the flux and fouling aspects.

Many models have been presented to determine and model hydrodynamic behaviour of microfiltration and ultrafiltration membrane processes (Fane, 1986; Davis, 1992; Belfort et al., 1994; Lojkine et al., 1992; Choi et al., 2000). However these are reviewed elsewhere and only the one that is applicable to the system in this research will be described in detail in the proceeding chapters.

Most of the models presented for crossflow microfiltration are basically based on the film theory. Classical film theory assumes diffusive transport in the cake layer to be determined by the degree of concentration polarization.

It can be stated that mass transfer for membrane processes can be categorized in two groups; (1) *Membrane controlled mass transfer*, (2) *Cake layer controlled mass transfer*

2.6.1 Membrane controlled mass transfer

In membrane controlled mass transfer, the resistance to flow is entirely related with the resistance of the membrane itself. For porous membranes flux can be mathematically expressed as;

$$J = \frac{\Delta P}{\mu R_m} \quad (2.4)$$

where J is the flux in m³/m²-h, ΔP is the transmembrane pressure, μ is the fluid viscosity and R_m is the resistance of the membrane in units of m⁻¹. For microporous membranes, specifically used for microfiltration, the Hagen-Poiseuille equation may be considered applicable for permeate undergoing laminar flow through membrane pores. The resistance of the membrane R_m can be defined as;

$$R_m = \frac{K(1 - \varepsilon_m)^2 S_m^2 l_m}{\varepsilon_m^3} \quad (2.5)$$

where ε_m is the porosity of the membrane, S_m is the pore surface area to volume ratio and l_m is the membrane thickness. K is a constant equal to 2 for membranes having cylindrical pores. However this constant will differ according to changing geometry of the pores.

2.6.2 Cake layer controlled mass transfer

2.6.2.1 The reknown resistance model

In the cake layer controlled mass transfer, the resistance model is the most applied one in explaining the mechanistic hydrodynamic behaviour of the membranes. The additional resistance offered by the material accumulating onto the membrane surface in the cake layer can be easily expressed by adding the cake layer resistance

to the membrane resistance accounting for the total resistance. In this case the flux will be;

$$J = \frac{\Delta P}{\mu(R_m + R_c)} \quad (2.6)$$

where R_c is the resistance of the cake layer in m^{-1} . R_c can be represented by the Hagen-Poiseuille equation in the same manner used for membrane resistance given in Equation 2.5.

$$R_c = \frac{K'(1 - \varepsilon_c)^2 S_c^2 l_c}{\varepsilon_c^3} \quad (2.7)$$

However in this case K' has a value of 5 for spherical geometry.

For crossflow filtration, the resistance is expected to reach a steady state condition when the adhesive forces that retain the solids deposition within the cake layer come into an equilibrium with the shear forces (air scouring) acting as a removal mechanism for the foulants. If there is sufficient information, the resistance of the cake layer can be calculated from Equation 2.7 and thus flux can be know from Equation 2.6. It is noteworthy to point out that flux will have a tendency to decrease over time due to varying properties of the cake layer, membrane and the bulk liquid.

2.6.2.2 The concentration polarization model

Concentration polarisation describes the tendency of the material to build up in the cake layer (membrane solution interfacial region) (Stephenson et al., 2000). The extent of this build up is dependant on the following factors;

- the diffusivity of the rejected materials (suspended and dissolved),
- the thickness of the stagnant region,
- the rate at which the materials are added to the stagnant region

The first factor is purely related to the properties of the solute where the others are effected by the operating conditions. The thickness of the cake layer, δ , can be determined from the rheological properties of the liquid and the hydrodynamic conditions of the flow channel. The rate of accumulation of the materials within cake layer is a function of the flux and rejection. The concentration polarization under steady state conditions based on film theory can be defined as:

$$J = \frac{D_B}{\delta} \ln\left(\frac{C^*}{C}\right) \quad (2.8)$$

where D_B is the Brownian diffusion coefficient in m^2s^{-1} , C^* and C are the respective concentrations at the membrane surface and in the bulk solution.

The ratio D_B/δ represents the mass transfer coefficient k in units of m s^{-1} . If the rejected materials comprise of dissolved ions or small molecules, as would be the case for pressure driven dense membrane processes (RO) then D_B can be expressed by the Stokes Einstein equation:

$$D_B = \frac{2\kappa T}{3\pi\mu r_p} \quad (2.9)$$

where κ is the Boltzmann constant, T is absolute temperature and r_p is the radius of suspended or dissolved rejected material. δ is only dependant on system hydrodynamics provided that the fluid exerts a Newtonian behaviour which is a function of ;

- the physical properties of the liquid,
- the shape and size of the flow channels within the module,
- the mean velocity and in particular the shear rate of liquid flowing through the channels of the membrane

This leads to the so called Leveque solution for laminar flow and Brownian diffusive transport (Leveque, 1928; Porter, 1972) where the length averaged flux is given by Equation 2.10.

$$\langle J \rangle = 0.0807 \left(\frac{D_B^2 \gamma_o}{L} \right)^{1/3} \ln\left(\frac{C^*}{C}\right) \quad (2.10)$$

where γ_o is the maximum shear rate and L is the hydraulic dimension. The shear rate is given by the ratio of the crossflow velocity U to the characteristic dimension and is geomtry dependant, thus for parallel flow channels of height h :

$$\gamma_o = \frac{6U}{h} \quad (2.11)$$

and for tubes of diamater d ;

$$\gamma_o = \frac{8U}{d} \quad (2.12)$$

Complications arise in the concentration polarisation model when it is specifically applied to systems in which colloidal and/or suspended material is present and accumulate in the cake layer. This implies that a correction for non-Newtonian behaviour is needed to account for the local solute concentration dependant changes in; *viscosity of the fluid, diffusivity of the solute and permeability of the cake*. Many equations have been proposed and derived to express these dependancies however these are reviewed elsewhere.

2.7 The Membrane Coupled Activated Sludge Process- Membrane Bioreactor (MBR)

Combination of the membrane technology with various types of bioreactors led to the concept of “*Membrane Bioreactor*” (MBR) which is now the fastest growing and developing technology for the treatment of low to high strength domestic and industrial wastewater. From a physical point of view, one can state that the only difference of the membrane bioreactor from a conventional activated sludge process lies in the technique of separation of the biomass from the liquid stream. In conventional final sedimentation tanks only the fraction of the activated sludge that forms flocs and settles can be retained. With membrane filtration all parts of the activated sludge that are larger than the cutoff of the membrane are retained. Hence it can be stated that in membrane bioreactors, *the separation of the activated sludge from the liquid stream is independent of sludge properties and settling characteristics*.

To retain the bacteria within the reactor, microfiltration membranes with a maximum nominal pore size of 0.4 μm are usually used. To control cake layer formation, fouling and clogging of the membranes, crossflow filtration is the most suitable way of removing the foulants away from the transition boundary layer. The continuous velocity on the membrane and/or the existence of turbulence near the membrane surface is defined as the *crossflow*.

The *membrane coupled activated sludge process* consists of an activated sludge tank and a dead-end/crossflow microfiltration membrane for the solid-liquid separation. There are two types of MBR configurations for dead-end/crossflow filtration;

- MBR with external membrane filtration

- MBR with internal, submerged membrane filtration

In the external configuration, the membrane modules are placed outside of the activated sludge tank. The influent enters the biological reactor where it comes into contact with the biomass. The mixture is then pumped through the membranes.

The retained concentrate and the rejected materials are then returned to the activated sludge tank. The transmembrane pressure and the crossflow velocity necessary for operation are both generated by pumps.

In the submerged configuration, filtration through the membranes is carried out within the same activated sludge tank, therefore a supply of activated sludge to the membranes and recirculation of the retained bacteria are not necessary. The driving force necessary to generate a transmembrane pressure across the membrane is actually the water level above the membrane modules. In most applications for the submerged configuration the TMP is generated by a suction pump. Control of the cake layer and fouling are achieved by air scouring where ascending air bubbles move near the membrane surface generating the necessary liquid shear velocity. A schematic representation of external and internal membrane filtration can be seen in Figure 2.16.

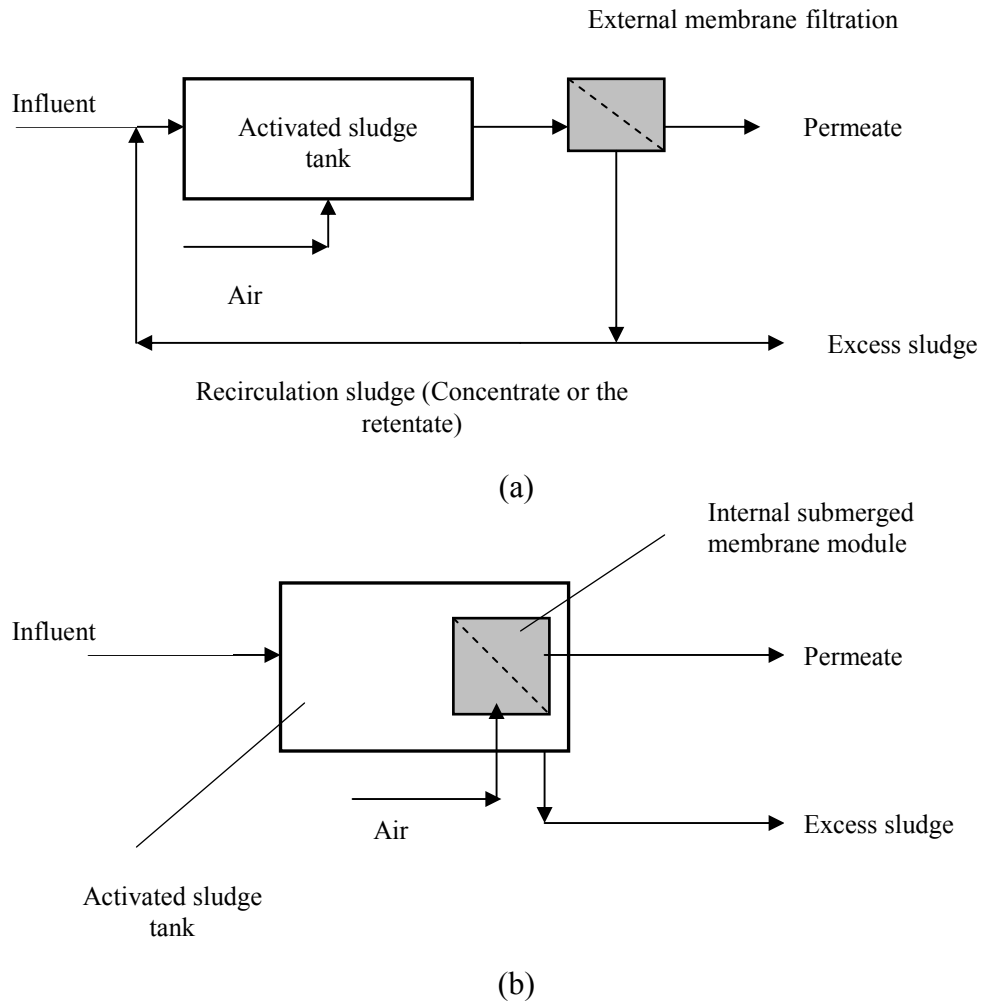


Figure 2.16: Schematic representation of MBR with (a) external membrane filtration, (b) internal submerged membrane filtration

The following operational measures are essential for proper functioning of membrane bioreactors;

- Supply of necessary oxygen for biological reactions
- Generation of transmembrane pressure for the filtration process
- Crossflow or air scouring for controlling the cake layer formation

In submerged membrane modules the air introduced into the reactor serves two purposes, (1) *generating the necessary crossflow with air scouring*, (2) *supplying of the necessary oxygen for biochemical reactions*. In some incidents the air introduced for air scouring can also be sufficient to deliver the necessary oxygen for the bacteria where this is mostly encountered in low to medium strength domestic sewage. The external configuration, on the other hand, comprises only supplying of the oxygen for the bacteria as the crossflow is generated by the circulation pump. At this point

one might think about the combination effect of the air for crossflow filtration and the air for biological reactions. The required oxygen for biological reactions can vary due to changing influent concentrations and peaking conditions, where on the other hand air scouring for constant crossflow requires constant air feed. The supply of oxygen to the bacteria is carried out mostly using fine bubble diffused aeration system where it can be stated that fine bubbles ascend slowly and produce less turbulence. Crossflow by air scouring is best when higher turbulence is promoted with fast ascending air bubbles on the membrane surface generation more liquid shear velocity. This condition can be attained with coarse bubble aeration system. Therefore it can be concluded that there is no combination or synergy effect of oxygen supply and crossflow in MBR in terms of serving different purposes.

2.7.1 Historical background of MBRs

The milestones in the development and evolution of membrane coupled activated sludge process dates back to 1966 with the joint research carried out in the Department of Environmental Engineering; Rensselaer Polytechnic Institute, Troy, New York and Dorr Oliver Inc., US. The aim of this research was to develop a new and efficient biological separation procedure for the treatment of municipal and industrial wastes (Stiefel and Washington, 1966; Hardt et al., 1970; Smith et al. 1969).

Stiefel et al.(1969) examined the oxygen transfer and consumption in an activated sludge process with MLSS concentrations in the range of 12,500-37,500 mg/l. The high MLSS concentrations were achieved using cloth filters. It was found that as the MLSS increased the respiration rate of the activated sludge decreased. This was explained by the deficiency of oxygen supply in high MLSS concentrations. To enhance the oxygen supply an additional mixer was installed to serve the purpose of blending.

Hardt et al. (1970) continued on with the research at the same institute by using ultrafiltration membranes for the separation of activated sludge. Three plate modules switched in series were used. MLSS concentrations of 25 g/l were achieved at TMPs of 3-5 bars and flux rates of 6-11 $\text{lt}/\text{m}^2\text{-h}$ where the flux rate is very low compared to present membrane filtration modules. The system was fed with synthetic waste

where no excess sludge production was observed at a COD loading of 0.2 g/g VSS-day.

The first realization of a membrane coupled activated sludge process took place in Connecticut in the mid sixties by Dorr Oliver, Inc. (Smith et al., 1969). Asymmetric external membranes were used to treat the domestic sewage of an industrial plant with 120 workers and employees. The plant was operated at 10 gr/l of MLSS and BOD values less than 5 mg/l were observed where on the other hand suspended solids were not detectable in the permeate.

Krauth and Staab (1988) investigated external membrane filtration characteristics in activated sludge with increased transmembrane pressures at 4 bars to achieve sufficient oxygenation. With MLSS concentrations of 25 gr/l and a crossflow velocity of 4m/sec, they have achieved fluxes of 150 lt/m²-h. The specific energy consumption increased to 10 kWh/m³ from 5 kWh/m³ where the investigations were carried out at a transmembrane pressure of 2 bars (Krauth and Staab, 1980).

Investigations of internal membrane modules submerged directly into the activated sludge tank were first reported by Yamamoto et al. (1989). Submerged hollow fiber membranes were used with a cutoff size of 0.1 µm. The system was operated at a constant flux of 10 lt/m²-h by intermittent operation at transmembrane pressure of 0.13 bar. The operational sequence was to filtrate for 10 minutes followed by a filtration pause for 5 minutes. MLSS concentrations of 10 and 47gr/l were set during loading with artificial substrate. It was founded that MLSS concentrations over 40 gr/l resulted in a severe decrease of oxygen transfer and efficiency.

Therefore to maintain a stable flux and a stable oxygen transfer efficiency avoiding oxygen deficient conditions it was recommended not to exceed MLSS concentrations over 30,000 mg/l.

2.8 Aerobic MBR's for Domestic Sewage Treatment- Performance and Operational Aspects

Application of the MBR technology to municipal wastewater treatment has attracted more attention than ever both commercially and academically over the past decade. The performance of a membrane bioreactor must be evaluated in three aspects as they constitute to the overall performance. These aspects can be categorized as (1)

Biological and solids removal performance, (2) Virus and Bacterial Elimination Performance (3) Physical (Hydraulic) performance and Fouling. In the following section the biological and physical performance of MBRs treating domestic sewage is discussed.

2.8.1 Biological and solids removal performance

The biological performance of the MBR can be evaluated in terms of (1) *carbon removal* and (2) *nitrogen removal* where the solids removal performance is evaluated by total suspended solids (TSS) removal.

2.8.1.1 Carbon and solids removal performance

The carbon removal covers the treatment capability of a plant to remove BOD and COD. The reported COD loading rates range between 1.2-3.2 kgCOD/m³-d corresponding to removal efficiencies to more than %95. Because the activated sludge effluent from MBR is treated by filtration through a nominal 0.40µm membrane, very low concentration of TSS, BOD and COD are reported. Murakami et al. (1999) reported consistent BOD effluent levels of less than 10 mg/lit regardless of the varying influent BOD concentrations of 100 to 250 mg/lit.

Cote et al. (1998) investigated the performance of a membrane bioreactor using submerged hollow fiber membranes with a nominal pore size of 0.2 µm. The system was operated at three different MLSS levels of 25, 20 and 15 gr/lit respectively and with influent COD levels ranging between 290-750 mg/lit. The COD loading rates were in the range of 1.2 – 2.3 kgCOD/m³-d. It was observed that COD removal was better than 96% averaging to effluent COD values of 10-16 mg/lit.

The reduction in effluent COD increased slightly when the mass loading (F/M ratio) decreased which corresponded to a larger hydraulic detention time. It was also reported that all suspended matter was removed from the treated water, where the turbidity was below 0.3 NTU.

Sewage treatment plant built in Swanage UK by MBR Technology has a capacity of 13,000 m³/day considered to be a large full scale MBR plant. The system has been in operation since 2000 and has an operational MLSS in the range of 15,000-25,000 mg/lit with effluent TSS levels not detectable. The BOD removal is reported to be in

the range of 95-98% regardless of the changing influent BOD concentration ranging between 100-389 mg/l.

Van der Roest et al. (2002) investigated the biological performance of both submerged hollow fiber and flat sheet membranes. They split the research into four phases each of them having different operating conditions the most important being the sludge age and the F/M ratio. The effluent COD concentrations varied between 21 and 31 mg/l with corresponding influent COD concentration in the range of 341 to 621 mg/l. They reported consistent COD removal efficiencies not being less than 95%. The studies with the hollow fiber membranes revealed nearly the same results with only a 2% decrease in the COD removal efficiency. TSS in effluent was not detectable in both of the plants.

Rosenberger et al.(2000) investigated lab scale and pilot scale activated sludge plants coupled with microfiltration membranes for a period of three years. During the entire operation period no excess sludge was removed from the bioreactors apart from sampling, resulting in highly concentrated biomass in the reactors. The MLSS concentration ranged from 15 to 23 gr/l for a plant fed with municipal wastewater and up to 60 gr/l for a lab scale plant fed with high strength industrial wastewater with a mean loading rate of 2 kgCOD/m³-d. Both plants showed very high and stable COD removal rates regardless of the MLSS concentration and the composition of the microorganisms. Mean COD removal efficiency for the pilot scale bioreactor treating municipal wastewater was 95% independent of the loading rate whilst the mean COD removal efficiency for the lab scale bioreactor was 86% in which the lower values were to operating failures. It was reported that COD removal efficiencies decreased for loading rates higher than 7 kgCOD/m³-d where this was explained by high MLSS concentrations and consequently decreasing oxygen mass transfer.

Nah et al.(2005) investigated the performance of a MBR fed with synthetic wastewater operated at very low sludge ages and hydraulic detention times in the ranges of 0.25 to 5 days and 3 to 6 hours respectively. Results showed that MBR was capable of achieving excellent effluent quality regardless of the extremely short sludge ages. The MBR removal efficiencies ranged from approximately 97.3-98.4% in terms of total COD and 94.1-97.0% in terms of soluble COD.

Günder (2001) studied the comparative performance of flat sheet and hollow fiber membrane bioreactors and reported minimum 90% removal efficiencies for COD in

both reactors regardless of the influent loadings. The different pore sizes (0.4 μm for flat sheet and 0.1 μm for hollow fiber MBR) did not show difference in terms of COD removal and a relationship could not be established with respect to pore size and degradation. It was concluded that the COD measured in the permeate can be defined as the inert soluble substrate of influent origin.

Various researches and reports indicate that the performance of the MBRs to be relatively independent of the hydraulic detention times with values between 2 to 24 h resulting in very high removal percentages. Sludge age also appears to have little influence of effluent quality where reports show operating sludge ages between 5 and zero sludge wastage. Comparison of the reported systems show a slight improvement in removal efficiency with increasing sludge age up to 30 d, where after no further improvement is encountered. The solids removal performance of the MBR's were never below 99% in any of the studies reported making this parameter of minor importance for the MBR.

2.8.1.2 Nutrient removal performance

Complete nitrification in a MBR was observed with a hydraulic residence time as low as 2 hours (Chazie and Huyard, 1991), Chiemchaisri et al.(1993a) and Müller (1994) found that more than 80% of the influent TKN could be nitrified to NO_3 in a MBR. Long sludge ages prevents nitrifying bacteria from being washed out from the bioreactor, improving the nitrification capability of activated sludge. Fan et al.(1996) investigated the nitrification capability of a MBR using ceramic ultrafiltration module having a pore size of 0.02 μm which was quite low compared to the present ultrafiltration pore size.

It was founded that the system exerted a consistent TKN removal efficiency of 99% at a sludge age of 20 days and a hydraulic detention times of 15 hours.

Sludge age has been shown to have an influence on nitrification in MBR's with reported ammonia removal efficiencies increasing from 80 to 99% on increasing the sludge age from 10 to 50 days (Cote et al., 1997) and from 94 to 99% on doubling the sludge age from 5 to 10 days (Fan et al., 1996). The mean nitrification activity for the MBR has also been demonstrated to be more than double that of an equivalent activated sludge plant where 2.28 $\text{kgNH}_4\text{-N/kgMLSS-h}$ was observed in MBR

against $0.96 \text{ kgNH}_4\text{-N/kgMLSS-h}$ for a conventional activated sludge process (Zhang et al., 1997).

Muller et al.(1995) investigated the nitrogen removal capability of a membrane bioreactor using external tubular filtration modules with cutoff sizes in the range 10,000 to 50,000 dextrons that lie in the ultrafiltration range. The system was operated with zero excess sludge discharge meaning a complete sludge retention. It was found that the nitrification capacity at 30°C was constantly around $0.2 \text{ mmol/grMLSS-g}$ which implied that the viability of the nitrifying population did not cease. In addition, up to 40% of nitrogen supplied was lost as a result of denitrification. TKN was almost completely removed from the system achieving removal efficiencies near 95%.

Total nitrogen removal through the inclusion of an anoxic reactor as in the conventional activated sludge systems is common in MBRs. Cote et al.(1997) operated a MBR with a separate anoxic tank whilst Nah et al.(2000) investigated the denitrification through an intermittent aeration system. As encountered in the conventional activated sludge systems denitrification was dependant on the oxic/anoxic cycle times, BOD/TKN ratio, with total nitrogen removal dropping from $>80\%$ to 50% on decreasing the BOD/TKN ratio from >2 to <1 (Nah et al.,2000). Suwa et al.(1992) also operated a MBR on the basis of intermittent aeration reaching denitrification rates of $0.0074 \text{ grN/grVSS-d}$ in an external ultrafiltration membrane filtration process fed with synthetic wastewater. Complete elimination of nitrogen was achieved at loadings up to $4 \text{ kgNH}_4\text{-N/m}^3\text{-d}$ for nitrification and $5 \text{ kgNO}_3\text{-N/m}^3\text{-d}$ for denitrification. Suwa et al.(1992) related the denitrification efficiency to BOD loadings where no denitrification was observed below 0.438 grBOD/l and immediately recovered over this loading. It was further stipulated that the total nitrogen removal was around 40% at BOD/TKN ratios of 10 and higher than 90% when the ratio increased to 25. Suwa et al.(1992) also investigated the effect of DO concentration on the sidestream MBR and have postulated that a decrease of DO concentration from $5 \pm 1 \text{ mg/l}$ to $1 \pm 0.5 \text{ mg/l}$ did not exert an increase in the denitrification rate; rather it was stated that intermittent aeration with sequencing on-off aeration intervals had a significant increase in nitrogen removal

Seo et al.(2000) demonstrated the nitrogen removal performance of a submerged and intermittently aerated membrane bioreactor consisting of two tanks. Hollow fiber membranes with a nominal pore size of 0.1 μm were inserted into the 2nd reactor and the system was fed with domestic sewage. The influent COD and TKN concentrations were in the range of 216 to 327 mg/l and 28 to 47 mgN/l. The system operation was separated into two phases where in the first phase, the aeration –non aeration times for the first and the second reactor were set to 30/90min and 60/60 min respectively and 60/60 in the second phase for both reactors. It was seen that the effluent TN was maintained at 10.7 mg/l after 10 days of operation and the removal efficiency was 73.6% whereas it was reduced to 3.5 mg/l in Phase 2 corresponding to a removal efficiency of 91.6%. The increase in TN removal efficiency was linked to the adjusted aeration-non aeration times in the second phase. It was also observed that the dissolved oxygen concentration dropped to zero in the 15 min after the non-aeration period started where a bending point appeared in ORP curve indicating a complete denitrification in the reactor.

Ujang et al.(2002) also operated a lab scale flat sheet membrane bioreactor having two compartments with intermittent aeration (aeration and non-aeration sequence). The study was divided into three stages where each stage had a different aeration and non-aeration sequence to assess it's impact on nitrification and denitrification. The time cycles of the first and second compartments for aeration and non-aeration sequences were 90/150,150/90 min; 60/120, 120/60 min and 120/120,120/120 respectively. Unlike Seo at al.(2000), Ujang et al.(2002) observed that the removal of nitrogen was similar although operated at different aeration and non-aeration times. The nitrogen removal for stages 1,2 and 3 were $96.0\pm 1.0\%$, $95.7\pm 1.0\%$ and $96.3\pm 1.0\%$ respectively.

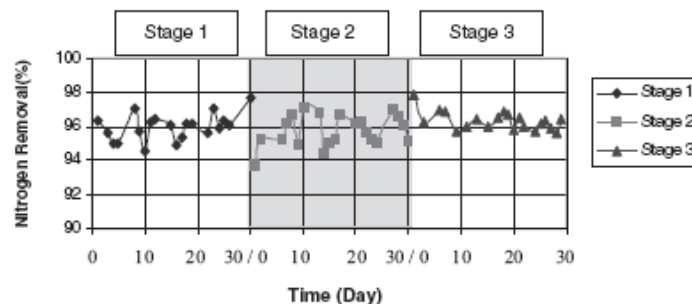


Figure 2.17: Nitrogen removal in intermittent MBR (Ujang et al., 2002)

The results show that there was not much difference in the efficiency of denitrification process although operated in varying aeration and non-aeration periods. Nagaoka (1999) also demonstrated the nitrogen removal capability of a membrane bioreactor fed with synthetic wastewater which was operated in intermittent aeration mode (30 minutes cycle) and found that the total nitrogen removal efficiency was 95%.

Zhang et al.(2005) compared a conventionally operated MBR (CMBR) with another membrane bioreactor operated in a sequencing batch mode named as a sequencing batch membrane bioreactor (SBMBR). It was found that the SBMBR achieved good results even at different influent COD/TN ratios. Even at low COD/TN ratios like 6.3 the TN and $\text{NH}_4^+\text{-N}$ removal efficiency were 65% and 90% respectively. The CMBR TN removal efficiency was 30.5% when the influent COD/TN ratio was 19.4 where the average $\text{NH}_4^+\text{-N}$ removal efficiency was 93.3%. This was linked to the conclusion that the limiting step of nitrogen removal in CMBR was denitrification. It was also observed that the variation of influent COD/TN ratio affected the CMBR more extensively than SBMBR.

Another intermittent aeration study was conducted with an MLSS concentration of 6000mg/lit and on/off aeration intervals of 15 min (Fernandez et al., 2000). An effluent total nitrogen concentration ranging from 7 to 10 mg/lit was achieved. Full nitrification was not possible at high MLSS concentrations up to 13,000mg/lit probably due to DO limitations in the activated sludge. In a laboratory study, an MBR was operated successfully at low DO concentrations (<1.0 mg/lit) to accomplish simultaneous nitrification-denitrification (Choo and Stensel, 2000). The reactor was operated with six 4 hour cycles per day consisting of 0.5, 2.0 and 1.5 hours for fill, aeration and effluent filtration-idle, respectively. Most of the nitrate was removed during the mixed and unaerated fill period, but it was found that a significant amount of nitrogen was removed by simultaneous nitrification and denitrification (SNdN) during aeration at dissolved oxygen concentrations less than 3.0 mg/lit. It was reported that the SNdN removal increased with decreasing dissolved oxygen concentrations however this had a negative impact on nitrification. Nitrogen removal efficiency ranged from 87% to 93% .

Timberlake et al.(1988) reported simultaneous carbon removal, nitrification and denitrification in a membrane bioreactors if the biofilms were sufficiently deep for

oxygen to be exhausted. The structure of a biofilm growing in a membrane bioreactor was described by the partition of the cake film into various layers each responsible for a biochemical reaction.

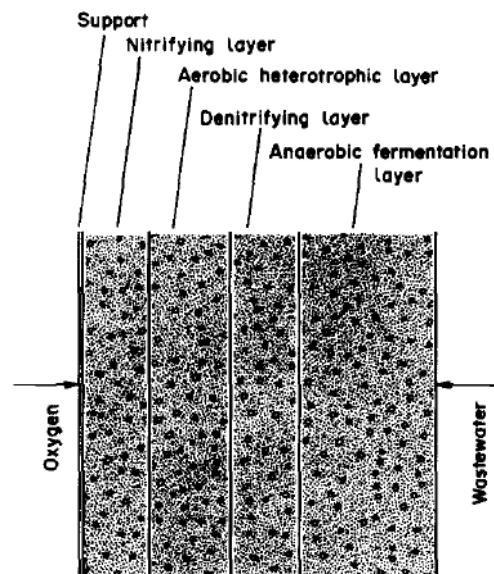


Figure 2.18: Structure of support aerated biofilm in a membrane bioreactor (Timberlake et al.,1988)

Semmens et al. (2003) studied the COD and nitrogen removal capabilities of a membrane aerated bioreactor with polyethylene hollow fiber and an ammonium acetate based synthetic wastewater. With a fixed COD:N ratio of 5, they achieved 75%, 90% and 95% COD removal at COD concentrations of 220, 270 and 290 mg/l respectively. At the highest COD concentration and with an ammonium concentration of 87 mg/l, the TN removal averaged 80% with a maximum of 95%. They concluded that MBRs are capable of simultaneous carbon removal, nitrification and denitrification at competitive rates.

Van der Roest et al. (2002) studied the nitrogen removal performance of pilot membrane bioreactors using both hollow fiber and flat sheet microfiltration membrane systems. In the first phase of the research with flat sheet membranes, primary sedimentation was included into the scheme where the nitrate in the permeate was relatively high with an average concentration above 10 mg/l. The COD/N ratio of the feed was 6 which is relatively low. The nitrogen removal improved in the second phase where the COD/N ratio was increased to 8. The nitrogen removal was even better in Phase 3 without primary sedimentation where the COD/N ratio was higher than 10. In the final phase, the effect of incorporation of

recirculation flow from the membrane tank to the anoxic tank was investigated. The nitrogen in the permeate did not improve much due to the low internal recirculation flow. The results showed similarity with the studies conducted with the hollow fiber membranes. It was emphasized that the COD/N ratio and the internal recirculation flow had the utmost impact on total nitrogen removal.

Ghyoot et al.(1999) investigated the nitrogen removal capability of a membrane bioreactor for the treatment of highly concentrated sludge reject water using ultrafiltration and microfiltration modules in two different runs. Denitrification was achieved using external carbon source. The average TKN concentrations for the first and second runs were 293 and 305 mg/l respectively. The use of an ultrafiltration unit with a positive displacement pump for sludge recirculation resulted in complete nitrification at an aerobic sludge loading rate of 0.16 kgN/kgSS-d, while the use of a microfiltration unit with a centrifugal pump for sludge recirculation resulted in complete nitrification at a max loading of 0.08 kgN/kgSS-d. The sudden decrease of nitrification using a centrifugal pump was explained due to the high shear stress created by this pump on the biomass passing through it. More than 80% denitrification was achieved via nitrite at a COD:N ration 2.3 g/g and via nitrate at a COD:N ratio of 3.8 g/g. Use of acetic acid as an extra carbon source resulted in a denitrification more than 90%. Maximal anoxic sludge loading rates of 0.4 and 0.2 kg NO_x-N/kgSS-d were achieved for dosage of respectively methanol and acetic acid.

It was reported by various researchers that, denitrification, the reduction of nitrate to various gaseous end products such as molecular nitrogen and dinitrogen oxide can proceed alongside of nitrification simultaneously if :

- Aeration is supplied intermittently (Chaize and Huyard, 1991; Chiemchaisri et al., 1992),
- Hydrodynamic are such that an anoxic area results (Chaize and Huyard, 1991),
- High organic loads are added allowing anoxic micro sites to develop within the flocs (Suwa et al., 1992; Chaize and Huyard, 1991; Ueada et al., 1996)

2.8.1.3 Virus and bacterial elimination performance

It has been reported that MBRs are capable of removing high number of bacteria and viruses. Chiemchaisri et al. (1992) observed an improvement in virus removal as a gel layer was formed on the membrane surface. Till et al. (1998) reported that the formation of a gel layer on the membrane surface decreases the effective cut-off size of the membrane contributing to better performance of bacteria removal. This can also be explained by the formation of a transition boundary layer in other words the cake layer.

Gander et al.(1999) reported 3-5 log rejections with pore sizes of 5 μm where on the other hand 8 log rejections of total coliforms encountered for membrane cut-off sizes of 4 μm . Findings indicated that as the membrane filtration resistance increased, membrane fouling played a significant role in removal through a reduction in effective pore size. Table 2.6. summarizes the disinfection performance of various membrane bioreactors (Stephenson et al., 2000).

Günder (2001) reported that with submerged plate modules having a cutoff size of 0.4 μm and hollow fiber modules having a cutoff size of 0.1 μm , an almost complete rejection of all indicator organisms were achieved. It was then concluded that microfiltration represents a purposeful disinfection because of the rejection of the organisms.

Similar results were reported in other investigations. In experiments with hollow fiber modules, no faecal coliforms could be measured in the permeate (Firk, 1997). Wummel et al.(1998) measured concentrations less than 500 in 100 ml for different indicator organisms. In investigations with flat sheet membrane modules, 10 to 500 faecal coliforms in 100 ml were found (Churchouse, 1997).

It can be concluded that the permeate from both flat sheet and hollow fiber membrane modules comply with the standards for bathing waters issued by the EC shown in Table 2.6.

Table 2.6: Microbiological quality requirements for bathing waters (EC Bathing Water Guideline dated 8.12.1975;76/160 EWG)

<i>Microbiological Parameter</i>		<i>Guide</i>	<i>Imperative</i>
Total Coliform	in 100ml	500 (80)	10.000 (95)
Faecal Coliform	in 100ml	100 (80)	2.000(95)
Streptococcus faecalis	in 100ml	100 (90)	-
Salmonella	in 1000ml		0 (95)
Enteric Virus	in 10 l		0 (95)

It has also been reported that both hollow fiber and flat sheet membranes having cutoff sizes of 0.2 and 0.4 μm respectively, are capable of removing the *cryptosporidium* virus. *Cryptosporidium* is a reknown virus that lives in the digestion system of the human beings and mostly result in fatality.

Table 2.7: Disinfection performance of various MBRs (Stephenson et al., 2000)

<i>Reference</i>	<i>System</i>	<i>Pore Size</i>	<i>Parameter</i>	<i>Influent</i>	<i>Effluent</i>	<i>Removal (log)</i>
Ciemchaisri (1992a,b)	subm. hollow fiber	0.3 μ m	Coliphage	7.1-7.5 log	1.2-3.5 log	4.6
Cote et al.(1997)	subm.hollow fiber	200.000 Daltons	total coliform bacteriophage	5.6-5.9x10 ⁷ 1.4-3.7x10 ³	20-43 -	6.1-6.4 >3.8->4.5
Buisson et al.(1998)	subm. hollow fiber	200.000 Daltons	faecal coliform	n/a	n/a	6.2
Jefferson et al. (2000)	subm. flat sheet	0.4 μ m	total coliform	2.5-7.4	1-15	Ca.7
Churchouse and Wildgoose (1999)	subm.flat sheet	0.4 μ m	Faecal coliform Faecal streptococcus Coliphage	0.9-64x10 ⁶ <30x10 ⁶ <29-6320	<20 <11 <0.19	>5.7 >99.9993% >99.98%
Gander et al.(1999)	subm. flat sheet	0.4 μ m	Total coliform	n/a	n/a	ca.8
Ueda and Horan (2000)	subm.flat sheet	0.4 μ m	Phage Faecal coliform Faecal streptococcus	1.5x10 ³ -1.1-10 ⁸ 8.8x10 ⁶ -1.2x10 ⁷ 5.2x10 ⁵ -7.7x10 ⁵	n/a	2.3-5.9 6.86 75.83

2.8.1.4 Physical (hydraulic) performance and fouling

Flux rates in MBR's range from 5 to 300 $\text{lt}/\text{m}^2\text{-h}$ and with specific flux values (hydraulic permeability) ranging from 20 to 200 $\text{lt}/\text{m}^2\text{-h-bar}$. A standard design flux of 0.5 $\text{m}^3/\text{m}^2\text{-d}$ (20.8 $\text{lt}/\text{m}^2\text{-h}$) has been suggested for a submerged flat sheet MBR with a membrane pore size of 0.4 μm (Ishida et al., 1993); yielding hydraulic permeabilities in the range of 75 to 100 $\text{lt}/\text{m}^2\text{-h-bar}$ depending on the TMP. Cote et al.(1997) reported hydraulic permeability values ranging from 125 to 175 $\text{lt}/\text{m}^2\text{-h-bar}$ for a submerged hollow fiber membrane microfiltration membrane backwashed every 15-30 minutes. It is known that sidestream MBR's exert a different hydrodynamic behaviour and can be subject to severe flux decline. Chaize and Huyard (1991) operated a sidestream polymeric ultrafiltration membrane at 1-2 bar TMP and a crossflow velocity of 1.5 m/sec. It was observed that the flux rate decreased from 90 $\text{lt}/\text{m}^2\text{-h}$ to 15 $\text{lt}/\text{m}^2\text{-h}$ in 80 days.

Gander et al. (2000) compared two different membrane materials, polysulphone and polypropylene using flat sheet modules with nominal pore sizes of 0.4 μm and 5 μm respectively. The initial flux of the polypropylene membrane was much higher (162.5 $\text{lt}/\text{m}^2\text{-h}$) than the polysulphone membrane (45 $\text{lt}/\text{m}^2\text{-h}$) however the decrease in the flux in the first day was more dramatic for the polypropylene membrane declining to 11.25 $\text{lt}/\text{m}^2\text{-h}$; whilst the polysulphone membrane flux declined to 41.75 $\text{lt}/\text{m}^2\text{-h}$. Steady state fluxes were sustained after 39 days of operation. The polysulphone membrane demonstrated a complete recovery of the flux after a chemical cleaning conducted on the 57th day where on the other hand the polypropylene membrane showed very little recovery. It was concluded that the polypropylene membrane was more prone to an irreversible fouling which was linked either to the pore size or the pore structure of the membrane material.

Chiemchaisri et al. (1992) reported that the intermittent suction could prevent the clogging of membranes to some extent (without any regular cleaning). Ujang et al. (2002) sustained flux rates varying from 0.14 to 0.18 $\text{m}^3/\text{m}^2\text{-day}$ at TMPs in the range of 0.5 to 3.4 kPa. The low operating TMP was linked to the intermittent suction applied to the membrane. Seo et al.(2000) also applied intermittent suction on a 5 min to 5 min basis for suction and pause to a membrane bioreactor where the flux rate was at 0.08 $\text{m}^3/\text{m}^2\text{-day}$ at 10-12 kPa suction pressure.

Günder (2001) operated two membrane bioreactors with flat sheet and hollow fiber modules in which the permeate pump operated at intervals. A filtration period of 8 minutes followed by a filtration pause of 2 minutes was applied, where not permeate was extracted during the pausing interval. Membrane manufacturers and some researchers define the filtration pause as the *relaxation* period. For the calculation of the average flux, the effective permeate volume in an entire filtration cycle was considered. Average flux is defined as the flux during non-steady state conditions with a dedicated time period (Δt) and the corresponding permeate volume (ΔV_p) in which it will be $\frac{\Delta V_p}{\Delta t}$. It was concluded that, with 8 minutes of filtration followed by 2 minutes relaxation intervals, the filtration flux was approximately 25% higher than the average flux for the entire cycle. The hollow fiber MBR was operated in a different sequence compared to the flat sheet MBR. The filtration process was interrupted by a periodic backwash occurring for 20 seconds at the end of 240 seconds of filtration period. As in the flat sheet membranes, the average flux was considered for the entire filtration cycle and it was lower than the flux in the filtration period. The relationship between the permeate volume vs time and the average flux were represented in Figure 2.19.

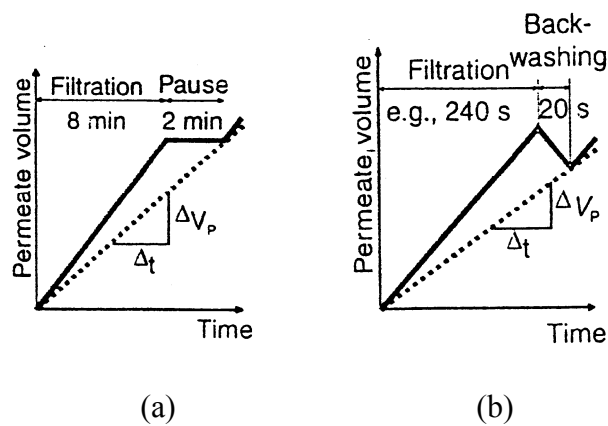


Figure 2.19: Relationship between the permeate volume and time (a) flat sheet membranes, (b) hollow fiber membranes (operational sequence) (Günder, 2001)

When the two plants were compared in terms of hydraulic performance, it was observed that the hollow fiber plant exerted higher transmembrane pressure at lower flux rates where this was vice versa for the membrane bioreactor equipped with flat sheet modules. This increase was explained by the influence of the cake layer getting

thicker at higher pressures or fluxes where another possibility foreseen was that the flow resistance on the permeate side of the plate module increased.

It was also concluded that this tendency was not visible for the hollow fiber membranes due to periodic backwashing. The TMP – Flux relationship was compared for flat sheet and hollow fiber in Figure 2.20 (Günder, 2001).

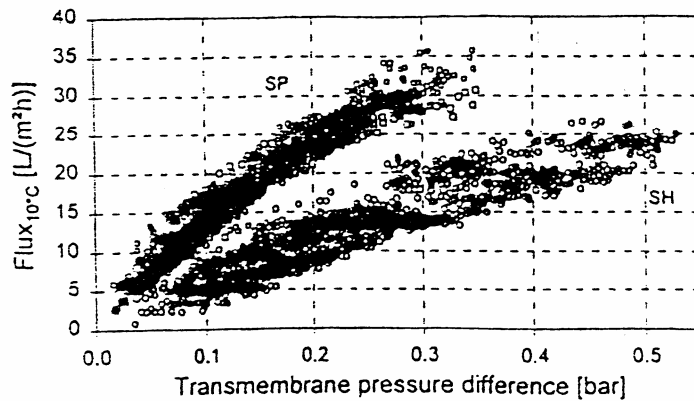


Figure 2.20: Relationship between transmembrane pressure and flux at 10°C (Günder, 2001)

Table 2.8. summarizes the hydraulic operational parameters for various membrane bioreactors equipped with hollow fiber fiber and flat sheet modules.

Chiemchaisri and Yamamoto (1993b) studied the effect of various temperatures on the permeate flux. It was found that a temperature decrease affected the permeate flux not only by increasing the viscosity of the mixed liquor and also by changing the membrane resistance. The increase in viscosity and total membrane resistance contributed in the same degree to the reduction of permeate flux in the 5-15°C range. According to Chiemchaisri and Yamamoto (1993b); the membrane resistance increased by a factor of 2 in the case when temperature is decreased to 5°C from 25°C and the flux gradually declined from 0.3 to 0.17 m³/m²-day where accordingly the transmembrane pressure increased to 85 kPa from 40 kPa.

Table 2.8: Hydraulic performance of various membrane bioreactors with submerged hollow fiber and flat sheet modules

<i>Wastewater</i>	<i>Type</i>	<i>V</i> (<i>m</i> ³)	<i>HRT</i> (<i>h</i>)	<i>Pore size</i> (<i>μm</i>)	<i>Crossflow velocity</i> (<i>m/sec</i>)	<i>Pressure</i> (<i>bar</i>)	<i>Initial flux</i> (<i>lt/m</i> ² - <i>h</i>)	<i>Mean flux</i> (<i>lt/m</i> ² - <i>h</i>)	<i>Specific flux</i> (<i>lt/m</i> ² - <i>h-bar</i>)	<i>Area</i>	<i>Reference</i>
Domestic	HF	3.12	13.4	0.4	-	0.04	16.6	-	4-5	20	Ueda and Hata, 1999
Municipal	HF	3.9	15.6	0.2	-	0.15-0.3	18	60-120	-	13.9	Doreau et al., 2000
Municipal	HF	-	2	0.02	-	0.2	35	175	0.14	-	Cote et al., 1997
Municipal	HF	-	2	0.02	-	0.2	25	125	0.24	8	
Raw Sewage	HF	21.4	13-16	0.1	0.4	0.15	12.1	80.5	-	4	Ueda et al., 1996
Domestic	HF	0.45	12	0.1	0.3-0.5	0.3	16.6	55	-	8	Shimizu et al., 1996
Domestic	HF	2.4	-	0.4	-	-	16.6	-	-	16.8	Murakami et al., 1999
Household	HF	0.04	10-15	0.1	-	0.04	10	166-250	-	0.5	Nah et al., 2000
Municipal	FS	-	7.6-11.4	0.4	0.5	0.03	20.8	69.4	-	-	Ishida et al., 1993
Greywater	FS	0.07	-	0.4	0.5	0.03	7.9	263	-	0.24	Jefferson et al., 2000
Municipal	FS	0.035	-	0.4	-	0.03	7	233	-	0.24	Gander et al., 2000
Municipal	FS	0.035	-	5	-	0.03	5	166	-	0.24	Gander et al., 2000
Municipal	FS	-	-	0.04	0.5	-	-	-	-	-	Gander et al., 2000b
Municipal	FS	-	-	-	-	0.1	27-32	270-320	-	240	Judd, 1997; Churchouse, 1997
Domestic	FS	3.12	13.4	0.4	-	0.17	16.6	98	-	20	Ueda and Hata, 1999
Municipal	FS	-	-	-	-	-	10	-	-	-	Kraft and Mende, 1995

HF: Hollow fiber ;PF :Plate frame

Oginer et al.(2002) concluded that the use of empirical relation between $d(\Delta P)/dt$ and J , obtained in short term experience is not adequate to predict the MBR performance for the long term. It is noted that the reversible nature of the fouling differs from one case to the other. If the fouling is reversible in the short term, it is noted that in the long term the fouling is irreversible in the first period, where as the major part of the fouling takes place in the second period which is reversible. This dilemma is explained by the fact that fouling can be modelled by an irreversible membrane pore blockage caused by the long contact time of deposited compounds with the membrane's surface.

Meng et al. (2005) investigated the effect of filamentous bacteria on membrane fouling. It was noted that the flocs with negligible filament would lead to severe pore blocking due to their too small floc size, and the flocs with filament would result in the formation of a non-porous cake layer affecting the permeability of the membrane. The excess growth of filamentous bacteria on the other hand led to too much production of EPS (extra cellular polymeric substances) which caused severe membrane fouling. It was finally concluded that the filamentous bacteria and EPS were the main factors governing membrane performance and the growth of filamentous bacteria in the bulk liquid had to be controlled.

2.9 Microbial Population Diversity in Membrane Bioreactors

Although the microbial community in the activated sludge process has been extensively studied, attempts at identifying the nitrifying and denitrifying bacteria and their correlation to nitrogen removal in the membrane bioreactor has been limited. Little information is available on the microbiological aspects of the highly concentrated biomass, which is mostly restricted to examinations with pure cultures. It can be assumed that if operated at high sludge ages, bacteria are facing conditions of extreme competition for the inflowing substrates. Rosenberger et al. (2000) operated a lab scale membrane bioreactor with 15 to 23 gr/l of MLSS where stable biomass concentrations were reached at F/M ratios as low as 0.07 grCOD/kgMLSS-d. Direct microscopic studies showed high amounts of freely suspended cells and at various times also a high number of filamentous bacteria resembling conditions of bulking in conventional activated sludge systems.

It was noted that most of the time only extremely low numbers of protozoa were observed indicating that the finally attained biomass was not controlled by floc forming activity. According to the findings, it was concluded that the bacteria in a highly concentrated sludge of a membrane bioreactor are not in a physiological state characteristic for growing cells which is linked to substrate limiting or in other words low F/M conditions. The highly concentrated sludge offers the advantage of high degradation rates with less sludge production compared to conventional activated sludge systems.

Sofia et al.(2004) used fluorescence in situ hybridization (FISH) technique to investigate the bacterial community involved in removing nitrogen from sewage and their preferred DO environment within in an anoxic/oxic membrane bioreactor. The results showed that *Nitrosospira* spp. and *Nitrospira* spp. were the predominant groups of ammonia and nitrite oxidizing group respectively. It was observed that nitrifying bacteria *Nitrosospira* spp. and *Nitrospira* spp. were located in the middle of the flocs, whereas the *Paracoccus* responsible for denitrification were found on the outside of the flocs as shown in Figure 2.21. The occurrence of the denitrifiers and nitrifiers at different locations suggested that the selection resulted from different growth rates and it was further concluded that the bacterial groups with higher growth rates (denitrifiers) dominated the outer floc layers while those with lower growth rate (nitrifiers) concentrated inside the flocs. The distribution of the nitrifiers and denitrifiers were also affected by the concentration of DO in the bulk liquid. These findings are very important to assess and mechanistically understand the behaviour of simultaneous nitrification and denitrification in MBRs.

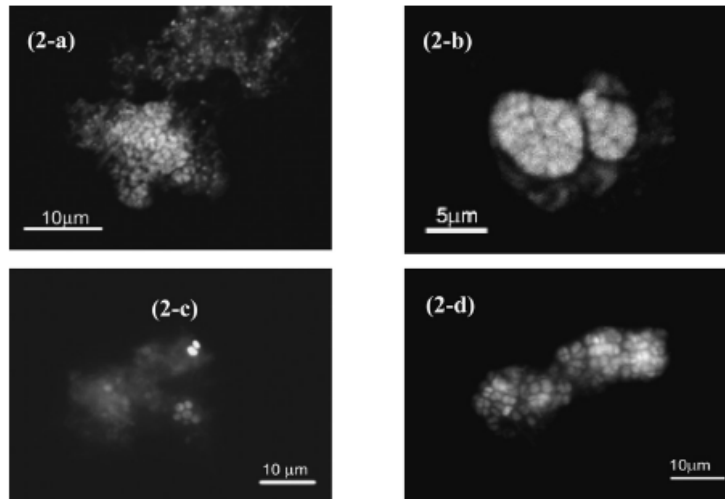
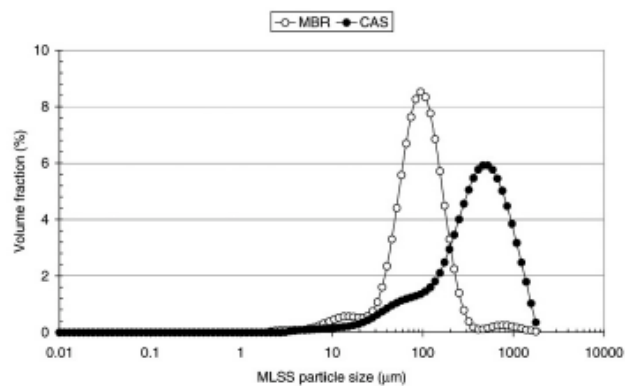
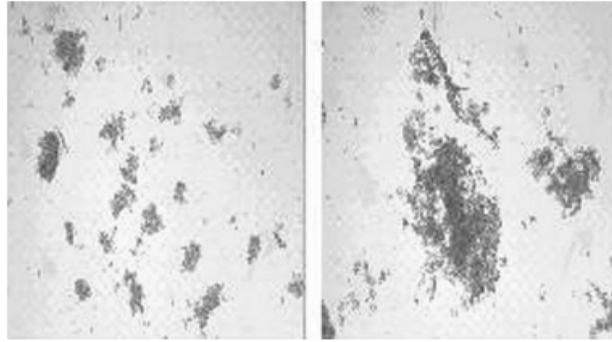


Figure 2.21: Clusters of *Nitrosospira* spp. (2-a), clusters of *Nitrosospira* spp. (2-b), genus *Paracoccus* cells (2-c,2-d), (Sofia et al.,2004)

Meng et al.(2005) observed the dominance of the filamentous bacteria in a microfiltration membrane bioreactor. It was stated that the filamentous bacteria form the backbone of activated sludge flocs to which floc forming bacteria attach by means of EPS and form strong flocs. However, an excess of filamentous bacteria would produce an abundance of filaments extending from the flocs into the bulk solution producing a bridging which prevents the agglomeration of floc particles (Sezgin et al., 1978). The flocs with excess filamentous bacteria have a high viscosity for the increase of EPS in sludge suspension. Smith et al. (2003) reported that MBRs include no sedimentation stage and consequently bacterial groups that are associated with floc formation no longer have an advantage hence dominance in the population will be by smaller sized flocs as can be seen in Figure 2.22 a,b.



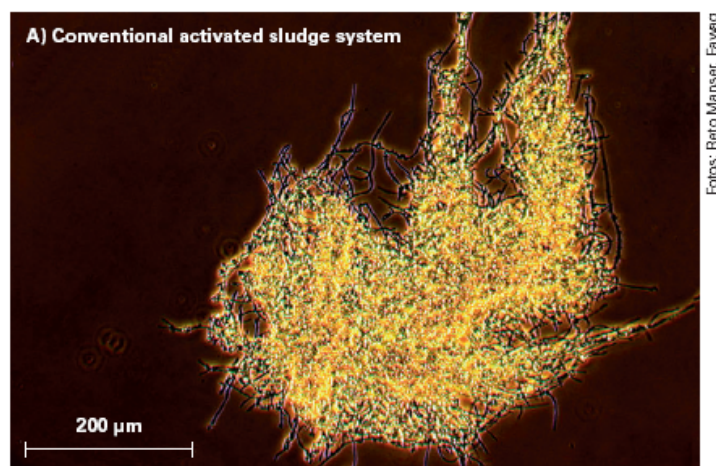
(a)



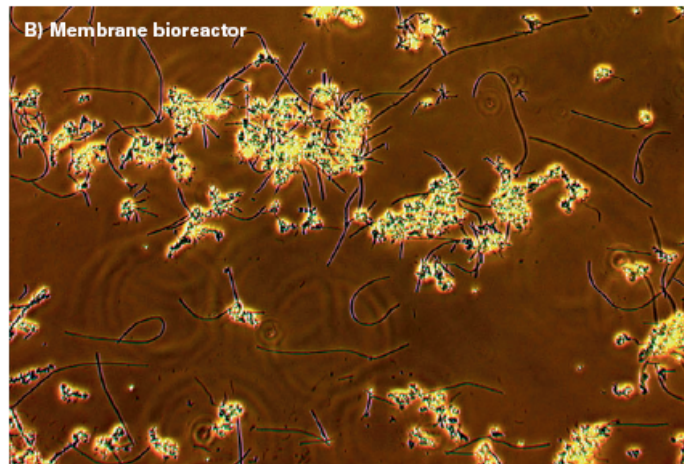
(b)

Figure 2.22: (a) Mixed liquor size distributions for membrane bioreactors and conventional activated sludge plants at 30 day sludge age, (b) Example photographs of biomass for the membrane bioreactor and conventional activated sludge plant at a 30 day sludge age (Smith et al., 2003)

Manser et al. (2005) compared the floc size and morphology of bacterial cells in a membrane bioreactor and a conventional activated sludge system. They concluded that floc size in membrane bioreactors were always smaller than in the conventional system (Figs. 2.23a and 2.23b). Flocs from the conventional plant had a mean diameter of 200–500 μm , although the size showed considerable seasonal variation. In the membrane bioreactor, the sludge received flocs with a diameter of approximately 100 μm at the beginning of the project and after almost 2 years of operation the floc size had declined to no greater than 40 μm .



(a)



(b)

Figure 2.23: Phase-contrast micrographs of activated sludge flocs from the (a) conventional activated sludge with a secondary clarifier (b) from the membrane bioreactor (Manser et al., 2005)

They also concluded that nitrifiers generally form dense clusters of 10–10,000 cells, growing only in the floc interior (Fig. 2.24, yellow stains). They are presumably overgrown by more rapidly replicating heterotrophic bacteria (i.e. bacteria dependent on organic substances).

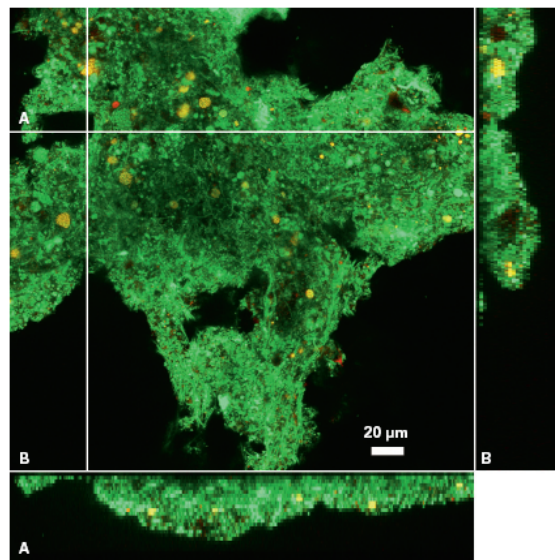


Figure 2.24: Confocal laser scanning microscopic sections through an activated sludge floc, stained with gene probes. Green: general probe for all bacteria; Yellow: specific probe for a group of ammonia-oxidizing bacteria.

2.10 Proposed Biological and Hydraulic Models for Membrane Bioreactors – A Review of Previous Studies

Various models have been proposed to understand the behaviour of membrane bioreactors treating domestic sewage. The models mainly focused on the physical aspects of the membrane bioreactors rather than the biological conversions taking place in the bulk liquid or in the biofilm formed on the surface of the membrane. The biological models proposed so far were lacking in explanation of especially nitrification and denitrification taking place in membrane bioreactors with highly concentrated biomass. Moreover, simultaneous nitrification denitrification capability of membrane bioreactors could not yet be fully explained. It is observed that dynamic modelling and calibration of models adopted to membrane bioreactors need to be further emphasized on. The physical models proposed in the previous studies on the other hand, focused on the mechanistic understanding of the hydraulic behaviour and flow resistance offered by the membrane.

Although the hydrodynamic behaviour of a membrane can be modelled and calibrated, still no solid mechanistic explanation could have been derived for understanding the fouling mechanism.

Lu et al. (2000) adopted a model for an intermittently aerated membrane bioreactor by incorporating the concept of soluble microbial product formation (SMP) into the activated sludge model No.1 (Henze et al., 1987).

The soluble microbial products were classified and incorporated into the model in two groups defined as utilization associated products and biomass associated products. The modelled system was operated in an intermittent aeration mode with aerobic cycle followed by an anoxic cycle for the removal of nitrogen based on 60/120 minutes sequence. A highly concentrated synthetic wastewater was used in the study where the influent COD and influent TKN were 2820 mg/lit and 720 mg/lit respectively. The model exerted good results against measured values in terms of the formation of soluble microbial products however it lacked in the explanation of simultaneous nitrification and denitrification. Separate environments were created within the reactor by turning the aeration on and off which cannot be attributed to a true simultaneous nitrification and denitrification and it can be concluded that it is no different than a conventional sequencing batch reactor operating regime. The model

showed no dependence and sensitivity to varying dissolved oxygen concentration in the bulk liquid which is very skeptical in a very concentrated biomass which further attention should be given to. The model should have included and investigated the temperature effect on the biochemical reactions in the membrane bioreactor. The adopted model provided a rational explanation in defining the total COD in the permeate dominantly consisting of soluble microbial products where it was increased with respect to increasing sludge age where the minimum effluent COD was detected at a sludge age of 20 days.

Lu et al. (2003) again proposed a model for the soluble microbial product formation in MBR by incorporating the concept into activated sludge model No.3 (Gujer et al., 1999).

It was found that SMP could not be ignored and it contributed to about 15% of the total COD in the reactor under a hydraulic detention time of 12 h and a sludge age of 10 days.

The effect of soluble microbial product formation on membrane fouling was investigated by Cho et al. (2003) through the combination of ASM No.1 with a membrane resistance in series model. The ASM No.1 was modified to incorporate the formation of soluble microbial products for the correct assessment of its impact on membrane fouling. From obtained results it was concluded that when the F/M ratio was less than 1.2, SMP would be considered as the main factor affecting membrane fouling in low SRT but TSS would appear to be the most important parameter to control membrane fouling. The SMP production was closely linked to biological kinetic parameters and it was noted that fouling in membrane systems should not be controlled apart from biological factors such as total suspended solids, sludge age and the F/M ratio. Wintgens et al.(2003) developed an integrated membrane bioreactor model for hollow fiber microfiltration MBR, consisting of a compartment describing the activated sludge process to account for the biological treatment performance and an element to describe the permeability of the filtration unit. The biological model was based on ASM 3 (Gujer et al., 1999) whilst the filtration was based on the resistance model.

Semmens and Shanahan (2005) developed a multi species biofilm model that includes aerobic heterotrophs, nitrifiers, denitrifiers, and acetoclastic methanogens in a membrane bioreactor. The model was used to predict the behaviour of the

membrane aerated biofilms under different operating conditions. As experienced in the other biofilms, the model was based on various assumptions which is believed to hinder the true understanding of the biological reactions taking place. The most important assumption was that *no growth or substrate removal occurs in the bulk fluid* which cannot be generalized for MBRs even a thick cake layer or biofilm forms on the surface of the membrane. The behaviour of the model was very sensitive to the diffusion coefficients. Semmens and Shanahan (2005) described the biofilm as a layer that is made up of different environments each responsible for certain biological reactions.

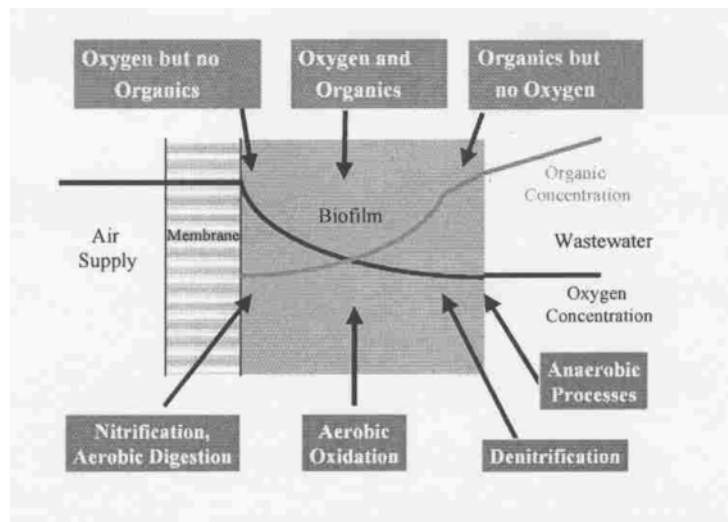


Figure 2.25: Different environments in a membrane aerated biofilm (Semmens and Shanahan,2005)

The effect of air sparging (AS), backflushing (BF) and combined application of both (AS+BF) were incorporated into the resistance model by Psoch and Schiewer (2006) to investigate the enhancement on permeate flux compared to non-enhanced filtration (NON). Scanning electron microscope (SEM) measurements of cake thickness served for evaluating cleaning effectiveness and as input data for the model calculations. It was concluded that the major factors that affect the resistance model are the geometric properties of the cake layer, i.e. cake layer thickness and specific surface area. The cake porosity and cake layer compression have significant but considerably smaller effect on resistance. The experimentally determined internal fouling resistance varied only by a factor of 2 between different techniques, decreasing in the order of NON>BF>AS+BF>AS. According to the resistance model and SEM observations, the combination of air sparging and backflushing showed the

highest flux yield and lowest total resistance over the investigated time. For AS+BF as well as AS, the total resistance was less than twice the membrane resistance, whereas for NON the cake resistance alone was already five times the membrane resistance.

3 MATERIALS and METHODS

A pilot scale membrane bioreactor was setup to investigate the biological and hydrodynamic behaviour of MBRs treating domestic sewage. Prior to setting up of the system an extensive investigation was carried out by reviewing the existing pilot and full scale MBRs. The purpose of this investigation was to compile the advantages and disadvantages of certain systems treating domestic and industrial sewage to guide in the selection of the new system to be used in this study.

3.1 MBR Selection

The major criteria considered in the selection of the new system were;

- Investment and operation costs,
- Technique used for maintaining a constant thickness of cake layer,
- Techniques used for extracting the permeate,
- Necessity for chemical in-situ cleaning,
- Flexibility for application of certain biological process schemes
- Pretreatment requirements,
- Membrane failure and ease of replacement,
- Placement of the membrane modules (submerged or external)

External MBRs require high recirculation flows which in turn needs high capacity pumps and thus consume much more power when compared to submerged MBRs. This was the main reason for the application of submerged systems to mid and large full scale membrane bioreactor plants around the world. The air entrained inside the pipes has also a negative impact on suction performance. Therefore the external membrane filtration systems were discarded from the selection.

Yamamoto et al.(1989) were the first researchers to introduce submerged membrane systems.

As explained in the previous chapter there were two types of submerged systems; (1) *Flatsheet (non-wovens)*, (2) *Hollow fiber (wovens)*. Hollow fiber membranes requires the extraction of the permeate with 40-80 kPa of suction pressure and periodic backflushing with air sparging. The backflushing is set to be occurring every 15 minutes for a duration of 0.5 to 1 minute with high flows. It has been reported that, due to this intensive backflushing the holes located on the fibers are prone to becoming larger year by year which can have an adverse effect in permeate quality within 5 years especially breakthrough of bacteria and viruses. Flatsheet membranes on the other hand offer the advantage of gravity permeate flow through the membranes without employing a suction pressure. The advantage of having a gravity flow is that it requires low transmembrane pressure which in turn has a positive effect on membrane fouling. Flatsheet membranes also have the flexibility to employ suction for the extraction of the permeate.

Hollow fiber membranes are based on ultrafiltration which have lower cut off sizes than flat sheet membranes based on microfiltration. This necessitates the need for a better pretreatment compared to flatsheet systems. Flatsheet systems only require 3 mm fine screening whilst hollow fiber membranes require 0.75 mm of very fine screening. Due to this very low cut off sizes wovens are also subject to clogging with oil and grease in the reactor.

Hollow fiber membranes require a high degree of automation due to the more number of equipments installed, whereas flatsheet membranes employ a very simple technique for operation and hence automation. The high degree of automation that is employed in hollow fiber membranes tends to increase both investment and operational costs.

Flatsheet membranes have 1538 installations worldwide, whilst hollow fiber membranes only 347 installations, however this statistic differs from the installations done in North America with 168 installation for hollow fiber and 51 installations for flatsheet membranes (Yang et al., 2005). It is suspected that this difference is due to the intensive and fancy marketing strategy conducted by Zenon, a reknown hollow fiber membrane supplier.

For especially specific applications such as extreme conditions of pH, wastewater with high temperatures or with an industrial waste flat sheet systems could be more appropriate because there is a broader choice of membrane and module materials with enhanced mechanical properties and resistance to specific chemicals (Lesjean et al., 2004).

With respect to the advantages and disadvantages explained above for the hollow fiber and flatsheet membranes; it was decided that flatsheet membrane microfiltration technology to be used for this study.

3.2 System Description

A pilot scale flatsheet membrane bioreactor based on microfiltration was set up at a domestic sewage treatment plant. The system was installed at the head works of the treatment plant to enable easy intake of raw sewage coming with the sewer network. The sewerage system feeding the sewage treatment plant was a combined sewer network.

3.2.1 Membrane and module specifications

The membranes had a cutoff size of $0.4\ \mu\text{m}$ where the supplier stated that the cutoff size decreases to $0.04\ \mu\text{m}$ after 3-4 months of operation. The submerged membrane unit manufacturer was Kubota Corporation Inc., Japan and the pilot plant supplier was MBR Wastewater Treatment Ltd., UK. The MBR was operated in a continuous mode where the permeate was extracted with gravity flow by maintaining a certain hydrostatic pressure over the module as schematically shown in Figure 3.1.

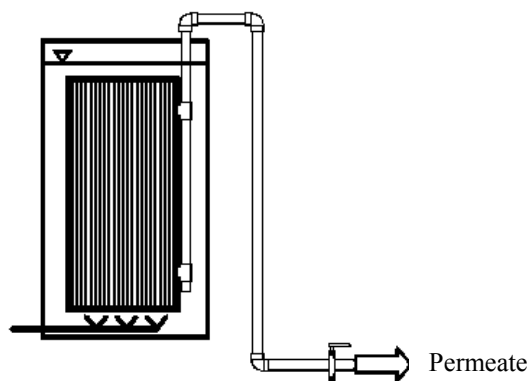


Figure 3.1: Schematic representation of permeate extraction in the pilot plant

No suction pressure was applied to the membranes during the entire operation. The driving force to achieve the desired permeate flow was established by maintaining a constant liquid level within the MBR tank. Table 3.1 summarizes the specifications for the flatsheet submerged membrane unit.

Table 3.1: Specification of the Kubota submerged membrane unit

<i>Parameter</i>	<i>Value/Description</i>
Mode	XL-10
Membrane Material	PVDF
Cartridge Number	10
Membrane Case Dry Weight	55
Membrane Case Maximum Weight*	100
Pore Size	0.4 μ m
Effective Membrane Area	8
Initial Flux with Clean water, minimum	0.42 m ³ /m ² -h
Aeration Type	Coarse bubble
Min diffuser air supply rate	0.13 m ³ /min
Max air supply Rate	0.2 m ³ /min
Filtration Pressure	20 kPa or lower
Water Temperature	5-40°C
In situ chemical cleaning	Sodium hypochloride, NaOCl (%0.5 solution) and oxalic acid %1 or less
In situ chemical cleaning period	6-12 months
Chemical injection pressure	7 kPa
MLSS concentration	8-25 g/l
pH Operation	5-10
Expected lifetime	10-20 years

Schematic of the submerged membrane unit is seen in Figure 3.2 and the pictures are shown in Figure 3.3.

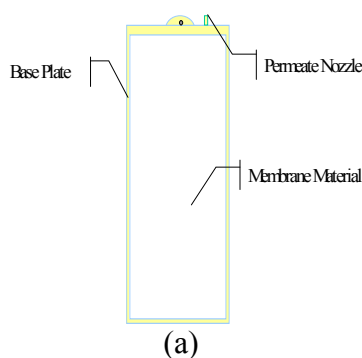
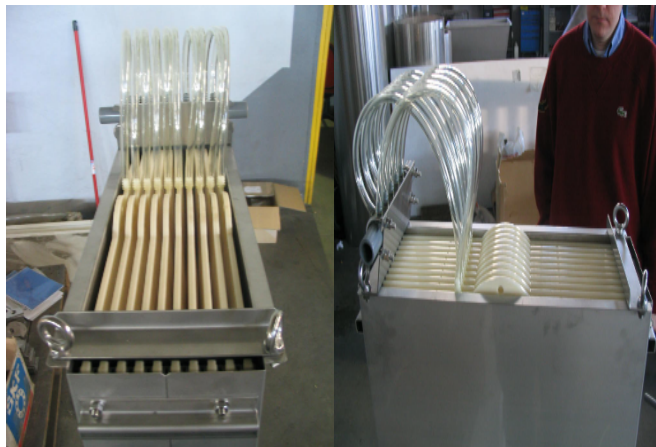


Figure 3.2: Schematics of (a) membrane panel (b) submerged membrane unit

The membrane panel consists of a base plate with a network of shallow grooves and a permeate nozzle. A flat felt material layer either side of the base plate which acts as a spacer between the membrane sheet and the flat ABS support. This felt material also acts as an emergency filter layer.



(a)



(b)

Figure 3.3: Pictures of the (a) submerged membrane module, (b) flatsheet membrane panel

An outer membrane sheet manufactured from poly-olefin with a pore size range of 0.1 to 0.4 μm covers the felt layers on the either side of the base plate. The membrane panels are placed 7 mm apart inside the submerged membrane unit. The permeate tube connects each membrane panel to the permeate manifold. This manifold connects the membrane panels via their individual permeate tubes to the permeate pipeline that transfers permeate out of the membrane bioreactor.

3.2.2 Pilot membrane bioreactor plant specifications

The pilot membrane bioreactor setup was arranged to have a predenitrification biological process scheme with the flexibility to incorporate an anaerobic reactor for biological excess phosphorus removal. It also had the flexibility to include an additional aeration compartment called the “fine bubble diffused aeration (FBDA)” tank to enable to work with high strength industrial wastewater. The purpose was to increase the hydraulic detention time. Specification of the pilot plant is illustrated in Table 3.2.

Table 3.2: Specifications of the pilot scale membrane bioreactor

<i>Parameter</i>	<i>Value</i>
<i>Tanks and Equipments</i>	
Total / Effective volume of Inlet Tank	0.27 / 0.20 m^3
Total / Effective volume of Anoxic Tank	0.28 / 0.21 m^3
Total / Effective volume of MBR Tank	1.5 / 1.20 m^3
Total / Effective volume of FBDA Tank	5.3 / 3.9 m^3
Volume of intermediate inlet lift station	0.7 m^3
Total/ Effective volume of permeate tank	0.28 / 0.25 m^3
Pretreatment	Two stage, 1 st stage 1 mm static screen, 2 nd stage ,0.75mm basket screen
Raw Sewage Pump	Submersible, 5 m^3/h , 5mwc
Intermediate lift pump	Submersible, 0.5 m^3/h , 6mwc
Sludge recirculation pump	Horizontal shaft, centrifugal, 1.5 m^3/h , 5mwc
Air Blower	Lateral channel, centrifuge, 40 m^3/h , 400mbar
Washwater pump	Horizontal shaft, centrifugal, 122 m^3/h , 2 bar
Aeration type in MBR tank	Coarse bubble
Aeration type in FBDA tank	Fine bubble diffused aeration with 9 ,9” membrane disc diffuser
Anoxic Tank mixer	Flash mixer, 0.18 kW

Instrumentation

Oxygen Meter	Qty :2; in MBR and FBDA tank
ORP meter	Qty : 1, in Anoxic tank
Flowmeter	Qty:3, on inlet line, on recirculation lline and on permeate line
pH Meter	Qty:2 , in inlet tank and MBR tank
Static Pressure meter and sensor	Qty:1 , in MBR tank
Dynamic pressure meter and sensor	Qty:1; on permeate line
Level sensors	Qty: 3, in intermediate lift tank, in inlet tank and in MBR tank

The pictures of the pilot plant is shown in Figure 3.4. The setup of the pilot plant is shown in Figure 3.5.



Figure 3.4: Pictures of the pilot plant

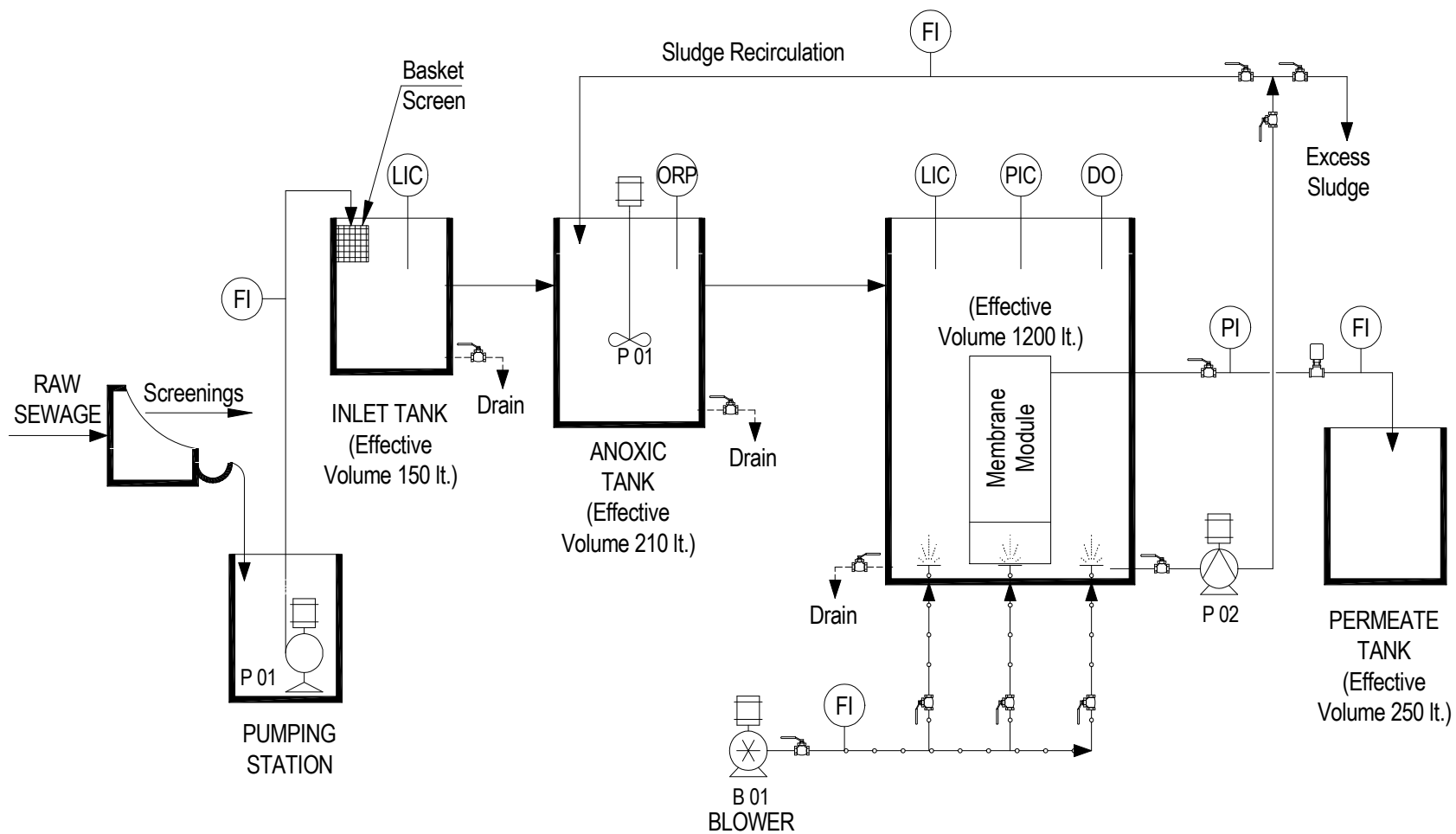


Figure 3.5: Schematic setup of the pilot plant

The system is designed so that all the tanks could be drained in case of emergency.

The raw sewage was passed through a static screen prior to being gravitated to an intermediate storage tank. As explained above the system was installed in a wastewater treatment plant where the raw sewage was transported by a combined sewer network. In the beginning of the operational period there was only one meshed basket screen with an opening of 1 mm, however due to the high amounts of debris and rags being transported within the sewer system causing clogging of the inlet pipework, an additional static screen with an opening of 0.75 mm was installed. The intermediate storage tank served two purposes; (1) collecting of raw sewage to be fed to the pilot plant during night times in case of extremely low flows, (2) serving as a pump station.

The intermediate pump transferred the screened sewage to the inlet tank where it was passed through the basket screen. The pump operated in an interlock mode with the level sensors installed in the inlet tank and the membrane tank. The main purpose of the inlet tank was to avoid the raw sewage coming in direct contact with the membranes and to avoid any grease or fine materials passing to the downstream tanks. The raw sewage then passed to the anoxic tank and then to the membrane tank by gravity. Anoxic tank was arranged so that the process had a predenitrification scheme. The anoxic tank was mixed by a surface flash mixer to keep the content in suspension and it was monitored through an oxidation-reduction potential (ORP) for the purpose of keeping a track of the level of nitrate reduction (denitrification) taking place within this tank.

The MBR tank was arranged as a completely mixed reactor where the membrane module was installed. The air necessary for scouring and for the biochemical reactions taking place was supplied through a blower and coarse bubble aeration system. The equilibrium between the amount of foulants building up on the cake layer and the amount that is removed by the shear forces was balanced through the cross flow velocity generated by the air introduced to the membranes. The oxygen level was monitored and recorded by the oxygen meter installed in this tank. The static pressure meter and the level sensor provided the MBR tank to have constant liquid level conditions for the hydrostatic pressure needed for permeate extraction.

Additional perforated diffuser pipes were added to the MBR tank during the summer season when there was a lack of oxygenation due to high air and wastewater temperature and high MLSS concentrations. The amount of air blown in to the new perforated diffuser pipes were adjustable. Temperature meter was also installed in anoxic, MBR and FBDA tanks.

The recirculation pump was installed to pump nitrate rich mixed liquor of the MBR tank back to the anoxic tank for denitrification. The pump had the capacity to adjust the recirculation flow in the range of 1Q to 8Q. The amount of recirculated flow was monitored and recorded by an electromagnetic double flange flowmeter. The excess sludge was wasted by a valve installed on the branch taken from the recirculation line. The FBDA tank was equipped with 9 nos of 9” membrane disc diffusers for fine bubble aeration in case of treating high strength domestic sewage. The level of dissolved oxygen was monitored by an oxygen meter.

The permeate line was equipped with a dynamic pressure meter, flow meter and an automatic valve. The amount of permeate and the pressure on the permeate was monitored and recorded continuously. The permeate of the system was collected in a covered permeate tank for sampling and visual control of the effluent. The amount of air introduced both into the MBR and FBDA tanks were monitored by vertically installed rotometers and it was adjustable by air valves installed in each line. The blower is equipped with a frequency converter to adjust to the varying demand of oxygen. The washwater pump was used to inject air into the coarse bubble diffusers through the air line to prevent clogging and blockage of the diffusers by highly concentrated sludge resulting in a possible decreased oxygenation efficiency. The control strategy of the pilot plant is as follows :

The Feed Pump

- a. The flow rate is set manually by valve.
- b. Normally operates with a constant flow, continuously 24 hours.
- c. The flow – rate will be checked manually by a V-notch at 2 points:
Inlet Tank and Wash Tank.
- d. Pump will be cut-out when one of the following conditions will occur:
Water level in Pump station – “low”
Water level in Inlet Tank – “high” (checked by electrode sensor)
Water level in Membrane Tank – “high” (checked by Ultrasonic device)
If the blower is switched off

Blower

Controlled manually by valves (flow rate will be checked by Rota meters of FBDA Tank and Membrane Tank).

Sludge Recirculation Pump

Controlled manually by valve (flow rate will be checked by V-notch in the Anoxic Tank or FBDA Tank)

Washing Pump

Controlled manually by valve

Alarms on Panel

The feed pump is stopped
The blower is stopped
The sludge recirculation pump is stopped
P-dosing pump is stopped

On-line control devices

- a. Flow meter
- b. Static pressure meter
- c. Dynamic pressure meter
- d. Electrode level meter
- e. DO meter
- f. ORP meter
- g. Blower for DO control with frequency converter
- h. Electrical controlled valves, permeate effluent

There was a blind stoppage along with a valve as branching on the permeate line to enable chemical in-situ cleaning of the membranes. The connection was made to this point from the sodium hypochlorite tank. The piping of the pilot plant enabled the flexibility to take the anoxic tank, FBDA tank and the bio-P tank off service.

3.3 Experimental Program and Testing Procedures

The research program for the pilot scale membrane bioreactor was divided into four experimental periods as shown in Table 3.3.

Table 3.3: List of the experimental periods

	<i>Duration (Days)</i>	<i>Remarks</i>
Run I	310	Constant hydraulic conditions and flux, $\theta_x=38$ d
Run II	43	Constant hydraulic conditions and flux, MLSS between 25.000 -30.000 mg/l, $\theta_x=74$ d
Run III	45	Constant hydraulic conditions without the anoxic tank in operation, $\theta_x=36,5$ d

Following a startup period of 30 days, a constant wastewater flow was supplied to the pilot plant with constant flux rate conditions. This experimental period accounted for the most important part of the research where especially carbon and nitrogen removal capabilities of MBR were investigated with varying operational factors such as dissolved oxygen and temperature. The system was operated under what is recommended to be the optimum conditions for MBRs by the supplier. In the following period the sludge age was increased to 109 days with an MLSS concentration over 35.000 mg/lt. The effects of increased MLSS concentration on biological processes and physical characteristics of the membrane and the effect of recirculation flow on nitrogen removal were investigated in this run. In order to assess the effect of anoxic tank on predenitrification, the system was operated only with the MBR tank. The stand alone performance of only the MBR tank on nitrogen removal was investigated and compared with the results of Run I. The system was operated with the same conditions for Run I. The objective of the final run was to assess the behaviour of the MBR under variable hydraulic conditions and flux. The entire experimental period including the startup period lasted for 615 days. Table 3.4. summarizes the operational figures for each run.

Table 3.4: List of crucial operating parameters for all experimental periods

<i>Parameter</i>	<i>Unit</i>	<i>Run I</i>	<i>Run II</i>	<i>Run III</i>
Influent Flow	m ³ /d	4	4	4-4.5
Recirculation Flow	m ³ /d	12	12	-
Hydraulic detention time	h	8.4	8.4	7.2
Sludge age	days	38	74	36,5
Flux	m ³ /m ² -d	0.5	0.5	0.5
Hydraulic permeability	lt/m ² -h-bar	182-410	175-230	214-260
Waste activated sludge flow	lt/d	36	18	32
MLSS	mg/lt	13,000-16,000	25,000-30,000	17,500-21,000
MLVSS	mg/lt	9,100-12,200	15,000-20,000	12,500-16,000
Temperature	°C	2-28	8-22	18-27
Excess sludge production	kg/d	0.528	0.45	0.498

3.4 Measurement and Analysis Procedure

3.4.1 Data acquisition

The pilot plant was continuously controlled and monitored through online measuring instruments, probes, sensors ...etc.(Figure 3.5) The daily data acquisition campaign is given in Table 3.5.

Table 3.5: Data acquisition campaign during experimental testing

<i>Parameter</i>	<i>Unit</i>	<i>Instrument Specifications</i>	<i>Frequency of Recording</i>
Inlet Flow	m ³ /h	Endress+Hauser, online electromagnetic double flanged type flowmeter with totalizer	Twice, daily
Recirculation Flow	m ³ /h	Endress+Hauser, online electromagnetic double flanged type flowmeter with totalizer	Twice, daily
Permeate Flow	m ³ /h	Endress+Hauser, online electromagnetic double flanged type flowmeter with totalizer	Twice, daily
Air Flow to MBR	Nm ³ /h	Gemü, Rotometer type flowmeter	Once, daily
Air Flow to FBDA	Nm ³ /h	Gemü, Rotometer type flowmeter	Once, daily
O ₂ in MBR	mg/l	Endress+ Hauser,transmitter and probe	Every 2 hours, daily
ORP in Anoxic Tank	mg/l	Endress+ Hauser,transmitter and probe	Every 2 hours, daily
Static Pressure in MBR	kPa	Vega, probe type	Every 2 hours, daily
Dynamic Pressure at Permeate	kPa	Vega, online probe type	Every 2 hours, daily
Temperature in inlet	°C	WTW, portable device	Twice, daily
Temperature in MBR	°C	Endress+ Hauser,transmitter and probe	Twice, daily
pH at inlet		WTW, portable device	Twice, daily
pH in MBR		WTW, portable device	Twice, daily

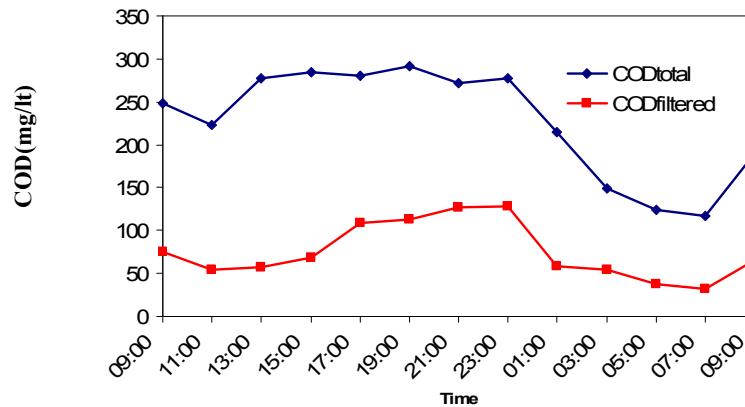
The instruments used to record the necessary data were routinely calibrated to avoid any unwanted errors.

3.4.2 Analytical methods

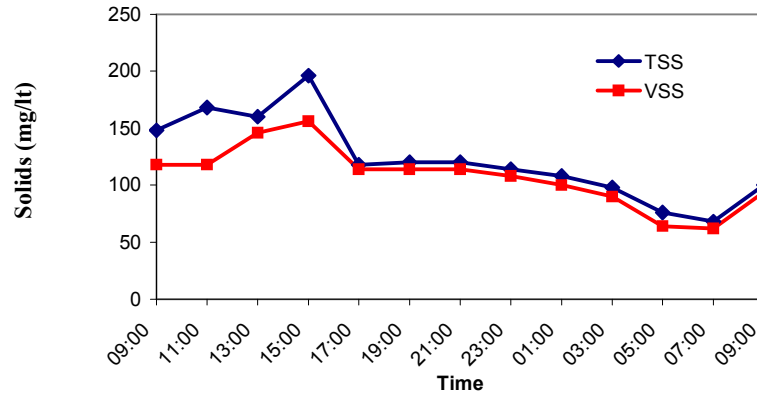
The performance of the MBR in terms of biological processes was monitored regularly by conducting the following analyses on the influent, effluent, anoxic and membrane tank.

- Total suspended solids (TSS)
- Volatile suspended solids (VSS)
- Chemical Oxygen Demand (COD)
- Ammonium Nitrogen (NH_4^+ -N)
- Nitrite Nitrogen (NO_2^- -N)
- Nitrate Nitrogen (NO_3^- -N)
- Total Kjeldahl Nitrogen (TKN)

The analyses were done on 8 hour (between 08.30 and 16.30) composite samples which reflected the representative sample of the incoming sewage to the wastewater treatment plant for the 24 hour period. Prior to deciding on the sampling interval for making composite samples, analysis were conducted for a 24 h period to find the most appropriate time of interval for composite sampling. The analyses were done on the influent COD and TSS parameters and it was found that the concentrations showed a significant decrease after 23:00 until 07:00 in the morning where afterwards it showed an increase. The interval between the 09.00 and 23.00 were near steady for COD and the same conditions could be accounted for the TSS. Figure 3.6 (a) and (b) shows the daily variations for the COD and TSS parameters respectively.



(a)



(b)

Figure 3.6: Daily variation of (a) Influent COD and (b) Influent TSS,VSS

Due to the nature of the sewer system the influent wastewater parameters showed significant fluctuations especially in rainy weather.

The methods for analysis used in the study are summarized in Table 3.6.

Table 3.6: Analysis methods

<i>Parameter</i>	<i>Method</i>	<i>Reference</i>
Total suspended Solids (TSS)	2540 D.	Standard Methods for the Examination of Water and Wastewater 19 th Edition, 1995
Volatile suspended Solids (VSS)	2540 E.	Standard Methods for the Examination of Water and Wastewater 19 th Edition, 1995
Chemical Oxygen Demand (COD)	5220 D.	Standard Methods for the Examination of Water and Wastewater 19 th Edition, 1995
Ammonium Nitrogen (NH ₄ ⁺ -N)	4500 NH ₃	Standard Methods for the Examination of Water and Wastewater 19 th Edition, 1995
Nitrite Nitrogen(NO ₂ ⁻ -N)	4500 NO ₂ ⁻	Standard Methods for the Examination of Water and Wastewater 19 th Edition, 1995
Nitrate Nitrogen (NO ₃ ⁻ -N)	4500 NO ₃ ⁻	Standard Methods for the Examination of Water and Wastewater 19 th Edition, 1995
Total Kjeldahl Nitrogen (TKN)	4500 N _{Org}	Standard Methods for the Examination of Water and Wastewater 19 th Edition, 1995
Biological Oxygen Demand (BOD)	5210	Standard Methods for the Examination of Water and Wastewater 19 th Edition, 1995

All analyses and sampling were performed in accordance with the Standards Methods for the Examination of Water and Wastewater, 19th Edition (APHA, AWWA and WEF, 1995).

Merck SQ Nova 60 wideband spectrofotometer and it's thermoreactor were used throughout the study. At the beginning of the study, Ion Chromotographic methods were used for the determination of all the anions and cations where afterwards this was not used.

Fluorescence in-situ hybridization (FISH) analysis of biomass samples was performed to the protocol described by Amann et al. (1995) for the identification and determination of bacterial communities. Oligonucleotide probes were used in the study for this prupose.

3.5 Application of FISH (Fluorescence in situ hybridization) Technique

In this study, the aim was also to identify and quantify the nitrifying bacteria present in a pilot-scale membrane bioreactor treating municipal wastewater by using fluorescence *in situ* hybridization (FISH).

The materials used in the FISH campaign are as follows:

- Phosphate Buffer Saline (PBS) consisting of 130 mM NaCl (provided from BDH GPR™) and 10 mM sodium phosphate (pH 7.2).
- Paraformaldehyde ((CH₂O)_n) provided from BDH GPR™.
- Absolute ethanol (C₂H₅OH) provided from Carlo Erba Reagents.
- Agarose provided from BDH Electran.
- +4°C refrigerator provided from Arçelik (Turkey).
- -20°C deep freezer provided from Arçelik (Turkey).
- Microfuge^R 18 Centrifuge provided from Beckman Coulter, Inc.
- Roller – Blot Hybridizer HB – 30 provided from Techne

The samples were taken from the oxic tank where nitrification takes place and were prefixed at site using absolute ethanol (1:1 (v/v)). They were stored in cool boxes at 4°C until the arrival to the laboratory. The samples were kept at -20°C and fixed at the same day as the sampling.

Using phosphate buffer saline (PBS), 500 µl of activated sludge – ethanol mix was washed and resuspended in 0.25 ml of PBS. After washing 0.75 ml of freshly prepared 4% paraformaldehyde (PFA) in PBS was added to the suspension. The suspension was incubated at 4°C for at least 3 hours or overnight. After fixation the samples were washed using PBS and resuspended in 1 ml of PBS – absolute ethanol (1:1, v/v), and they were stored at 20°C.

Total cell counts of the samples were obtained using the universal DNA stain 4',6-diamidino-2-phenylindole (DAPI). Serial dilutions of the fixed samples were prepared with PBS containing DAPI at a final concentration of 3.3 µg/ml and incubated for 15 min. Counts were obtained using an Olympus BX 50 Epifluorescence Microscope equipped with a 100 W high-pressure mercury lamp, U-MWIB and U-MWG filter cubes. Dilutions that resulted in between about 50 and

300 cells per field of view were used for the counts. For each sample counts for 10 random fields of view were obtained, and the average cell count was calculated.

The 16S rRNA-targeted oligonucleotide probes were used in this study in order to target different microbial groups. Figure 2.2 gives the microorganisms associated with nitrification process and the location of these organisms in the phylogenetic tree which the probes used in this study are specifically designed for. The target groups of these probes and their optimum hybridization conditions are given in Table 2.4. All probes were made, labeled and obtained commercially from Qiagen Corp. (Germany).

For each sample, negative controls that are lacking a probe were prepared in order to see the level of nonspecific binding and to monitor autofluorescence. Additionally one positive control was prepared to find out the whole microbial community in the MBR activated sludge sample.

50 μ l of the fixed samples were first washed once using PBS solution and dehydrated by applying the sample to increasing concentrations of ethanol (50, 80 and 100 % v/v) at room temperatures. After dehydration the samples were fixed on gelatin-coated slides. 13 μ l of hybridization buffer and 2 μ l of probe were added on the fixed cells. Following these additions, the samples were hybridized at the optimum hybridization temperature given in the literature for three hours. In the last 10 minutes of hybridization the samples were stained with 4 μ l of DAPI. After hybridization, the samples were washed twice in a washing buffer for 15 minutes at the optimum washing temperature and after washing a final washing procedure with MilliQ water was applied.

Slides were visualized by using an Olympus BX 50 Epifluorescence microscope equipped with a 100 W high-pressure mercury lamp and a Spot RT charged coupled device (CCD) camera having a special software supplied by the camera manufacturer (Diagnostic Instruments Ltd., UK). The obtained images were processed and analyzed with Image-Pro Plus version 5.1 image analysis software (Media Cybernetics, USA). The hybridized microorganisms were visualized from the fluorescence image obtained.

Using DAPI images and probe images the quantifications results were obtained and rated. Finally percentage values for each probe were calculated.

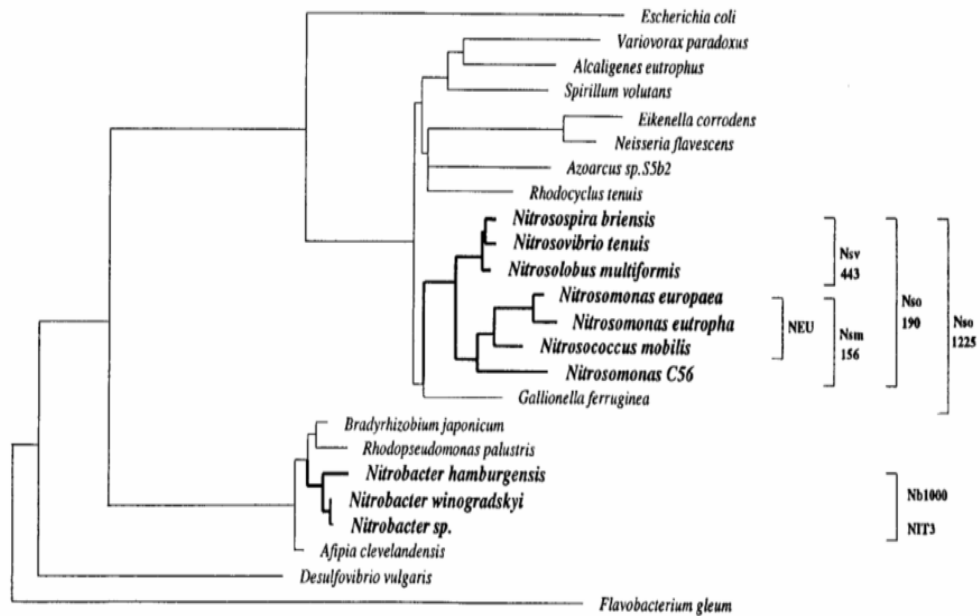


Figure 3.7: Phylogenetic tree inferred from comparison of 16S rRNA sequences. (Target organisms for probes Nso190, Nso1225, Nsm156, Nsv443, NEU, NIT3, and Nb1000) (Mobarry et al., 1996)

3.6 Tools used for Modelling

Computer simulators were used to assess and model the behaviour of MBRs treating domestic sewage. A simulator is a computer program that allows the user to link various unit processes together (such as bioreactors and clarifiers) according to the flow scheme of a particular treatment plant and then to assess the performance of the plant for specified operational and influent loading conditions. The simulator may also incorporate models describing unit processes beyond the activated sludge system such as chemical precipitation, anaerobic digesters and sludge handling processes. Each unit process incorporates one or more mathematical models of which the bioreactor model usually is the most complex.

The potential benefit of simulators in the analysis, design and operation of wastewater treatment plants is widely recognized. Such tools can provide a better understanding of the mechanistic basis of models, in that they allow users to appreciate system responses to changes in control variables. Simulators may also be used effectively for the calibration of complex models.

Two different simulators were used in this study as they are concentrated on different aspects of MBRs.

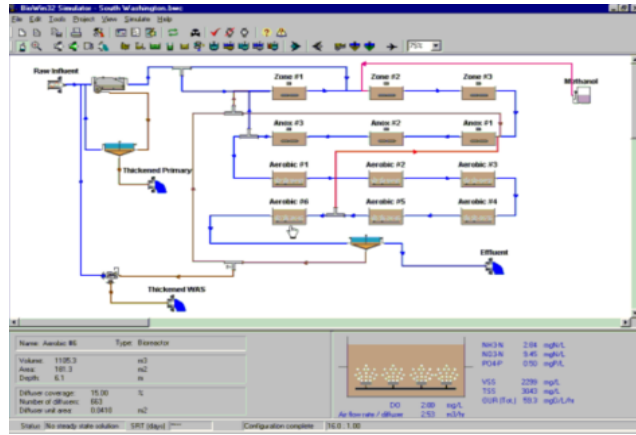
1. BioWin 2.2® by EnviroSim Associates Ltd.
2. GPS-X® by Hydromantis, Inc.

BioWin 2.2 was used mainly for the assessment and calibration of biological reactions and the kinetic model proposed, while on the other hand GPS-X was used for the mechanistic explanation of the physical behaviour of the MBR used in this study. Therefore the study can be considered in two aspects; (1) *Biological performance and calibration of the model proposed*, (2) *Physical performance and calibration of the hydrodynamic model*.

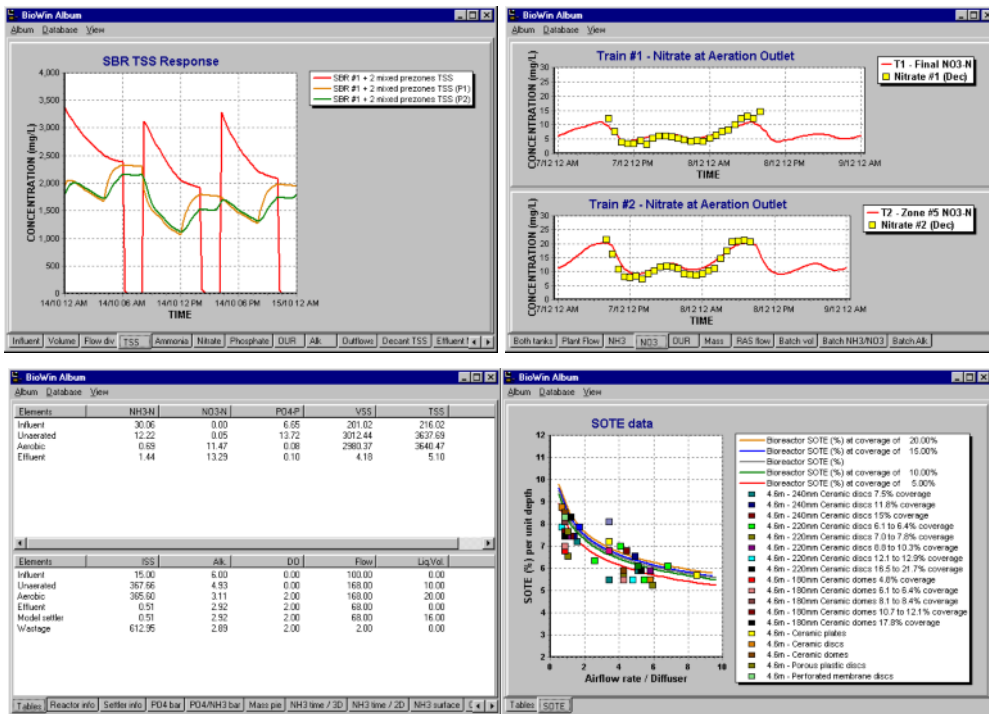
BioWin is a Microsoft Windows based simulator used world wide in the analysis and design of wastewater treatment plants. The latest full plant version 2.2 was used in this study in which the major aspects of the simulator can be listed as;

- It contains an integrated biological model for BNR activated sludge, fermenters and anaerobic digesters,
- Models pH changes in addition to alkalinity in activated sludge and digesters,
- Includes a specific methanol utilizing biomass population,
- Predicts struvite and hydroxyapatite formation
- Includes the membrane bioreactor process module,
- Predicts digester biogas composition including CO₂, CH₄ and H₂.
- Includes dynamic settling state point analysis (SPA) diagrams
- Includes a single model matrix as opposed to interfacing multiple disparate models.
- Includes a model builder unit where the users can enter their own process matrix and define the relevant processes, kinetic and stoichiometric coefficients.

The BioWin 2.2. user interface and the album pages which show the results can be seen in Figure 3.7.



(a)



(b)

Figure 3.8: (a) BioWin 2.2. user interface, (b) album pages of BioWin

BioWin is used by many contracting, consultancy companies as well as academic institutions and public utilities. On the other hand BioWin has been referenced in many technical papers. Due to the extensive list of clients and technical papers referencing BioWin, only the major clients list and some of the technical papers referencing BioWin are listed in Tables 3.7. and 3.8 respectively.

Table 3.7: Client list of BioWin

<i>Engineering Service Companies</i>	<i>Academic Institutions</i>	<i>Public Utilities</i>
Binnie Black & Veatch	Clemson University	Thames Water
Biwater International	Georgia Institute of Tech	Brisbane Water
Brown & Caldwell Env. Eng. and Consultants	University of Washington	City of Cape Town
CDM	Virginia Polytech.Inst.	District of Columbia Water & Sewer Authority
CH2M Hill	University of British Columbia	MPWiK S.A. Krakow
Earth Tech	Kyonggi University	US Army Corps of Engineers
Hazen & Sawyer Env. Eng. & Consultants	Marquette University	City of Atlanta
Metcalf & Eddy	University of Connecticut	South Australia Water Corporation
MWH	University of Central Florida	Alberta Capital Region Wastewater Commission
Parsons	University of Toronto, Civil Engineering Faculty	
Tetra Tech	University of Canterbury	
Western Australia Water Corporation	Iowa State University	
LEMTECH Consulting		
MASS Aritma Sistemleri A.Ş.		
Brentwood Industries		
Burns & McDonnell		

Table 3.8: Some of the technical papers referencing BioWin

<i>No</i>	<i>Technical Paper Reference</i>
1	J.L. Barnard, K. Abraham. Key features of successful BNR operation. Proceedings of the IWA Specialized Conference on Nutrient Management in Wastewater Treatment Processes and Recycle Streams, Krakow, Poland, September 19 – 21, 2005.
2	M. Hintze, S. Pratt, and A. Shilton. Effect of sludge retention time on phosphorus removal in a full- wastewater treatment plant. Proceedings of the IWA Specialized Conference on Nutrient Management Treatment Processes and Recycle Streams, Krakow, Poland, September 19 – 21, 2005.
3	D. Andrews, P. Huck, and O. Natvik. Nitrification / denitrification – a comparison of operational benefits and the removal of pharmaceuticals and personal care products. Proceedings of the IWA Specialized Conference on Nutrient Management in Wastewater Treatment Processes and Recycle Streams, Krakow, Poland, September 19 – 21, 2005.
4	R.M. Jones, P.L. Dold. The importance of considering the interaction between the solid and liquid train in design and operation of biological nutrient removal processes. Proceedings of the IWA Specialized Conference on Nutrient Management in Wastewater Treatment Processes and Recycle Streams, Krakow, Poland, September 19 – 21, 2005.
5	T. Friedrich, J. McLellan, T. Deniz, and J. Milligan. Biological nutrient removal process enhancement analysis of the Marshall Street Advanced pollution control facility, Clearwater, Florida . Proceedings of the Water Environment Federation 78th Annual Technical Exhibition & Conference, Washington, D.C., USA, October 29 – November 2, 2005.
6	L. Lei, R. McCandless, Q. He, P. Olszewski, and J. Coughenour. Use of BioWin as a tool for wastewater treatment plant capacity evaluation. Proceedings of the Water Environment Federation 78th Annual Technical Exhibition & Conference, Washington, D.C., USA, October 29 – November 2, 2005.
7	D. Phagoo, D. Fry, J. Machisko, and J. Penny. Enhanced BNR with MBR – a unique combination. Proceedings of the Water Environment Federation 78th Annual Technical Exhibition & Conference, Washington, D.C., USA, October 29 – November 2, 2005.
8	D. Sen, C.W. Randall. Unified computational model for activated sludge, IFAS, and MBBR systems. Proceedings of the Water Environment Federation 78th Annual Technical Exhibition & Conference, Washington, D.C., USA, October 29 – November 2, 2005.
9	D. Marrs, J. Newman, S. Sen, N. Boswell, M. Lubarsky, and H. Melcer. Field application of WERF low F/M protocol to measure nitrifier growth and endogenous decay. Proceedings of the Water Environment Federation 77th Annual Technical Exhibition & Conference, New Orleans, Louisiana, USA, October 2 - 6, 2004.
10	R. Jones and I. Takács. Modeling the impact of anaerobic digestion on the overall performance of biological nutrient removal wastewater treatment plants. Proceedings of the Water Environment Federation 77th Annual Technical Exhibition & Conference, New Orleans, Louisiana, USA, October 2 - 6, 2004.

Table 3.8. continued

11	C. Tang, P. Prestia, R. Kettle, D. Chu, B. Mansell, J. Kuo, R. W. Horvath, J. F. Stahl. Start-up of a nitrification/denitrification activated sludge process with a high ammonia side-stream: challenges and solutions. Proceedings of the Water Environment Federation 77th Annual Technical Exhibition & Conference, New Orleans, Louisiana, USA, October 2 - 6, 2004.
12	K. Mahoney, J. Mueller, C. Villari, D. Katehis, E. Proffitt. Evaluation of alternative DO control strategies for high rate BNR processes. Proceedings of the Water Environment Federation 76th Annual Technical Exhibition & Conference, Los Angeles, California, USA, October 11 - 15, 2003.
13	A. van Niekerk, J. Ruhl, P. Pitt, D. Parker, S. Kharkar, A. Tesfaye. Upgrading of the nitrification/denitrification facility at the Blue Plains advanced wastewater treatment plant. Proceedings of the Water Environment Federation 76th Annual Technical Exhibition & Conference, Los Angeles, California, USA, October 11 - 15, 2003.
14	R.M. Jones, C.M. Bye, P.L. Dold. Nitrification parameter measurement for plant design – experience with new methods. Proceedings of the Water Environment Federation 76th Annual Technical Exhibition & Conference, Los Angeles, California, USA, October 11 - 15, 2003.
15	P.L. Dold, H.D. Stensel, D.L. Ke, R.M. Jones, C.M. Bye, H. Melcer. Importance of decay rate in assessing nitrification kinetics. Proceedings of the Water Environment Federation 75th Annual Technical Exhibition & Conference, Chicago, Illinois, USA, September 28 - October 2, 2002.
16	J.R. Bratby, B. Gaines, M. Loyer, F. Luiz, D. Parker. Merits of alternative MBR systems. Proceedings of the Water Environment Federation 75th Annual Technical Exhibition & Conference, Chicago, Illinois, USA, September 28 - October 2, 2002.
17	C. Hertle, J. Crofts, R. Whittle, P. Turl, G. Johnston. Picnic bay membrane bioreactors for wastewater treatment at Magnetic Island, Australia. Proceedings of the Enviro 2002 Convention & Exhibition and IWA 3rd World Water Congress, Melbourne, Victoria, Australia, April 7-12, 2002.
18	J.L. Barnard, P. Weston, P. Coleman. Design and operational considerations for the largest SBR plant. Proceedings of the Water Environment Federation 74th Annual Conference & Exposition, Atlanta, Georgia, USA, October 13-17, 2001.
19	C.D.M. Filipe, G. Crawford, B. Johnson, G.T. Daigger. Integrating ASM 2d models into whole plant mass balance simulators. Proceedings of the Water Environment Federation 74th Annual Conference & Exposition, Atlanta, Georgia, USA, October 13-17, 2001.
20	B. Lesjean, P. Sztajn bok, S. Zeghal, H. Buisson. Comparison of three activated sludge processes: conventional, BNR, and membrane (BIOSEP) activated sludge. Proceedings of the Water Environment Federation 72nd Annual Conference & Exposition, New Orleans, Louisiana, USA, October 9-13, 1999.

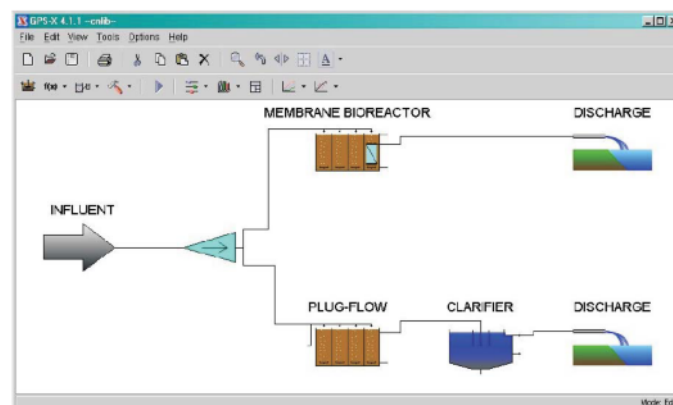
GPS-X 5.0. developed by Hydromantis, Inc. is also special a software program specifically designed for the modelling and simulation of municipal and industrial wastewater treatment plants. Advanced simulating features of GPS-X 5.0 are as follows:

- Customizable open model code (user can change models, can change interface forms, and add new models)
- Contains built in routines for On-Off P,PI,PID and feedforward controller simulation
- Built in PID controller tuning facility
- Automatic sensitivity analysis module for performing steady state, time dynamic and phase dynamic processes
- Optimization module for calibrating models (i.e. parameter estimation) and optimizing processes
- Dynamic parameter estimation module for estimation of time varying parameters using on-line or historical data.
- Model developer module for creating new process matrixes from scratch

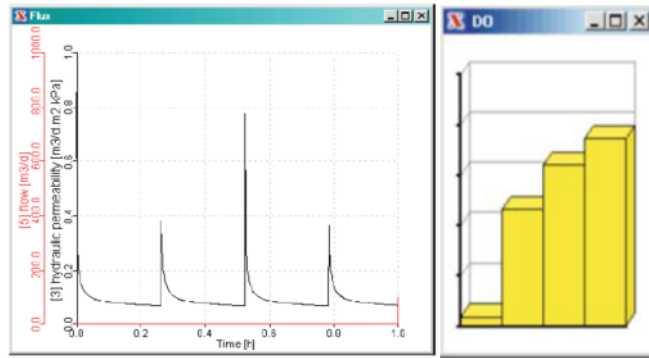
The major advantage of using GPS-X in this study was that it specifically included a MBR model which has the following features;

- Simulation of membrane fouling and it's affect on MBR teratment process
- A sophisticated membrane resistance model for calculating transmembrane flux
- Dynamic modelling of cake formation on the membrane filter
- The ability to specify backwash, relaxation and chemical/physical cleaning schedules
- The ability to specify different membrane types and resistances
- The ability to determine the dynamic transmembrane flux
- The ability to look at the relationship between MLSS,SRT and cake formation on the surface of the membrane

The interface of GPS-X illustrating a sample MBR configuration and the results page is shown in Figure 3.8.



(a)



(b)

Figure 3.9: (a) GPS-X user interface, (b) Result pages of GPS-X

The available process modules in GPS-X are illustrated in Figure 3.9.



Figure 3.10: Available process modules in GPS-X

Some of the client's names and the technical papers referencing GPS-X are shown in Tables 3.9 and 3.10 respectively. Due to the vast number of companies and technical papers using GPS-X, the lists presented herein are in short form.

Table 3.9:Client list of GPS-X

<i>Engineering Service Companies</i>	<i>Academic Institutions</i>	<i>Public Utilities</i>
AQUA Contact	Cranfield University	Anglian Water
Black & Veatch	Michigan State University	Brisbane Water
CH2M Hill	Trinity College, Dublin	Helsinki Water
Earth Tech	Brigham Young University	Severn Trent Water
ITT Industries Sanitaire Europe	Chemical Engineering National Taiwan University	Stockholm Vatten Company
Ondeo Degremont	ENIT	Yorkshire Water Services
Scottish Water	École Polytechnique of Montreal	Melbourne Water Corporation
Proentec East GmbH	Instituto Tecnológico de Orizaba	Environment Canada
Halcrow Group Limited	McMaster University	City of Austin
Geomatrix Consultants	Middle East Technical University	City of Ottawa
Metcalf & Eddy Inc	New Jersey Institute of Technology	Alexandria Sanitation Authority
MASS Aritma Sistemleri A.Ş.	University of Toyko	DOW Benelux NV
Capaccio Environmental Engineer Inc.	University of Trento	
CODESA	University of Udine	
Delcan Corporation	University of Venice	
Suez-Lyonnaise des Eaux	Universität Karlsruhe	
	University of Girona	

Table 3.10: Some of the technical papers referencing GPS-X

<i>No</i>	<i>Technical Paper Reference</i>
1	Alex J., Beteau, J.F., Copp J., Hellinga C., Jeppsson U., Marsili-Libelli S., Pons M.N., Spanjers H. and Vanhooren H. (1999). Benchmark for evaluating control strategies in wastewater treatment plants. <i>Proc. the ECC'99 Conference, Karlsruhe, Germany, 31 August - 3 September</i>
2	Andreottola G., Foladori P., Gelmini A., Guglielmi G. and Romani S. (2001). Verification of a municipal wastewater treatment plant through a dynamic simulation model: a case study. <i>Ingegneria Ambientale</i> . n. 10, October.
3	Averill D. and Gall B. (2000). The design of intermittent treatment processes for variable loading conditions. <i>Proceedings of the Water Environment Federation's 2000 Wet Weather Specialty Conference</i> . May 7-10, Rochester, New York.

Table 3.10. continued

<i>No</i>	<i>Technical Paper Reference</i>
4	Barnet M.W. and Gall B. (1995). A robust rule-based system for on-line diagnosis of nitrification problems in activated sludge treatment. <i>Proceedings of the Water Environment Federation 68th Annual Conference and Exposition, Volume I.</i> October 21-25, Miami, Florida.
5	Bertanza G., Pedrazzani R., Brunori L. and Prandini F. (2003). Biomass monitoring in activated sludge plants by means of respirometry and dehydrogenase activity measurement: Bench and full scale tests. <i>Submitted to IA - Ingegneria Ambientale.</i>
6	Bingley M., Stokes L. and Upton J. (1996). Modeling as a design tool: experiences using Hydromantis-GPS-X. <i>Proc. Forum for Applied Biotechnology Conf.,</i> Belgium.
7	Copp J.B. and Spanjers H. (2002). Activated sludge toxicity mitigation using a respirometric measurement. <i>15th IFAC World Congress on Automatic Control,</i> Barcelona, Spain, July.
8	Copp J.B. editor (2001). The COST Simulation Benchmark: Description and Simulator Manual, Office for Official Publications of the European Communities, Luxembourg (144 pages) ISBN 92-894-1658-0.
9	Daigger G.T. and Nolasco D. (1995). Evaluation and design of full-scale wastewater treatment plants using biological process models. <i>Water Science and Technology,</i> Vol.31, No.2, pp. 245-255.
10	Gall B., Stephenson J. and Wolfe L. (1994). Modeling the effects of plant upgrade scenarios on treatment plant performance. <i>Proceedings of the Water Environment Federation 67th Annual Conference and Exposition, Volume II.</i> October 15-19, Chicago, Illinois.
11	Hvala, N., Zec M., Roš M. and Strmčnik S. (2001). Design of a sequencing batch reactor sequece with an input load partition in a simulation-based experimental environment. <i>Water Environment Research,</i> 73(2), 146-153.
12	Ketchen S., Takács I. and Lockwood S. (1997). Model helps operators with process decisions at the GEP-Selkirk plant. <i>Proceedings of the Water Environment Federation 70th Annual Conference and Exposition,</i> Chicago, Illinois.
13	Ky R.C., Y.Comeau, M. Perrier and I. Takács. (2001). Modeling biological phosphorus removal from a cheese factory effluent by an SBR. <i>Wat. Sci. Tech.</i> 43(3), 257-264.
14	Makinia J., Swinarski M. and Dobiegala E. (2002). Experiences with computer simulation at two large wastewater treatment plants in northern Poland. <i>Water Science and Technology</i> Vol 45 No 6 pp 209-218.
15	Nolasco D., Daigger G., Stafford, D., Stephenson J. and Kaupp D. (1998). The use of mathematical modeling and pilot plant testing to develop a new biological phosphorous and nitrogen removal process. <i>Water Environment Research,</i> Vol. 70, No. 6, pp. 1205-1215.
16	Novák, L. and Havrlíková, D. (2003). Performance intensification of Prague wastewater treatment plant. submitted to: <i>The 9th IWA Specialized Conference: Design, Operation and Economics of Large Wastewater Treatment Plants,</i> September 1th - 4th, Prague.

Table 3.10. continued

<i>No</i>	<i>Technical Paper Reference</i>
17	Shaw A.R. and Barnard J.L. (2002). The respirometric determination of nitrification kinetics and the implication for modeling and the design of activated sludge processes. <i>Proceedings WEFTEC 2002.</i> 75 th Annual Conference and Exhibition, Chicago, Ill.
18	Spérandio M. and Queinnec I. (2002). On line estimation of wastewater nitrifiable nitrogen, nitrification and denitrification rates using ORP and DO dynamics. <i>IWA conference on Trends in Sustainable Production</i> , Nimes, France, 13-15 November (accepted in <i>Water Science and Technology</i>).
19	Stokes L. and Coyle L. (1994). Dynamic modeling of an ASP sewage works combining simulation and on-line monitoring. <i>BHR 2nd Conference on Hydraulic modeling</i> , pp131-142, Stratford UK.
20	Takács I., Patry G.G., Gall B. and Patry J. (1998). The integrated computer control system: a comprehensive model-based control technology. <i>Dynamic and Control of Wastewater Systems</i> , Technomic Publishing, Lancaster, PA.
21	Torcu E.C. and Gökçay C.F. (2002). Modeling of Izmir Wastewater Treatment Plant by GPS-X Software. <i>EPMR-2002 International Conference on Environmental Problems of the Mediterranean Regions</i> , Nicosia, N. Cyprus. 12-15 April, pp 60-68.

4 MODELLING OF MEMBRANE BIOREACTORS

Modelling is a powerful tool in assessing the mechanistic behaviour of highly sophisticated activated sludge systems. The first known model was developed in 1986 by a group of scientists appointed by the International Association on Water Pollution Research and Control (IAWPRC) incorporating carbon removal, nitrification and denitrification in a single matrix (Grady et al., 1986). It was later on proposed that certain changes be made in particular to the way in which the fate of organic nitrogen was modelled. These changes were subsequently adopted in the final version of the IAWPRC Activated Sludge Model No.1 named as ASM1 (Henze et al., 1987). ASM1 has the importance of providing the benefit for establishing a common framework in understanding the biochemical reactions occurring in an activated sludge system. ASM1 was later on developed to incorporate biological phosphorus removal in ASM2 (Henze et al., 1995) and ASM3 (Gujer et al., 1999) was introduced to overcome the defects of ASM1 by incorporating the storage phenomena. Many limitations were also noted for the models however, they provided a good understanding in assessing and predicting the behaviour of biological processes. The models to be used in assessing the behaviour of various activated sludge systems have to be properly selected in accordance with the final objective of the research. The model variables and processes in the matrix should be able to provide a mechanistic explanation of the biochemical reactions occurring in a wastewater treatment plant like carbon oxidation, nitrification and denitrification.

Activated sludge models, ASM1, ASM2, ASM2d and ASM3 proposed by the IWA Task group are the most commonly used for mathematical modelling of biological sections of wastewater treatment plants. These models distinguish between the mechanisms acting on different components in the influent wastewater stream. The task group regarded COD to be the best measure of the concentration of organic matter in wastewater, because it alone provides a link between electron equivalents in the organic substrate, the biomass and the oxygen utilized. Therefore the

concentration of organic matter and the biomass is expressed in COD units in the IWA based models. The organic matter along with nitrogenous components are divided into a number of categories based on their biodegradability and on being soluble or particulate. The partitioning of influent organic material as being biodegradable or nonbiodegradable is referred to as wastewater characteristics which is very important in terms of modelling and has a significant effect on system performance in particular for nitrification and denitrification.

Due to their high operating sludge age and high MLSS concentration retained in the system, IWA based models in its original form do not deliver the mechanistic explanation required to assess the performance of membrane bioreactors treating domestic and industrial wastewater. It has been observed that a new approach and a framework must be developed in order to fully understand the biological processes occurring in MBRs and especially nitrogen removal. In this context, a new model was developed incorporating carbon removal, nitrification and denitrification where special attention was given to explain the level simultaneous nitrification-denitrification (SNdN) occurring in the submerged membrane bioreactor. The adopted model was dynamically calibrated with success and sensitivity of the model was derived. This section of the study aims to give a comprehensive explanation for the adopted model.

4.1 Wastewater Characterization

4.1.1 Organic material

The organic matter in a raw sewage can be partitioned in different categories in which the most important one to be biodegradability, where some portion of the influent organic substances can be *biodegradable* and some *nonbiodegradable*. The influent total COD, C_{Tin} , is the sum of total nonbiodegradable COD, C_{lin} , and total biodegradable COD, C_{S1} .

$$C_{Tin} = C_{lin} + C_{S1} \quad (4.1)$$

The total nonbiodegradable COD can be further subdivided as soluble inert COD, S_{lin} and particulate inert COD, X_{lin} . Both components are assumed to be unaffected by the biological processes where S_I flows through the system in soluble form with no change whilst X_I gets accumulated in the system by being entrapped in the activated

sludge with respect to the sludge age of the system. S_I leaves the system via secondary settling tank overflow and X_I gets wasted via the surplus activated sludge to a line. The mass of X_I retained in the system will be equal to the inlet mass per day of influent entering multiplied by the sludge age, therefore X_I can contribute to a significant portion of the mixed liquor in systems operated at high sludge ages especially for the membrane bioreactors. S_I and X_I can be quantified by fractional parameters of f_{SI} and f_{XI} respectively in relation to the total influent COD.

$$S_{In} = f_{SI} \cdot C_{Tin} \quad (4.2)$$

$$X_{In} = f_{XI} \cdot C_{Tin} \quad (4.3)$$

$$C_{In} = (f_{SI} + f_{XI})C_{Tin} = f_I C_{Tin} \quad (4.4)$$

f_{SI} =fraction of total COD which is soluble nonbiodegradable

f_{XI} =fraction of total COD which particulate nonbiodegradable

f_I =total nonbiodegradable fraction of influent COD

The biodegradable portion of the organic material is subdivided into two categories, readily biodegradable COD, S_S and slowly biodegradable COD, X_S . The readily biodegradable COD is hypothesized to consist of organic material that can be readily taken up by the bacteria to be metabolized for growth and maintenance. The slowly biodegradable COD however is assumed to be made up of complex macro organic molecules which cannot be taken up by the bacteria and has to undergo though an enzymatic breakdown which can be defined as hydrolysis. Although X_S is assumed to be of particulate nature, it has been proposed that some portion of it is in soluble form on the basis of different hydrolysis rates. (Henze, 1992) The sum of these two components is equal to the total biodegradable COD.

$$C_{Sin} = S_{Sin} + X_{Sin} \quad (4.5)$$

S_S and X_S can be quantified likewise done for the nonbiodegradable portions of influent COD.

$$S_{Sin} = f_{SS} \cdot C_{Tin} \quad (4.6)$$

$$X_{Sin} = f_{XS} \cdot C_{Tin} \quad (4.7)$$

$$C_{Sin} = (f_{SS} + f_{XS})C_{Tin} = f_S C_{Tin} \quad (4.8)$$

f_{SS} =fraction of total COD which is soluble biodegradable

f_{XS} =fraction of total COD which is particulate biodegradable

f_S =total biodegradable fraction of influent COD

The readily biodegradable fraction usually consists of 8-25% of the total COD in raw sewage and 10-35% in primary settled sewage. (Ekama and Marais, 1984) Henze (1992) reported that acetic acid, volatile fatty acids, alcohols, amino acids and carbohydrates are the compounds that contribute to the readily biodegradable portion of COD. A further division of readily biodegradable COD has to be made for modelling of excess phosphorus removal comprising of short chain volatile fatty acids-acetate, S_A and fermentable readily biodegradable substrate, S_F (Henze et al., 1995). These fractions will not be considered in this research as biological excess phosphorus removal is not part of the study.

At this point the term “soluble” must be clearly defined as it generally refers to material that passes through a 0.45 μ m membrane filter (Grady, 1989). However in many cases other types like glass fiber filters with nominal pore size of 1.2 μ m-1.5 μ m are also used which may result in discrepancies of influent COD measurements because the amount of soluble material passing through these filters may significantly vary due to the fact that some portion of the COD may be in colloidal form. Presumably most of the colloidal COD passes through the glass fiber filter however a major portion is retained by the 0.45 μ m membrane filter. Barker and Dold (1997) subdivided the slowly biodegradable COD into colloidal and particulate forms clearly distinguishing between 1.2 μ m glass fiber filtrate COD and 0.45 μ m membrane filtrate COD. In this study both glass fiber filters and membrane filters were used in determination of particulate and soluble COD components.

The importance of colloidal COD as a model parameter increases when assessing the performance of primary settling and its effect on the activated sludge system or when modelling types of treatment systems like contact stabilization, very low sludge aged systems....etc where adsorption of colloidal material is incomplete. Due to the long operating sludge ages in membrane bioreactors, the colloidal portion of COD will rapidly get adsorbed onto the sludge, therefore the colloidal/particulate distinction for X_S will not be considered in this study with the assumption that it covers a wide range of particle size distribution.

$$X_{Sm} = C_{Sin} - S_{Sin} \quad (4.9)$$

In municipal wastewater, slowly biodegradable COD accounts to approximately 40-60% of the total influent COD and it is expected that only colloidal fraction of X_S passes to the activated sludge system following primary settling where the colloidal/particulate X_S distinction has to be made in order to quantify the percentage removal. Distribution of COD fractions is shown in Figure 4.1.

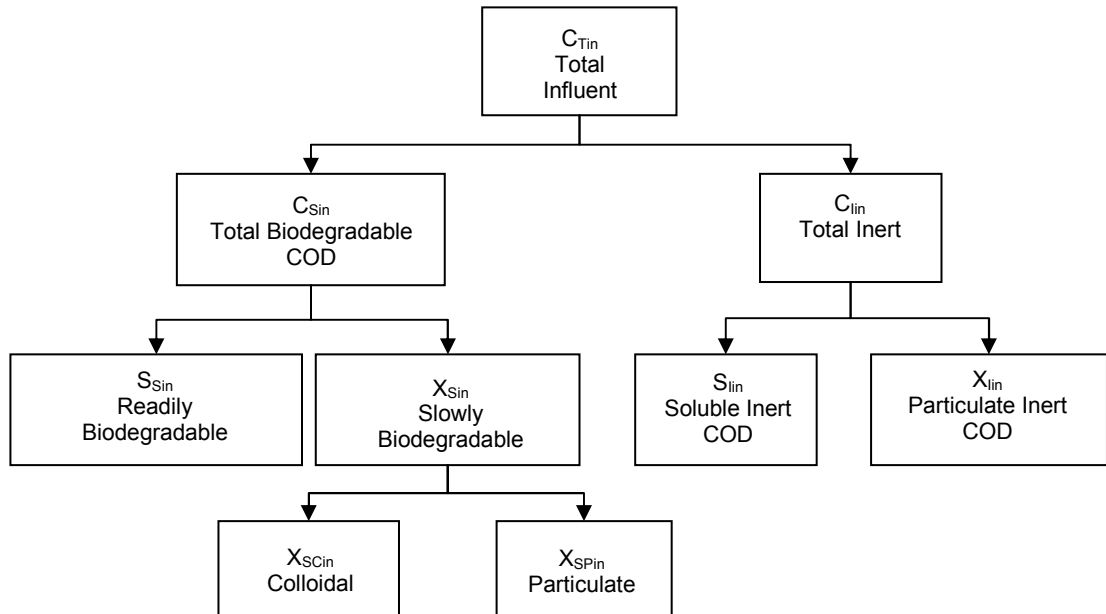


Figure 4.1: Categorization of COD components in raw sewage

Recently biomass COD in the influent, X_{Hin} , has gained significant emphasis to constitute a major component of the influent COD with reported values of 7- 25% of the total influent COD (Orhon and Çokgör, 1997) and 10-80% of the volatile suspended solids (Kappeler and Gujer, 1992).

$$X_{Hin} = f_{XH} \cdot C_{Tin} \quad (4.10)$$

f_{XH} =heterotrophic biomass fraction in the influent

On the contrary, most of the models do not include this component as a parameter in the process matrix where in this case it should be noted that the influent biomass COD has to be considered as part of slowly biodegradable COD and influent particulate inert COD. Henze (1992) schematically illustrated the COD components of raw domestic sewage on the basis of distinction between slowly (X_{Sin}) and rapidly hydrolyzable COD (S_{Hin}). (Figure 4.2)

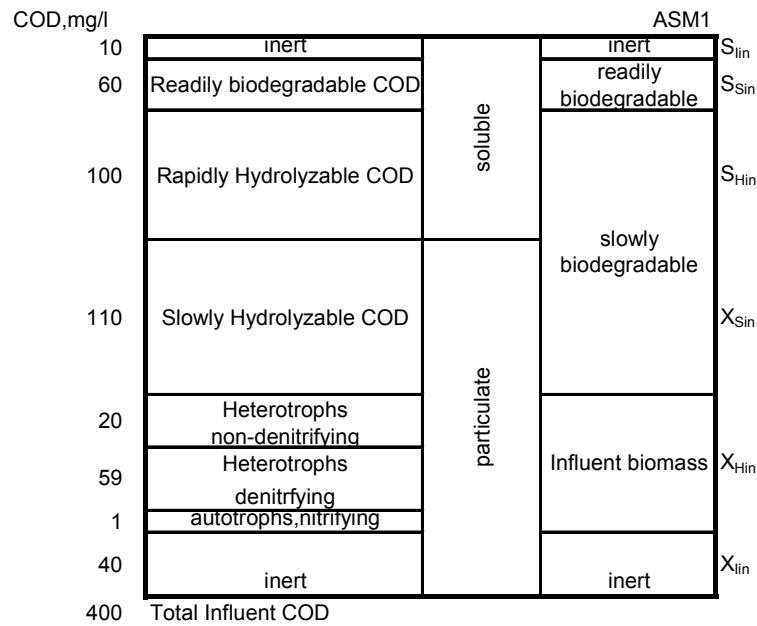


Figure 4.2: Quantified COD components in raw sewage , $C_{Tin}=400\text{mg/l}$

Typical COD fractions collected from different sources are illustrated in Table 4.1.

Table 4.1: COD fractions in domestic sewage

	<i>COD Fractions (%)</i>					<i>Reference</i>
	f_{SI}	f_{XI}	f_{SS}	f_{XS}	f_{XH}	
Raw Sewage						
South Africa	5	13	20	62	-	Siegrist andTschui, 1992
Switzerland	11	11	32	45	-	Henze et al., 1987
Hungary	9	20	29	43	-	Henze et al., 1987
Denmark	8	19	24	49	-	Henze et al., 1987
Switzerland						
Flawill(22°C)	20	9	11	53	7	Kappeler and Gujer, 1992
Tuffenwies(13°C)	10	8	7	60	15	Kappeler and Gujer, 1992
Dietikon(15°C)	12	10	8	55	15	Kappeler and Gujer, 1992
Denmark-Lundtofte	2	18	20	40	20	Henze, 1992
Settled Sewage						
Denmark-Lundtofte	3	11	29	43	14	Henze, 1992
Switzerland-Zurich	10	9	16	40	25	Sollfrank, 1998
France-Pilot	10	13	33	44	-	Lesouef et al., 1992
France-Valenton	6	8	25	41	-	Lesouef et al., 1992
South Africa	8	4	28	60	-	Ekama et al., 1986

The COD components in an activated sludge system is not limited with the influent stream as the process itself exerts COD that is related to the biological processes

which in return changes the composition of the COD in the effluent stream. Gaffney and Heukelekian (1961) were the first researchers to experimentally prove the existence of soluble organic material where Chudoba et al. (1968) conducted an extensive study on soluble microbial products. Orhon et al. (1989) proposed the formation of soluble microbial products (S_{SMP}) into mathematical models which were defined to be growth or decay associated processes. IWA based models do not include this mechanism in the process matrix of ASM1, ASM2-2d and ASM3. Since the exertion of this component cannot be avoided, it is better to include this in mathematical models to correctly assess the effluent COD, if not then the best approach would be to measure the effluent COD in predicting the amount of soluble product formation as the difference between the influent inert soluble COD based on the assumption that all the readily biodegradable COD is depleted.

Similarly the nonbiodegradable COD of influent origin (X_{in}) is not the only inert COD fraction that is enmeshed in the mixed liquor. Particulate inert products, X_P is generated during decay or death–regeneration phase of the metabolic activities of the microorganisms. Dold et al. (1980) included this mechanism in their general activated sludge model to be an important process parameter affecting especially the solids balance and likewise this mechanism was also included in ASM1. (Henze et al., 1987)

It is now widely known that formation of both soluble and particulate inert products are decay associated which means that the applied process scheme has significant impact on the existence of these compounds. On the basis of this approach it should be expected that the level of formation of these components would be at the highest in membrane bioreactors. Therefore S_{SMP} along with X_P are introduced as a process component into the adopted model for membrane bioreactors.

4.1.2 Influent solids characterization

The organic material characterization is very important in determining the effluent quality, biological reactor dimensioning, aeration requirements and volatile solids production. However raw sewage contains significant amount of inorganic fixed solids that contribute to total solids production of the system by getting entrapped in the activated sludge. This effect will have substantial difference in the sizing of the biological reactors and secondary settling tanks. Therefore, correct setting of influent

solids characterization is a prerequisite in assessing the true performance of a system by modelling.

Determination of influent inorganic suspended solids, X_{ISS} , requires the measurement of influent total and volatile suspended solids where the difference between the latter will be equal to inorganic suspended solids.

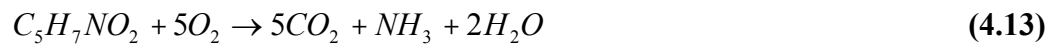
$$X_{ISSin} = TSS_{in} - VSS_{in} \quad (4.11)$$

Measurement of X_{ISS} involves filtering of the raw sewage sample through a glass fiber filter in order to retain the suspended solids. The IWA based models as well as the general activated sludge model (Dold et al.,1980) are based on COD as the parameter for quantifying organic material. The influent volatile suspended solids in the influent stream is a derived parameter based on specifying a ratio for the COD_p/VSS (f_{CV}) for the particulate COD components which plays a key role in modelling of the solids balance. The ratio of COD to VSS in the influent stream for solid components can be determined by the following analysis.

$$COD_p / VSS = \frac{UnfilteredCOD_{in} - GlassfiberfiltrateCOD_{in}}{VSS_{in}} \quad (4.12)$$

Some models predict the same COD_p/VSS ratio for all particulate COD components however X_I and X_P accounts to a major portion of of the VSS in the activated sludge especially at long sludge ages setting a somewhat different COD_p/VSS ratio for the mixed liquor. Therefore it would be more rational to use different COD_p/VSS ratios for the influent and the mixed liquor enabling near precise estimation of the solids balance. The influent stream contains only X_I and X_S contributing to the particulate COD therefore it would not be wrong to use the same COD_p/VSS ratio for these two components. Typical domestic sewage contains 15-45 mg/l X_{ISS} and the f_{CV} values are in the range of 1.5-1.5 mg COD_p /mgVSS.

The biomass COD/VSS ratio can be derived from the stoichiometric oxidation equation of $C_5H_7NO_2$ (chemical composition of biomass) to carbon dioxide and water. The resultant ratio, f_X is 1.42 mg COD /mgVSS.



In light of the aspects mentioned above two different COD/VSS values will be used in this study for the solids balance modelling of the pilot membrane bioreactor.

4.1.3 Nitrogenous material

Raw domestic sewage contains unoxidized forms of nitrogen which is identified by Total Kjeldahl Nitrogen (TKN). However if in cases that raw sewage contains oxidized forms of nitrogen like nitrite and nitrate, these should be included as separate components into the model matrix as they will significantly affect the design and performance of nutrient removal systems. TKN is the sum of ammonia nitrogen, $\text{NH}_4^+\text{-N}$ (S_{NH}) and organic nitrogen (C_{ND}). Characterization of nitrogenous material is done with respect to their biodegradation properties and a further subdivision according to their form of being soluble or particulate. The major categorization is done for the organic nitrogen as ammonia nitrogen, S_{NH} is readily available for incorporation into cell for growth and maintenance of autotrophs and/or oxidation to $\text{NO}_2^-\text{-N}$ and $\text{NO}_3^-\text{-N}$.

Biodegradable organic nitrogen consists of soluble biodegradable organic nitrogen, S_{ND} and particulate biodegradable organic nitrogen, X_{ND} . The particulate organic nitrogen is hydrolyzed to soluble organic nitrogen, S_{ND} where soluble organic nitrogen is further converted to ammonia nitrogen, S_{NH} by means of the ammonification process driven by heterotrophic activities. It has been reported that conversion of biodegradable organic nitrogen to ammonia is a very rapid process and it is expected to be complete for sludge ages greater than three (Orhon and Artan, 1994).

The nonbiodegradable organic nitrogen components are related to the particulate and soluble nonbiodegradable COD fractions, X_{I} and S_{I} . The quantification can be defined by means fractions adopted to each component.

$$S_{\text{Nin}} = f_{\text{SNI}} \cdot S_{\text{In}} \quad (4.14)$$

$$X_{\text{Nin}} = f_{\text{XNI}} \cdot X_{\text{In}} \quad (4.15)$$

where

f_{SNI} = N content of influent nonbiodegradable soluble COD

f_{XNI} = N content of influent nonbiodegradable particulate COD

X_{Nin} = influent nonbiodegradable particulate organic nitrogen

S_{Nin} = influent nonbiodegradable soluble organic nitrogen

The total influent biodegradable organic nitrogen will be the difference between the influent TKN and the nonbiodegradable fractions and the ammonia nitrogen, S_{NH} .

$$C_{NDin} = S_{NDin} + X_{NDin} = C_{TKNin} - S_{NHin} - S_{Nlin} - X_{Nlin} \quad (4.16)$$

The total ammonia available for oxidation can be calculated as

$$C_{NDin} + S_{NHin} = C_{TKNin} - S_{Nlin} - X_{Nlin} \quad (4.17)$$

Like it's COD counterpart, S_I , the soluble organic nitrogen flows through the system without being affected by biological processes. Aside from the soluble nonbiodegradable organic nitrogen, S_{NI} , the effluent may contain some minor fraction of unoxidized ammonia nitrogen, organic nitrogen entrapped in the effluent VSS and nonbiodegradable soluble nitrogenous products. The soluble nonbiodegradable nitrogenous products, S_{NP} , is assumed to be resulting from growth or decay associated processes. Composition of the effluent in terms of nitrogenous material can be expressed as;

$$S_{NE} = S_{Nin} + S_{NH} + S_{ND} + S_{NP} \quad (4.18)$$

S_{NP} can be quantified by a fraction of soluble organic microbial products, S_{SMP} .

$$S_{NP} = f_{SNP} \cdot S_{SMP} \quad (4.19)$$

The total particulate organic nitrogen in the mixed liquor is comprised of the autotrophic active biomass, X_H , portion of particulate inert products and inert particulate matter of influent origin.

$$X_{NT} = i_{XB} X_H + i_{XP} X_P + i_{XI} X_I \quad (4.20)$$

X_H =active biomass concentration

X_P =endogenous biomass concentration

X_I =inert biomass concentration

i_{XB} =nitrogen content of active biomass

i_{XP} =nitrogen content of endogenous biomass

i_{XI} =nitrogen content of inert biomass

i_{XB} can be approximately found from the fraction of N in the chemical composition of biomass ($C_5H_7NO_2$) which is 0.086 grN/grcellCOD or 0.123 grN/grVSS. Eckenfelder (1989) experimentally found the N content of endogenous biomass to be 0.07 grN/grVSS or 0.05 grN/grCOD by experimentally measuring the mixed liquor

suspended solids with varying sludge age. Böhnke (1989) proposed that N content of inert biomass is nearly equal to the N content endogenous matter. Influent wastewater characterization for nitrogenous components is shown in Figure 4.3.

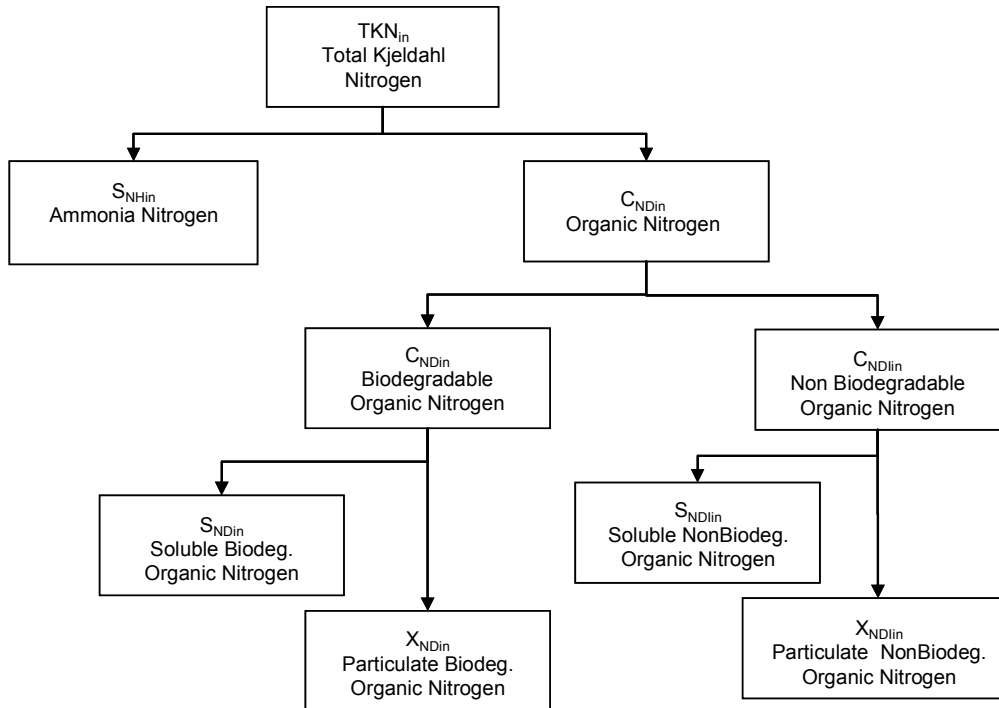


Figure 4.3: Influent wastewater characterization for nitrogenous material

Table 4.2. lists magnitudes for nitrogenous fractions typically encountered with municipal wastewaters (Melcer et al., 2003) and Table 4.3. illustrates nitrogen fractions for Istanbul raw sewage.

Table 4.2: Typical nitrogen fractions for domestic sewage

<i>Nitrogenous Material</i>	<i>Concentrations</i>	<i>Units</i>	<i>Fractions</i>	<i>Fraction Units</i>
TKN	25-70	gN/m ³	-	
Ammonia Nitrogen, S _{NH}	20-30	gN/m ³	0.50-0.75	g N/g TKN
Soluble unbiodegradable TKN	0-5	gN/m ³	0-0.07	g N/g TKN
Biodegradable TKN	0-10	gN/m ³	0-0.25	g N/g TKN
Particulate unbiodegradable TKN	2-8	gN/m ³	0.03-0.07	g N/g X _I

Table 4.3: Nitrogenous material in Istanbul domestic sewage

<i>Parameter</i>	<i>Unit</i>	<i>Sözen (1995)</i>	<i>TPB and UBM(1993)</i>
Influent TKN, C_{TKN}	g N/m ³	57	44
Organic Nitrogen, C_{ND}	g N/m ³	42	11
Ammonium Nitrogen, S_{NH}	g N/m ³	13	31

4.2 Measurement Techniques for Wastewater Characterization

The development of IWA based activated sludge models led to a better understanding of the biological processes in activated sludge system however this in return required a thorough and intensive wastewater characterization. Many researchers have worked on different techniques for wastewater characterization with some focus given to the biodegradable components and some to the nonbiodegradable influent fractions. However in general, the methods that are used to determine the influent wastewater characteristics can be divided into two main groups;

- i. Direct measurement techniques which use standard method analytical techniques,
- ii. Bioassay methods where information is derived from the observation of a lab or pilot scale biological system like continuous flow or sequencing batch reactor activated sludge system.

Direct methods may also include characteristics that can be inferred from direct measurements, such as the estimation of inert suspended solids X_{ISSin} as the difference between the measured total suspended solids (TSS_{in}) and volatile suspended solids (VSS_{in}).

Bioassay methods enable the identification of numerous influent wastewater characteristics by observing the responses in tests in which an activated sludge system is fed with raw sewage or synthetic wastewater. This is accomplished by setting up lab scale or pilot scale continuous flow reactors or sequencing batch reactor systems.

The alternative approach to wastewater characterization has been recently developed by the Dutch Foundation for Applied Waster Research (STOWA). The guidelines for wastewater characterization in this approach are based on physical-chemical methods to characterize the sum of soluble COD fractions S_I and S_S (Roeleveld and van Loosdrecht, 2002). Physical-chemical methods have been used as the basis for wastewater characterization in this research. The structure of the characterization is based on four steps which are combined with a BOD analysis for determining the biodegradable fraction of the influent COD.

- i. Soluble inert influent COD, S_I , is determined based on soluble COD in the effluent of a wastewater treatment plant filtered through $0.45\mu\text{m}$ membrane filter,
- ii. Readily biodegradable COD, S_S , is determined based on soluble COD in the influent minus the soluble COD in the effluent,
- iii. Slowly biodegradable COD, X_S , is determined by measuring the total concentration of biodegradable material from a BOD analysis where the BOD is measured as a function of time. The ultimate BOD is calculated from measured BOD_5 by using k_{BOD} constant derived through least squares method,
- iv. Influent particulate COD, X_I is determined by the equation,

$$X_I = C_{Tin} - S_S - X_S - S_I \text{ or } X_{In} = C_{Tin} - S_I - BCOD \quad (4.21)$$

The result of this characterization sequence implies that all errors and inaccuracies are reflected on X_I which is a very sensitive parameter for modelling. Inaccuracies in the X_I component will be directly reflected in the sludge production and solids balance of the system which can be calibrated against measured data. This approach does not take into account the formation of soluble microbial products in the system for the determination of soluble inert influent COD, S_I . Therefore, soluble microbial products have to be subtracted from the effluent soluble COD analysis filtered through $0.45\mu\text{m}$ membrane filter. S_P is a process generated component which can be estimated as a fraction (f_{ES}) of endogenous biomass. In this case, S_I will be,

$$S_I = S_E(0.45\mu\text{m}) - S_P \quad (4.22)$$

STOWA wastewater characterization guidelines recommend the use of membrane filtration to retain all colloidal material on the filter without a pre-flocculation step (Roeleveld and van Loosdrecht, 2002). These guidelines also apply correction factors to account for soluble microbial products in the effluent. The guidelines also assume the non-existence of active biomass in the raw sewage. The equations necessary for wastewater characterization in ASM1 as per STOWA guidelines are presented in Table 4.4 (Roeleveld and van Loosdrecht, 2002).

Table 4.4: Equations used in wastewater characterization using physical-chemical methods (ASM1)

<i>Equations for ASM1</i>
$C_{Tin} = S_{Sin} + S_{Lin} + X_{Sin} + X_{Lin} + X_{Hin} + X_{Ain}$
Assumption: $X_{Hin} = 0$; $X_{Ain} = 0 - 0.1$
$C_{Tin} = S_{Sin} + S_{Lin} + X_{Sin} + X_{Lin}$
$C_{Tin} = S_{Tin} + X_{Tin}$
$S_{Tin} = S_{Sin} + S_{Lin}$
$X_{Tin} = X_{Sin} + X_{Lin}$
$C_S (BCOD) = S_{Sin} + X_{Sin}$
<i>Conversion to ASM1 wastewater characterization</i>
$S_{Lin} = 0.9S_{Teff}$ (low loaded wastewater treatment plants)
$S_{Lin} = 0.9S_{Teff} - 1.5BOD_{eff}$ (high loaded wastewater treatment plants)
$S_{Sin} = S_{Tin} - S_{Lin}$
$X_{Sin} = C_{Sin} - S_{Sin}$
$X_{Lin} = C_{Tin} - S_{Lin} - S_{Sin} - X_{Sin}$
$X_{Hin} = 0$; $X_{Ain} = 0 - 0.1$

Since the major portion of influent nitrogen is in the form of ammonia, which has no link to organic components, there is no need for a very detailed estimation of nitrogen fractions. It is more appropriate to use fixed nitrogen fractions (i_N) for the organic part of nitrogen as it has been done in ASM1 and ASM2 and proven to be a reliable characterization method (Henze et al., 1987; Henze et al., 1995). Roeleveld and van Loosdrecht (2002) suggest that nitrogen characterization should be able to predict the nitrogen content of the sludge. On the other hand the amount of available

oxidizable nitrogen determines the autotrophic oxygen demand and hence the denitrification capacity required. The practical equations for influent nitrogen fractionation proposed by STOWA are presented in Table 4.5.

Table 4.5: Equations for nitrogen fractionation

Equations for Nitrogen fractionation

$$S_{NH} = NH_4^+ - N_{in}$$

$$TKN_{in} = S_{NH} + (i_{NSF} \cdot S_F) + (i_{NSI} \cdot S_I) + (i_{NXI} \cdot X_I) + (i_{NXS} \cdot X_S)$$

in ASM1 ($i_{NSS} \cdot S_S$) for ($i_{NSF} \cdot S_F$) with $i_{NSS}=0.02$ by default

$$TKN_{in,sol} = S_{NH} + (i_{NSF} \cdot S_F) + (i_{NSI} \cdot S_I) \text{ membrane filtered}(0.1\mu\text{m}) \text{ or flocculation}$$

$$TKN_{eff,sol} = i_{NSI} \cdot S_I + S_{NH\,eff} \text{ membrane filtered}(0.1\mu\text{m}) \text{ or flocculation}$$

$$TKN_{in,part} = TKN_{in,total} - TKN_{in,sol} = (i_{NXI} \cdot X_I) + (i_{NXS} \cdot X_S)$$

The conceptual approach adopted for wastewater characterization in recent studies significantly affects the basic structure of the mathematical models for carbon and nutrient removal. The number of process components needs to be increased to account for all the parameters identified in the wastewater and activated sludge.

4.3 Process Kinetics for Carbon Removal

Careful evaluation and interpretation of the fate of each model component is necessary before the formulation of a mathematical model for design and performance prediction. Detailed characterization of influent wastewater has to be coupled with the processes occurring in an activated sludge system which is very important for a correct assessment of process performance. The processes can be evaluated on the basis of the compound's physical situation of being soluble or particulate.

4.3.1 Fate of carbonaceous particulate components

The heterotrophic biomass, X_H , being the most important particulate component is responsible for the biodegradation of organic matter under anoxic and aerobic conditions but it is assumed to cease under anaerobic conditions. Heterotrophic biomass is generated by growth on readily biodegradable substrate, S_S where two different approaches have been made with respect to the available and usable

substrate. Dold et al. (1980) proposed that heterotrophic biomass can grow both on readily (S_S) and slowly (X_S) biodegradable substrate. The readily biodegradable substrate can be directly taken up by the bacteria for cell growth and maintenance whilst the slowly biodegradable substrate has to undergo some other enzymatic processes. The uptake of readily biodegradable organic matter can be described by means of Monod function.

$$\frac{dX_H}{dt} = \mu_{H \max} \frac{S_S}{K_S + S_S} X_H \quad (4.22)$$

It is known that the maximum rate of substrate removal under anoxic conditions is lower than it is in aerobic conditions. Henze et al. (1987) explains this situation as either the maximum specific growth rate being lower in anoxic conditions or only a fraction of the heterotrophic biomass can utilize nitrate as the terminal electron acceptor. It is also pointed out that it would be very hard to differentiate between these possibilities therefore from a modelling point of view an empirical correction factor for growth (η_g) is proposed to be incorporated into the rate expression.

$$\frac{dX_H}{dt} = \eta_g \mu_{H \max} \frac{S_{NO}}{K_{NO} + S_{NO}} X_H \quad (4.23)$$

Batchelor (1982) proposed the anoxic correction factor to be $\eta_g < 1.0$. In anoxic conditions the heterotrophic bacteria use nitrate nitrogen as the electron acceptor in the absence of oxygen. This also requires the presence of readily biodegradable substrate which will be discussed in denitrification stoichiometry.

According to the general activated sludge model (Dold et al., 1980), the slowly biodegradable substrate is first adsorbed and then stored on the active biomass where afterwards this stored material is hydrolyzed by extracellular enzymes. The resulting compounds of this hydrolysis process can then be directly absorbed by the active biomass. The latter two processes are explained by saturation type functions where the hydrolysis of the stored component is defined as the rate limiting step.

$$\frac{dX_S}{dt} = - \frac{K_{MP}(X_S / X_H)}{K_{SP} + (X_S / X_H)} X_H \quad (1^{st} \text{ step}) \quad (4.24)$$

and

$$\frac{dX_H}{dt} = Y_H \frac{K_{MP}(X_S / X_H)}{K_{SP} + (X_S / X_H)} X_H \quad (2^{\text{nd}} \text{ step}) \quad (4.25)$$

where

K_{MP} = maximum specific utilization rate for slowly biodegradable substrate

K_{SP} = half saturation coefficient

ASM1 proposes that the readily biodegradable organic matter is the only substrate available for growth and cell maintenance. On the contrary to the general activated sludge model, it is postulated that the slowly biodegradable organic matter is not adsorbed onto the biomass, rather it is entrapped in the activated sludge where it is hydrolyzed to readily biodegradable substrate through extra cellular enzymatic activity which can also be defined by a saturation type rate equation. This process constantly generates readily biodegradable substrate which is slower than the uptake of S_S for growth and cell maintenance of active biomass and again it is the rate limiting step for heterotrophic activity.

$$\frac{dX_S}{dt} = -k_h \frac{(X_S / X_H)}{K_X + (X_S / X_H)} X_H \quad (4.26)$$

where

k_h = maximum specific hydrolysis rate

K_X = half saturation constant for hydrolysis of slowly biodegradable substrate

The hydrolysis of X_S does not require energy utilization and thus there is no utilization of an electron acceptor. The rate of hydrolysis in anoxic conditions is slower than that in aerobic conditions as it is also expected to be for growth under anoxic conditions. The hydrolysis rate under anoxic conditions is adjusted in the same manner done for growth under anoxic conditions with a correction factor of η_{HYD} which is less than 1.

$$\frac{dX_S}{dt} = -\eta_{HYD} k_h \frac{(X_S / X_H)}{K_X + (X_S / X_H)} X_H \quad (4.27)$$

The loss of active biomass is also a known mechanism that affects the overall fate of particulate components and brings forward the term net growth which can be explained by two different universally accepted approaches, death-regeneration (Dold et al., 1980) and endogenous decay.

Death regeneration approach which is also the basis for ASM1 stipulates that decay is assumed to result in the conversion of viable biomass into slowly biodegradable substrate, X_S and particulate products, X_P , which are inert to further biological activity (Henze et al, 1987).

$$\frac{dX_H}{dt} = -b_{H(d-r)} \cdot X_H \quad (4.28)$$

$$\frac{dX_P}{dt} = f_{XP} \cdot b_{H(d-r)} \cdot X_H \quad (4.29)$$

and

$$\frac{dX_S}{dt} = (1 - f_{XP}) b_{H(d-r)} \cdot X_H \quad (4.30)$$

where

$b_{H(d-r)}$ = rate of death for heterotrophic active biomass

f_{XP} = inert fraction of particulate organic matter

Loss or death of viable biomass in death-regeneration is also assumed to occur at a rate independent of the presence of an electron acceptor. However the second step, regeneration, which can be defined as the conversion of the resultant slowly biodegradable substrate to a form (S_S) that can be utilized by the bacteria requires the presence of an electron acceptor. Oxygen is the terminal electron acceptor in the regeneration phase which consumes oxygen where no oxygen is directly consumed in the death phase. The rate of heterotrophic biomass generated from the regenerated substrate can be expressed as follows;

$$\frac{dX_H}{dt} = Y_H (1 - f_{XP}) \cdot b_{H(d-r)} \cdot X_H \quad (4.31)$$

The oxygen consumption expression for the regeneration step will be;

$$\frac{dS_O}{dt} = -(1 - Y_H) (1 - f_{XP}) b_{H(d-r)} \cdot X_H \quad (4.32)$$

Further usage of regenerated S_S is dependant on the conditions of the bulk liquid being aerobic, anoxic or anaerobic. If the conditions are aerobic then S_S will be utilized for growth and maintenance, if in the case of anoxic conditions prevail then

anoxic growth will occur at the expense of available nitrate nitrogen. Anaerobic conditions will result in the accumulation of formed X_S during the death phase.

The second approach, endogenous decay, can be defined as the overall decrease in the volatile suspended solids by means of a decay coefficient, k_d , in traditional modelling. However following the concept of viability, it was reported that the decay of active biomass generates particulate inert organic products, X_P with a fraction of f_{EX} . This component does not undergo any further biological reaction and accumulates in the system where it is removed only through the waste sludge stream. McKinney (1962), defined the total biomass in the system as the sum of decrease in the heterotrophic active biomass and the increase in generation of the particulate inert organic products which can be expressed as:

$$\frac{dX_T}{dt} = \frac{dX_H}{dt} + \frac{dX_P}{dt} \quad (4.33)$$

The rate of generation of particulate inert organic products can be expressed as a fraction, f_{EX} , of the heterotrophic biomass under decay.

$$\frac{dX_P}{dt} = -f_{EX} \frac{dX_H}{dt} \quad (4.34)$$

where

f_{EX} = inert fraction of heterotrophic active biomass

A value of 0.20 is universally accepted for f_{EX} in models based on endogenous decay. (McCarty et al., 1962; Washington et al., 1965)

Marais and Ekama (1976) showed that the decrease in heterotrophic active biomass can be described by a first order rate expression.

$$\frac{dX_H}{dt} = -b_H X_H \quad (4.35)$$

where b_H is the endogenous decay coefficient for heterotrophic active biomass. The formation of particulate inert organic products, X_P , can be re-expressed by combining equations (4.32) and (4.33).

$$\frac{dX_P}{dt} = f_{EX} b_H X_H \quad (4.36)$$

The loss of heterotrophic active biomass through endogenous decay is considered to be a process requiring the utilization of an electron acceptor which is oxygen. The rate of oxygen consumption can be expressed as;

$$\frac{dS_O}{dt} = -(1 - f_{EX})b_H \cdot X_H \quad (4.37)$$

The endogenous decay process is also considered to be occurring under anoxic conditions where the terminal electron acceptor is nitrate nitrogen (S_{NO}). It is further postulated that the rate of anoxic decay is lower than aerobic decay with a correction factor of η_D . Siegrist et al. (1999) reported an average anoxic respiration activity (nitrate respiration) of 35 to 40% as compared with the aerobic decay of heterotrophs. The anoxic decay rate (b_{HD}) can be determined using respirometric analysis on activated sludge samples taken from the anoxic zones of activated sludge system. The rate of nitrate nitrogen consumption under anoxic conditions can be expressed as;

$$\frac{dS_{NO}}{dt} = -\left(\frac{1 - f_{EX} - f_{ES}}{2.86}\right)b_{HD}X_H \quad (4.38)$$

or

$$\frac{dS_{NO}}{dt} = -\left(\frac{1 - f_{EX} - f_{ES}}{2.86}\right)\eta_D \cdot b_H X_H \quad (4.39)$$

The decay coefficient, $b_{H(d-r)}$, in the death-regeneration approach will be different from the usually used lysis rate in the endogenous decay models due to the recycling of the substrate. When the readily biodegradable COD is used for cell growth and maintenance, only a fraction of a unit of oxygen will be required because of the energy incorporated into the active biomass. The biomass in turn must undergo decay before the unit of oxygen is removed. This leads to the conclusion that the decay rate for the death regeneration approach should be higher than in the endogenous decay to give the same amount of oxygen utilization due to decay. The relationship between the two decay rates can be derived by combining equations (4.32) and (4.37) for dissolved oxygen and (4.29) and (4.36) for inert particulate products.

$$(1 - f_{EX})b_H X_H = (1 - Y_H)(1 - f_{XP})b_{H(d-r)}X_H \quad (4.40)$$

$$f_{EX}b_H X_H = f_{XP}b_{H(d-r)}X_H \quad (4.41)$$

Unlike the decay rate, the fraction (f_{XP}) of heterotrophic biomass converted to inert particulate organic products in the death regeneration rate will be less than the fraction (f_{EX}) used for in the endogenous decay model. Solving equations (4.40) and (4.41) simultaneously yields the relationship between the decay rates and fraction of particulate inert organic products for the two model approaches.

$$f_{XP} = \frac{(1 - Y_H)}{1 - Y_H f_{EX}} f_{EX} \quad (4.42)$$

$$b_{H(d-r)} = \frac{b_H}{1 - Y_H (1 - f_{XP})} \quad (4.43)$$

Figure 4.4 and 4.5 gives a schematic illustration of the death-regeneration and the endogenous decay models respectively under aerobic and anoxic conditions.

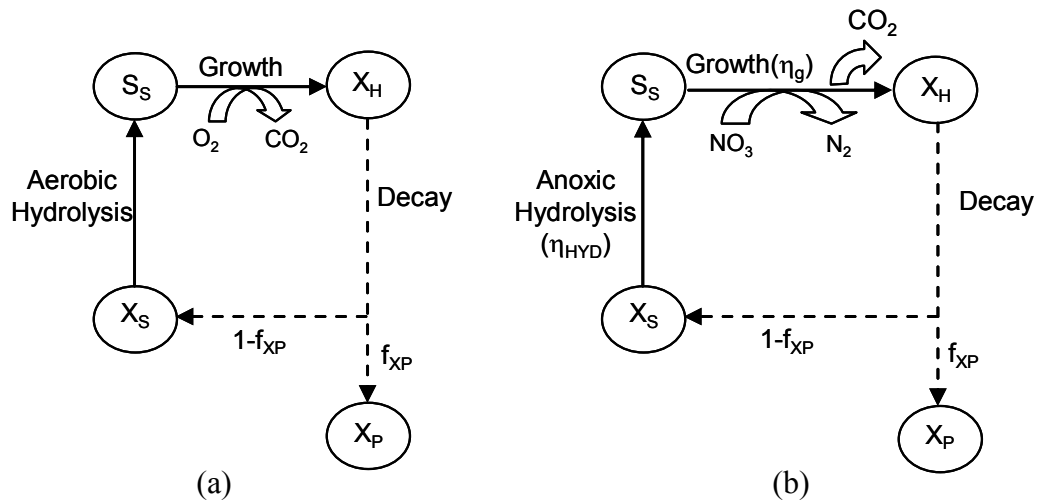


Figure 4.4: Schematic illustration of death-regeneration model (basis of ASM1) under (a) aerobic (b) anoxic conditions (Henze et al., 1987)

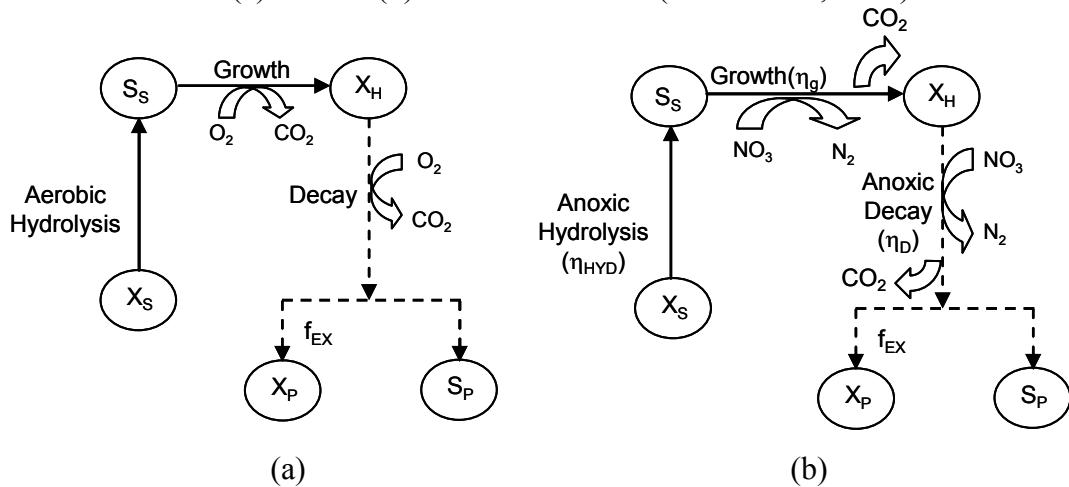


Figure 4.5: Schematic illustration of endogenous decay model (basis of for this research) under (a) aerobic (b) anoxic conditions

The major disadvantage of the death-regeneration model is that, it does not distinguish between the slowly biodegradable substrate of influent origin and the one that is being recycled through regeneration. It is evident that the rate of hydrolysis of the slow biodegradable substrate will not be the same for one formed through regeneration. This is approved in a recent study conducted with a soluble synthetic waste in which the hydrolysis rate constant, k_h , was found to be $0.65d^{-1}$ much lower than the value proposed in ASM1. The hydrolysis phenomena should be carefully dealt with when using death-regeneration approach for the loss of viable biomass.

The last but the most important particulate component in terms of solids balance is the inert particulate COD, X_I . The magnitude of this component is important in the description of activated sludge system behaviour, particularly with respect to volatile solids production. At steady state the mass of X_I entering the system will be balanced with the mass of X_I leaving the system through the sludge wastage stream and in the effluent with overflowing solids. From a mass balance standpoint, the X_I will be accumulated in the system with direct proportion to the sludge age of the activated sludge plant. It is important to note that X_I does not contribute to BOD in the influent which means that increasing proportion of X_I in total influent COD will increase the COD/BOD ratio in the raw sewage.

4.3.2 Fate of carbonaceous soluble components

The most important carbonaceous soluble component is the readily biodegradable substrate, S_S , which is considered to be the only substrate that the heterotrophic active biomass can grow on. The fate of readily biodegradable substrate again depends on the model adopted for the loss of viable heterotrophic biomass. In the endogenous decay model, the magnitude of this soluble component is not affected by the decrease of active biomass and it is depleted by the heterotrophic biomass only for cell growth and maintenance by means of the yield coefficient, Y_H . The utilization of S_S can be expressed with a Monod equation.

$$\frac{dS_S}{dt} = -\frac{\mu_{H\max}}{Y_H} \frac{S_S}{K_S + S_S} X_H \quad (4.44)$$

However in the death-regeneration model, the readily biodegradable substrate is simultaneously generated through hydrolysis of the slowly biodegradable substrate

which is the result of decay of the viable biomass. In this approach Equation (4.44) is modified by adding Equation (4.26) to incorporate generation of readily biodegradable substrate .

$$\frac{dS_S}{dt} = -\frac{\mu_{H\max}}{Y_H} \frac{S_S}{K_S + S_S} X_H + k_h \frac{(X_S / X_H)}{K_X + (X_S / X_H)} X_H \quad (4.45)$$

Depletion of readily biodegradable substrate is considered to take place under aerobic conditions where dissolved oxygen is the terminal electron acceptor. However the readily biodegradable substrate is also utilized during anoxic growth of active biomass where the electron acceptor is nitrate nitrogen in the absence of dissolved oxygen.

$$\frac{dS_S}{dt} = -\eta_g \frac{\mu_{H\max}}{Y_H} \frac{S_S}{K_S + S_S} X_H \quad (4.46)$$

The soluble inert COD, S_I , in raw sewage is unaffected by the biological reactions and it leaves the system in the effluent and wastage streams. The magnitude of this component is important in assessing the carbon removal performance of an activated sludge system.

The existence of soluble microbial products, S_{SMP} , generated by microbial activity in activated sludge systems has been widely demonstrated by Barker and Stuckey (1999). S_{SMP} , which partly contributes to the effluent COD plays an important role in wastewater treatment processes, especially in membrane bioreactors where the biomass can be completely retained in the bioreactor and a fraction of SMP with macromolecule can be retained from the permeate. The first model to characterize microbial product formation was proposed by Luedeking and Piret (1959) for the fermentation of glucose to lactic acid with the following expression:

$$\frac{dS_P}{dt} = \alpha \frac{dX}{dt} + \beta X \quad (4.47)$$

Two different categories of SMP are classified according to Namkung and Rittmann (1986) based on the bacterial phase from which they are derived; *i.*) *Products arising from growth associated mechanisms (utilization associated products)* and *ii.*) *Products arising from decay associated products (biomass associated products)*. Eckhoff and Jenkins (1967) were the first researches to apply this phenomena to

treatment kinetics in which they stipulated that the soluble residual products were formed by growth associated mechanisms with the following expression;

$$\frac{dS_p}{dt} = \alpha\mu X \quad (4.48)$$

Eckhoff and Jenkins (1967) also formulated the effluent total COD concentration as a function of C_{Sin} ;

$$S_T = \alpha Y_H C_{Sin} + (1 - \alpha Y_H) \frac{\mu_H}{Y_H k_m} \quad (4.49)$$

where α , representing the fraction of biodegradable COD converted to soluble residual products was proposed to be 0.1. On the contrary to the above expression Cimşit (1986) postulated that decay associated mechanism was the predominant step in the formation of residual products and formulated this phenomena with the expression;

$$\frac{dS_p}{dt} = \beta k_h \frac{(X_S / X_H)}{K_X + (X_S / X_H)} X_H \quad (4.50)$$

The nature of the soluble residual or microbial products are still not well established. Most studies claim that they are nonbiodegradable whilst others claim that they are biodegradable at a much slower rate than the biodegradable COD in the raw sewage. This rate could be considered negligible as the effect in a wastewater treatment would not seem so visible resulting in an assumption to consider them as inert. The formulation of the rate or residual product generation or accumulation again depends on the structure of model adopted. In the death regeneration approach, the formation of residual products are linked with *i.) a fraction of biodegradable COD being converted to soluble residual products* and *ii.) a fraction of slowly biodegradable substrate formed as a result of lysis yields soluble residual products during hydrolysis* in which these can be expressed as;

$$\frac{dS_p}{dt} = \alpha_R \mu_{H \max} \frac{S_S}{K_S + S_S} + f_{PS} k_h \frac{(X_S / X_H)}{K_X + (X_S / X_H)} X_H \quad (4.51)$$

where

α_R =growth associated soluble inert product formation fraction for the death regeneration model

f_{PS} = fraction of endogenous particulate matter converted into soluble inert microbial products

In the endogenous decay model the above mentioned approach can be used to define growth associated soluble inert products.

$$\frac{dS_P}{dt} = \alpha_D \mu_{H \max} \frac{S_S}{K_S + S_S} X_H \quad (4.52)$$

The α_D in equation (4.52) represents only the fraction of influent biodegradable substrate converted to soluble residual products as α_R in equation (4.51) represents the fraction of both the influent and the regenerated biodegradable substrate transformed into residual products.

The most practical approach in modelling of the formation of soluble microbial products is to consider a fraction, f_{ES} , of the endogenous biomass converted to soluble microbial products.

$$\frac{dS_P}{dt} = f_{ES} b_H X_H \quad (4.53)$$

Where f_{ES} is the fraction of endogenous biomass converted to soluble microbial products. The soluble microbial product formation in endogenous decay models is considered to be aerobic where the oxygen is the electron acceptor. However it is also postulated that the formation continues under anoxic conditions at a reduced rate. The oxygen consumption in the case of aerobic conditions can be expressed as;

$$\frac{dS_O}{dt} = -(1 - (f_{EX} + f_{ES})) b_H X_H \quad (4.54)$$

In a recent study, Lu et al. (2002) incorporated the formation soluble microbial products into ASM3 matrix for the modelling of membrane bioreactors. They stipulated that some fraction of SMP formed having macro molecular weight is retained in the bioreactor with further assumption that both growth and decay associated products can be degraded again by heterotrophs directly according to the multiplicative Monod expression. The SMP, which includes both growth and decay associated products along with the hydrolysis of particulate biodegradable substrate is calculated as one parameter in model simulation with the following expression:

$$\begin{aligned}
\frac{dS_{SMP}}{dt} = & \gamma_{UAP} \mu_{H \max} \frac{S_S}{K_S + S_S} X_H (1 + \eta_g) + \\
& (\gamma_{UAP} - \frac{1}{Y_{SMP}}) \mu_{SMP} \frac{S_{SMP}}{K_{SMP} + S_{SMP}} X_H (1 + \eta_g) + (1 - f_B) (b_{BAP,H} X_H + b_{BAP,A} X_A) + \\
& k_h \frac{(X_S / X_H)}{K_X + (X_S / X_H)} X_H (1 + \eta_{HYD}) \tag{4.55}
\end{aligned}$$

Where $\gamma_{UAP,H}$ and $\gamma_{UAP,A}$ are the fraction of biodegradable organic substrate converted to soluble microbial products and $b_{BAP,H}$ and $b_{BAP,A}$ are the decay coefficients for the formation of biomass associated products. They proposed a value of 0.30 for the utilization associated product formation for both heterotrophs and autotrophs and rates $b_{BAP,H}$ and $b_{BAP,A}$ of 0.01 and 0.001d⁻¹ respectively for biomass associated product formation. The major difference of this approach from the previous modelling attempts for residual product formation is that the heterotrophs can grow directly on the soluble microbial products formed with a smaller maximum specific growth rate, μ_{SMP} .

4.4 Process Kinetics for Nitrification

Nitrification is governed by three major processes: *i.) Growth of autotrophs, ii.) Decay of autotrophs, iii. Ammonification of organic nitrogen.*

4.4.1 Growth of autotrophs

The rate expression for the nitrifying bacteria growing on ammonia nitrogen, S_{NH} and nitrite nitrogen, NO_2^- , is expressed by the Monod type equation as done for the heterotrophs. Nitrification is considered as a two step process where in the first step Nitrosomonas grows on ammonia nitrogen by utilizing it whilst in the second step Nitrobacter consume nitrite for growth and cell maintenance. The first step of nitrification is regarded as the rate-limiting step for the overall growth of autotrophs.

$$\mu_A = \mu_{A \max} \frac{S_{NH}}{K_{NH} + S_{NH}} \tag{4.56}$$

where

μ_A =specific growth rate of nitrifying bacteria

μ_{Amax} =maximum specific growth rate of nitrifying bacteria

S_{NH} =ammonia nitrogen concentration in the bulk liquid

K_{NH} =ammonia half saturation constant

The growth of autotrophs can be expressed by the product of the specific growth rate and the concentration of the nitrifying bacteria;

$$\frac{dX_A}{dt} = \mu_A X_A = \mu_{Amax} \frac{S_{NH}}{K_{NH} + S_{NH}} X_A \quad (4.57)$$

where

X_A =autotrophic biomass concentration

The relationship between the autotrophic growth rate and ammonia nitrogen consumption rate will be governed by the yield coefficient for the nitrifying bacteria,

$$\frac{dS_{NH}}{dt} = -\frac{1}{Y_A} \frac{dX_A}{dt} \quad (4.58)$$

The ammonia oxidation during nitrification can be stoichiometrically expressed by combining equations (4.57) and (4.58);

$$\frac{dS_{NH}}{dt} = -\frac{\mu_{Amax}}{Y_A} \frac{S_{NH}}{K_{NH} + S_{NH}} X_A \quad (4.59)$$

The oxidized ammonia nitrogen will be converted to nitrate nitrogen in terms nitrification kinetics with the assumption that no nitrite build up will take place;

$$\frac{dS_{NO}}{dt} = -\frac{dS_{NH}}{dt} \quad (4.60)$$

The growth of nitrifying bacteria and ammonia oxidation occurs in full aerobic conditions where the electron acceptor is oxygen. Unlike the heterotrophs, the growth of autotrophs is not considered to be continuing under anoxic conditions even with a reduced rate. The oxygen consumed during nitrification can be expressed with respect to the stoichiometry of this process;

$$\frac{dS_O}{dt} = -\frac{4.57 - Y_A}{Y_A} \mu_A X_A \quad (4.61)$$

or

$$\frac{dS_O}{dt} = (4.57 - Y_A) \frac{dS_{NH}}{dt} \quad (4.62)$$

where S_O is the dissolved oxygen concentration.

The performance of nitrification is most affected by the parameters μ_{Amax} and K_{NH} where the maximum specific growth rate of nitrifying bacteria is severely influenced by temperature. Therefore nitrifying systems are designed according to minimum sewage temperature measured which will have the most adverse effect on the growth rate. The temperature effect on nitrification is best explained by Arrhenius type functions where EPA Design Manual for Nitrogen Control (U.S. EPA, 1993) suggests the following temperature dependency;

$$\mu_A = 0,47.e^{0,098(T-15)} = 0,47.1,103^{(T-15)} \quad (4.63)$$

Researchers have suggested temperature dependency coefficients in the range of 1.076 to 1.127 where a higher temperature dependency factor implies a larger temperature dependency.

Values for μ_{Amax} (20°C) ranging from 0.2 to 1.0d⁻¹ have been observed in activated sludge systems treating a number of different wastewaters. Dold and Marais (1986) reported μ_{Amax} (20°C) values in the range of 0.20 to 0.65d⁻¹ and 1.0 mg/l for the half saturation constant of ammonia.

4.4.2 Decay of autotrophs

As observed for the heterotrophs, nitrifiers also undergo through decay which is associated with predation and lysis. Decay is considered to be a first order reaction which can be expressed by;

$$\frac{dX_A}{dt} = -b_A X_A \quad (4.64)$$

where b_A is the autotrophic decay rate.

A number of studies have been conducted for the determination of 20°C autotrophic decay rate, b_A . Nowak et al. (1994) reported 0.20d⁻¹ for aerobic systems whilst Siegrist et al. (1999) reported 0.21±0.05d⁻¹. Copp and Murphy (1995) reported 20°C b_A values in the range of 0.14 to 0.17d⁻¹ for studies with nitrifier enrichments. Henze et.al (1987, 1995) suggested 20°C b_A values of 0.05d⁻¹ and 0.03-0.06d⁻¹ respectively. Katehis et al. (2002) performed bench scale testing on SBR's having 15 days of sludge age finding a b_A value of 0.09d⁻¹.

4.4.3 Ammonification of organic nitrogen

Ammonification can be described as the conversion of soluble organic nitrogen, C_{ND} , into ammonia nitrogen, S_{NH} which is a sequential process involving two consecutive reactions (Figure 4.6). The first step is involved in the conversion of particulate organic nitrogen into soluble organic nitrogen by hydrolysis where in the second process the formed soluble organic nitrogen is converted into ammonia nitrogen. The hydrolysis step can be mathematically expressed by a surface saturation type expression as given for the hydrolysis of slowly biodegradable substrate;

$$\frac{dX_{ND}}{dt} = -k_h \frac{(X_{ND} / X_H)}{K_X + (X_{ND} / X_H)} X_H \quad (4.65)$$

The conversion of soluble organic nitrogen into ammonia nitrogen can be expressed by a first order reaction;

$$\frac{dS_{ND}}{dt} = -k_a S_{ND} X_H \quad (4.66)$$

where k_a is the ammonification rate constant. Henze et al. (1987) suggests 0.04 l/mg-day.

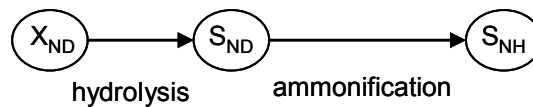


Figure 4.6: Schematic illustration for conversion of organic nitrogen to ammonia

Ekama and Marais (1984) stipulate that the overall breakdown of total organic nitrogen to ammonia is regarded to be a single step reaction which again was defined by first order kinetics;

$$\frac{dC_{ND}}{dt} = -k_R C_{ND} X_H \quad (4.67)$$

A k_R value of 0.015 l/mg-day has been used for the single step conversion reaction.

4.5 Process Kinetics for Denitrification

Three major process are responsible for denitrification which can be defined as the conversion of +5 valenced nitrate nitrogen (NO_3^- -N) into gaseous nitrogen (N_2). i.)

Growth of denitrifiers, ii.) Anoxic hydrolysis of slowly biodegradable COD iii.)
Decay of denitrifiers.

4.5.1 Growth of denitrifiers

Denitrification is considered to be occurring under anoxic conditions without the presence of dissolved oxygen and stoichiometrically it requires a carbon source. Nitrate nitrogen, S_{NO} is the electron acceptor in the absence of dissolved oxygen. Nitrate reduction is carried out by common facultative heterotrophic bacteria in the activated sludge process (Randall et al., 1992). The specific growth of denitrifiers can be expressed by Monod type equation with the incorporation of carbon source. Readily biodegradable COD can be utilized as the carbon source for denitrifiers.

$$\mu_{HD} = \mu_{HDmax} \frac{S_S}{K_S + S_S} \frac{S_{NO}}{K_{NO} + S_{NO}} \quad (4.68)$$

where

μ_{HD} =specific growth rate of denitrifiers

μ_{HDmax} =maximum specific growth rate of denitrifiers

S_S =readily biodegradable COD

K_S =half saturation constant for readily biodegradable COD

S_{NO} =nitrate nitrogen concentration

K_{NO} =half saturation constant for nitrate nitrogen

Two principal factors control the rate of denitrification in activated sludge systems:

- i. The rate of utilization of readily biodegradable COD derived from the influent wastewater,
- ii. Once the readily biodegradable COD is consumed, the rate of denitrification is controlled by the rate of hydrolysis of slowly biodegradable COD

The rate of readily biodegradable substrate consumption by the denitrifying bacteria can be expressed with the yield coefficient for the denitrifiers:

$$\frac{dS_S}{dt} = -\frac{\mu_{HD}}{Y_{HD}} X_{HD} = -\frac{\mu_{HDmax}}{Y_{HD}} \frac{S_S}{K_S + S_S} X_{HD} \quad (4.69)$$

where X_{HD} is the concentration of denitrifiers. The nitrate utilization rate can be expressed on oxygen equivalent basis:

$$\frac{dS_{NO}}{dt} = -\frac{1-Y_{HD}}{2.86Y_{HD}}\mu_{HD}X_{HD} \quad (4.70)$$

Equation (4.70) also defines the denitrification yield, Y_D , which gives the amount of cell COD produced per unit of nitrate nitrogen consumed.

$$Y_D = \frac{2.86Y_{HD}}{1-Y_{HD}} \quad (4.71)$$

In single sludge systems, heterotrophic biomass is responsible for carbon and nitrogen removal in which it is very hard to distinguish between the heterotrophs and denitrifiers. Heterotrophs adjust themselves to the changing environment whether being anoxic or aerobic. They use oxygen as the electron acceptor in aerobic tanks and nitrate nitrogen in anoxic tanks. The rate of substrate utilization and endogenous activity has been observed to be lower when nitrate instead of oxygen is used as the electron acceptor. A significant result of the lower activity with nitrate present is that the rate of nitrate utilization on an oxygen equivalent basis is lower than the oxygen utilization rate under aerobic conditions. The other factor for lower substrate utilization rate is that not all of the heterotrophic bacteria are facultative organisms that can uptake nitrate. These factors have to be considered in the rate expressions for heterotrophs. IWA based models compiled these rate reducing factors in one correction factor, η_g for heterotrophs' microbial activity under anoxic conditions. The value of η_g was found to vary from 0.30 to 0.85 for different activated sludge processes. This approach also simplifies the model equations and brings an ease in solving the set of equations for a particular activated sludge system. Equation (4.69) can be rearranged to incorporate the anoxic growth reduction factor;

$$\frac{dS_S}{dt} = -\eta_g \frac{\mu_H}{Y_H} X_H = -\eta_g \mu_{H\max} \frac{S_S}{K_S + S_S} X_H \quad (4.72)$$

4.5.2 Anoxic hydrolysis of slowly biodegradable substrate

Van Haandel et al. (1981) showed that the removal rate of slowly biodegradable substrate was significantly lower than in aerobic conditions. Particulate biodegradable substrate is hydrolyzed to readily biodegradable substrate to be utilized by the bacteria which makes this step rate-limiting under anoxic conditions. Once the readily biodegradable substrate is consumed the rate of denitrification is controlled by the rate of hydrolysis of slowly biodegradable substrate. As done for

anoxic growth, the hydrolysis under anoxic conditions can be expressed by rearranging equation (4.26) to incorporate the anoxic hydrolysis correction factor, η_{HYD} ;

$$\frac{dX_S}{dt} = -\eta_{HYD} k_h \frac{(X_S / X_H)}{K_X + (X_S / X_H)} X_H \quad (4.73)$$

Henze et al. (1987) suggested a value of 0.40 for η_{HYD} .

4.5.3 Decay of denitrifiers

The microbial decay is also considered to be occurring under anoxic conditions in the endogenous decay approach. The death–regeneration approach takes into consideration a different decay rate under anoxic conditions where the biomass is partially converted to slowly biodegradable substrate and partially to inert endogenous particulate matter.

$$\frac{dX_H}{dt} = -b_H' X_H \quad (4.74)$$

It is explained above that not all of the heterotrophic biomass is of facultative origin that can contribute to the growth and decay of denitrifiers. Therefore the same approach of applying a correction factor, η_D , can be used to explain decay of denitrifiers under anoxic conditions for heterotrophs.

$$\frac{dX_{HD}}{dt} = -b_{HD} X_{HD} = -\eta_D b_H X_H \quad (4.75)$$

Decay rate for denitrifiers, b_{HD} , can also be measured with an anoxic culture using batch tests. Siegrist et al. (1999) proposed a reduction in anoxic decay rate of 40-50% for autotrophs and heterotrophs by performing batch experiments.

4.5.4 Switching functions

The Task Group employed the concept of switching functions to activate and deactivate the process rate equations with respect to changing environmental conditions such as changing of dissolved oxygen levels. The switching functions became more important in processes that required an electron acceptor. For example nitrification is strongly dependant on the existence of an electron acceptor where it is very well known that ammonia oxidation will not be prevailing under anoxic

conditions. This is regardless of the substrate and other process kinetics. The Task Group modelled this phenomena by incorporating an dissolved oxygen switch that turned on or off the process under certain environmental conditions;

$$\frac{S_o}{K_o + S_o} \quad (4.76)$$

Under full oxic conditions S_o will be greater than the half saturation constant of oxygen, K_o which will turn on the process rate equation. Similarly processes that occur in the absence of oxygen must incorporate an oxygen switch that represents these conditions ;

$$\frac{K_o}{K_o + S_o} \quad (4.77)$$

The value of the half saturation constants will be the governing factor in setting the the environmental conditions for that particular process. Consequently, half saturation constants play an important role in the modelling of activated sludge systems.

Matrix representation of Activated Sludge Model No.1 can be seen in Table 4.6.

Table 4.6: Process kinetics and stoichiometry for carbon oxidation, nitrification and denitrification, ASM1 (Henze et al., 1987)

j	Component i	1	2	3	4	5	6	7	8	9	10	11	12	13	Process Rate ρ_j , $\text{ML}^{-3}\text{T}^{-1}$
	Process	S_i	S_S	X_i	X_S	X_H	X_A	X_P	S_O	S_{NO}	S_{NH}	S_{ND}	X_{ND}	S_{ALK}	
1	Aerobic growth of heterotrophs		$\frac{1}{Y_H}$			1			$-\frac{1-Y_H}{Y_H}$			$-i_{XB}$		$-\frac{i_{XB}}{14}$	$\hat{\mu}_H \left(\frac{S_S}{K_S + S_S} \right) \left(\frac{S_O}{K_{OH} + S_O} \right) X_H$
2	Anoxic growth of heterotrophs		$\frac{1}{Y_H}$			1			$-\frac{1-Y_H}{2.86Y_H}$			$-i_{XB}$		$\frac{1-Y_H}{14.286Y_H} - \frac{i_{XB}}{14}$	$\eta_g \hat{\mu}_H \left(\frac{S_S}{K_S + S_S} \right) \left(\frac{K_{OH}}{K_{OH} + S_O} \right) \left(\frac{S_{NO}}{K_{NO} + S_{NO}} \right) X_H$
3	Aerobic growth of autotrophs						1		$-\frac{4.57-Y_A}{Y_A}$	$\frac{1}{Y_A}$		$-i_{XB} - \frac{1}{Y_A}$		$-\frac{i_{XB}}{14} - \frac{1}{Y_A}$	$\hat{\mu}_A \left(\frac{S_{NH}}{K_{NH} + S_{NH}} \right) \left(\frac{S_O}{K_{OA} + S_O} \right) X_A$
4	Aerobic decay of heterotrophs				$1-f_p$	-1		f_p							$b_H X_H$
5	Aerobic decay of autotrophs				$1-f_p$		-1	f_p							$b_A X_A$
6	Ammonification of soluble organic nitrogen										1	-1		$\frac{1}{14}$	$k_a S_{ND} X_H$
7	Hydrolysis of entrapped organics		1		-1										$k_h \frac{X_S}{K_X + \frac{X_S}{X_H}} \left[\left(\frac{S_O}{K_{OH} + S_O} \right) + \eta_h \left(\frac{K_{OH}}{K_{OH} + S_O} \right) \left(\frac{S_{NO}}{K_{NO} + S_{NO}} \right) \right] X_H$
8	Hydrolysis of entrapped organic nitrogen											1	-1		$\rho_T \left(\frac{X_{ND}}{X_S} \right)$

Kinetic Parameters : $\mu_H, K_S, b_H, \mu_A, K_{NH}, b_A, K_{NO}, k_h, K_X, K_{NH}, K_{ALK}, K_{OA}, K_{OH}, k_a$

Stoichiometric Parameters : $Y_H, Y_A, \eta_g, \eta_h, i_{XB}, i_{XP}, f_p$

4.6 Model Development for Carbon and Nitrogen Removal in MBR

The first approach in modelling of the membrane bioreactors was no different than conventional activated sludge systems with differences only in biomass separation and the amount of biomass that can be retained in the reactor due to complete separation of liquid and solids phases. However over the years many studies and researches have been made on the behaviour of membrane bioreactors for carbon and nutrient removal. It has been seen that complete solids retention can have detrimental effect on the floc formation and physiological state of the microorganisms. It can be assumed that if operated at high sludge ages bacteria are facing conditions of extreme competition for incoming substrate. Rosenberger et al. (2000) operated lab and pilot scale membrane bioreactors for the examination of the physiological state and morphology of the bacterial cultures within the the MBRs. It has been reported that due to the correspondingly low ribosome content the bacteria in the highly concentrated sludge of the membrane bioreactor are not in a physiological state characteristics for growth of bacteria which is linked to substrate limitation. This can lead to the conclusion that the membrane bioreactors run on decay dominant processes.

Sofia et al.(2004) observed high denitrification activity in a laboratory scale anoxic/oxic sequential MBR in which the authors did not attributed this solely to the presence of *Paracoccus* responsible for nitrogen removal. It was further stated that there could be other bacterial species in the MBR culture apart from the predominantly reported species which can also be capable of mediating the nitrate reduction process.

Fernandez et al. (2000) reported simultaneous nitrification and denitrification in on/off aeration cyclic MBR. Timberlake et al. (1988) linked the simultaneous nitrification and denitrification phenomena to the depth of the biofilm formed on the membrane surface. Suzuki et al. (1993) and Osa et al. (1997) also reported simultaneous nitrification and denitrification in a single reactor. The nitrification rates of membrane aerated bioreactors reported in the literature are also high ehwn compared to other biological nitrification processes. Brindle et al. (1998) achieved more than 99% ammonia removal usind dead-end hollow fibers supplied with pure oxygen.

Semmens et al. (2003) developed a model for the mechanistic explanation of carbon oxidation, nitrification and denitrification based on attached growth biofilm formed on the membrane surface. The multiple population biofilm model provided a rational basis for the processes occurring in a membrane bioreactor however the model was limited to the biochemical reactions occurring only on the biofilm and the major assumption of the model was that no growth or substrate removal occurred in the bulk fluid.

Cho et al. (2003) combined activated sludge model No.1 including SMP with resistance in series model. The purpose of the model was to investigate the interaction between the formation of soluble microbial products and fouling. Lu et al. (2002) coupled the formation of soluble microbial products with the activated sludge model No.3 and it was emphasized that soluble products of macromolecular weight were also retained in the membrane reactor which did not contribute to the effluent COD of the system.

De Silva et al. (1998) adopted a model to predict the behaviour of a membrane bioreactor for the sludge concentration and the effluent quality obtained through anoxic/oxic cycles. It was concluded that the major trade-off of cyclic operation is that the effluent ammonia concentration was high. The model included biomass associated and utilization associated formation of soluble microbial products.

All of the ambiguities and anomalies detected by many researchers for the membrane bioreactors in terms of performance and with respect to conventional activated sludge processes imply the necessity for further research and model development in the mechanistic explanation of the biochemical reactions taking place in this new technology. This necessity has verified itself in this research as well.

The measured data for the pilot plant membrane bioreactor in this study within the operational time period could not be explained by neither the conventional IWA based activated sludge models nor by the models recently adopted for membrane bioreactors. Therefore a new model had to be adopted to incorporate and mechanistically explain the reactions occurring in the system which would be fitting the measured data.

4.7 A New Proposed Model for Membrane Bioreactor Activated Sludge Systems

Activated Sludge Model No.1 (Henze et al., 1987) was chosen as the basis for the development of a new model for MBR. ASM1 based on death regeneration approach had the disadvantage of not distinguishing between the slowly biodegradable COD of influent origin and the one that is regenerated through lysis. It has been reported that MBRs run on substrate limited and decay dominant conditions due to the high active biomass concentration and high sludge ages which creates a competition environment for both the heterotrophs and autotrophs. (Rosenberger et al., 2000)

ASM1, based on death-regeneration approach was modified to endogenous decay model (Orhon and Artan, 1994) where the overall decrease in the VSS concentration is explained by means of an endogenous decay coefficient, b_H , in which some portion (f_{EX}) is converted to particulate inert organic products (X_P). Membrane bioreactors operate at high sludge ages, hence high MLSS concentrations will inevitably shift the biological processes from being growth dominant to decay dominant which requires the existence of an electron acceptor where ASM1 neglects the usage of an electron acceptor during the decay mechanism.

It can be postulated that the bacteria in MBR's consume nitrate extensively as the electron acceptor during the decay process where this consumption increases with decreasing dissolved oxygen levels in the reactor. Processwise explanation of this mechanism was done by adding two more processes to the original matrix of ASM1 which includes the anoxic decay of autotrophs and heterotrophs bound to an electron acceptor (S_{NO}). The soluble product formation was also added to the matrix to account for the soluble products (S_{SMP}) formed during decay. (Orhon et al., 1992) The new adopted model for the MBR systems contain 14 components and 10 processes representing a system of coupled ordinary differential equations which can be solved for a given set of initial concentrations in the bioreactors. The proposed process matrix is given in Table 4.7.

Table 4.7: Process kinetics and stoichiometry for carbon oxidation, nitrification and denitrification in membrane bioreactors

j	Component i	1	2	3	4	5	6	7	8	9	10	11	12	13	14	Process Rate ρ_j , ML ⁻³ T ⁻¹
	Process	S _I	S _S	X _I	X _S	X _H	X _A	X _P	S _O	S _{NO}	S _{NH}	S _{ND}	X _{ND}	S _{SMP}	S _{ALK}	
1	Aerobic growth of heterotrophs		$\frac{1}{Y_H}$			1			$-\frac{1-Y_H}{Y_H}$						$\frac{i_{XB}}{14}$	$\hat{\mu}_H \left(\frac{S_S}{K_S + S_S} \right) \left(\frac{S_O}{K_{OH} + S_O} \right) X_H$
2	Anoxic growth of heterotrophs		$\frac{1}{Y_H}$			1			$-\frac{1-Y_H}{2.86 Y_H}$						$\frac{1-Y_H}{14.286 Y_H} - \frac{i_{XB}}{14}$	$\eta_g \hat{\mu}_H \left(\frac{S_S}{K_S + S_S} \right) \left(\frac{K_{OH}}{K_{OH} + S_O} \right) \left(\frac{S_{NO}}{K_{NO} + S_{NO}} \right) X_H$
3	Aerobic growth of autotrophs						1		$-\frac{4.57-Y_A}{Y_A}$	$\frac{1}{Y_A}$					$\frac{i_{XB}}{14} - \frac{1}{Y_A}$	$\hat{\mu}_A \left(\frac{S_{NH}}{K_{NH} + S_{NH}} \right) \left(\frac{S_O}{K_{OA} + S_O} \right) X_A$
4	Aerobic decay of heterotrophs					-1		f _{EX}	$-(1-f_{EX}-f_{ES})$				i _{XB} -f _{EX} i _{XP}	f _{ES}		$b_H \left(\frac{S_O}{K_{OH} + S_O} \right) X_H$
5	Aerobic decay of autotrophs						-1	f _{EX}	$-(1-f_{EX}-f_{ES})$				i _{XB} -f _{EX} i _{XP}	f _{ES}		$b_A \left(\frac{S_O}{K_{OA} + S_O} \right) X_A$
6	Anoxic decay of heterotrophs					-1		f _{EX}	$-\frac{1-f_{EX}-f_{ES}}{2.86}$					f _{ES}		$\eta_D b_H \left(\frac{K_{OH}}{K_{OH} + S_O} \right) \left(\frac{S_{NO}}{K_{NO} + S_{NO}} \right) X_H$
7	Anoxic decay of autotrophs						-1	f _{EX}	$-\frac{1-f_{EX}-f_{ES}}{2.86}$					f _{ES}		$\eta_D b_A \left(\frac{K_{OA}}{K_{OA} + S_O} \right) \left(\frac{S_{NO}}{K_{NO} + S_{NO}} \right) X_A$
8	Ammonification of soluble organic nitrogen										1	-1			$\frac{1}{14}$	$k_a S_{ND} X_H$
9	Hydrolysis of entrapped organics		1		-1											$k_h \frac{X_S}{K_X + \frac{X_S}{X_H}} \left[\left(\frac{S_O}{K_{OH} + S_O} \right) + \eta_h \left(\frac{K_{OH}}{K_{OH} + S_O} \right) \left(\frac{S_{NO}}{K_{NO} + S_{NO}} \right) \right] X_H$
10	Hydrolysis of entrapped organic nitrogen											1	-1			$\rho_T \left(\frac{X_{ND}}{X_S} \right)$

Kinetic Parameters : $\mu_H, K_S, b_H, \mu_A, K_{NH}, b_A, K_{NO}, k_h, K_X, K_{NH}, K_{ALK}, K_{OA}, K_{OH}, k_a$

Stoichiometric Parameters : $Y_H, Y_A, \eta_g, \eta_D, \eta_h, i_{XB}, i_{XP}, f_{EX}, f_{ES}$

The new adopted model provides a scientific basis for the explanation of simultaneous nitrification and denitrification in membrane bioreactors operated at low to medium dissolved oxygen levels ($0.3 < DO < 1.0$ mg/l). The heterotrophs and autotrophs excessively uptake nitrate nitrogen as the terminal electron acceptor during decay contributing to more nitrate utilization than for growth in anoxic conditions. The decay of heterotrophs and autotrophs occur at a lower rate compared to aerobic conditions.

This process can be expressed by incorporating a correction factor, η_D , for the decay rate, b_H , and the switching function for absence of oxygen in the rate equation.

$$\frac{dX_H}{dt} = -\eta_D \cdot b_H \frac{K_{OH}}{K_{OH} + S_O} \frac{S_{NO}}{K_{NO} + S_{NO}} X_H \quad (4.78)$$

The decay of autotrophs under anoxic conditions can be expressed in the same way done for the heterotrophs;

$$\frac{dX_A}{dt} = -\eta_D \cdot b_A \frac{K_{OA}}{K_{OA} + S_O} \frac{S_{NO}}{K_{NO} + S_{NO}} X_A \quad (4.79)$$

The nitrate nitrogen uptake during anoxic decay for heterotrophs and autotrophs can be respectively expressed as;

$$\frac{dS_{NO}}{dt} = -\frac{1 - f_{EX} - f_{ES}}{2.86} \eta_D \cdot b_H \frac{K_{OH}}{K_{OH} + S_{NO}} \frac{S_{NO}}{K_{NO} + S_{NO}} X_H \quad (4.80)$$

and

$$\frac{dS_{NO}}{dt} = -\frac{1 - f_{EX} - f_{ES}}{2.86} \eta_D \cdot b_A \frac{K_{OA}}{K_{OA} + S_O} \frac{S_{NO}}{K_{NO} + S_{NO}} X_A \quad (4.81)$$

The nitrate uptake during growth in anoxic conditions can be expressed as done in the same way for Equation (4.70) with dual Monod type function

$$\frac{dS_{NO}}{dt} = -\frac{1 - Y_H}{2.86 Y_H} \eta_g \mu_{H \max} \frac{S_S}{K_S + S_S} \frac{K_{OH}}{K_{OH} + S_O} \frac{S_{NO}}{K_{NO} + S_{NO}} \quad (4.82)$$

The overall nitrate uptake in the system can be expressed by combining the utilization rates of nitrate both in growth and decay phases.

$$\frac{dS_{NO}}{dt} = -\frac{1 - Y_H}{2.86 Y_H} \eta_g \mu_{H \max} \frac{S_S}{K_S + S_S} \frac{K_{OH}}{K_{OH} + S_O} \frac{S_{NO}}{K_{NO} + S_{NO}}$$

$$+ \frac{1 - f_{EX} - f_{ES}}{2.86} \eta_D \frac{S_{NO}}{K_{NO} + S_{NO}} \left[b_H \frac{K_{OH}}{K_{OH} + S_O} X_H + b_A \frac{K_{OA}}{K_{OA} + S_O} X_A \right] \quad (4.83)$$

The switching functions play a more important role in the modelling of membrane bioreactors as the highly concentrated activated sludge will limit the diffusion of the electron acceptor or the donor from the bulk liquid into the cell for growth and maintenance. Therefore the switching functions cannot be kept apart from the rate expressions in the modelling of membrane bioreactors due to the fact that MBRs are always operated with MLSS concentrations between 10,000-30,000 mg/l. Highly concentrated biomass will decrease the diffusion of oxygen and substrate into the cell thereby changing the floc structure to incorporate an anoxic mass fraction. This anoxic mass fraction can trigger the high level of denitrification that is experienced by researchers. Simultaneous nitrification and denitrification (SNdN) can be explained by diffusion limitation concept which can only be defined by half saturation constants in switching functions for the systems based suspended growth processes.

The high concentration in the bulk liquid and the population diversity result in a size distribution of flocs where in MBR it is assumed to be larger in the size of 50-110 μm . It is stipulated that a substantial anoxic mass fraction exists in the center of the biomass flocs (Figure 4.7) resulting in an oxygen diffusion limitation into the flocs. (Pochana and Keller, 1999)

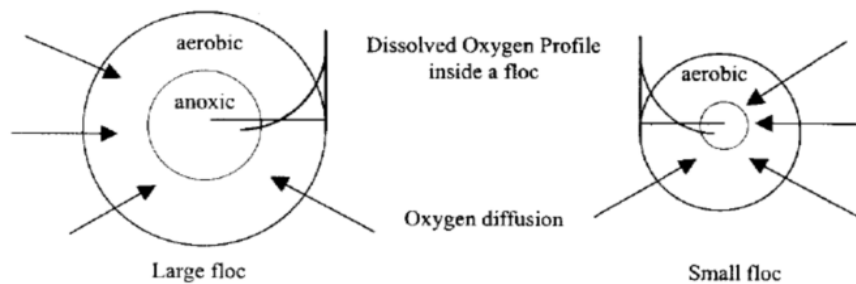


Figure 4.7: Oxygen profile inside (a) Large flocs (b) small flocs

The level of SNdN occurring in a membrane bioreactor suggests that this level of diffusion limitation is so high that it is even causing the anoxic fraction of biomass inside the floc to be dominant during low to mid DO levels. It can be concluded that during high DO levels this fraction of biomass shifts from being anoxic to aerobic

decreasing the level of SNdN. The half saturation constants proposed in IWA based activated sludge models are listed in Table 4.8.

Table 4.8: Half saturation constants used in ASM1, ASM2, ASM2d and ASM3

<i>Half Saturation Constant</i>	<i>Unit</i>	<i>ASM1</i>	<i>ASM2&2d</i>	<i>ASM3</i>
K_{OH}	mg/l	0,2	0,2	0,2
K_{OA}	mg/l	0,4	0,5	0,5
K_{NH}	mg/l	1	1	1
K_{NO}	mg/l	0,5	0,5	0,5

Increase in diffusion limitation would be implying higher half saturation constants. It is believed that the bulk liquid conditions in a membrane bioreactor is totally different than in a bioreactor operated under conventional activated sludge process scheme. The existence of highly filamentous bacteria (Nagaoka et al., 1996; Lee et al., 2001; Zhang et al., 2005) in MBRs leads to the formation of extra cellular polymeric substances (EPS) which can also be related to the diffusion limitation apart from highly concentrated biomass.

It would be misleading to account for the major processes in MBR to be occurring under dedicated environmental conditions like the conventional activated sludge systems. For example decay may be occurring only under aerobic conditions in conventional activated sludge systems whilst it may be occurring both in anoxic and aerobic conditions fully dependant on the diffusion limitation related to the biomass concentration of the bulk liquid of a membrane bioreactor. On the other hand anoxic growth may be occurring even under dissolved oxygen levels up to 1 mg/l due to diffusion limitation and the existence of an anoxic mass fraction inside the floc. This means that nearly 2-3 times more nitrate uptake can take place by the heterotrophs in the MBRs compared to conventional activated sludge systems under the same operating dissolved oxygen concentrations.

The same approach would be valid for the diffusion of substrates that can be readily used by the heterotrophs and autotrophs like the readily biodegradable COD, S_s , ammonia nitrogen, S_{NH} and nitrate nitrogen, S_{NO} . As the biomass concentration in the bulk liquid is increased it will create an environment causing the electron donors not to be able to fully diffuse into the flocs. This will result in some portions of the soluble substrate remaining in the bulk liquid which would mean an increase in the effluent soluble substrate levels.

The formation of soluble microbial product formation is also introduced as a new component into the adopted model as it plays an important role for both biological and physical operational aspects of a membrane bioreactor. In this regard the SMP formation is considered to be related to decay associated mechanisms however occurring both in aerobic and anoxic conditions. Namkung and Rittmann (1986) partitioned the soluble microbial products into two different categories based on their bacterial process phase from which they are derived from; utilization associated products (UAP) and biomass associated products (BAP). There is still dispute among researchers on the biodegradability of the soluble residual products. Rittmann (1987) stipulated that SMP is biodegradable after culture acclimation. Gaudy and Blachy (1985) studied the biodegradability of residual COD and with respect to the findings it can be stated that only a very small portion of the SMP undergo biodegradation at a very slow rate that they can be considered inert. In view of the findings, the adopted model takes into consideration the SMP formed no longer biodegradable. The rate equation for the formation of SMP under aerobic and anoxic conditions can be expressed together with the switching functions respectively for heterotrophs and autotrophs;

$$\frac{dS_{SMP}}{dt} = f_{ES} b_H X_H \left(\frac{S_O}{K_{OH} + S_O} + \eta_D \frac{K_{OH}}{K_{OH} + S_O} \frac{S_{NO}}{K_{NO} + S_{NO}} \right) \quad (4.84)$$

and

$$\frac{dS_{SMP}}{dt} = f_{ES} b_A X_A \left(\frac{S_O}{K_{OA} + S_O} + \eta_D \frac{K_{OA}}{K_{OA} + S_O} \frac{S_{NO}}{K_{NO} + S_{NO}} \right) \quad (4.85)$$

Oxygen will be utilized during aerobic decay of the heterotrophs and autotrophs;

$$\frac{dS_O}{dt} = -(1 - f_{EX} - f_{ES}) \left[b_H \frac{S_O}{K_{OH} + S_O} X_H + b_A \frac{S_O}{K_{OA} + S_O} X_A \right] \quad (4.86)$$

Unlike ASM1, the adopted model incorporates the formation of particulate inert organic products under anoxic conditions with the following stoichiometric equation;

$$\frac{dX_P}{dt} = f_{EX} \eta_D \frac{S_{NO}}{K_{NO} + S_{NO}} \left[b_H \frac{K_{OH}}{K_{OH} + S_O} X_H + b_A \frac{K_{OA}}{K_{OA} + S_O} X_A \right] \quad (4.87)$$

The relationship between the process components and the model parameters are derived on the basis of continuity equations defining mass balance around the influent –effluent streams and around each individual reactor.

4.8 Modelling of Carbon Removal, Nitrification and Denitrification in MBR with the New Adopted Model

The steady state mass balance equations can be written on the basis of the process kinetics and stoichiometry given in Table 4.7 and the schematic process diagram of the membrane reactor for carbon and nitrogen removal shown in Figure 4.8.

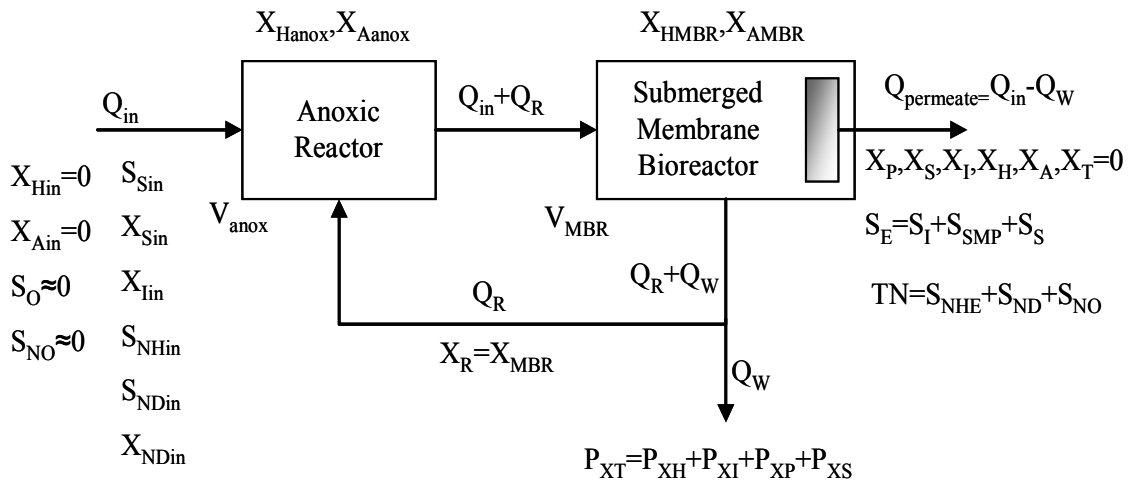


Figure 4.8: Schematic process diagram for carbon and nitrogen removal in submerged membrane bioreactor

The components can be derived from steady state analysis of the mass balance equations written for each reactor and for the system. The solids balance, carbon removal, nitrification and denitrification performance can be derived separately.

4.8.1 Solids balance

Heterotrophic and autotrophic active biomass can grow on readily biodegradable COD, S_S and ammonia nitrogen, S_{NH} respectively (Dold et al., 1980, Henze et al., 1987). Mass balance for biomass and substrate around the inlet and outlet of the system will yield the amount of generation of the active biomass.

$$V \frac{dS_S}{dt} = Q_{in} C_{Sin} - Q_p S_S - V_{anox} \frac{\mu_H}{Y_H} \eta_g X_{Hanox} - V_{mbr} \frac{\mu_H}{Y_H} X_{Hmbr} \frac{S_O}{K_{OH} + S_O} = 0 \quad (4.88)$$

Substrate and oxygen diffusion limitation is a very important phenomena in MBRs due to the fact that it considerably affects the rate of a particular process dependant especially on an electron acceptor. Therefore correct assessment of the MBR process through stoichiometric equations require the use of switching functions for electron acceptors and donors. The results obtained by neglecting these switching functions will be misleading and it will not fit the measured data and modelling results. It can be concluded that a specific dedication of a process to a reactor being anoxic or aerobic cannot be made in a membrane bioreactor system as the process can occur in both type of reactors dependant on the environmental conditions. The oxygen switching function for heterotrophs can be expressed by,

$$\frac{K_{OH}}{K_{OH} + S_o} = f_{DNH} \Rightarrow \frac{S_o}{K_{OH} + S_o} = 1 - f_{DNH} \quad (4.89)$$

Since the amount of waste sludge is very small in MBRs, it would not be misleading to consider the permeate flow equal to the inlet flow. The substrate-biomass equation can also be written for autotrophs on the basis of nitrification occuring only in the MBR tank with relation to the sustained dissolved oxygen level,

$$V \frac{dS_{NH}}{dt} = Q_{in} S_{NHin} - Q_p S_{NH} - V_{mbr} \frac{\mu_A}{Y_A} X_{Ambr} (1 - f_{DNA}) = 0 \quad (4.90)$$

Since complete retention of the sludge is maintained in the MBR, the heterotrophic active biomass will be higher in this tank when compared to anoxic tank. The relationship of heterotrophic biomass between these two tanks can be derived by writing a net growth steady state equation for the anoxic reactor.

$$V \frac{dX_H}{dt} = RQX_{Hmbr} + V_{anox} X_{Hanox} (\eta_g \mu_H - \eta_D b_H) - (1 + R)QX_{Hanox} = 0 \quad (4.91)$$

Rearranging Equation (4.91) will yield the relationship between these two components :

$$X_{Hanox} = \frac{\frac{R}{1+R}}{1 - \frac{\theta_{Hanox}}{1+R} (\eta_g \mu_H - \eta_D b_H)} X_{Hmbr} \quad (4.92)$$

$$\frac{R}{1+R} = f_R \quad (4.93)$$

The above expression implies that the heterotrophic active biomass in the anoxic tank will be equal to the concentration in the MBR tank with a fraction related to the recirculation ratio and the net growth occurring in the anoxic tank. The net growth is related to the level of available readily biodegradable substrate and nitrate nitrogen. The presence of nitrate nitrogen in the anoxic reactor is related to the level of DO sustained in the MBR which will be discussed in the proceeding sections. Since nearly all of the readily biodegradable substrate is depleted for anoxic growth, it would not be misleading to neglect the net growth when deriving the relationship of active biomass between the two reactors. The measured data and modelling results also confirm this approach. In this case, the following equation can be used for practical stoichiometric equation derivation,

$$X_{Hanox} = \frac{R}{1+R} X_{Hmbr} = f_R X_{Hmbr} \quad (4.94)$$

Sludge age is defined as the ratio of the amount of solids retained in the system to the amount of solids wasted. It can also be mathematically expressed as the inverse of net growth occurring in the system.

$$\theta_x = \frac{V_T \cdot X}{P_X} \quad (4.95)$$

or

$$\frac{1}{\theta_x} = \mu_H - b_H = \frac{Q_W}{V_T} \Rightarrow \frac{1}{\theta_x} = \frac{Q_W}{V_T}; \quad (4.96)$$

where P_{XH} is the amount of excess heterotrophic biomass generated.

Growth and decay of heterotrophs occur both in the anoxic and the membrane bioreactor. These processes occur in a reduced rate in the anoxic tank when compared to the MBR reactor which is kept under aerobic conditions. Growth and decay of heterotrophs have correction factors of η_g and η_D respectively in anoxic conditions. However unlike the conventional activated sludge systems, anoxic conditions can also prevail in the MBR reactor which will result in a reduced growth and decay activity in relation with the oxygen switching function of heterotrophs. Neglecting the use of oxygen switching functions in membrane bioreactors will lead to inaccurate results as it will not be possible to reflect the changes happening during varying dissolved oxygen levels especially for systems operated under certain

conditions to achieve simultaneous nitrification and denitrification (SNdN). Therefore it is a must to take into account this function in the stoichiometric equations. This phenomena can be explained by the following mass balance equation for heterotrophs with reduced activity in the anoxic tank coupled with oxygen switching functions:

$$(\mu_H - b_H)X_{Hmbr}(V_{mbr}(1 - f_{DNH}) + \eta_g \eta_D f_R V_{anox}) = P_{XH} \quad (4.97)$$

Since a min level of dissolved oxygen dependant on the temperature has to be maintained in the MBR tank for nitrification the correction factors for growth and decay can not be applied to the membrane bioreactor. Under these circumstances, growth and decay in the MBR tank operated at minimum dissolved oxygen levels will be reduced in relation with the switching function for oxygen. Otherwise process rates for these activities would be underestimated as the minimum oxygen concentration in the MBR tank is always higher than the anoxic tank. The sum of anoxic and MBR reactor volumes in relation to the reduced correction factor and switching functions can be defined as a fraction of the the total volume of reactors in the system.

$$V_{mbr}(1 - f_{DNH}) + \eta_g \eta_D f_R V_{anox} = \beta V_T \quad (4.98)$$

where β can be derived by substituting $V_T - V_{anox}$ for V_{mbr} in Equation (4.98);

$$\beta = 1 - f_{DNH} - (1 - f_{DNH} - \eta_g \eta_D f_R) \frac{V_{anox}}{V_T} \quad (4.99)$$

Substituting β in equation (4.99) will result in,

$$\mu_H - b_H = \frac{1}{\theta_X} = \frac{Q_W}{\beta V_T} = \frac{1}{\beta \theta_X} \quad (4.100)$$

The specific heterotrophic growth rate can be derived from Equation (4.100),

$$\mu_H = \frac{1 + b_H \beta \theta_X}{\beta \theta_X} \quad (4.101)$$

The concentration of heterotrophic biomass in the membrane bioreactor can be obtained by using Equation (4.101) in Equation (4.88);

$$X_{Hmbr} = \frac{Y_H Q (C_{Sin} - S_S) \beta \theta_X}{(1 + b_H \beta \theta_X) (V_{anox} f_R \eta_g + V_{mbr} (1 - f_{DNH}))} \quad (4.102)$$

Interpretation of the above expression reveals that the level of heterotrophic active biomass in the MBR tank is also inversely proportional to the level of dissolved oxygen level. This can be linked to the diffusion limitation where it is expected that the half saturation constant to be higher compared to conventional activated sludge systems. The growth process rate would be lower in the same influent and environmental conditions in a membrane bioreactor due to the oxygen diffusion limitation. Hence, the heterotrophic active biomass concentration will be affected by the level of dissolved oxygen sustained in the membrane bioreactor. Increasing dissolved oxygen levels will result in a decrease in the concentration of heterotrophic active biomass whilst decreasing oxygen levels will have the opposite effect. The total heterotrophic active biomass in the system can be expressed as;

$$V_T X_{HT} = M_{XHT} = V_{anox} X_{Hanox} + V_{mbr} X_{Hmbr} = X_{Hmbr} (V_{anox} f_R + V_{mbr}) \quad (4.103)$$

In the simplified approach the heterotrophic active biomass concentration in the anoxic reactor will then be,

$$X_{Hanox} = f_R \cdot \frac{Y_H Q (C_{Sin} - S_S) \beta \theta_X}{(1 + b_H \beta \theta_X) (V_{anox} f_R \eta_g + V_{mbr} (1 - f_{DNH}))} \quad (4.104)$$

Similarly, it can be stipulated that autotrophic growth will occur in the membrane bioreactor whilst autotrophic decay can occur both in both tanks. This can be expressed by using the correction factor for decay of autotrophs under anoxic conditions coupled with the oxygen switching function for this type of bacteria as given in Equation (4.97) for the heterotrophs;

$$(\mu_A - b_A) X_{Ambr} V_{mbr} (1 - f_{DNA}) - b_A \eta_D f_R X_{Ambr} V_{anox} = P_{XA} \quad (4.105)$$

The above expression is different from the one derived for the heterotrophs due to the fact that no autotrophic growth occurs in the anoxic reactor where only decay persists. Therefore it would be very complex and mathematically not correct to derive an equation for net growth in the membrane bioreactor systems as done for the heterotrophs. In order to obtain the concentration of autotrophs in the MBR tank the second expression defining decay in equation (4.105) can be neglected. The growth rate of autotrophs can be expressed as,

$$\frac{1}{\theta_{XA}} = (\mu_A - b_A) (1 - f_{DNA}) \Rightarrow \mu_A = \frac{1 + b_A (1 - f_{DNA}) \theta_{XA}}{\theta_{XA} (1 - f_{DNA})} \quad (4.106)$$

The concentration of autotrophic biomass in the MBR can be derived by incorporating equation (4.108) into the steady state analysis of Equation (4.90),

$$X_{Ambr} = \frac{Q(S_{NHin} - S_{NHE})\theta_{XA}Y_A}{(1 + b_A(1 - f_{DNA})\theta_{XA})V_{mbr}} = \frac{QY_{NA}N_{OX}\theta_{XA}}{V_{mbr}} \quad (4.107)$$

where

$$\theta_{XA} = \frac{\theta_X}{1 + \frac{V_{anox}}{V_T}} \quad \text{and} \quad Y_{NA} = \frac{Y_A}{1 + b_A(1 - f_{DNA})\theta_{XA}} \quad (4.108)$$

Particulate organic matter will be generated by a fraction of the decay activity of both heterotrophs and autotrophs which can be expressed by,

$$\frac{V_T X_P}{\theta_X} = V_T [f_{EX} b_H X_H (1 - f_{DNH}) + f_{EX} b_A X_A (1 - f_{DNA}) + f_{EX} \eta_D b_H X_H f_{DNH} + f_{EX} \eta_D b_A X_A f_{DNA}] \quad (4.109)$$

where

$$\frac{V_T X_P}{\theta_X} = P_{XP} \quad (4.110)$$

For simplifying purposes, the particulate organic matter generation due to the decay of autotrophs will be lower compared to the rate of generation from the heterotrophs. Therefore it would not be misleading in practical stoichiometric calculations to account the X_P accumulation on the decay of heterotrophs which can be expressed by rearranging Equation (4.109),

$$X_P = f_{EX} b_H X_H ((1 - f_{DNH}) + \eta_D f_{DNH}) \theta_X \quad (4.111)$$

The above expression implies that the rate of generation of the particulate inert organic matter will be in direct proportion with the operating sludge age of the MBR. Since MBRs are operated at very high sludge ages, the amount of accumulated X_P in the system will be higher and the percentage of this fraction in total biomass will also be higher when compared to conventional activated sludge systems.

The particulate inert organic matter of influent origin will be entrapped in the activated sludge and will leave the system via the waste sludge stream. The corresponding mass balance is expressed as,

$$V \frac{dX_I}{dt} = QX_{Iin} - P_{XI} = 0 \quad (4.112)$$

Substituting the value of P_{XI} in Equation (4.95) to (4.112) will yield the amount of X_I entrapped in the activated sludge.

$$X_I = X_{I1} \frac{\theta_X}{\theta_{HT}} \quad (4.113)$$

The above equation indicates that the influent inert particulate COD accumulates in the biological reactor by the ratio of the sludge age to the hydraulic detention time maintained in the system.

The slowly biodegradable COD, X_S , of particulate nature will be hydrolyzed to readily biodegradable COD, S_S , and the portion that is not hydrolyzed will also be entrapped in the activated sludge which will be wasted from the system through the waste sludge stream in accordance with the following continuity equation;

$$\begin{aligned} V \frac{dX_S}{dt} = & QX_{Sin} - P_{XS} - Vk_h \frac{X_S / X_H}{K_X + X_S / X_H} X_H (1 - f_{DNH}) \\ & + V\eta_{HYD} k_h \frac{X_S / X_H}{K_X + X_S / X_H} X_H f_{DNH} = 0 \end{aligned} \quad (4.114)$$

Equation (4.109) can be arranged by substituting the expression for P_{XS} ,

$$QX_{Sin} - Q \frac{\theta_H}{\theta_X} X_S - Vk_h \frac{X_S / X_H}{K_X + X_S / X_H} X_H ((1 - f_{DNH}) + \eta_{HYD} f_{DNH}) = 0 \quad (4.115)$$

The saturation type expression of the hydrolysis of X_S brings out the difficulty in mathematically and stoichiometrically defining the amount of X_S in the system. The model and simulator solve the set of differential equations simultaneously without any difficulty for saturation type functions. For practical reasons, it would be possible to adopt first order rate expression for hydrolysis with the assumption of $K_X \gg X_S / X_H$. Then the Equation (4.115) can be rearranged as;

$$QX_{Sin} - Q \frac{\theta_H}{\theta_X} X_S - Vk_h X_S ((1 - f_{DNH}) + \eta_{HYD} f_{DNH}) = 0 \quad (4.116)$$

Solving Equation (4.116) for X_S in MBR will yield;

$$X_S = \frac{X_{Sin} \frac{\theta_X}{\theta_H}}{1 + k_h \theta_X ((1 - f_{DNH}) + \eta_{HYD} f_{DNH})} \quad (4.117)$$

The process model formulation for the overall influent solids balance can be calculated through a set of equations. X_{VASS} (volatile active suspended solids) is the sum of all the influent active biomass components converted X_{VSS} with their influent COD/VSS ratio ($f_{CV, (X_{Tin}/VSS_{in})}$) where X_{VSS} includes all the particulate components.

$$X_{VASS} = \frac{X_H}{f_{CV}} + \frac{X_A}{f_{CV}} \quad (4.118)$$

$$X_{VSS} = X_{VASS} + \frac{X_P}{f_{CV}} + \frac{X_I}{f_{CV}} + \frac{X_S}{f_{CV}} \quad (4.119)$$

X_{TISS} (total inert suspended solids) is the sum of all inert/inorganic solids from ISS, precipitated solids and the organism ash content (synthesis ISS) in which this is simplified to,

$$X_{TISS} = X_{ISS} + \left[X_{VASS} + \frac{X_P}{f_{CV}} \left(\frac{1}{1 - \frac{ashcontent}{100}} - 1 \right) \right] \quad (4.120)$$

where the ash content of the biomass is taken as %8 by default. The overall total influent suspended solids will then be,

$$X_{TSS} = X_{VSS} + X_{TISS} \quad (4.121)$$

The influent solids balance is very important in determining the total solids and biomass content of the membrane bioreactor system. The effect of inorganic suspended solids and the correct assessment of influent volatile active and volatile suspended solids are among vital issues to be taken into consideration.

4.8.2 Stoichiometric assessment of sludge production in MBR

Sludge production is related to all of the particulate components of the process.

$$P_{XT} = P_{XH} + P_{XA} + P_{XS} + P_{XI} + P_{XP} + P_{XISS} \quad (4.122)$$

Excess sludge production of heterotrophic active biomass can be calculated by combining Equations (4.95) and (4.102),

$$P_{XH} = \frac{Y_H}{(1 + b_H \beta \theta_X)} \frac{Q(C_{Sin} - S_S) \beta}{(V_{anox} f_R \eta_g + V_{mbr} (1 - f_{DNH}))} (V_{anox} f_R + V_{mbr}) \quad (4.123)$$

Incorporating Y_{NH} into Equation (4.123) will result in,

$$P_{XH} = Y_{NH} Q(C_{Sin} - S_S) \beta \frac{(V_{anox} f_R + V_{mbr})}{(V_{anox} f_R \eta_g + V_{mbr} (1 - f_{DNH}))} \quad (4.124)$$

P_{XP} can be derived by combining Equations (4.102), (4.110) and (4.111);

$$P_{XP} = f_{EX} b_H ((1 - f_{DNH}) + \eta_D f_{DNH}) Y_{NH} Q(C_{Sin} - S_S) \beta \theta_X \frac{(V_{anox} f_R + V_{mbr})}{(V_{anox} f_R \eta_g + V_{mbr} (1 - f_{DNH}))} \quad (4.125)$$

The excess sludge production of inert particulate organic matter can be expressed in a simplified form with respect to the heterotrophic excess sludge production;

$$P_{XP} = f_{EX} b_H ((1 - f_{DNH}) + \eta_D f_{DNH}) \beta \theta_X P_{XH} \quad (4.126)$$

The sludge resulting from the accumulation of inert particulate COD will directly proportional to the amount in the influent,

$$P_{XI} = Q f_{XI} C_{Tin} = Q \frac{f_{XI}}{f_S} C_{Sin} \quad \text{or} \quad P_{XI} = Q X_{I1} \quad (4.127)$$

where Q_W is the excess sludge flow.

The particulate slowly biodegradable COD will also be wasted from the system through the sludge stream on the basis of Equations (4.95) and (4.117);

$$P_{XS} = \frac{Q X_{Sin}}{1 + k_h \theta_X ((1 - f_{DNH}) + \eta_{HYD} f_{DNH})} \quad (4.128)$$

The amount of autotrophic biomass to be wasted can be derived from the mass balance equation written for X_A ,

$$P_{XA} = \frac{V_T X_A}{\theta_{XA}} \quad (4.129)$$

where,

$$V_T X_A = X_{Ambr} (V_{anox} f_R + V_{mbr}) \quad (4.130)$$

By combining Equations (4.105), (4.129) and (4.130), P_{XA} can be defined as,

$$P_{XA} = QY_{NA}(S_{NHin} - S_{NHE}) \frac{V_{anox}f_R + V_{mbr}}{V_{mbr}} \quad (4.131)$$

The influent inorganic suspended solids will also get enmeshed within the activated sludge significantly contributing the total mass retained in the system. The influent inorganic suspended solids will behave in the same way as inert particulate COD of influent origin by not contributing to any of the processes and it's amount will increase with the sludge age of the system.

$$P_{ISS} = QX_{ISSin} \quad (4.132)$$

4.8.3 Nitrification stoichiometry

The steady state mass balance equation for ammonia nitrogen based on the process kinetics given in Table 4.7 will lead to the daily amount of ammonia nitrogen oxidized per unit amount of total biomass in the reactor which can be identified as the nitrification rate.

$$V \frac{dS_{NH}}{dt} = Q_{in}S_{NHin} - Q_p S_{NH} - V_{mbr} \left(-i_{XB} - \frac{1}{Y_A}\right) X_A \mu_{Amax} \frac{S_{NH}}{K_{NH} + S_{NH}} \frac{S_O}{K_{OA} + S_O} = 0 \quad (4.133)$$

The above expression can be rearranged as,

$$S_{NHin} - S_{NH} = \frac{V_{mbr}}{Q} \left(i_{XB} + \frac{1}{Y_A}\right) X_A \mu_A (1 - f_{DNA}) \quad (4.134)$$

The amount of nitrogen that is incorporated into biomass for cell synthesis during growth of autotrophs can be neglected for simplifying purposes. Then the amount of ammonia nitrogen used as the energy source for aerobic growth of autotrophs in nitrification will be;

$$S_{NHin} - S_{NH} = \frac{V_{mbr}}{Q} \frac{\mu_A}{Y_A} X_A (1 - f_{DNA}) = q_A \theta_H X_A (1 - f_{DNA}) \quad (4.135)$$

The nitrification rate, R_N , is defined as the daily amount of ammonia nitrogen oxidized per unit amount of total active biomass in the reactor,

$$R_N = \frac{QN_{OX}}{V_T X_T} = f_A \frac{N_{OX}}{X_A \theta_H} \quad (4.136)$$

where f_A is the autotrophic fraction of the total biomass which can be estimated from the daily amount of biomass production for the heterotrophic and autotrophic portions.

$$f_A = \frac{P_{XA}}{P_{XA} + P_{XH}} \quad (4.137)$$

The amount of nitrogen incorporated into heterotrophic biomass, N_X , can also be derived from the following mass balance equation,

$$N_X = \frac{VX_H}{Q} [i_{XB}(\mu_H(1 - f_{DNH}) + \eta_g f_{DNH}) + b_H f_{EX} i_{XP} ((1 - f_{DNH}) + \eta_D f_{DNH})] \quad (4.138)$$

In a more simple way, the mass of nitrogen incorporated into biomass will be equal to the sum of nitrogen associated with the heterotrophic biomass by the fraction of i_{XB} and the nitrogen associated with the endogenous products by the fraction of i_{XE} . This can be expressed as;

$$QN_X = i_{XB}Q_W X_H + i_{XP}Q_W X_P \quad (4.139)$$

where $Q_W X_H = P_{XH}$ and $Q_W X_P = P_{XP}$

$$N_X = i_{XB}P_{XH} + i_{XE}f_{EX}b_H((1 - f_{DNH}) + \eta_D f_{DNH})P_{XH}\beta\theta_X \quad (4.140)$$

Substitution of the values of P_{XH} and P_{XP} in Equations (4.124) and (4.127) respectively will result in the following equation for the amount of nitrogen incorporated into heterotrophic biomass per unit volume of wastewater treated, N_X ,

$$\frac{N_X}{Q} = [i_{XB} + f_{EX}i_{XP}b_H((1 - f_{DNH}) + \eta_D f_{DNH})\beta\theta_X]Y_{NH}(C_{Sin} - S_S)\beta \frac{V_{anox}f_R + V_{mbr}}{V_{anox}f_R\eta_g + V_{mbr}(1 - f_{DNH})} \quad (4.141)$$

The expected effluent ammonia nitrogen concentration can be found as a function of the sludge age and the sustained dissolved oxygen level by equating the specific growth rate of the nitrifiers in Equation (4.106) to,

$$\frac{1 + b_A(1 - f_{DNA})\theta_{XA}}{\theta_{XA}(1 - f_{DNA})} = \mu_{Amax} \frac{S_{NH}}{K_{NH} + S_{NH}} \quad (4.142)$$

Rearranging equation (4.144) for S_{NH} will yield the effluent ammonia nitrogen concentration in a membrane bioreactor system;

$$S_{NH} = \frac{K_{NH}(1 + b_A(1 - f_{DNA})\theta_{XA})}{\theta_{XA}(1 - f_{DNA})(\mu_{Amax} - b_A)} - 1 \quad (4.143)$$

Unlike the conventional activated sludge systems, the effluent ammonia nitrogen concentration in the membrane bioreactor is also related to the dissolved oxygen level in the membrane reactor which also affects the decay of autotrophs under low DO conditions.

The oxidizable ammonia nitrogen, N_{OX} , can be expressed as the difference between the influent ammonia nitrogen and effluent ammonia nitrogen plus the nitrogen incorporated into biomass.

$$N_{OX} = S_{NHin} - S_{NHE} - N_X \quad (4.144)$$

Under full nitrification conditions the oxidizable ammonia nitrogen, N_{OX} will be equal to the formed nitrate nitrogen, S_{NO} .

4.8.4 Denitrification stoichiometry

In the conventional activated sludge systems, the conversion of already formed nitrate nitrogen into nitrogen gas is expected to occur only in unaerated tanks of the system where anoxic conditions prevail. However due to the oxygen diffusion limitation phenomena expected in the membrane bioreactor systems denitrification can occur both in the anoxic and the MBR tank with a level defined in relation to the sustained dissolved oxygen level. Therefore correct assessment of the denitrification potential in a membrane bioreactor system involves the investigation of this process in both tanks. Denitrification potential, N_{DP} , can be defined as the amount of nitrate nitrogen that can be potentially removed by means of denitrification. It is defined on the basis of nitrate requirement rate which may be calculated as the electron acceptor demand (Orhon and Artan, 1994) in the anoxic and MBR tanks. The nitrate requirement rate for the MBR reactor can be defined as,

$$R_{NDmbr} = \frac{1 - Y_H}{2.86Y_H} \eta_g \mu_{Hmax} \frac{S_S}{K_S + S_S} f_{DNH} \frac{S_{NO}}{K_{NO} + S_{NO}} X_H + \frac{1 - f_{EX} - f_{ES}}{2.86} \eta_D b_H f_{DNH} \frac{S_{NO}}{K_{NO} + S_{NO}} X_H + \frac{1 - f_{EX} - f_{ES}}{2.86} \eta_D b_A f_{DNA} \frac{S_{NO}}{K_{NO} + S_{NO}} X_A \quad (4.145)$$

The nitrate requirement rate for the anoxic tank can be defined in the same way done for the MBR reactor ,

$$R_{ND_{anox}} = \frac{1-Y_H}{2.86Y_H} \eta_g \mu_{H_{max}} \frac{S_S}{K_S + S_S} \frac{S_{NO}}{K_{NO} + S_{NO}} X_H + \frac{1-f_{EX} - f_{ES}}{2.86} \eta_D b_H$$

$$\frac{S_{NO}}{K_{NO} + S_{NO}} X_H + \frac{1-f_{EX} - f_{ES}}{2.86} \eta_D b_A \frac{S_{NO}}{K_{NO} + S_{NO}} X_A \quad (4.146)$$

The oxygen switching function in the anoxic reactor can be neglected as it is always low and it is not affected severely by the dissolved oxygen level in the MBR tank. Equations (4.147) and (4.148) can be further simplified by neglecting the nitrate uptake of autotrophs during decay as the contribution in the total uptake would be negligible with respect to heterotrophs. During denitrification the level of produced nitrate will be very high compared to the half saturation concentration of nitrate nitrogen ($S_{NO} \gg K_{NO}$). Therefore the switching function for nitrate nitrogen can be eliminated with the assumption that denitrification fully takes place in these reactors however in relation to the dissolved oxygen level in the MBR tank. Substituting the value of $\mu_H X_H$ and X_H in Equation (4.101) and (4.102) into Equations (4.145) and (4.148) will yield the following expressions for MBR and anoxic tank respectively;

$$\frac{N_{DP_{mbr}}}{Q} = \frac{V_{mbr}}{V_{anox} f_R \eta_g + V_{mbr} (1 - f_{DNH})} \frac{(C_{Sin} - S_S)}{2.86} f_{DNH} \left[(1 - Y_H) \eta_g + \frac{(1 - f_{EX} - f_{ES}) \eta_D b_H Y_H \beta \theta_X}{(1 + b_H \beta \theta_X)} \right] \quad (4.147)$$

and

$$\frac{N_{DP_{anox}}}{Q} = \frac{V_{anox}}{V_{anox} f_R \eta_g + V_{mbr} (1 - f_{DNH})} \frac{(C_{Sin} - S_S)}{2.86} f_R \left[(1 - Y_H) \eta_g + \frac{(1 - f_{EX} - f_{ES}) \eta_D b_H Y_H \beta \theta_X}{(1 + b_H \beta \theta_X)} \right] \quad (4.148)$$

Combining Equations (4.147) and (4.148) will yield the overall denitrification potential of a membrane bioreactor system.

$$\frac{N_{DP}}{Q} = \left[((1 - Y_H) \eta_g + \frac{(1 - f_{EX} - f_{ES}) \eta_D b_H Y_H \beta \theta_X}{(1 + b_H \beta \theta_X)}) \right] \frac{V_{mbr} f_{DNH} + f_R V_{anox}}{V_{anox} f_R \eta_g + V_{mbr} (1 - f_{DNH})} \frac{(C_{Sin} - S_S)}{2.86} \quad (4.149)$$

Although an overall expression defining the total denitrification potential in the system can be defined however it is very important to assess the denitrification potential for each reactor. Orhon and Artan (1994) postulated the approach that the entire readily biodegradable substrate will be depleted in the anoxic tank and the remaining portion of the biodegradable substrate is to be distributed between the anoxic and aerobic zones in the ratio of V_D/V_T for conventional activated sludge systems. The same approach can be adopted to membrane bioreactor systems however in a different way. The readily biodegradable substrate will be depleted in both the anoxic and MBR reactors as a fraction of the nitrate nitrogen equivalent of the total electron donor demand associated with the heterotrophic growth whilst readily and slowly biodegradable substrate will be utilized in both tanks with the electron donor demand associated with anoxic and aerobic endogenous respiration. The level of nitrate uptake in the presence of an electron donor will be varying in the MBR tank with respect to the dissolved oxygen levels. This approach can be stoichiometrically expressed for the anoxic and MBR tanks respectively with the following equations ;

$$\frac{N_{DPanox}}{Q} = \left[(1 - Y_H) \frac{S_{Sin}}{2.86} \eta_g + \frac{(1 - f_{EX} - f_{ES}) \eta_D b_H Y_H \beta \theta_X}{(1 + b_H \beta \theta_X)} \frac{C_{Sin}}{2.86} \right] \frac{V_{anox}}{V_T} \quad (4.150)$$

and

$$\frac{N_{DPmbr}}{Q} = \left[(1 - Y_H) \frac{(C_{Sin} - S_{Sin})}{2.86} \eta_g + \frac{(1 - f_{EX} - f_{ES}) \eta_D b_H Y_H \beta \theta_X}{(1 + b_H \beta \theta_X)} \frac{C_{Sin}}{2.86} \eta_{anox} \right] f_{DNH} \left(1 - \frac{V_{anox}}{V_T} \right) \quad (4.151)$$

The remaining biodegradable substrate for nitrate utilization during anoxic and aerobic decay is corrected by a factor of η_{anox} when estimating the denitrification potential of the membrane tank due to the fact that some portion of the readily biodegradable COD will be depleted and some portion of the slowly biodegradable COD will be hydrolyzed in the anoxic tank. The readily biodegradable substrate to be used for growth in the MBR tank will be generated by the hydrolysis of the slowly biodegradable substrate remaining from the anoxic tank. The electron donor that will be used for the uptake of nitrate during the anoxic and aerobic endogenous respiration will be equal to the slowly biodegradable COD that is remaining from the hydrolysis within the anoxic tank. Therefore using the correction factor for

hydrolysis, η_{HYD} , in the anoxic tank, the denitrification potential of the MBR tank can be reexpressed as,

$$\frac{N_{DPmbr}}{Q} = \left[(1 - Y_H) \frac{(C_{Sin} - S_{Sin})}{2.86} \eta_g + \frac{(1 - f_{EX} - f_{ES}) \eta_D b_H Y_H \beta \theta_X}{(1 + b_H \beta \theta_X)} \frac{X_{Sin}}{2.86} \eta_{HYD} \right] f_{DNH} \left(1 - \frac{V_{anox}}{V_T} \right) \quad (4.152)$$

It is more practical and technically correct to quantify the hydrolysis that is taking place under the anoxic conditions. ASM1 (Henze et al., 1987) recommends 0.40 for the correction factor of hydrolysis under anoxic conditions. It is expected that this ratio to be higher in the membrane bioreactor systems.

Mass balance for nitrate nitrogen on the entire system determines the nitrate concentration, S_{NOE} in the effluent.

$$QS_{NOin} - QS_{NOE} + QN_{OX} - QN_{DP} = 0 \quad (4.153)$$

The effluent nitrate nitrogen is also related to the recirculation of the produced nitrates back to the anoxic tank. Unlike the conventional systems, the membrane bioreactors do not have internal recirculation lines dedicated for recycling of the nitrified mixed liquor. The sludge and the formed nitrates are returned back to the anoxic reactor together by a single recycle line from the membrane tank. If the denitrification potential of the system is sufficient, then all of the nitrate nitrogen recirculated into the anoxic zone will be consumed. It should also be noted that the recirculation also carries dissolved oxygen into the anoxic tank which causes a reduction in the denitrification potential. In this case the expected effluent nitrate nitrogen concentration can be expressed as follows;

$$S_{NOE} = S_{NOin} + N_{OX} - N_{DP} + R \frac{S_O}{2.86} \quad (4.154)$$

The denitrification potential of a system can exceed the amount of nitrate nitrogen to be denitrified. In this case effluent nitrate nitrogen is expected to be zero.

Furthermore, it should be noted that decreased dissolved oxygen levels in the membrane tank will promote anoxic conditions that will enable the uptake of nitrate nitrogen both in the anoxic growth and decay phases resulting in simultaneous nitrification and denitrification in the membrane tank. The level of simultaneous nitrification and denitrification (SNdN) is solely dependant on the sustained dissolved oxygen levels due to oxygen diffusion limitation. Oxygen diffusion

limitation in a suspended process can only be explained by the half saturation concentration oxygen for both the heterotrophs and autotrophs. Equation (4.149) implies that as the dissolved oxygen in the membrane tank decreases the denitrification potential of this reactor increases resulting in increase amount of nitrate uptake. Consequently, there is a tendency of the denitrification process to completely shift to the MBR reactor with decreasing oxygen levels resulting in a less need for the anoxic reactor as decreased level of nitrate nitrogen will be recycled back to the anoxic reactor.

During increased levels of dissolved oxygen, the denitrification will be occurring in the anoxic tank. Therefore, switch function of nitrate is important because it will define the limitation on the extent of denitrification occurring in a particular tank. However since the level of nitrate nitrogen that is to be produced is dependant on the level of dissolved oxygen in the MBR reactor, it is practically not possible to involve this switch function in the stoichiometric equations derived for the denitrification potential. This can only be assessed by the simultaneous solving of the set of differential equations for the processes and components given in table 4.7. A computer simulator or a program is essential in evaluating this phenomena. Simultaneous nitrification and denitrification (SNDN) is a complex process especially in a MBR where oxygen diffusion limitation govern the diffusivity of oxygen from the bulk liquid into the bacterial cell.

4.8.5 Oxygen utilization

The oxygen utilization is related to three processes, *i.) Growth of Heterotrophs, ii.) Growth of Autotrophs, iii.) Endogenous Respiration of both Heterotrophs and Autotrophs*

The oxygen requirement for heterotrophs, OR_H , in the MBR can be expressed as follows

$$V_{mbr} OUR_H = V_{mbr} R_{HSO} = \left(\frac{1 - Y_H}{Y_H} \mu_H X_{Hmbr} + (1 - f_{EX} - f_{ES}) b_H X_{Hmbr} \right) (1 - f_{DNH}) \quad (4.155)$$

Substituting the value of $\mu_H X_H$ and X_H in Equation (4.101) and (4.102) into Equations (4.157) will yield the oxygen requirement of heterotrophs;

$$\frac{OR_H}{Q} = \frac{(C_{Sin} - S_S)(1 - f_{DNH})}{V_{anox} f_R \eta_g + V_{mbr}(1 - f_{DNH})} \left[(1 - Y_H) + (1 - f_{EX} - f_{ES}) b_H \beta \theta_X \frac{Y_H}{1 + b_H \beta \theta_X} \right] \quad (4.156)$$

The oxygen requirement for nitrification, OR_A , is function of the oxygen utilization rate for autotrophs, R_{ASO} ,

$$V_{mbr} OUR_A = V_{mbr} R_{ASO} = \left(\frac{4.57 - Y_A}{Y_A} \mu_A X_A + (1 - f_{EX} - f_{ES}) b_A X_A \right) (1 - f_{DNA}) \quad (4.157)$$

Substituting the value of $\mu_A X_A$ and X_A in Equation (4.106) and (4.107) into Equations (4.159) will yield the oxygen requirement of autotrophs ;

$$\frac{OR_A}{Q} = \frac{(S_{NHin} - S_{NHE})}{V_{mbr}} \left[(4.57 - Y_A) + (1 - f_{EX} - f_{ES}) b_A (1 - f_{DNA}) \theta_{XA} \frac{Y_A}{1 + b_A (1 - f_{DNA}) \theta_{XA}} \right] \quad (4.158)$$

The required oxygen is related to the amount of oxidizable ammonia nitrogen, therefore it would be more appropriate to use N_{OX} value instead of $(S_{NHin} - S_{NH})$.

$$\frac{OR_A}{Q} = \frac{N_{OX}}{V_{mbr}} \left[(4.57 - Y_A) + (1 - f_{EX} - f_{ES}) b_A (1 - f_{DNA}) \theta_{XA} Y_{NA} \right] \quad (4.159)$$

where

$$N_{OX} = S_{NHin} - S_{NHE} - N_X \quad (4.160)$$

Since the amount of autotrophs in the system is very low compared to heterotrophs the oxygen requirement related to endogenous respiration during decay of autotrophs is mostly neglected. In this case the oxygen requirement for nitrification can be expressed in the simplest way;

$$OR_A = \frac{4.57 Q N_{OX}}{V_{mbr}} \quad (4.161)$$

In denitrification systems, the overall rate of oxygen requirement can be calculated by subtracting the oxygen equivalent of the nitrate nitrogen removal rate in denitrification from the sum of carbonaceous and nitrogenous oxygen demands,

$$OR_T = OR_H + 4.57 Q N_{OX} - 2.86 Q (N_{OX} - S_{NOE}) \quad (4.162)$$

where $N_{OX} - S_{NOE}$ will be equal to the nitrate nitrogen removal rate, N_D . Then Equation (4.163) can be rewritten as,

$$OR_T = OR_H + 4.57QN_{OX} - 2.86QN_D \quad (4.163)$$

4.9 Dynamic Modelling of Membrane Bioreactors with the New Adopted Process Matrix using a Computer Simulator

Computer based process simulation is ideal to predict and assess the behaviour of activated sludge systems. BioWin 2.2® by EnviroSim Associates Ltd has been used to simulate and assess the behaviour of membrane bioreactor systems with the new adopted process matrix incorporating simultaneous nitrification and denitrification (SNdN). The usage of the simulator has been done in a stepwise manner based on a methodology. Figure 4.9 illustrates the general methodology adopted in setting up the simulation model for pilot membrane bioreactor.

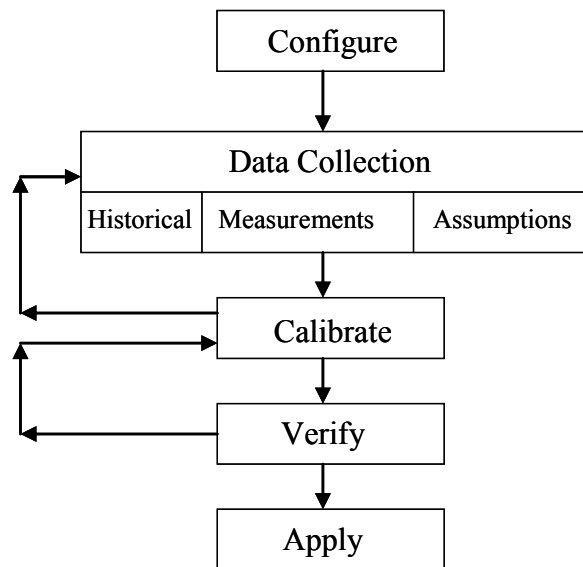


Figure 4.9: Methodology followed for using the process simulator (Dold et al., 2003)

The summary of steps followed for the usage of the simulator in accordance with the methodology given in Figure 4.9 are as follows,

- i. The simulator is configured with the physical characteristics of the pilot membrane bioreactor system including but not limited to unit sizes, flowrates, flow routings and modelling frame work which comprises of model selection for biokinetics, settling, oxygenation..etc
- ii. Necessary data is collected on wastewater characteristics, plant performance, recordings of daily pH, dissolved oxygen, oxidation-reduction potential, flows..etc to be used in the simulation and calibration of the new biological adopted process matrix for MBR.
- iii. Calibration step involves adjustment of the operational and controllable parameters of the model and the pilot plant to fit the actual measured performance data. This step usually involves reverting back to the previous steps on data gathering or reassessing the adopted biokinetic model until a match is achieved.
- iv. Verification involves applying the calibrated simulator to a different set of operating points other than that used for calibration to check the validity and consistency. The types of model parameters that are adjusted at this step usually consists for those which direct measurements cannot be made.
- v. The last step of the methodology involves the application of the calibrated and verified model for the intended end use.

Dynamic modelling and calibration have been conducted for the pilot scale membrane bioreactor.

4.9.1 Configuration of the MBR pilot plant in the simulator

Configuration and setup of the actual conditions in the process simulator is very important to achieve the most accurate results. Setup includes entering of the process arrangement along with the unit sizes of the reactors, input and sludge recirculation streams. Bioreactor step up in the process simulator is the most important and vital step of configuring the system. Important considerations for bioreactors include compartmentalization into aerated and unaerated zones, the length width and depth ratios of each zone and the number and size of completely mixed or plugflow vessels used to model the mixing regimes.

The pilot plant MBR includes two bioreactors connected in series; *i.) Anoxic Tank* and *ii.) MBR tank*. The permeate of the membrane modules leaves the system as the effluent whilst the content of the MBR tank is being recirculated back to the anoxic tank. The system consists only one recirculation stream which serves the purposes of both recycling back the nitrified mixed liquor and the biomass. Both of the tanks have completely mixed regimes where anoxic tank is mixed by a surface agitator and the MBR tank is mixed and aerated through a blower coarse bubble diffuser system. The identification and setup of the aeration system is also important as the oxygen transfer efficiencies will be different for fine bubble and coarse bubble systems.

The configuration of the pilot plant MBR in the process simulator in accordance with the process flow diagram given in Figure 3.5 is illustrated in Figure 4.10.

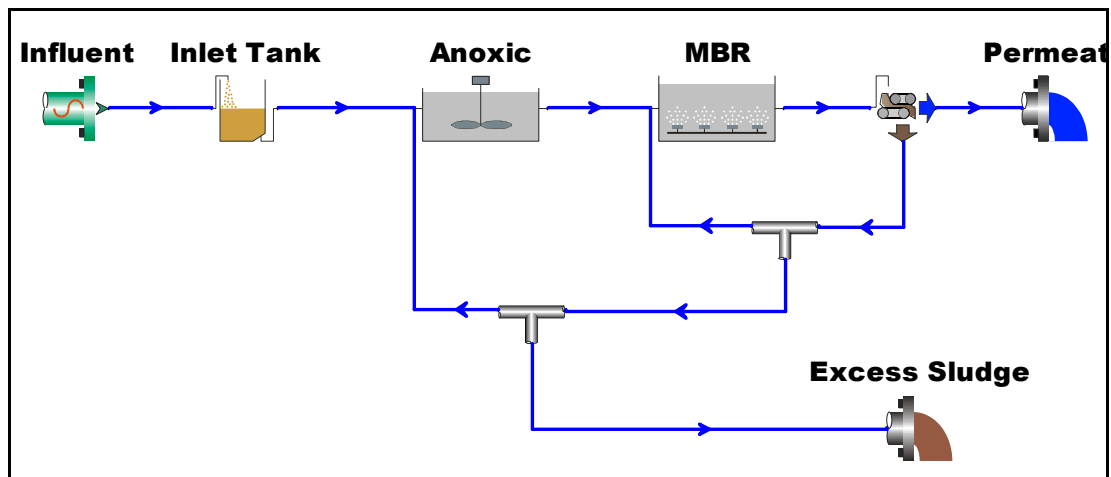


Figure 4.10: Plant layout implemented in BioWin 2.2® software

Although it has been mentioned that there is only one recirculation in the actual plant setup it is clearly seen in Figure 4.10. that there are two recirculation streams in the process simulator setup. The BioWin 2.2 uses a membrane process module to illustrate the complete retention of the solid particles and biomass greater than $4\ \mu\text{m}$. As it is known, unlike the externally configured microfiltration/ ultrafiltration/nanofiltration and reverse osmosis systems, the retained solids remain within the MBR tank where the membrane module is submerged and there is no separate line for discharging the retentate from the system. To illustrate the complete retention of the solids within the MBR tank, the plant layout in the process simulator consists of second recirculation line from the MBR process module back to the MBR tank. This recirculation stream having a very high flow ($>50Q_{in}$) is

designated as an internal recirculation stream representing the total solids entrapment within the MBR tank in terms of modelling purposes in the simulator. This very high flowrate of the internal recirculation becomes irrelevant and does not affect the amount of solids entrapment within the MBR tank above five times in the inlet flow. However to illustrate complete sludge retainment seen in the actual pilot plant setup a higher internal recirculation flow has been chosen. The excess sludge flow is being wasted from the recirculation line going back to the anoxic tank in the simulator layout as done in the actual plant.

The inlet tank serves the purpose of buffering the daily flow variations and enables a constant continuous feed to the MBR system. It also holds a fine basket screen to separate the solids from the inflow.

The influent stream has been modelled to incorporate the inlet wastewater characterization in accordance with the process components outlined in Figure 4.1. and Figure 4.3. The new adopted process matrix has been implemented using the “model builder” unit of BioWin which is illustrated in Figure 4.11.

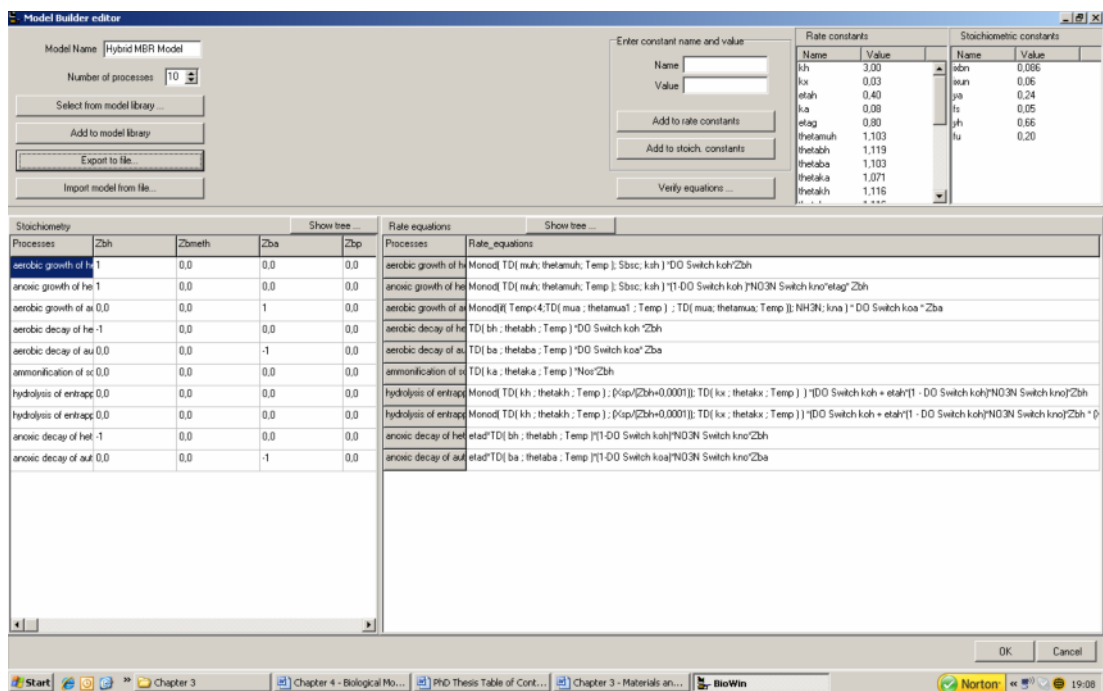


Figure 4.11: Model builder unit in BioWin for implementing the new adopted MBR process matrix

4.9.2 Data collection

The data collection along with the measurement and analysis campaign have been explained and defined in detail in Section 3.3. This section must be referred to for details.

4.9.3 Calibration protocol

Calibration is regarded as the process in which model parameters are adjusted until model predictions match selected sets of data linked to the performance of the actual plant. The objective would be to minimize the error between the datasets and model predictions. The following generalized procedure have been followed for calibration;

- i. The simulation has been dynamically ran for a scenario and time interval for which the measured data were available,
- ii. The simulation results were compared with the observed and measured data by making an error estimation. The error estimation can be defined as the visual observation of time series plots predicted by the model against appropriate data,
- iii. Parameters that are likely to affect the errors have been identified and the relevant parameters were adjusted to minimize these errors by making a loop for returning to the first step.

The kinetics and stoichiometry for autotrophs and heterotrophs are taken from ASM1 except for the decay rate where ASM1 is based on death regeneration approach whilst the new adopted model incorporates the endogenous decay mechanism. The default values of the parameters were taken at the starting point of calibration.

A stepwise long term dynamic calibration methodology was developed by initial introduction of three iterative steps in the order of VSS, TSS, $\text{NH}_4^+\text{-N}$, O_2 and $\text{NO}_3^-\text{-N}$ profiles respectively. For each iteration, the duration of the study (310 days) was resimulated each time when a parameter was changed to fit the plant data. The initial conditions which play an important role in dynamic simulations were carefully measured and set in the process simulator to account for the real conditions. In this way the initial conditions for all variables were properly estimated. The starting point of the calibration was to obtain and fit the measured solids data for MLVSS and MLSS profile. In the first attempts with the default parameter values, the solids

balance was underestimated with respect to the measured data. As a result, the decay rate for the heterotrophs, b_H and the maximum specific growth rate for heterotrophs, μ_{Hmax} were iteratively changed until a fit for the solids balance was achieved. However numerous attempts made for long dynamic simulation runs did not achieve a best fit especially for diurnal variations. The VSS and TSS concentrations simulated were observed to be lower than the measured results. Respirometric analysis has also been made with the membrane sludge for the specific determination of the decay rate for heterotrophs. The results can be seen in Appendix A.

Next, the maximum specific growth rate of autotrophs, μ_{Amax} , had to be increased to sustain autotrophic growth, whilst the decay rate for autotrophs, b_A , the half saturation constant for ammonia, K_{NH} , and the oxygen half saturation constant for autotrophs, K_{OA} had to be iteratively adjusted to enable for the levels of nitrification taking place in the membrane bioreactor. These parameters also played an important role in achieving the best fit for the effluent ammonia nitrogen concentration profile with respect to changing dissolved oxygen levels throughout the study. The observed high nitrification efficiencies under very low temperatures not resulting in a nitrifier washout was calibrated by adopting a higher Arrhenius type temperature factor. This enabled the observation of partial nitrification in the process simulator as observed in the measured results.

In the third step, the oxygen half saturation constant for the heterotrophs, K_{OH} and the correction factor, η_D , for the decay of heterotrophs under anoxic conditions were adjusted to fit the long term measured nitrate nitrogen profile. Siegrist et al. (1999) proposed a reduction in anoxic decay rate of 40-50% for autotrophs and heterotrophs by performing batch experiments. K_{OH} was increased to account for the oxygen diffusion limitation from the bulk liquid into the floc which promoted more nitrate uptake for a given dissolved oxygen concentration in the membrane bioreactor systems. This would have been very low for a conventional activated sludge system operating under the same dissolved oxygen concentration. The correction factor for the decay of heterotrophs under anoxic conditions were also increased considerably with respect to the reported values in the literature. Both of the latter two can be accounted to simultaneous nitrification and denitrification (SNdN). The calibration of oxygen profiles have done simultaneously in this step by changing oxygen half saturation constants for heterotrophs and autotrophs.

Interestingly, when the oxygen half saturation constant for the heterotrophs, K_{OH} was adjusted to fit the nitrate nitrogen profile the VSS and TSS profile resulted in a best fit against the measurement results. This aspect explained the reason for the non fitted VSS, TSS curve in the first iterative phase. Although it would seem that a decrease in the oxygen half saturation constant for heterotrophs would promote a higher heterotrophic activity in a conventional activated sludge system however this has proven to be opposite in a membrane bioreactor system. With a higher oxygen half saturation constant for heterotrophs, K_{OH} , it is evident that the overall growth for any given dissolved oxygen concentration in a membrane bioreactor is higher compared to a conventional system due to the contribution of anoxic growth. On the contrary with a higher half saturation constant for heterotrophs the decay rate for a given dissolved oxygen concentration would be lower. The combined affect of this would result in an overall increase in the heterotrophic and autotrophic microbial community. The increased value of the oxygen half saturation constant for heterotrophs, K_{OH} , verifies the oxygen diffusion limitation in MBRs and the existence of an anoxic mass fraction within the floc of microbial culture acclimated in a membrane bioreactor. The calibration results also prove that the stoichiometric equations derived for the determination of active heterotrophic and autotrophic biomass should always be used in conjunction with their oxygen switch functions (f_{DNH} and f_{DNA}).

The affect of the oxygen half saturation constant on the heterotrophic and autotrophic biomass resulted in the decrease of the iterative steps to two in the calibration protocol. In the revised and final calibration methodology, first the nitrification and the ammonia nitrogen profile was calibrated and afterwards MLVSS and the nitrate nitrogen profile were fitted in the same step by changing the growth and decay rates for heterotrophs and the oxygen half saturation constant for heterotrophs. The adopted and used calibration methodology is presented in Figure 4.12 (Insel et al., 2006). Each iteration step comprises the preceding steps to maintain good of VSS, TSS, $\text{NH}_4^+\text{-N}$, O_2 and NO_3^-N profiles.

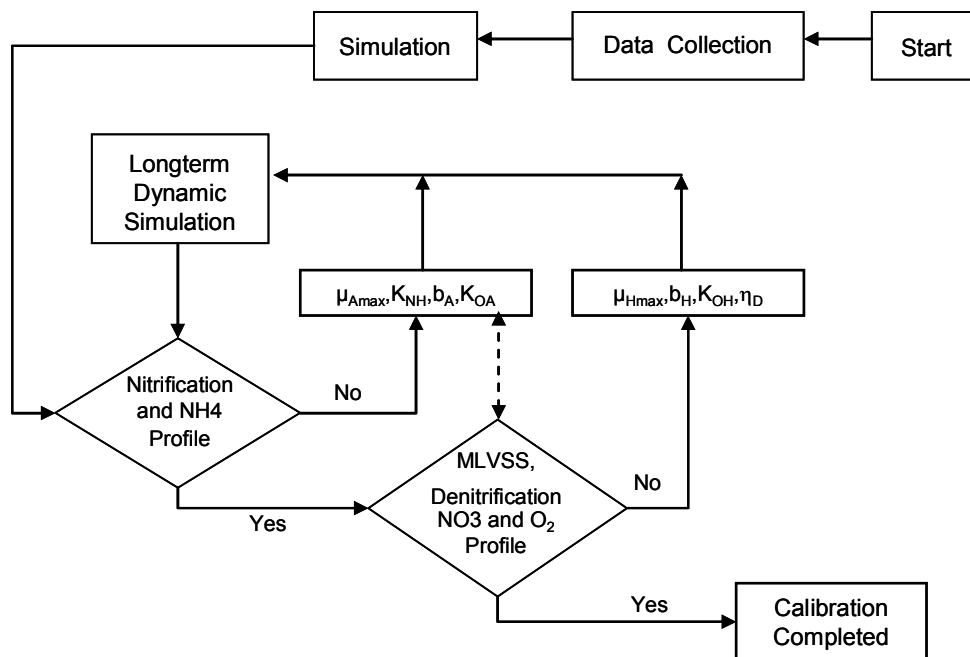


Figure 4.12: Calibration methodology of the new adopted process matrix for MBR (Insel et al., 2006)

The calibration of the VSS, NO₃ and O₂ profiles had to be conducted under the same iterative step as the parameters that affected each of these profiles were interrelated to another. The values of the calibrated parameters together with their default values are listed in Table 4.9.

Table 4.9: Summary of the calibrated ASM1 parameters to the new adopted process matrix for MBR

<i>Parameter</i>	<i>Units</i>	<i>ASM1</i>	θ <i>(ASM1)</i>	<i>Calibrated</i>	θ <i>(Calibrated)</i>
<i>Stoichiometric</i>					
Heterotrophic Yield, Y_H	gcellCOD gCOD ⁻¹	0.67	-	0.66	
Autotrophic Yield, Y_A	gcellCOD gN ⁻¹	0.24	-	0.24	
Fraction of biomass leading to particulate products, f_p (f_{EX})	dimensionless	0.08	-	0.20	
Fraction of biomass leading to soluble products, f_{ES}	dimensionless	-	-	0.05	
Mass of nitrogen per mass of COD in biomass, i_{XB}	gN gCOD ⁻¹ in biomass	0.086	-	0.086	
Mass of nitrogen per mass of COD in products from biomass, i_{XE}	gN gCOD ⁻¹ in end.mass	0.06	-	0.06	
<i>Kinetic</i>					
Max specific growth rate for heterotrophic biomass, μ_{Hmax}	d ⁻¹	6	1.029	6	1.103
Half saturation constant for heterotrophic biomass, K_S	g m ⁻³	20	-	20	
Decay rate for heterotrophic biomass, b_H	d ⁻¹	0.62	1.029	0.24	1.119
Oxygen half saturation constant for heterotrophs, K_{OH}	g O ₂ m ⁻³	0.20	-	1	
Ammonia half saturation constant for autotrophic biomass, K_{NH}	g Nm ⁻³	1	-	2	
Max specific growth rate for autotrophic biomass, μ_{Amax}	d ⁻¹	0.80	1.072	1	1.123
Decay rate for autotrophic biomass, b_A	d ⁻¹	0.05- 0.15	1.029	0.06	1.119
Correction factor for μ_{Hmax} under anoxic conditions, η_g	dimensionless	0.80	-	0.80	
Correction factor for hydrolysis under anoxic conditions, η_h	dimensionless	0.40	-	0.6	
Correction factor decay under anoxic conditions, η_D	dimensionless	-	-	0.90	
Max specific hydrolysis rate, K_h	gX _S (gcell COD.d) ⁻¹	3	1.05	3	1.116
Half saturation constant for hydrolysis of slowly biodeg. subs., K_X	gX _S gcell COD ⁻¹	0.03	1.029	0.03	1.116
Nitrate half saturation constant for denitrifying het. Biomass, K_{NO}	gNO ₃ -N m ⁻³	2	-	2	
Ammonification rate, k_a	m ³ COD (g .d) ⁻¹	0.08	1.05	0.08	1.071

The oxygen half saturation constant for heterotrophs, K_{OH} , and autotrophs, K_{OA} , were calibrated at 1.0 mg/l and 1.25 mg/l respectively which is very high compared to used values in ASM1. Higher oxygen half saturation constants imply less diffusivity of oxygen from the bulk liquid into the bacterial flocs. The correction factor, η_D , for

decay under anoxic conditions was set at 0.90 suggesting a higher decay rate and hence a higher nitrate uptake rate compared to conventional systems. The higher oxygen half saturation constant coupled with a higher decay rate under anoxic conditions favor the conditions for simultaneous nitrification and denitrification (SNdN).

Nitrification which is solely dependant on oxygen was also sensitive to changing dissolved oxygen levels. The effluent ammonia nitrogen concentration, S_{NH} , were fitted to the measured data with the calibration of the oxygen half saturation constant of autotrophs, K_{OA} , and the half saturation constant for ammonia, K_{NH} . The half saturation constant for ammonia was set to 2 mg/lit which is double the value used in ASM1 whilst the half saturation constant for nitrate nitrogen, K_{NO} , was also calibrated at 2 mg/lit. The typical value used for K_{NO} in ASM1 is 0.50 mg/lit. The calibration task was completed when the simulated profiles were closest to the to all measured data.

4.9.4 Sensitivity analysis

Sensitivity analysis have been conducted on the calibrated model to identify those model parameters that have the largest effect on the model variables. Linear sensitivity analysis has been applied by developing sensitivity functions around a certain operating point. The relative change in state y_j for a 100% change in parameter θ_i is used which is expressed as follows;

$$\delta_{i,j} = \frac{\theta_i}{y_j} \frac{\partial y_j}{\partial \theta_i} \quad (4.164)$$

where i is the n number of parameters and j is the m number of states.

Parameters for which $\delta_{i,j} > 100\%$ are considered to be very sensitive therefore for a thorough evaluation relative sensitivities between the parameters should be taken into account. The sensitivity analysis has been performed by perturbing each individual parameter one at a time by an appropriately selected perturbation value $\Delta\theta$ (IWA and WERF, 2003) which is represented in Equation (4.167),

$$\delta_{i,j} = \frac{\theta_i}{y_j(\theta_i)} \frac{y_j(\theta_i) - y_j(\theta_i + \Delta\theta_i)}{\Delta\theta_i} \quad (4.165)$$

Sensitivity functions in steady state have been developed around a certain operating point. The analysis was performed by providing a %1 positive perturbation to three different sets of parameters in the model;

- i. Stoichiometric and kinetic parameters
- ii. Influent parameters
- iii. Operation parameters

The following steps were performed for the preparation of the sensitivity tables around a defined operating point,

1. Steady state was established and then the results were saved into a spreadsheet.
2. The sensitivity functions according to equation (4.167) were calculated in a matrix, one for each operating point expressed as percent change in calculated variables for 100% change in parameters. Since the models are nonlinear and both parameters and calculated variables have physical bounds, it would be meaningless to change parameters by 100%. Therefore the results are expressed of a 1 percent perturbation scaled up to 100% which is done only for the purpose of presentation.
3. The sum of absolute values of sensitivities for each row and column was calculated as an additional row and column for matrices.
4. In the last step the matrices were sorted by the sum of absolute values, both for parameters and calculated variables. Sorting left to right and top to bottom in descending order results in the most sensitive cells being moved to the top left corner.

The readability of the sensitivity table has been increased by discarding low sensitivity values of $\delta_{i,j} < 10\%$ and the highest sensitivity values of $\delta_{i,j} > 100\%$ were marked with bold font. The sensitivity table for the stoichiometric and kinetic parameters derived based on the above approach is given in Table 4.10. The sensitivity table for the influent and operational parameters of the calibrated new adopted process matrix for the pilot scale membrane bioreactor system is given in Table 4.11.

Table 4.10: Model parameter sensitivity table

% Sensitivity	Rank Variables	1 X_{ND}	2 S_{NO}	3 X_A	4 S_{NH}	5 X_S	6 X_P	7 S_{ND}	8 S_S	9 X_H	10 S_{ALK}	11 VSS	12 X_I	13 S_I	14 S_O	15 S_P	16 SRT	
Rank	Value (with defaults)	0,71	5,58	514,09	1,39	9,71	3365,92	0,16	1,43	4438,58	0,12	10555	4874,97	12,08	0,76	7,74	37,01	
1	K_{OH}		-163			52			70	25								
2	K_{NH}		-18		152													
3	K_{OA}		-18		143													
4	m_A		14		-156													
5	b_A		-20	-59	139													
6	h_d		-108	-26	72	21			70	-26							13	
7	K_h	-142				-127												
8	K_X	140				105												
9	b_H		-18			11	20		139	-80		-18					25	
10	Y_H		18	-28		-41	97			94		46					103	
11	f_U		18			-11	101					21						
12	i_{XBN}		-72	-14		11			70									
13	m_H		-18						-80									
14	f_{es}																103	
15	h_g		-54			12			-71									
16	h_h					-52												
17	Y_A		-14	100													13	
18	i_{XUN}																	
19	K_{NO}		36			12												
20	k_a																	
21	K_S					-11			139									

Table 4.11: Influent and operational parameters sensitivity table

% Sensitivity	Rank Variables	1 X_{ND}	2 S_{NO}	3 X_A	4 S_{NH}	5 X_S	6 X_P	7 S_{ND}	8 S_S	9 X_H	10 S_{ALK}	11 VSS	12 X_I	13 S_I	14 S_O	15 S_P	16 SRT	
Rank	Value (with defaults)	0,71	5,58	514,09	1,39	9,71	3365,92	0,16	1,43	4438,58	0,12	10555	4874,97	12,08	0,76	7,74	37,01	
1	CODinf	140	-314	21		176	81		70	145		107	100	100			91	
2	Qwas		17	-50	71		-122		69	-24		-81	-100				-26	-100
3	Qinf	141	18	100		103	100			101		100	100					
4	TKNinf		358	79	72	-72	20		-70	-49								25
5	DO		143	-14		-62				-25								13
6	T°C		-36	-75	-73		38			-131		-33						39

The number -163 in the nitrate nitrogen, S_{NO} , column and K_{OH} row in Table 4.10 represents a strong sensitivity of nitrate nitrogen to oxygen half saturation constant of heterotrophs in a negative way. For %1 increase in the oxygen half saturation constant for heterotrophs the nitrate nitrogen concentration will drop by 1.63 percent. In the same manner, 1 percent increase in the ammonia half saturation concentration, K_{NH} , will result in a 1.52 percent increase in the effluent ammonia concentration, S_{NH} .

4.10 Dynamic Physical Modelling of Membrane Bioreactors using a Computer Simulator

The pilot plant membrane bioreactor was dynamically simulated for physical properties using GPS-X Software by Hydromantis Inc. The structure of the MBR models combines a conventional activated sludge tank model (plug-flow or CSTR) with an in-tank solids separation filter, as shown in Figure 4-13. In the case of the plug-flow MBR, the filter placed in the final tank (an optional internal recycle is shown for illustrative purposes). Permeate flow is drawn through the filter at a rate determined by the filter model.

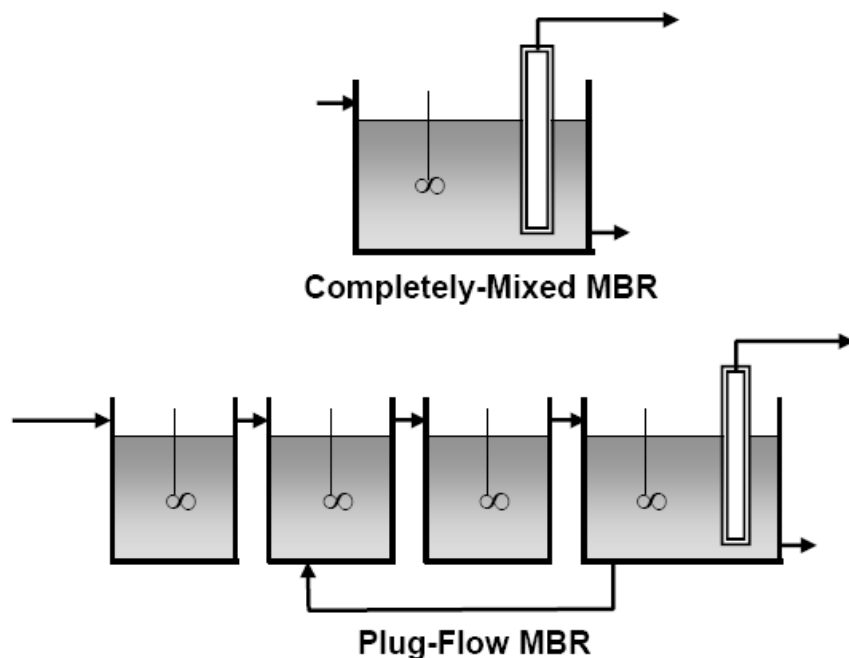


Figure 4.13: Membrane bioreactor model structures

The two MBR objects used in GPS-X are shown in Figure 4.14. with the connection points illustrated.

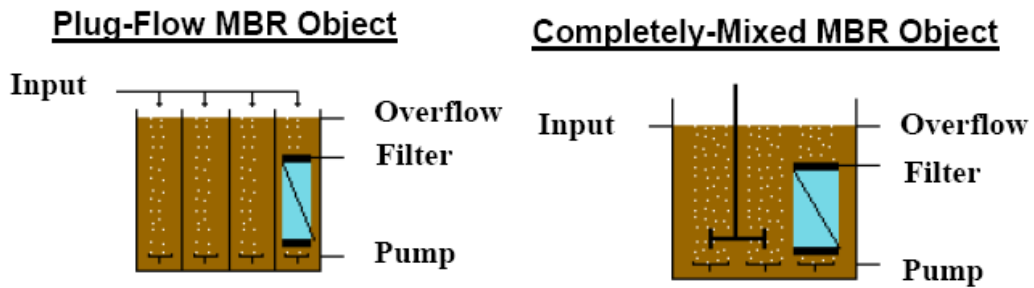


Figure 4.14: GPS-X membrane bioreactor objects

Both of the MBR models in GPS-X feature two different modes of operation; “Simple Mode” and “Advanced Mode”. Simple Mode operation assumes that the filter is operated adequately to properly remove flow, and does not consider the effects of transmembrane pressure (TMP), backwashing, and filter resistance. Table 4-12. summarizes the difference between Simple Mode and Advanced Mode.

Table 4.12: MBR model modes

	Simple Mode	Advanced Mode
Flow Balance and Reactor Volume	Model assumes flow in = flow out, and there is no change in reactor volume. All incoming flow is assumed to exit via the filter (and it is assumed there will be no tank overflow).	Permeate flow is determined from filter model. Reactor volume increases and decreases depending on the difference between flow in and flow out. If the permeate flow is insufficient to remove enough flow from the reactor, overflow can occur. Conversely, too much permeate flow will drain the reactor. A reactor level controller (which adjusts backwashing period length) is provided to help keep the reactor from overflowing or draining.

Filter Operation	Filter operation is ignored	User must specify TMP, backwashing/relaxing cycles, and cross-flow aeration.
Cross Flow Air	Filter-cake solids removal from cross-flow aeration is ignored, but oxygen transfer from the cross-flow air to the bulk liquid is calculated and included in the biological activity.	Both solids removal and oxygen transfer are considered for cross-flow aeration.
Solids Capture	The solids capture rate determines what fraction of the mixed liquor solids remain in the reactor. These solids remain suspended in the bulk liquid.	The solids capture rate determines what fraction of the mixed liquor solids remain in the reactor. These solids makeup the filter cake and can be returned to the bulk liquid through backwashing or crossflow aeration.
Biological Activity	There is no difference in the biological model when using simple or advanced modes.	

The specification of the membrane filter physical characteristics is done in the Input Parameters > Physical – Membrane menu, as shown in Figure 4-15. Note that all parameters except solids capture rate are ignored (and greyed-out on these menus) when the model is set to Simple Mode.

The screenshot shows a dialog box titled "Physical - Membrane" with three sections:

- Membrane Properties:**
 - [6] solids capture rate: 0.999, unit: -
 - [6] total membrane surface area: 4000, unit: m2
 - More... button
- Membrane Resistance:**
 - [6] intrinsic membrane resistance: 1e+11, unit: 1/m
- Membrane Fouling:**
 - [6] maximum fouling resistance: 1e+13, unit: -
 - [6] fouling rate constant: 0.001, unit: 1/d

Buttons for "Accept" and "Cancel" are located at the bottom right.

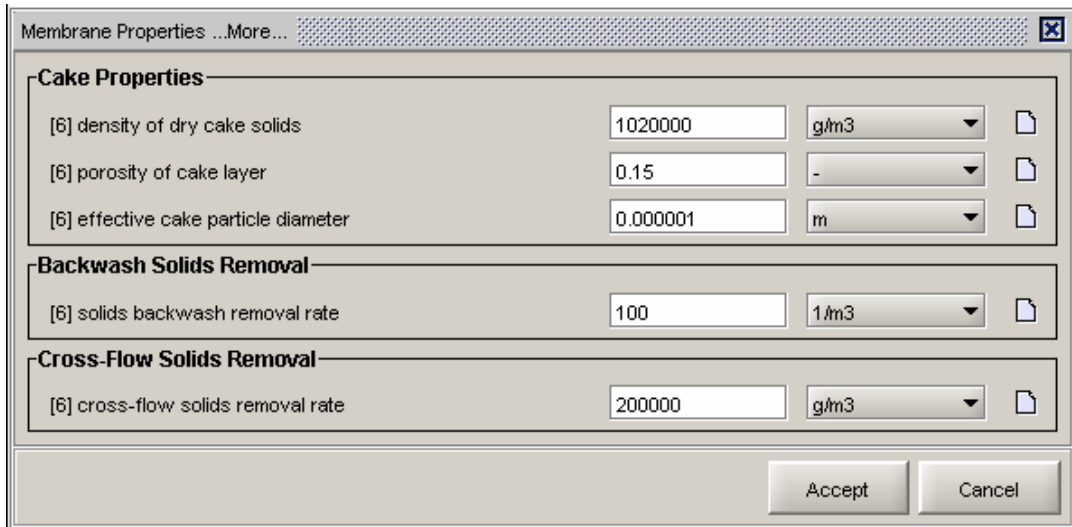


Figure 4.15: Physical membrane properties

Total membrane surface area and solids capture rate are used (along with the transmembrane pressure) to determine the amount of solids retained on the filter, forming cake layer. The cake thickness is determined from the total cake solids and the physical cake parameters shown in the Membrane Properties menu.

The intrinsic membrane resistance and maximum fouling resistance are used (along with the cake resistance, calculated from cake thickness) to determine the overall resistance using the “resistance in series model” (Choi et al., 2000). The resistance in series model is expressed with the following equation,

$$J = \frac{TMP}{\mu \cdot R_t} = \frac{TMP}{\mu(R_m + R_c + R_f)} \quad (4.166)$$

where,

J= permeate flux (m/s)

TMP=transmembrane pressure (kPa)

μ =dynamic viscosity (Pa.s)

R_m =intrinsic membrane resistance (1/m)

R_c =cake resistance (1/m)

R_f =fouling resistance (1/m)

The solids backwash removal rate is the mass of solids removed from the filter cake per unit flow of backwash through the filter. The crossflow solids removal rate is the

mass of solids removed from the filter cake, per unit of cross flow air, per unit surface area of the filter.

All models are based on the Carman-Kozeny equation, which describes the head loss (h) for filtration through a porous medium in which the flow channel radius corresponds to the pore volume divided by the wetted surface ($\varepsilon / ((1 - \varepsilon)A_s)$).

$$h(m) = \frac{\sigma \mu k A_s^2 (1 - \varepsilon)_2 J}{\rho_L g \varepsilon^3} \quad (4.167)$$

where

σ = cake layer thickness (m)

k =Kozeny constant (dimensionless)

A_s =specific surface of a cake layer particle (1/m)

ε =filter cake porosity (dimensionless)

ρ_L =density of the feed solution (kg/m³)

g =gravitational constant (m/s²)

The pressure difference across the cake layer is related to the head loss by;

$$\Delta P(Pa) = h \rho_L g \quad (4.168)$$

The pressure drop in the cake layer is related to the resistance in that layer via an equation analogous to Equation (4.166);

$$\Delta P(Pa) = R_c \mu J \quad (4.169)$$

Inserting Equation (4.168) into Equation (4.167) to eliminate the head loss term, substituting the resistance for the pressure difference by inserting Equation (4.169) and solving for the cake resistance yields;

$$R_c = \frac{\sigma k A_s^2 (1 - \varepsilon)^2}{\varepsilon^3} \quad (4.170)$$

In the membrane filtration systems, membrane fouling is common and will cause the flux to decrease. Fouling resistance can be defined as;

$$R_f = \alpha M_d \quad (4.171)$$

M_d is the amount of deposit (time-dependent parameter) and can be expressed as ;

$$\frac{dM_d}{dt} = k_f(M_d^* - M_d) \quad (4.172)$$

Integration of Equation (4.172) will yield;

$$M_d = M_d^* (1 - e^{-k_f t}) \quad (4.173)$$

From Equations (4.171) and (4.173), fouling resistance can be expressed as;

$$R_f = \alpha M_d^* (1 - e^{-k_f t}) \quad (4.174)$$

Where α is a proportional constant, M_d^* is the maximum deposition value and k_f is the deposition rate. Deposition rate k_f increases significantly with protein concentration.

The specific cake resistance can be expressed defined in terms of cake thickness which involve Karman-Kozeny equation. The specific cake resistance is defined as the resistance per unit thickness of a cake layer,

$$R_c = \int_0^{\delta_c} r_c d\delta_c \quad (4.175)$$

where r_c is the specific cake resistance and δ_c is the cake layer thickness. If the cake layer is assumed to be homogenous, the above equation becomes,

$$R_c = r_c \delta_c \quad (4.176)$$

For a homogenous cake, the cake thickness is

$$\delta_c = \frac{m_p}{\rho_p (1 - \varepsilon) A_m} = \text{volume of cake/area of membrane} \quad (4.177)$$

where m_p is the total dried mass of a cake layer, ρ_p is the density of a particle, ε is the porosity of a cake layer, and A_m is the effective membrane area. Substituting Equation (4.177) into (4.176) and combining with Karman-Kozeny equation gives R_c as,

$$R_c = 180 \frac{(1 - \varepsilon)^2}{d_p^2 \varepsilon^3} \frac{m_p}{(1 - \varepsilon) A_m \rho_p} = 180 \frac{(1 - \varepsilon) m_p}{d_p^2 \varepsilon^3 A_m \rho_p} \quad (4.178)$$

The permeate flux in the resistance in-series model as expressed in Equation (4.166) can be re-expressed as ;

$$J = \frac{\Delta P}{\mu \left[R_m + 180 \frac{(1-\varepsilon)m_p}{d_p^2 \varepsilon^3 A_m \rho_p} + \alpha M_d^* (1 - e^{-k_f t}) \right]} \quad (4.179)$$

As shown in Equation (4.179), the membrane resistance, R_m , cake resistance, R_c , and fouling resistance, R_f can be considered simultaneously.

4.10.1 Configuration of the MBR pilot plant in the simulator

Processwise, the configuration of the pilot plant is done in the same way done in BioWin 2.2. The pilot plant MBR includes two bioreactors connected in series; *i.*) *Anoxic Tank* and *ii.*) *MBR tank*. The permeate of the membrane modules leaves the system as the effluent whilst the content of the MBR tank is being recirculated back to the anoxic tank. The system consists only one recirculation stream which serves the purposes of both recycling back the nitrified mixed liquor and the biomass. Both of the tanks have completely mixed regimes where anoxic tank is mixed by a surface agitator and the MBR tank is mixed and aerated through a blower coarse bubble diffuser system. The oxygen necessary for air scouring and biological oxidation have been setup separately. Due to the membrane process module, the recirculation lines are not visible in GPS-X.

The configuration of the pilot plant MBR in GPS-X is illustrated in Figure 4.16.

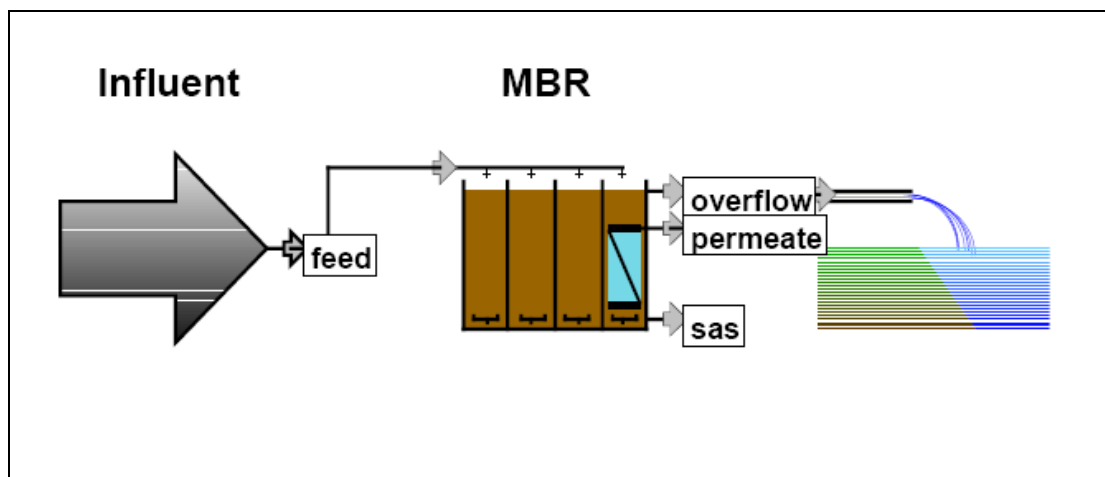


Figure 4.16: Plant layout implemented in GPS-X® software

The excess sludge is wasted from the line designated as sas whereas the filtered effluent leaves the system through the permeate line. The MBR is modelled in GPS-X using the flux controller which enables to simulate the system with constant flux, permeate and variable TMP. In this option, the TMP is increased over time. The operational mode of the MBR is based on 12 hour filtration and 10min relaxation with air scouring in a 24 h period. This has been done by adjusting the relevant parameters in the membrane backwash section of the operational parameters of the membrane. The crossflow air amount and the type of aeration system used to create the crossflow velocity is also entered in the operational parameters of the membrane.

The major setup parameters of the model is given in Table 4.13.

Table 4.13: MBR setup parameters in GPS-X

<i>Parameter</i>	<i>Unit</i>	<i>Value</i>
Solids capture rate	-	%99.9999
Total membrane surface area	m ²	8
Density of dry cake solids	g/m ³	1020000
Porosity of cake layer	-	0,36
Effective cake particle diameter diameter	m	0,000001
Solids backwash removal rate	1/m ³	100
Crossflow solids removal rate	g/m ³	200000
Flux Controller		ON
Controller constant	-	0,001
Flux setpoint	lt/m ² -h	20
Frequency of crossflow air backwash	h	12
Duration of crossflow air backwash	min	10
Backwash flow	m ³ /h	0
Level controller		ON
Crossflow airflow	m ³ /h	8
α factor for crossflow aeration	-	0,35
SOTE for crossflow (coarse bubble)	%	6
Waste activated sludge flow	lt/d	36
Recirculation flow	m ³ /d	12

5 EXPERIMENTAL RESULTS AND EVALUATION

The new adopted model was applied to the pilot membrane bioreactor to evaluate the performance and assess the model's accuracy against measured data. The system was operated for 308 days under dynamic and diurnal conditions and the model was also ran against dynamic input data of the actual plant. The experimental period can be divided into two segments. The first segment can be defined as the time period that has elapsed to reach steady state conditions and the second segment is the interval where the pilot plant was operated under steady state however dynamic conditions. The adopted model was simulated under dynamic conditions during both phases. The experimental and simulated results are discussed in detail in this section.

5.1 Influent Wastewater Characterization

Influent was measured based on composite samples taken over an average of 10 hours period during day time. During the recorded period wet weather events have occurred which had an impact on the influent concentrations and loads. The increased flow was buffered in the intermediate balancing tank as the flowthrough capacity of the membrane bioreactor was limited with the installed area of the membrane.

The influent characterization was performed according to Roeleveld and van Loosdrecht (2002) which is also applied by the Dutch Foundation for Applied Waster Research (STOWA). Physical-chemical methods were used to determine the influent readily biodegradable COD(S_S) and the influent inert COD(S_I), where afterwards this was coupled with a BOD analysis campaign which included the measurement of BOD as a function of time to determine the biodegradable fraction (S_S+X_S) of the influent total COD (Roeleveld and van Loosdrecht, 2002). The fraction X_I was determined by subtracting the sum of other COD fractions from total influent COD. The value of k was determined by using the least squares method which involved fitting a curve through a set of data points so that the sum of the squares of the residuals (the difference between the observed value and the value of

the fitted curve) would be minimum. f_{BOD} is a correction factor to determine the exact BCOD concentration with respect to the determined BOD_{tot} value as in the long term measurements part of the biodegradable COD is converted to inert fraction. (Roeleveld and van Loosdrecht, 2002). The f_{BOD} factor ranges between 0.10 to 0.20, where in this study the factor was set at the lower value of 0.1. The fractions were determined through a set of equations based on ASM1 parameters. In this method the influent X_I / X_T ratio is determined from BOD_5 measurements. STOWA wastewater characterization guidelines recommend the use of membrane filtration to retain all colloidal material on the filter without a pre-flocculation step (Roeleveld and van Loosdrecht, 2002). These guidelines also apply correction factors to account for soluble microbial products in the effluent. The guidelines also assume the non-existence of active biomass in the raw sewage. The fitted BOD curve for the determination of k_{BOD} , BOD_T and BCOD is illustrated in Figure 5.1.

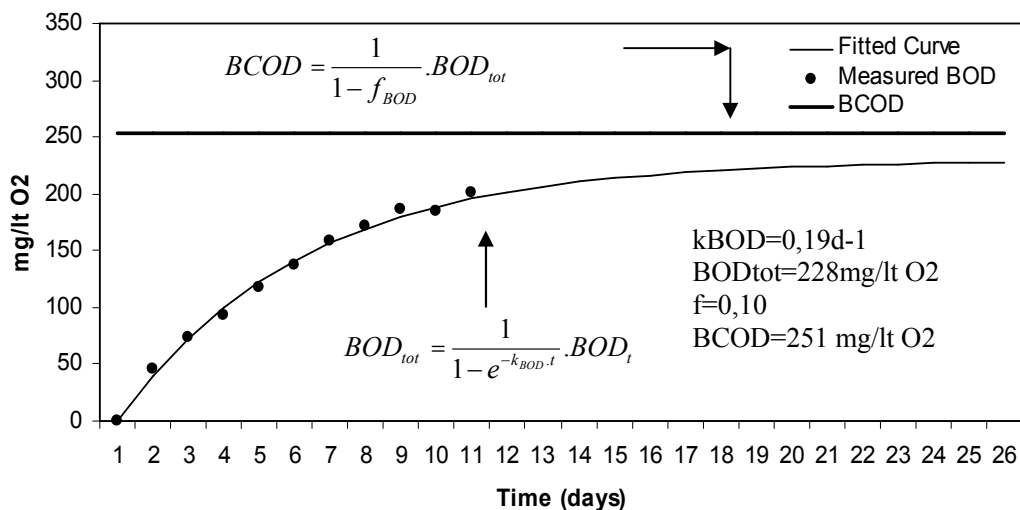


Figure 5.1: Fitted BOD curve for the set of measured BOD₅ data points

The resultant average wastewater characterization for the first half of the study was slightly different from the second half. This was linked to the fact that the second half of the study corresponded to winter conditions where the combined sewer network carried storm water to the plant thereby diluting the raw sewage. The resultant COD fractions are presented in Table 5.1 and 5.2.

Table 5.1: Influent COD concentration of raw sewage (average)

<i>Sample</i>	<i>COD component (mg COD/lt)</i>								
	C_T	S_T	X_T	S_S	S_I	X_S	X_I	$X_{SC}(S_H)$	X_{SP}
Raw (first half of the study)	464	293	171	159	14	245	46	120	125
Raw (second half of the study)	292	180	112	92	13	148	38	72	77

Table 5.2: Influent COD fractions of raw sewage (average)

<i>Sample</i>	<i>COD fraction (%)</i>					
	S_S	X_S	S_I	X_I	$X_{SC}(S_H)$	X_{SP}
Raw (first half of the study)	34,3	53	3	9,8	26	27
Raw (second half of the study)	31	50	4,5	13	25	26

Henze (1992) further subdivided the slowly biodegradable COD (X_S) to rapidly hydrolyzable COD (X_{SC} or S_H) assumed to be of colloidal/soluble nature and slowly hydrolyzable COD (X_{SP}) to be of particulate nature. The measured soluble COD accounted to not less than %60 of the total COD throughout the study which was different from a typical domestic sewage which is in the range of %25-%37 (Orhon et al., 1997).

The resultant COD fractionation was different from a typical domestic raw sewage. Orhon et al. (1997) characterized the raw sewage of Istanbul metropolitan area where the results were different from the characterization derived in this study. The S_S , X_S , S_I and X_I constituted to %9, %77, %4 and %10 respectively of the total influent COD. It is clearly seen that the raw sewage for the pilot plant in this study had more readily biodegradable COD available in the influent and less slowly biodegradable portion when compared to the typical Istanbul wastewater characterization. This also verified that the soluble fraction of the incoming total COD was higher than the particulate fraction which also showed that a significant portion of the slowly biodegradable COD was of colloidal/soluble nature (X_{SC}/S_H). The influent total, particulate and soluble COD are illustrated in Figure 5.2.

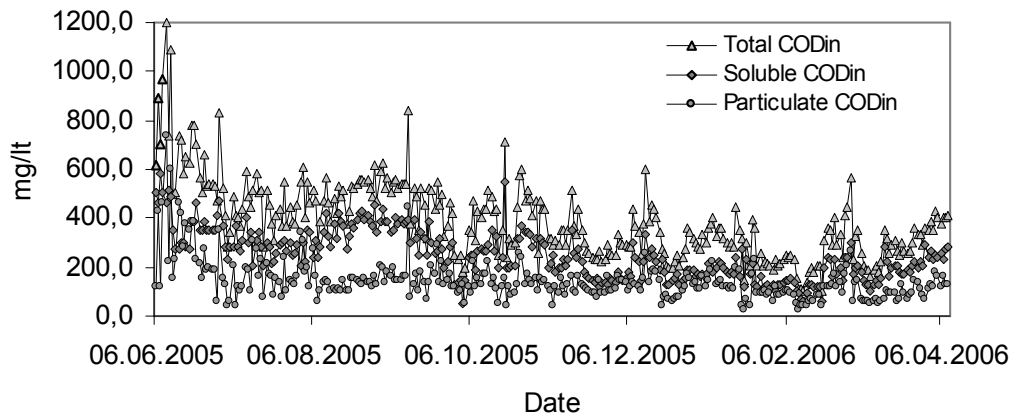


Figure 5.2: Influent total, particulate and soluble COD

According to Henze et al. (1995), the nitrogen in domestic wastewater is in biodegradable form. Fixed nitrogen fractions (i_N) are used for various COD components related to the organic part. Roeleveld and van Loosdrecht (2002) state that this approach is also applicable for ASM1. The influent nitrogen concentrations and nitrogen fractions used in this study are given in Table 5.3. The influent nitrogen concentrations did not show significantly different results as seen for the influent organic components.

Table 5.3: Influent nitrogen concentration and fractions

	<i>Unit</i>	<i>Min</i>	<i>Average</i>	<i>Max</i>
TKN	mgN/l	25	55	105
S_{NH}	mgN/l	18	41	78
C_{ND}	mgN/l	7	14	27
S_{ND}	mgN/l	3,2	6,3	12,2
X_{ND}	mgN/l	3,8	7,7	14,8
i_{XBN}	grN/grCOD	0,086	0,086	0,086
i_{XPN}	grN/grCOD	0,06	0,06	0,06
S_{NH}/TKN	%	70	74	88
C_{ND}/TKN	%	12	26	30
S_{ND}/C_{ND}	%	-	45	-
X_{ND}/C_{ND}	%	-	55	-

The influent TKN and ammonia nitrogen profiles are seen in Figure 5.3.

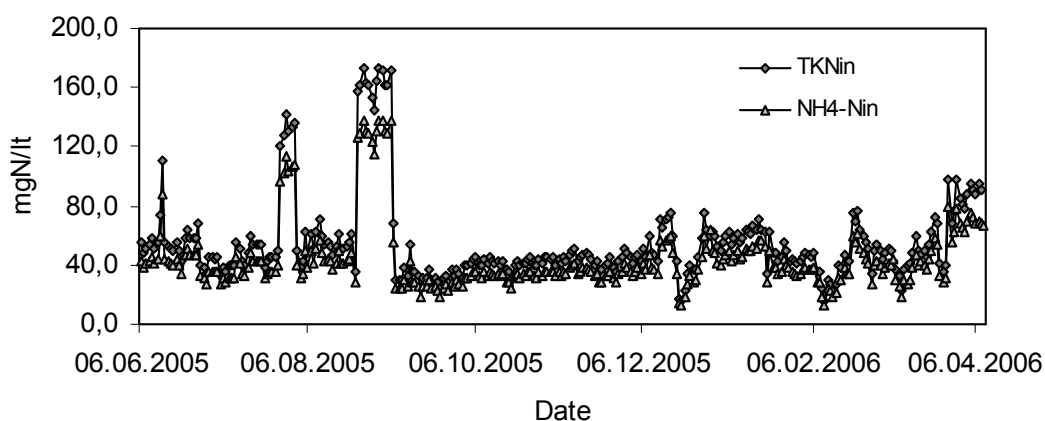


Figure 5.3: InfluentTKN and ammonia nitrogen profiles

The spikes in the influent conditions seen in the graphs represent the industrial wastewater contribution to the influent stream in which the influent TKN and NH_4^+ -N values have reached up to 174 mg/lt and 133 mg/lt, respectively.

The influent VSS to particulate COD ratio ($F_{CV}(X_T/VSS)$) which is the most important parameter for the solids balance was not in the range for a typical domestic sewage, revealing that the soluble fraction of COD was higher than expected; $S_{T1}/C_{T1} > X_{T1}/C_{T1}$. As expected, the slowly biodegradable fraction of the influent COD was at least %20-25 less than a typical raw sewage (Henze, 1992). Influent solids concentrations are presented in Table 5.4 and the influent TSS, VSS and ISS profiles are illustrated in Figure 5.4.

Table 5.4: Average influent solids concentration

<i>Unit</i>		<i>Value</i>						<i>Typical Range</i>
		<i>First Half of the Study(0-159 days)</i>			<i>Second Half of the Study (160-310 days)</i>			
		Min	Ave	Max	Min	Ave	Max	
TSS	mg/lt	68	200	780	53	143	364	
VSS	mg/lt	56	163	640	40	119	250	
ISS	mg/lt	12	37	140	13	26	114	
F_{CV} (X_T/VSS)	mgCODpart/ mgVSS		1,02			0,94		1,5-1,7

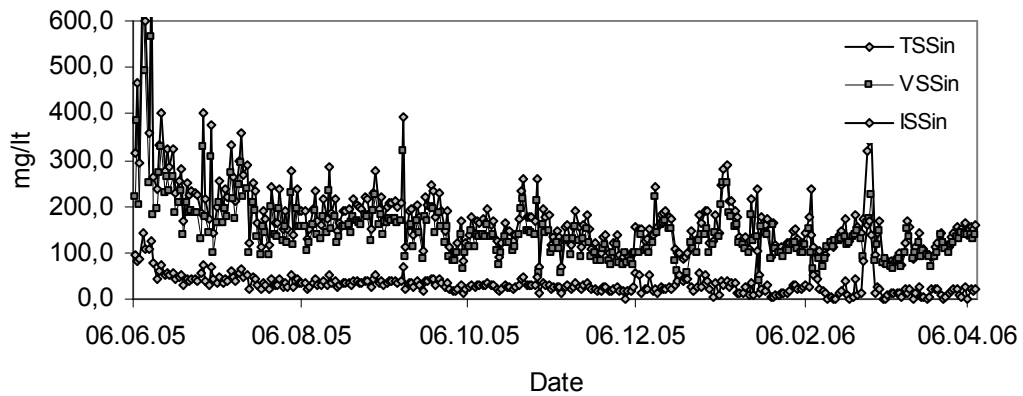


Figure 5.4: Influent TSS,VSS and ISS profiles

The max influent TSS concentration was measured as 780 mg/l. Due to the contribution of storm water the ISS values hence the influent F_{CV} value decreased in the second half of the study. F_{CV} values were calculated as 1.02 and 0.96 respectively for the first and second part of the study. The overall influent wastewater characterization for Run I is given in Table 5.5.

Table 5.5: Influent wastewater characterization (Run I)

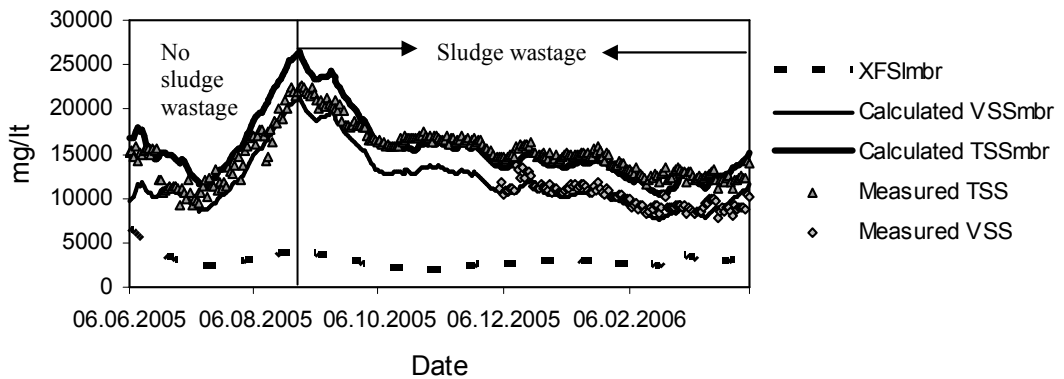
<i>Parameter</i>	<i>Unit</i>	<i>Min</i>	<i>Max</i>	<i>Average</i>	<i>%70'ile</i>	<i>%90'ile</i>
COD	mg/l	101	1204	392	459	564
TSS	mg/l	53	780	176	192	263
VSS	mg/l	40	639	145	158	210
TKN	mg/l	15	173	55	55	77
NH ₄ -N	mg/l	12	138	44	44	65

5.2 Solids Balance

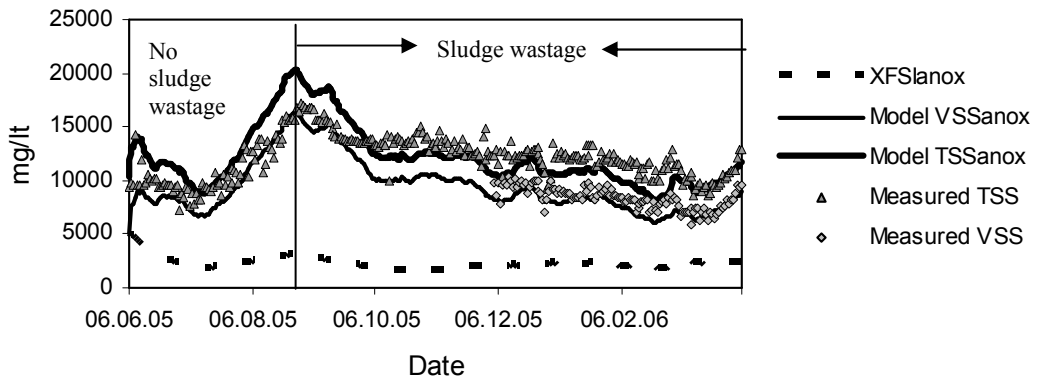
The system was operated for 307 days and the model was dynamically calibrated for solids balance, carbon and nitrogen removal. The particulate components reached a steady state for non-varying influent conditions and the model reacted well to the changing conditions in the influent thereby setting various steady states throughout the study (Figure 5.5a, 5.5b). The sludge was wasted from the system for the first 40 days of operation and then it was stopped until the 84th day where afterwards there was constant excess sludge wastage to reach the preset operating sludge age of 38 days where the MLSS reached a steady state value of 16,000mg/l. The system preserved this steady state for two months where afterwards the MLSS value

decreased due to changing influent conditions. The adopted dynamic model for the solids balance matched the measured MLSS and MLVSS values.

The new model also simulated the fate of other particulate components X_H , X_A , X_P , X_I , X_S and the results show that X_H was the major component that fluctuated with the changing influent conditions which was the driving parameter in setting up new steady states for the solids. (Figure 5.6a, 5.6b)

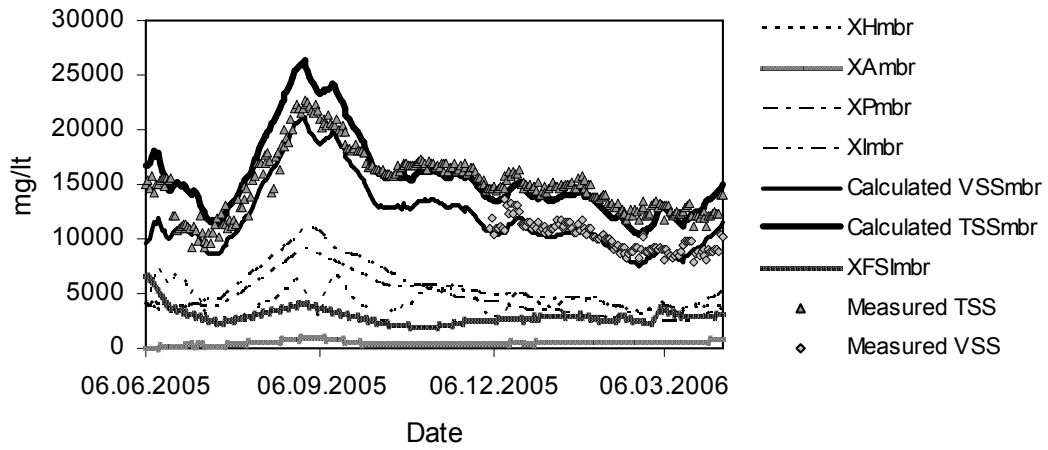


(a)



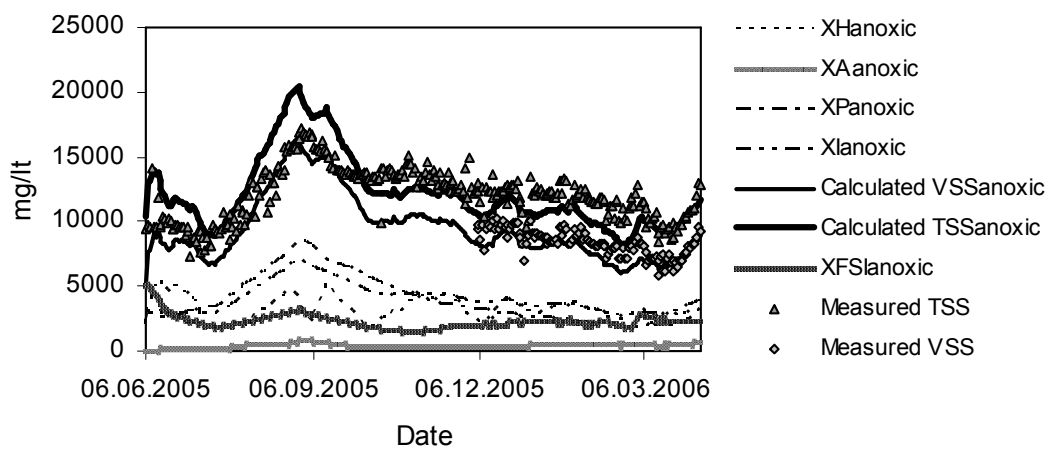
(b)

Figure 5.5: Solids balance (a) MBR Reactor, (b) in anoxic reactor



(a)

MLVSS/MLSS measurements and respirometric analysis have been done for the determination of the endogenous decay rate for heterotrophs, b_H , resulting in 0.31 d^{-1} and 0.36 d^{-1} respectively (Appendix A).



(b)

Figure 5.6: Fate of particulate components (a) MBR Reactor, (b) in anoxic reactor

Marais and Ekama (1976) proposed the endogenous decay rate to be $b_H=0.24 \text{ d}^{-1}$ at 20°C where lower values in the range of $0.15 - 0.20 \text{ d}^{-1}$ have recently been used. (Henze, 1992;Orhon and Artan, 1994) The model and the solids balance calibrated at $b_H=0.24\text{d}^{-1}$ less than what has been measured and higher than default values used so far , once again verifying the fact that MBR's run on decay dominant activated sludge process. The reason for the calibrated value of b_H being less than the one analyzed can be related to the nature of the sludge being sticky and jelly far away from a conventional activated sludge which has caused problems in the respirometer

resulting in retries of the analysis. Although the decay rate is higher than in a conventional activated sludge system the rate of the decay process is regulated by the attached switching functions both to the anoxic and aerobic decay processes. For example, the net decay rate of heterotrophs will be less due to the higher half saturation constants under aerobic conditions and the rate will be higher under anoxic decay conditions. This phenomena also applies to the decay rate of autotrophs. The decay rate for the nitrifiers, b_A , were calibrated at $0,06d^{-1}$ where Dold and Marais (1986) proposed values in the range of $0.04 - 0.16 d^{-1}$. Henze et al. (1987, 1995) suggested b_A values at $20^\circ C$ of $0.05d^{-1}$ and $0.03-0.06d^{-1}$ respectively. Katehis et al. (2002) performed bench scale testing on SBRs having 15 days of sludge age finding a b_A value of $0.09d^{-1}$. Both autotrophic and heterotrophic decay rates play an important role in parameter estimation of the model as it affects sensitivity severely where effluent S_{NH} is most influenced by the autotrophic decay rate, b_A .

The active heterotrophic biomass concentration in the anoxic reactor is smaller than in the MBR reactor with a fraction related to the recirculation ratio.

The TSS concentration in the effluent was less than $5mg/l$ and following the 32^{nd} day of the experiment this analysis was abandoned. The system produced TSS free permeate all throughout the study with no deterioration.

As it can be seen from the above solids balance figures the MLSS and MLVSS curves have fluctuated from the 122^{nd} day till the end of the study thereby setting different steady states in terms of solids balance. This is related to changing influent wastewater conditions and the operating conditions mainly, i.) Temperature and ii.) Dissolved Oxygen. Temperature has direct effect on the growth and decay rates through Arrhenius type equations. Since the membrane bioreactor process is decay dominant and the temperature increase has a proportional affect on the decay rate; the mixed liquor concentration within the system decreases with increasing temperature for a given dissolved oxygen level. This can be demonstrated by the adopted model at steady state conditions and can be compared with the stoichiometric equations derived for steady state conditions given below for the active heteorrophic and autotrophic biomass,

$$X_{Hmbr} = \frac{Y_H Q (C_{Sin} - S_S) \beta \theta_X}{(1 + b_H \beta \theta_X) (V_{anox} f_R \eta_g + V_{mbr} (1 - f_{DNH}))} \quad (6.1)$$

and

$$X_{Ambr} = \frac{Q(S_{NHin} - S_{NHE})\theta_{XA}Y_A}{(1 + b_A(1 - f_{DNA})\theta_{XA})V_{mbr}} = \frac{QY_{NA}N_{OX}\theta_{XA}}{V_{mbr}} \quad (6.2)$$

On the other hand, due to the diffusion limitation which is explained by higher oxygen half saturation constants for autotrophs and heterotrophs the mixed liquor volatile suspended solids concentration decreases with increasing dissolved oxygen levels for a given temperature. Figure 5.7. illustrates the variation in active biomass with respect to changing dissolved oxygen concentration for a given temperature.

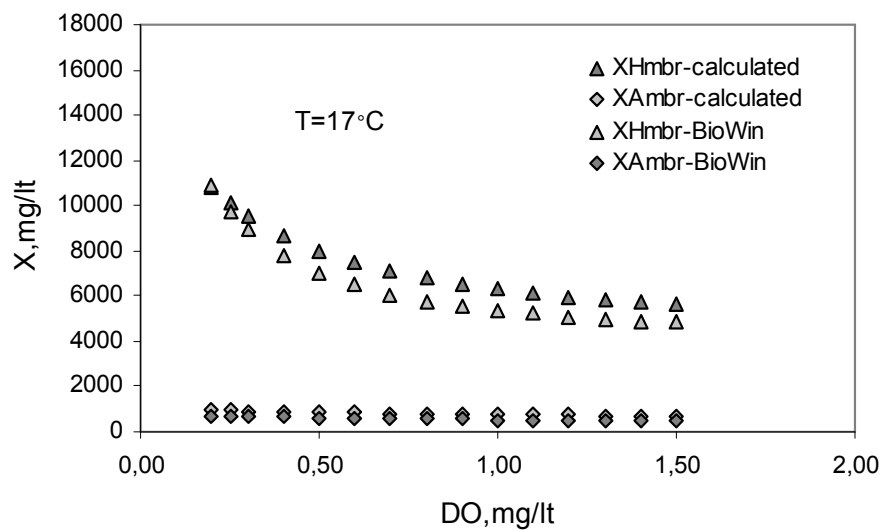


Figure 5.7: Variation of active biomass concentration with respect to changing dissolved oxygen concentration

Steady state model results reveal that an increase in dissolved oxygen level will have a decrease effect on the active biomass concentration both for heterotrophs and autotrophs. This fact is verified by the stoichiometrically driven equations for heterotrophic and autotrophic biomass given in Chapter 4. Figure 5.8. illustrates the variation in the active biomass with respect to changing temperature for a given dissolved oxygen concentration.

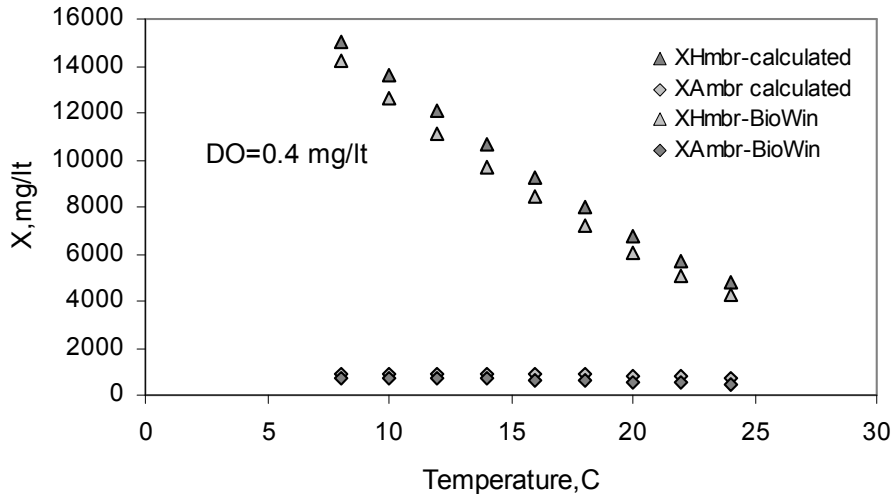


Figure 5.8: Variation of active biomass concentration with respect to changing temperature

Temperature increase has a detrimental effect on the heterotrophic biomass concentration due to increasing decay rates at higher temperatures. Since the membrane coupled activated sludge process is decay dominant the active biomass decreases with increasing temperature. The longterm observed dynamic mixed liquor suspended solids concentrations also fluctuate with dissolved oxygen and temperature. The stoichiometric calculations mimicked the model results thereby validating the mass balance derived stoichiometric equations for the heterotrophic and autotrophic active biomass concentrations.

5.3 Organics Removal

The average organic removal efficiency was 95% in terms of COD removal reaching upto a max of 99% independent from the influent loading where BOD in the effluent was not detectable (Figure 5.9). Gnder (2001) reported minimum COD removal efficiencies of 90% for MBR's whilst Van der Roest et al. (2002) recorded consistent organic removal efficiencies not being less than 95%. The effluent total COD values were in the range of 10-20 mg/l where it only consists of inert soluble fraction (S_I) and soluble microbial products (S_{SMP}). Both colloidal (X_{SC}) and particulate (X_{SP}) slowly biodegradable COD is completely depleted within the reactor where it is converted to readily biodegradable COD, S_S . The model characterized the measured effluent COD efficiently.

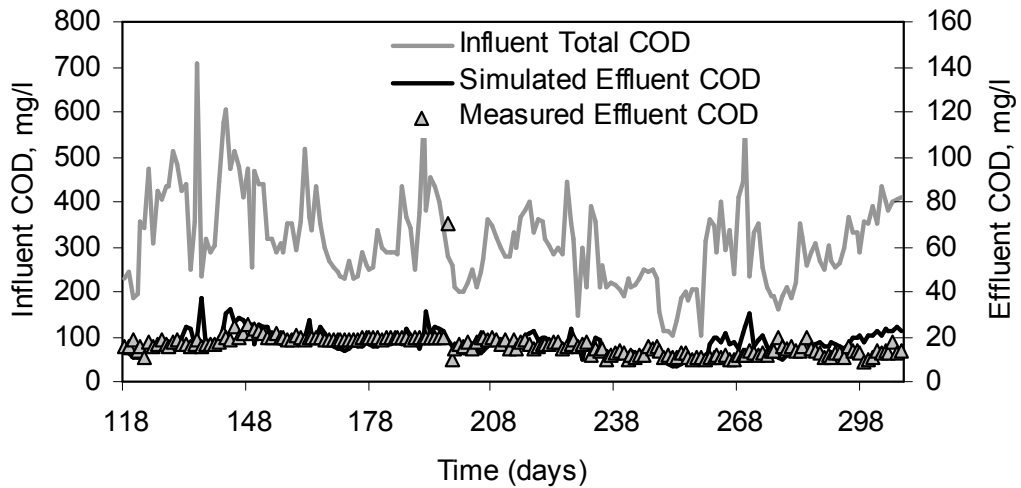


Figure 5.9: Influent COD and simulated/calculated effluent COD concentration profiles

The simulated effluent COD fractions according to the new adopted model are illustrated in Figure 5.10.

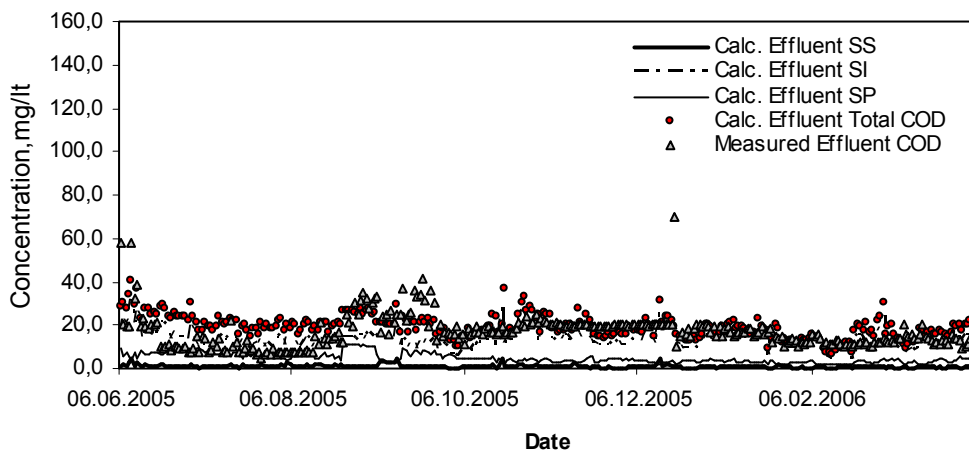


Figure 5.10: Simulated effluent COD fractions

The initial mismatch between the simulated and measured effluent COD values in the first 80 days of operation corresponds to the interval where there was no sludge wastage which excessively increased the biomass concentrations. Modelwise; this had an increasing affect on the S_{SMP} values due to high heterotrophic biomass and sludge age where in the contrary this was not experienced in the measured effluent COD values. On the other hand, this could also be explained by the fact that the system was in the startup phase that lasted for some time to reach stable operating conditions.

5.4 Oxygen Utilization

As in the conventional activated sludge systems the oxygen utilization is related to three processes, *i.) Growth of Heterotrophs*, *ii.) Growth of Autotrophs*, *iii.) Endogenous Respiration of both Heterotrophs and Autotrophs*. Coarse bubble aeration has been used throughout the study to supply the necessary oxygen to the bulk liquid and to remove the cake layer off the membrane surface to avoid fouling. The dissolved oxygen in the reactor was set by adjusting the air flowrate into the membrane bioreactor however a min of 8 m³/h of air was introduced into the tank for the necessary scouring of the cake layer on the surface of the membrane whilst the blower capacity enabled a max of 12 m³/h air flow. The MBR air supply rate against recorded dissolved oxygen concentration is illustrated in Figure 5.11.

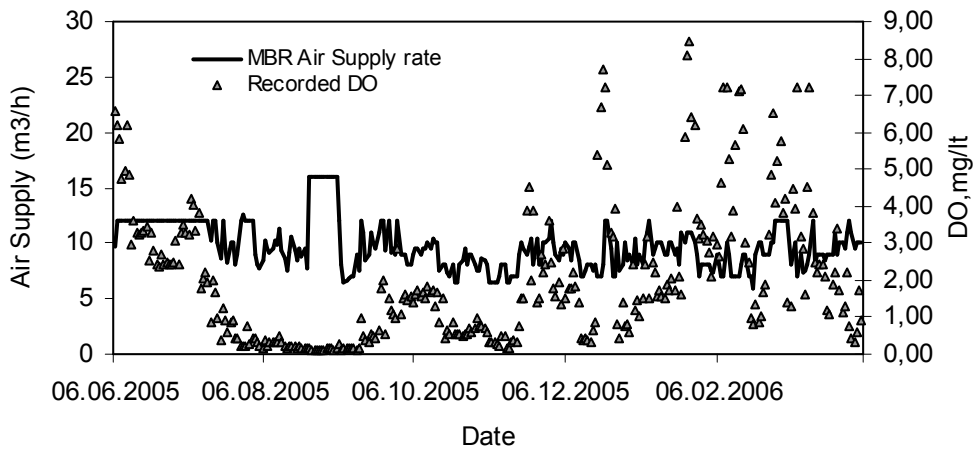


Figure 5.11: MBR air supply rate vs recorded DO

The DO level was intentionally kept in between 0.3 to 0.5 mg/l from day 50 until day 100 to assess the SNdN behaviour and performance of the membrane bioreactor. The DO concentration in the reactor is the difference between the air supplied and the OUR level in the reactor. The aeration model incorporated in the dynamic model resembled the recorded DO level which meant that the OUR in the reactor is also correct. The initial mismatch of the simulated and measured DO profiles is due to the startup period of the MBR (Figure 5.12).

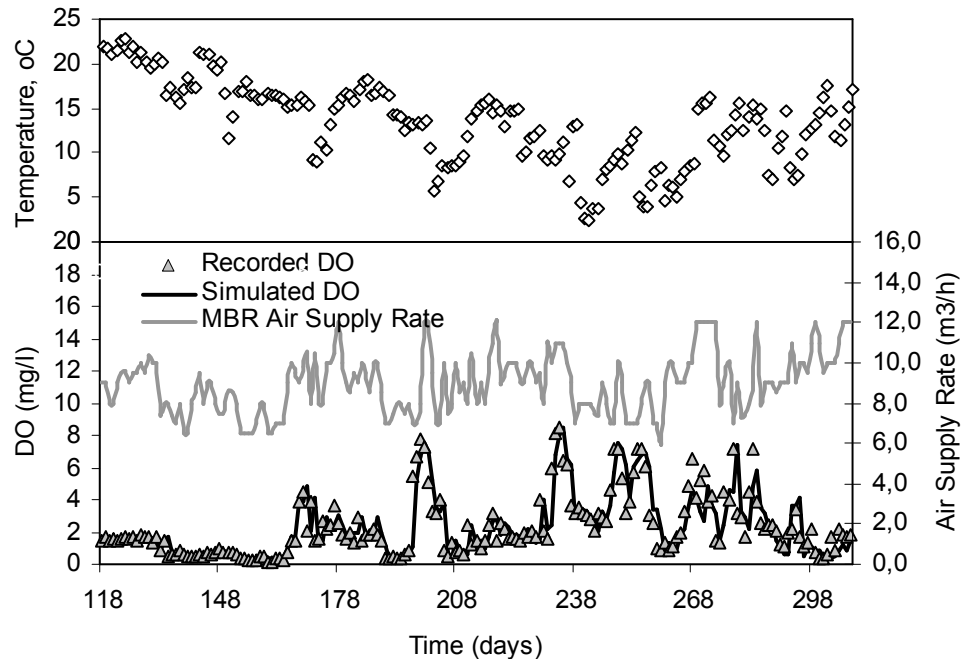


Figure 5.12: Airflowrate vs. measured and simulated DO in MBR unit

The oxygen transfer model used in this study was calibrated at α factor of 0.4 for the MLSS values in the range of 14-16 mg/l. Gnder (2001) stated that oxygen transfer is reduced with higher MLSS concentrations. It was also concluded that the α factor which defined the relation of oxygen transfer in pure water to oxygen transfer in activated sludge decreases from 0.5 at MLSS of 8 g/l to 0.12 at MLSS of 25 g/l. Gnder (2001) also derived an empirical relationship between the α factor and MLSS (gr/l);

$$\alpha = e^{-0.083.MLSS} \quad (6.3)$$

However further research has to be conducted for the affect of α on oxygen transfer and energy consumption for increased MLSS values.

5.5 Nitrogen Removal

5.5.1 Nitrification

A superficial interpretation of the experimental data regardless of the kinetics may easily lead to conclude that nitrification is sustained throughout the study with temperatures as low as 4°C where on the contrary Murat et al. (2002) reported nitrifier washout at 14°C for tannery wastewater. The German Wastewater Ordinance (AbwV, 1999) takes into account minimum 12°C of design temperature for

nitrification which is also used as a threshold value in seeking effluent regulations for $\text{NH}_4^+\text{-N}$. Partial nitrification was observed in which the wastewater temperature dropped below 4°C without nitrifier washout. This is explained by the high sludge age of the system and the high dissolved oxygen concentration in the membrane bioreactor. It is also well known that temperature has the most impact on the maximum autotrophic growth rate ($\mu_{A\text{max}}$). The temperature effect on the pilot plant can be evaluated by an Arrhenius type of equation with a temperature coefficient of 1.2 much higher than what is normally derived for domestic sewage (Henze et al., 1995) Higher temperature dependency factor implies a larger temperature dependency and it has a negative impact on plant design for the necessity to increase the sludge age at low temperatures. This is the only phenomena behind the nitrifiers not being washed out of the system even at temperatures below 4°C whilst their growth rate is largely decreased when compared to suggested temperature dependency factors.

$$\text{for Temp} < 4^\circ\text{C} \Rightarrow \mu_{A\text{max}}(T^\circ\text{C}) = \mu_{A\text{max}}(20^\circ\text{C}) \cdot 1.2^{T-20} \quad (6.4)$$

Magnified nitrification performance of the pilot MBR in a certain time interval including partial nitrification is shown in Figure 11a and 11b both with DO and temperature effect. Since sludge age was very high and pH was neutral throughout the study, dissolved oxygen and temperature were the two most important parameters affecting nitrification. The system nitrified with dissolved oxygen concentrations as low as 0.5 mg/l where it partially nitrified with dissolved oxygen concentrations down to 0.3 mg/l. Wuhmann(1964) studied three identical high rate activated sludge plants in which dissolved oxygen was maintained at 1.0, 4.0, 7.0 mg/l, respectively. Only 10% nitrification was observed in the unit with the lowest dissolved oxygen level, while in the others, 90% of the nitrogen was oxidized. The effect of dissolved oxygen level on nitrification can be explained by a switching function having an impact on growth kinetics.

$$\mu_A = \mu_{A\text{max}} \left(\frac{S_{\text{NH}}}{K_{\text{NH}} + S_{\text{NH}}} \right) \left(\frac{S_{\text{O}}}{K_{\text{OA}} + S_{\text{O}}} \right) \quad (6.5)$$

K_{OA} , is the half saturation constant for S_{O} and 0.4 mg/l is the recommended and adopted value for model simulation purposes. (Henze et al., 1987) However K_{OA} is related to the mixing intensity and mostly to the physical properties of flocs and

oxygen diffusion rate into the flocs where it can be stipulated that the oxygen level within the floc where the consumption takes place can be less than what it is in the bulk liquid. The high sludge concentration in the bulk liquid and the morphology of the bacteria (filaments and microthrix parvicella) have an adverse effect on the diffusivity of oxygen from the bulk liquid into the floc which can be explained by a higher half saturation constant for the autotrophs and mainly heterotrophs. The adopted model was calibrated for the half saturation concentration of autotrophs, K_{OA} being 1.25 mg/lit which is nearly 3 times higher than what is normally adopted. Although this phenomena would seem that the nitrification performance, especially the specific growth rate of nitrifiers in a MBR is less than a conventional activated sludge process, the high sludge age of the system ensures stable nitrification unless dissolved oxygen levels less than 0.3 mg/lit are not pertained. Nitrite build up was observed in some number of days where the dissolved oxygen levels dropped below 0.3 mg/lit which is explained by the Nitrobacter being more affected by low dissolved oxygen concentrations than Nitrosomonas (Knowles et al., 1965) where on the other hand no nitrite build up was also observed with the same low dissolved oxygen levels. Temperature did not have an effect on nitrite build up. The only difference in the two observations is the MLSS concentration in the bulk liquid where nitrite build up was more effective during high MLSS concentration whilst the MLSS was lower when no nitrite build up was observed during low dissolved oxygen levels. It can be concluded that the MLSS concentration within the reactor plays an important role in the diffusivity of oxygen into the flocs of Nitrosomonas and Nitrobacter thereby affecting the growth rate kinetics. The average ammonia removal efficiency calculated and measured throughout the study were %96 and 92% respectively.

Unlike the conventional activated sludge systems, the effluent ammonia nitrogen concentration in the membrane bioreactor is also related to the dissolved oxygen level in the membrane reactor which also affects the decay of autotrophs under low DO conditions.

The maximum nitrifier growth rate, μ_{Amax} , was calibrated to be $1.0d^{-1}$, slightly higher than what has been proposed by Henze et al. (1987) being $0.8d^{-1}$. Ammonia half saturation constant (K_{NH}) was found to be at 2.0 mg/lit; much higher than the proposed value of 1.0 mg/lit in conventional activated sludge modelling. The three parameters, μ_{Amax} , K_{NH} and b_A have the most impact on nitrification performance

where in the conventional activated sludge having low sludge ages only μ_{Amax} , and at high sludge ages μ_{Amax} and K_{NH} have noticeable impacts on overall nitrification performance. Figure 5.13 illustrates the performance of nitrification with respect to dissolved oxygen.

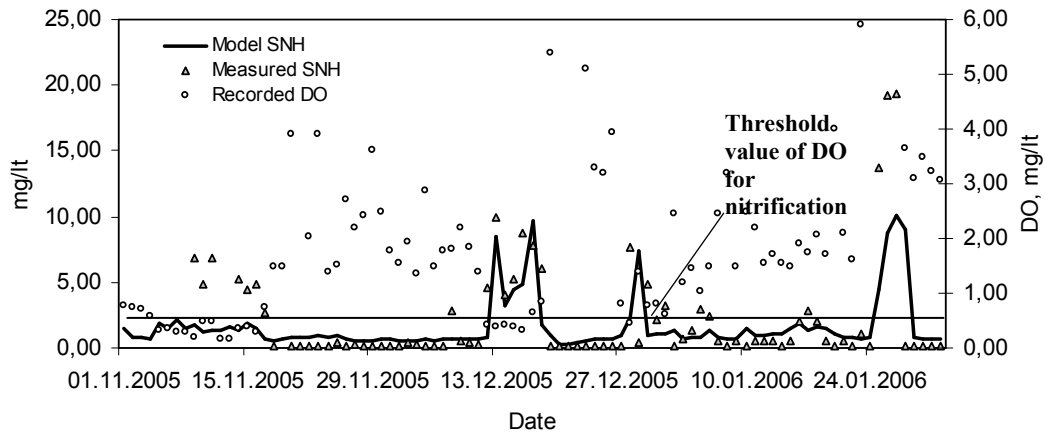


Figure 5.13: Nitrification performance of the pilot membrane bioreactor with respect to dissolved oxygen

Nitrification took place at dissolved concentrations less than 1.00 mg/l. This was linked to the fact that the sludge age of the system was extremely high and hence there was an abundance of autotrophic population when compared to conventional activated sludge systems. Nitrification performance of the pilot membrane bioreactor was also higher than a conventional activated sludge system. The system fully nitrified at temperatures as low as 4°C. However the sustainable temperature limit for nitrification was observed to be 8°C (Figure 5.14).

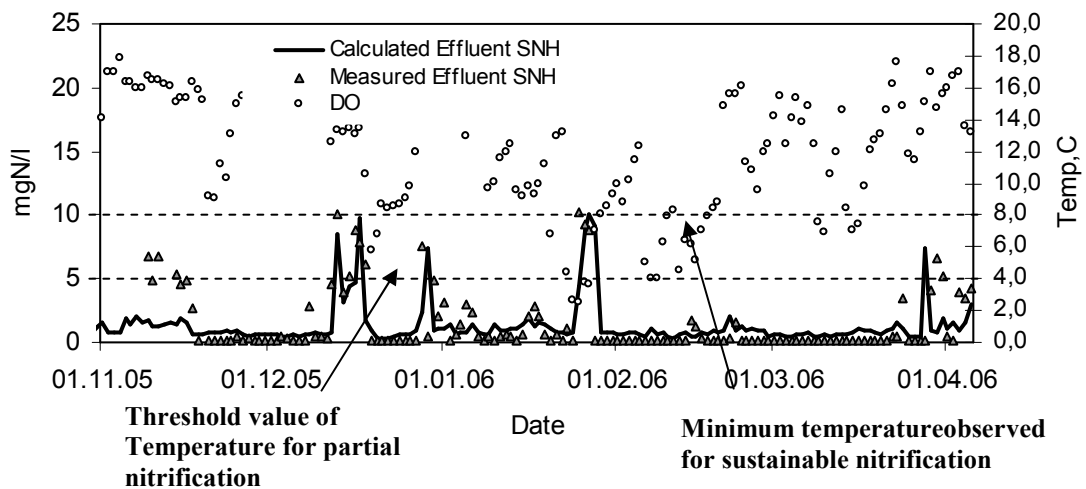


Figure 5.14: Nitrification performance of the pilot membrane bioreactor with respect to temperature

5.5.2 Denitrification

Significant simultaneous nitrification denitrification (SNdN) have been observed during the experimental study gaining the most attention in this research. It can be concluded that the factors and parameters triggering SNdN in MBR can be listed as i.) dissolved oxygen concentration, ii.) floc size, iii.) MLSS concentration of the bulk liquid which the latter two severely affects diffusion limitation of oxygen from the bulk liquid into the floc. The extent of SNdN has been both investigated in low DO levels ($0.3\text{mg/lt} < \text{DO} < 0.6\text{mg/lt}$) and high DO levels ($>1.5\text{ mg/lt}$).

At high DO levels, ($>1.5\text{mg/lt}$) the ammonia concentrations observed in the MBR tank was below 1 mg/lt , whilst the nitrate levels in the same tank which are to be pumped back to the anoxic reactor for denitrification was in the range of $8\text{-}16\text{ mg/lt}$. Considering that the average influent TKN and ammonia concentrations are $45\text{-}60\text{ mg/lt}$ and $30\text{-}45\text{ mg/lt}$ respectively, the level of denitrification in the MBR tank which is oxic was observed to be approximately $20\text{-}30\text{ mg/lt}$. This corresponds to a nitrate removal rate of nearly $50\text{-}60\%$ in the MBR tank itself. The level of denitrification is of course related to the denitrification potential, N_{DP} within the MBR reactor which is solely dependant on available COD. However in membrane bioreactors, it can be stated that the level of oxygen inside the MBR also plays an important role in defining denitrification potential in addition to the available carbon source and it must be evaluated in the mass balance derived equations. It has also been experimentally found that a DO concentration around 0.5 mg/lt in a sequencing batch reactor was suitable to achieve a nitrification rate equal to the denitrification rate which therefore lead SNdN (Münch et al., 1996). According to the modelling results, $80\text{-}85\%$ of readily biodegradable COD is depleted in the anoxic reactor as the only COD fraction available for denitrification which leaves the remaining S_s and hydrolysis of X_s to be the carbon source in the MBR tank.

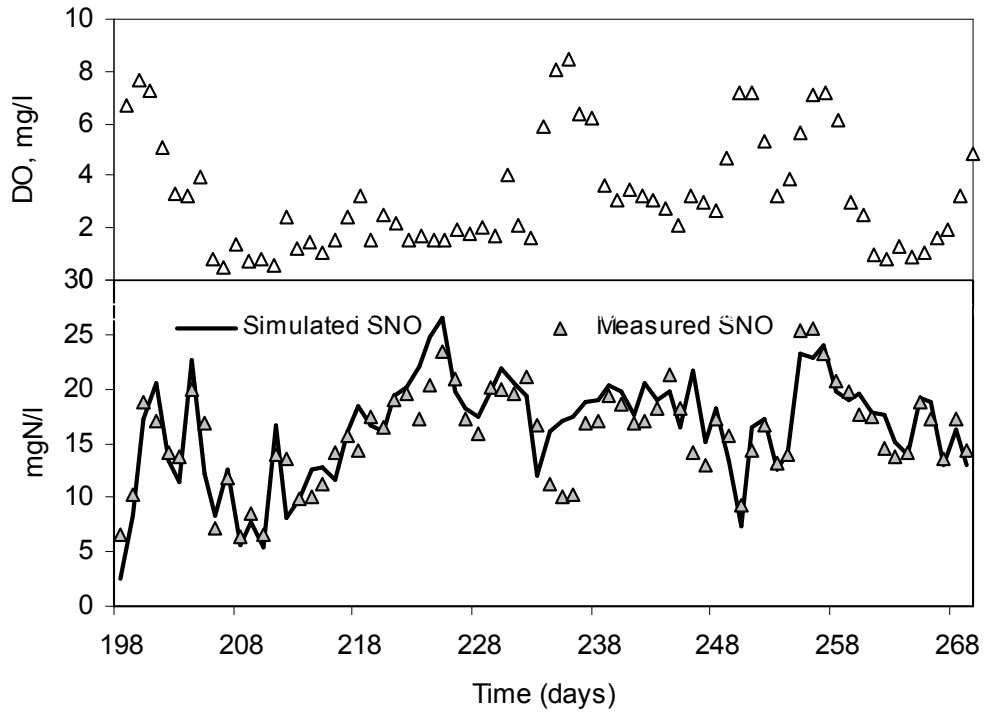
The high concentration in the bulk liquid and the population diversity results in a size distribution of flocs where in MBR it is assumed to be larger in the size of $50\text{-}110\mu\text{m}$. It is stipulated that a substantial anoxic mass fraction exists in the center of the biomass flocs resulting in an oxygen diffusion limitation into the flocs (Pochana and Keller, 1999). The level of SNdN occurring in the membrane bioreactor suggests that this level of diffusion limitation is so high that it is even causing the anoxic fraction of biomass inside the floc to be dominant during low DO levels. It can be

concluded that during high DO levels this fraction of biomass shifts from being anoxic to aerobic decreasing the level of SNdN. The oxygen diffusion limitation from the bulk liquid into the flocs can be explained by assigning specific values to half saturation constants in the corresponding switching functions namely $K_{OH}=1$ mg/l, $K_{OA}=1.25$ mg/l, $K_{NH}=2$ mg/l and $K_{NO}=2$ mg/l which are much higher than the values adopted to previous models (Henze et al., 1987, Henze et al., 1995, Gujer et al., 1999).

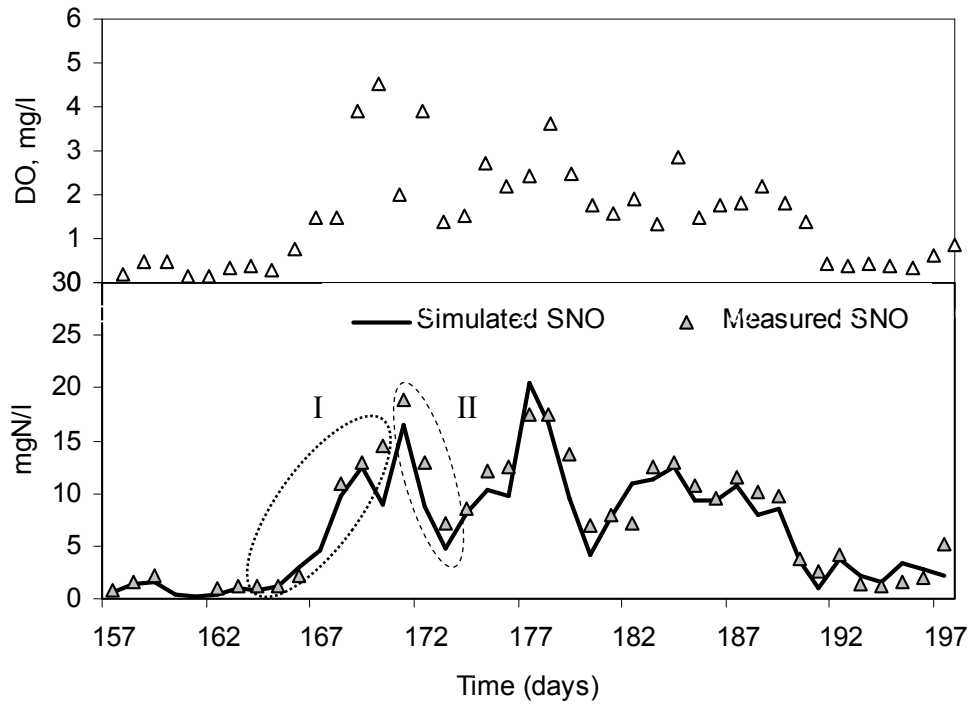
Table 5.6: Calibrated half saturation constants for MBR (Run I)

Half Saturation Parameter	Unit	This Study (Run I)	Reference (Henze et al.,1987;1995; Gujer et al.,1999)		
			ASM1	ASM2(d)	ASM3
K_{OH}	mgO ₂ /l	1.0	0.2	0.2	0.2
K_{OA}	mgO ₂ /l	1.25	0.4	0.5	0.5
K_{NH}	mgN/l	2.0	1.0	1.0	1.0
K_{NO}	mgN/l	2.0	0.5	0.5	0.5

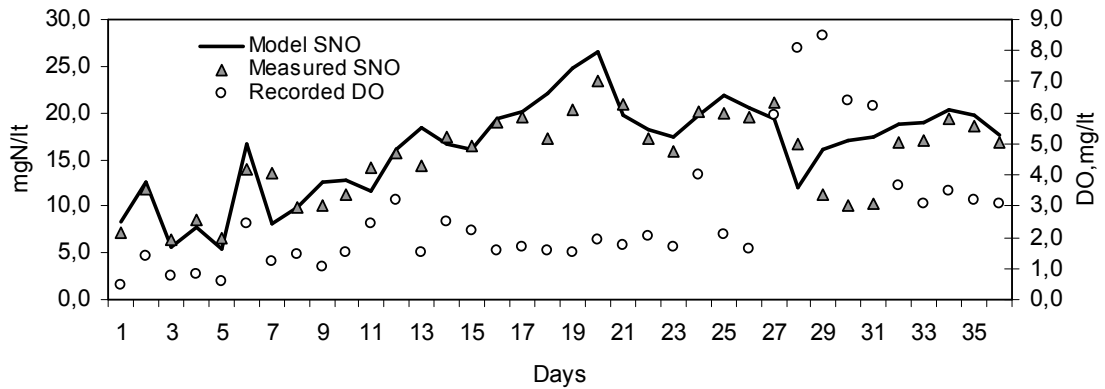
Assessment of the experimental results and mass balance verifications indicated that the level of SNdN cannot be only accounted for the diffusion limitations rather some other process was occurring both in the anoxic tank and the MBR tank during low DO levels causing the nitrate levels to drop. The adopted model fitted well to the experimental data with the two new processes *i.)Anoxic decay of heterotrophs* and *ii.)Anoxic decay of autotrophs* introduced into the original matrix of ASM1 revised for endogenous decay. These processes utilize nitrate nitrogen (S_{NO}) as the final electron acceptor. Anoxic decay occurs slower than aerobic conditions by incorporating an anoxic decay reduction factor, η_D into the process rate. η_D has been determined through calibrating the model to the nitrate response by adjusting the value to fit the data. The value of η_D has been calibrated to be 0.90 which is also quite high indicating that the anoxic decay is occurring nearly with the same rate as in aerobic conditions. Siegrist et al. (1999) proposed a reduction in anoxic decay rate of 40-50% for autotrophs and heterotrophs by performing batch experiments. This seems to be quite low when compared to MBRs, suggesting that the system is decay dominant and only a slight decrease should be expected triggering nitrate uptake at high rates. The magnified nitrate removal performance of the MBR pilot can be seen in Figure 5.15.



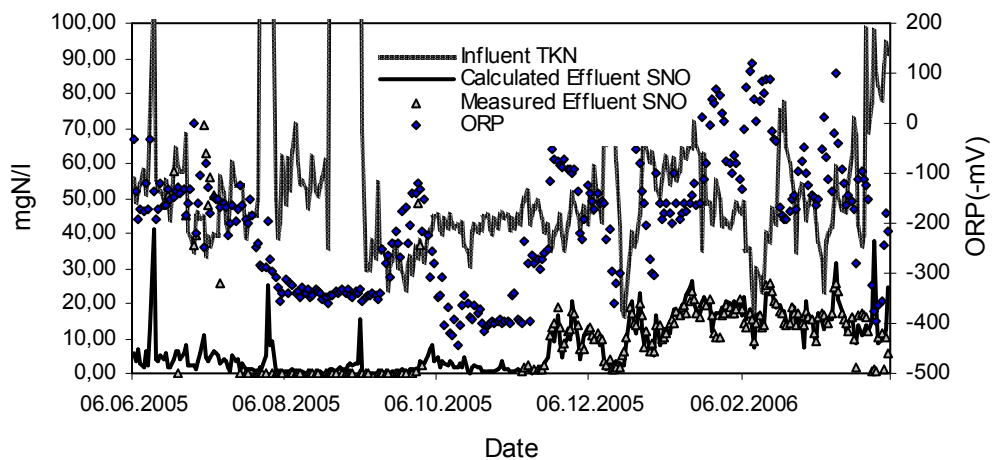
(a)



(b)



(c)



(d)

Figure 5.15: Nitrate removal performance (a) overall longterm results, (b) magnified results for low DO conditions (c) magnified results for high DO conditions (d) influent TKN and effluent S_{NO} results with respect to ORP values

The adopted model also fit well to the observed values in terms of $SNdN$. Figure 5.15b clearly shows the response of the model to fluctuating DO levels. The system was producing very low nitrate levels for low DO levels until day 10 of the experiment, where afterwards a sudden increase in DO resulted in a sudden increase of nitrate levels (I) and the opposite of this has been observed after day 15 of the experimental study (II) in which the sudden drop DO resulted in low nitrate levels in the permeate (Figure 5.15 c/d). Figure 5.16 shows the magnified simulation trajectories and experimental data for illustrating a good fit for longterm dynamic conditions under steady state conditions.

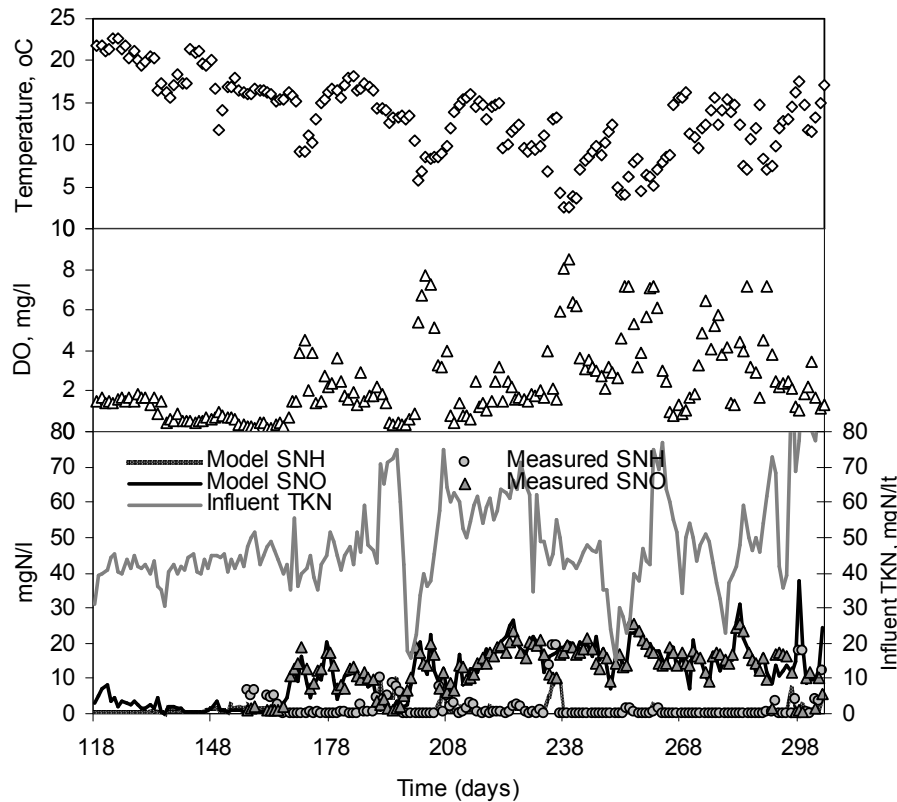


Figure 5.16: Dynamic simulation results and experimental data for S_{NH} and S_{NO}

Stoichiometry of denitrification requires the presence of an electron acceptor (NO_X) and a carbon source as the electron donor for the anoxic growth of heterotrophs. In practice this is evaluated as the ratio of influent COD to influent TKN where COD/TKN must be ≥ 10 for complete denitrification as lower values will dramatically decrease the efficiency of nitrate uptake (Orhon and Artan, 1994). The COD/TKN ratio throughout the study had an average of 8 where it can be concluded that there was not enough carbon source for denitrification levels achieved in the experimental study. The denitrification potential (N_{DP}) of a single sludge system is directly related to the amount of readily biodegradable substrate available catalyzing the uptake of nitrate during anoxic growth, however the levels of overall nitrate uptake observed in the experimental study imply that this is not the only process contributing to nitrogen removal in MBR. Heterotrophs also go through an endogenous respiration phase under anoxic conditions with a reduction factor (η_D) and using nitrate as the terminal electron acceptor instead of oxygen. Therefore mechanistic explanation of nitrogen removal in MBR require the addition of anoxic decay of heterotrophs and autotrophs with a significantly higher reduction factor of 0.90 for η_D .

The COD/TKN ratio exhibits high variation in the range of 5-20. Under low DO (from day 50 to 100 days) the system yielded high and stable nitrogen removal performance in spite of oscillating COD/TKN ratio in the influent. The system exhibited nearly full TN removal under low DO set-points.

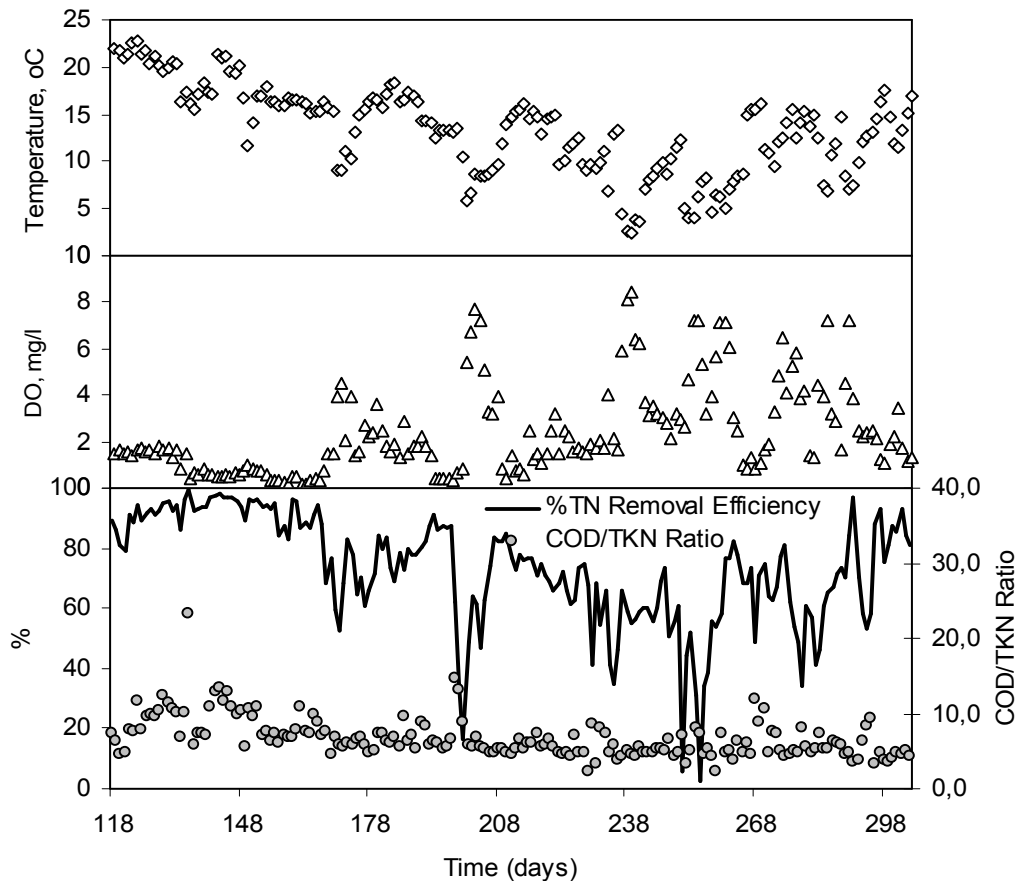


Figure 5.17: Total nitrogen removal efficiency vs. DO and influent COD/TKN ratio

The effect of increase in DO level in the reactor has negative effect on system performance with respect to TN removal. For instance, increase in DO level from 0.3 to 1.8 mg/l caused a gradual decrease in TN removal performance from 100% to 70%. According to Figure 5.17 the impact of COD/TKN level is much more pronounced under high DO levels in MBR reactor. At high DO levels, (>1.5mg/l) the ammonia concentrations observed in the MBR tank was below 1 mg/l, whilst the nitrate levels in the same tank was in the range of 8-16 mg/l. Considering that the average influent TKN and ammonia concentrations were 45-60 mg/l and 30-45 mg/l respectively, the level of denitrification in the MBR tank which is oxic was observed to be approximately 20-30 mg/l. This corresponds to a nitrate removal rate of nearly 50-60% in the MBR tank itself. The level of denitrification is related to the denitrification potential, N_{DP} within the MBR reactor which is solely dependant on

available COD. However in membrane bioreactors, it can be stated that the level of oxygen inside the MBR also plays an important role in defining denitrification potential.

The magnified TN removal evaluation with respect to Figure 5.17 reveals that the system produced low effluent TN concentrations ($TN < 15$ mg/l) with COD/TKN ratios below 10 indicating carbon deficiency for denitrification. It should also be noted that the pilot system had a V_D/V_T ratio of 0.14 which is the most important parameter in defining nitrogen removal efficiency in conventional activated sludge systems with predenitrification. German ATV DVWK Standards A131 (2000) recommends V_D/V_T ratio of 0.4 for COD/TKN ratio of 10 and 0.3 for a COD/TKN ratio 11 for design purposes of predenitrification systems (conversion has been made on the assumption that $COD = 2 \times BOD$ and $N_{OX} = \%70$ TKN) meaning that the V_D/V_T and the COD/TKN ratios for the pilot system would not be sufficient to reach the observed TN levels in a conventional activated sludge system.

It can be concluded that the factors and parameters triggering SNdN in MBR can be listed as *i.) dissolved oxygen concentration, ii.) floc size, iii.) MLSS concentration of the bulk liquid* which the latter two severely affects diffusion limitation of oxygen from the bulk liquid into the floc. Figure 5.18 shows the simulated ammonia (S_{NH}) and nitrate (S_{NO}) concentration for the entire duration of the study.

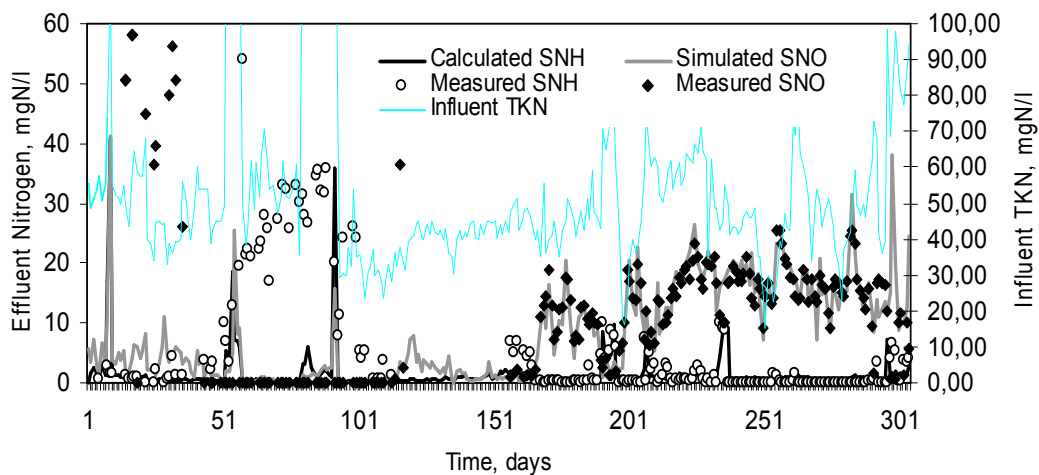


Figure 5.18: Simulated and calculated effluent ammonia (S_{NH}) and nitrate (S_{NO}) concentrations

The effluent nitrate (S_{NO}) can be expressed as the difference between available oxidizable nitrogen (N_{OX}) and the denitrification potential (N_{DP}) and the efficiency

can be expressed as the ratio between these two parameters. The denitrification potential can be expressed for each tank in the system with respect to the available COD fraction. Orhon and Artan (1994) postulated the approach that the entire readily biodegradable substrate will be depleted in the anoxic tank and the remaining portion of the biodegradable substrate is to be distributed between the anoxic and aerobic zones in the ratio of V_D/V_T for conventional activated sludge systems. The same approach can be adopted to membrane bioreactor systems however in a different way. The readily biodegradable substrate will be depleted in both the anoxic and MBR reactors as a fraction of the nitrate nitrogen equivalent of the total electron donor demand associated with the heterotrophic growth whilst readily and slowly biodegradable substrate will be utilized in both tanks with the electron donor demand associated with anoxic and aerobic endogenous respiration. The remaining biodegradable substrate for nitrate utilization during anoxic and aerobic decay is corrected by a factor of η_{HYD} when estimating the denitrification potential of the membrane tank due to the fact that some portion of the readily biodegradable COD will be depleted and some portion of the slowly biodegradable COD will be hydrolyzed in the anoxic tank. The denitrification potential for the anoxic tank and the MBR tank can be stoichiometrically and respectively defined with the equations given below;

$$\frac{N_{DPanox}}{Q} = \left[(1 - Y_H) \frac{S_{Sin}}{2.86} \eta_g + \frac{(1 - f_{EX} - f_{ES}) \eta_D b_H Y_H \beta \theta_X}{(1 + b_H \beta \theta_X)} \frac{C_{Sin}}{2.86} \right] \frac{V_{anox}}{V_T} \quad (6.6)$$

and

$$\frac{N_{DPMbr}}{Q} = \left[(1 - Y_H) \frac{(C_{Sin} - S_{Sin})}{2.86} \eta_g + \frac{(1 - f_{EX} - f_{ES}) \eta_D b_H Y_H \beta \theta_X}{(1 + b_H \beta \theta_X)} \frac{C_{Sin}}{2.86} \eta_{anox} \right] f_{DNH} \left(1 - \frac{V_{anox}}{V_T} \right) \quad (6.7)$$

The denitrification potential and hence the effluent total nitrogen concentration can be stoichiometrically calculated using the above equations. The validation of the above equations have been done by comparing the stoichiometrically driven results with the results of the adopted model at steady state conditions. The comparison has been done for constant temperature-varying dissolved oxygen concentrations (Figure 5.19) and constant dissolved oxygen concentration-varying temperature (Figure

5.20). This is to make a correct assessment on the impact of dissolved oxygen and temperature on total nitrogen removal.

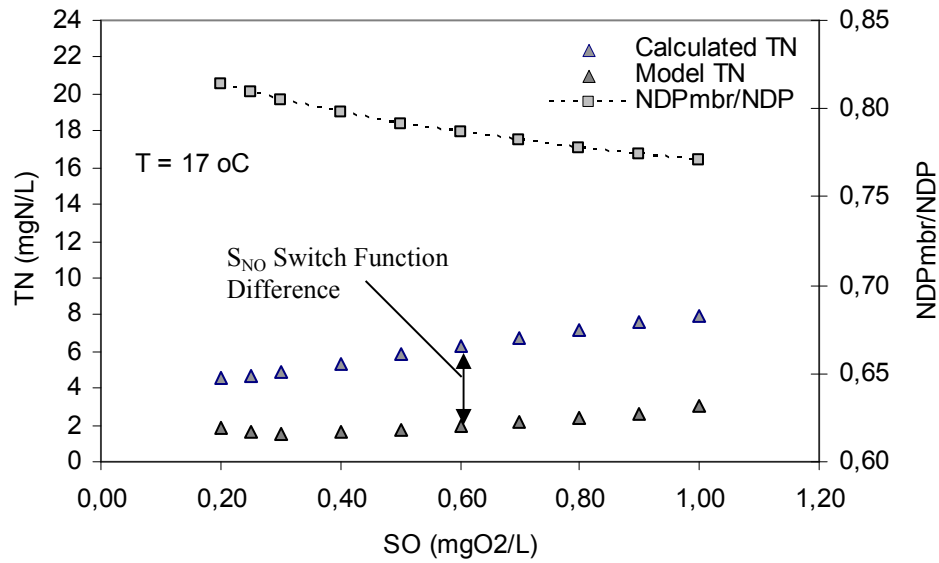


Figure 5.19: Comparison of total effluent nitrogen level with respect to stoichiometric and model results for varying dissolved oxygen

Denitrification requires the existence of a terminal electron acceptor which is nitrate where non-existence will cause the process not to occur. Modelwise, this is arranged by incorporating a switch function for nitrate and the model is simultaneously solved for each parameter. However since this is not possible to do in stoichiometric equations, there will be a difference in the denitrification potential and hence the total effluent nitrogen concentration (Figure 5.19).

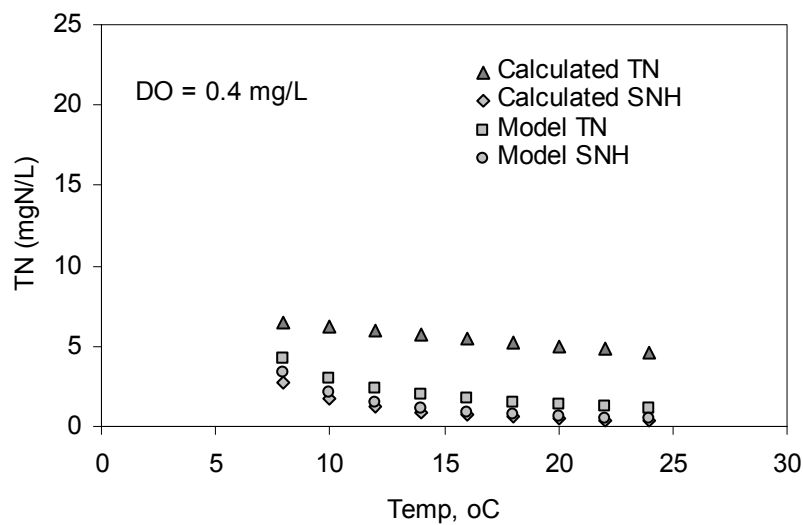


Figure 5.20: Comparison of total effluent nitrogen level with respect to stoichiometric and model results for varying temperature

The stoichiometric calculations mimicked the model results thereby validating the mass balance derived stoichiometric equations for the denitrification potential of each reactor and the total effluent nitrogen concentrations.

In order to assess the effect of diffusion limitation and the half saturation constant of oxygen for heterotrophs and autotrophs at increased biomass concentrations, Run II was conducted at biomass levels between 25,000-30,000mg/l. The steady state solids balance occurred in the range of 25,000-27,000 mg/l due to varying influent conditions. Nitrogen removal with special emphasis on denitrification was the main focus of the second run.

At first, nitrification and denitrification simulation results did not match the measured values with respect to the adopted and calibrated new MBR model. On the other hand, solids balance and organics removal results were explained efficiently with the new adopted model. From the preliminary assessment of the measured nitrogen removal results it was obvious that the diffusion limitation had been increased due to higher biomass concentration. This phenomena is directly related to the half saturation constants of oxygen for heterotrophs (K_{OH}) and autotrophs (K_{OA}) which regulate nitrification and denitrification by means of switching functions. It is expected that the half saturation constant of oxygen for both species to be increased with increasing MLSS values. The dominant partial nitrification results of the second run also imply that the diffusion limitation of oxygen into the nitrifying flocs is more dominant and effective at high biomass concentrations. The ammonia nitrogen (S_{NH}) profile for the second run is illustrated in Figure 5.21. The overall influent wastewater characterization for Run II is given in Table 5.7.

Table 5.7: Influent wastewater characterization (Run II)

<i>Parameter</i>	<i>Unit</i>	<i>Min</i>	<i>Max</i>	<i>Average</i>	<i>%70'ile</i>	<i>%90'ile</i>
COD	mg/l	538	798	679	726	775
TSS	mg/l	180	1545	334	319	412
VSS	mg/l	153	945	261	281	302
TKN	mg/l	79	124	97	99	114
NH ₄ -N	mg/l	63	99	77	79	91

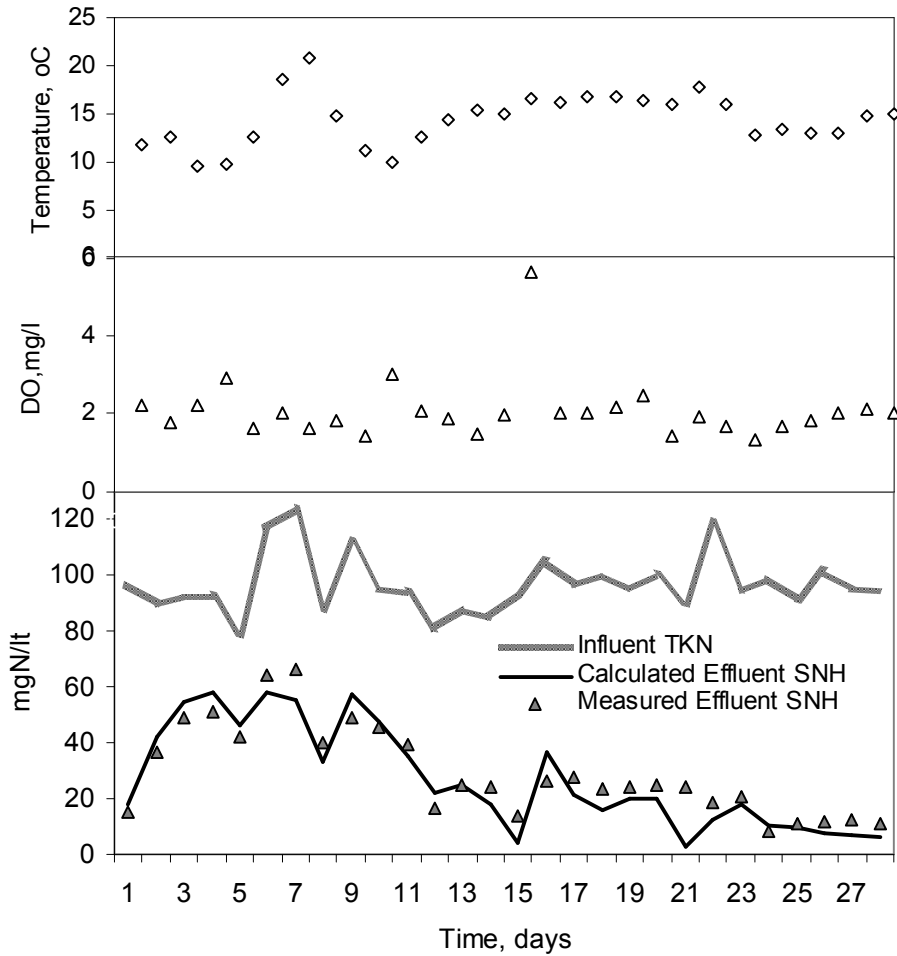


Figure 5.21: Ammonia (S_{NH}) profile for Run II

It can be clearly seen that not all of the incoming TKN load is fully oxidized and partial nitrification conditions prevail. On the other hand, denitrification performance has been increased with respect to the available nitrate and the level of oxygen in the bulk liquid when compared with the results of the first run. The nitrate nitrogen profile can be seen in Figure 5.22.

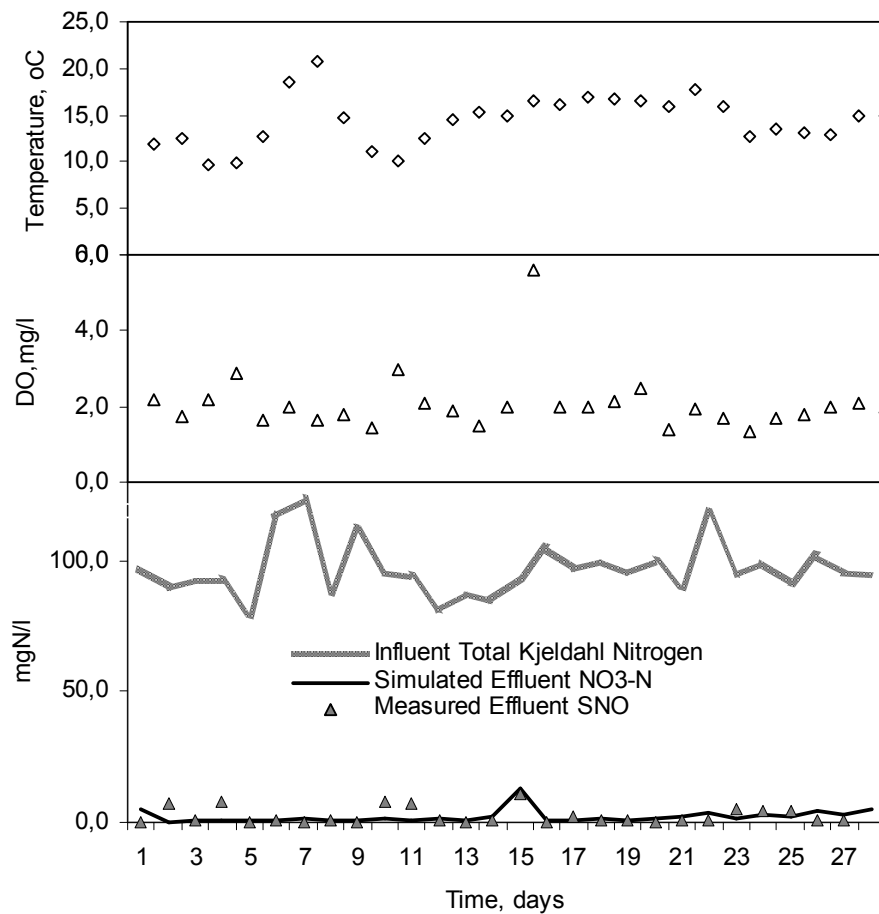


Figure 5.22: Nitrate (S_{NO}) profile for Run II

The nitrate profile is calibrated by increasing the oxygen half saturation constant of heterotrophs until a match is achieved with the measured results. By implementing a higher oxygen half saturation constant of heterotrophs at this biomass level the nitrate profile and hence denitrification were successfully calibrated. Taking into account the influent COD/TKN and the available V_D/V_T ratio, the system sustained denitrification efficiencies beyond the available denitrification potential which in conventional systems are thought to be bound to only these two factors. As explained in the previous sections, the denitrification potential of the system has been increased with respect to increased diffusion limitation meaning that the system had more denitrification potential than the available nitrate which resulted in increased nitrate removal efficiencies over 90%.

As it can be seen from Figure 5.23; the denitrification potential and total nitrogen removal efficiencies are very much higher than that of expected in a conventional system with respect to the available COD in the raw sewage and the dissolved oxygen concentration in the membrane reactor. This clearly shows the detrimental effect of mass transfer and hence diffusion limitation.

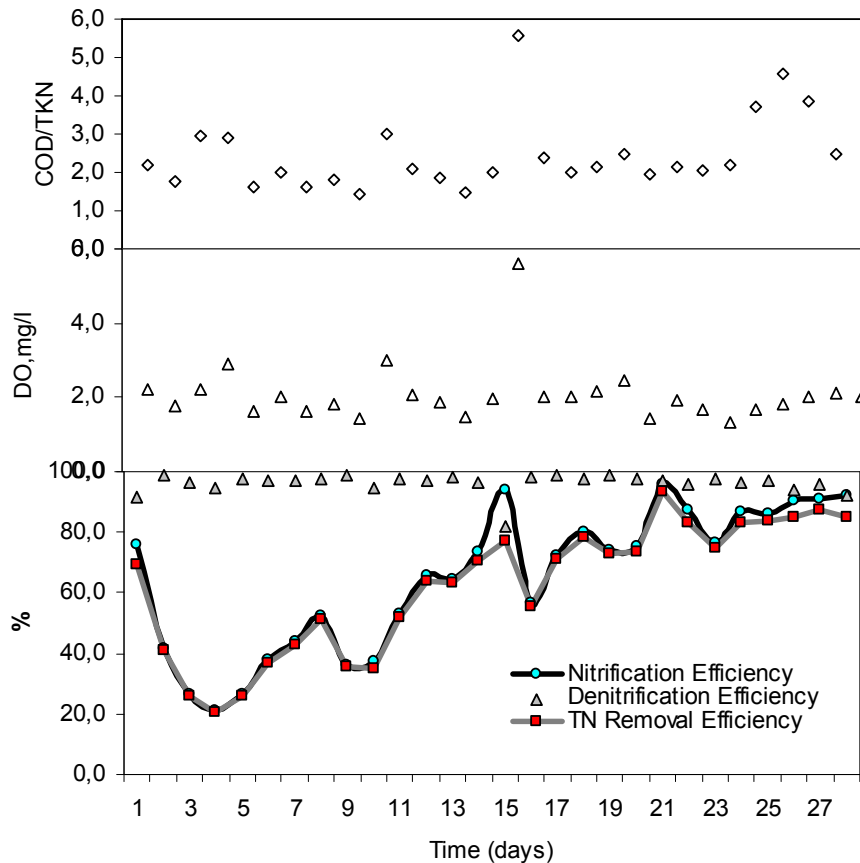


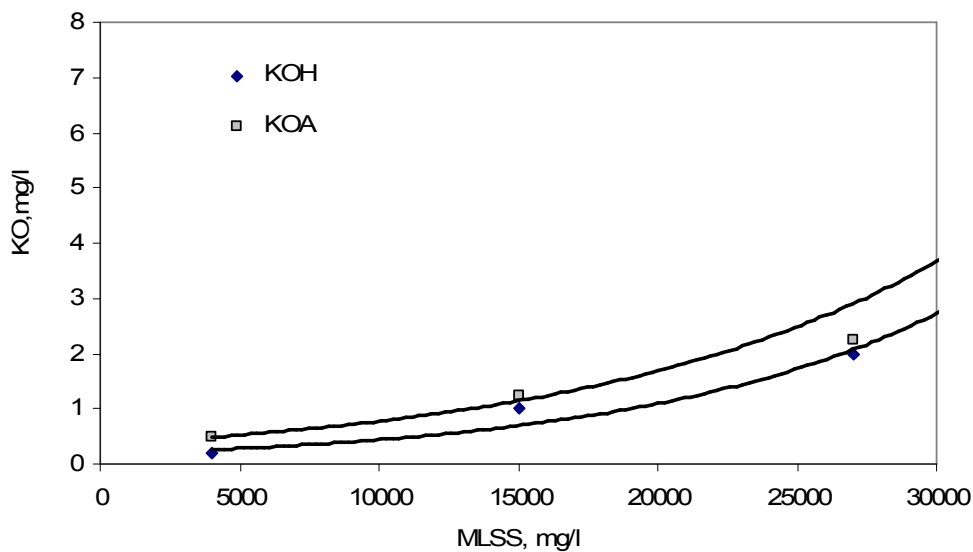
Figure 5.23: Efficiencies nitrification, denitrification and total nitrogen

Higher K_{OH} value meant increased diffusion limitation of oxygen from the bulk liquid into the floc sustaining a higher anoxic mass fraction within the bacteria even at higher DO levels resulting in an improved efficiency of nitrate removal. The half saturation constants K_{OA} and K_{OH} were calibrated at 2.25mg/l and 2.0 mg/l respectively for biomass levels in the range of 24,000-27,000mg/l in the second run (Table 5.8). According to the half saturation constants for oxygen at different biomass levels, the trend of this parameter can be fitted to give an indication of the diffusion limitation at biomass levels higher than 30,000mg/l.

Table 5.8: Calibrated half saturation constants for MBR (Run II)

Half Saturation Parameter	Unit	This Study (Run II)	Reference (Henze et al., 1987; 1995; Gujer et al., 1999)		
			ASM1	ASM2(d)	ASM3
K_{OH}	mgO ₂ /l	2.0	0.2	0.2	0.2
K_{OA}	mgO ₂ /l	2.25	0.4	0.5	0.5
K_{NH}	mgN/l	2.0	1.0	1.0	1.0
K_{NO}	mgN/l	2.0	0.5	0.5	0.5

Figure 5.24 implies that in case of MLSS concentrations higher than 40,000mg/l, it would practically not be possible for the autotrophic bacteria to uptake the oxygen in the bulk liquid due to the mass transfer limitation and as a result nitrification will cease. This will be also be the case for heterotrophic bacteria however they are less prone to diffusion limitation when compared to autotrophs.

**Figure 5.24:** Variation of K_{OA} and K_{OH} with respect to MLSS

It can be clearly stated that higher biomass levels will promote mass transfer limitation in terms of both substrate and oxygen. However due to the floc morphology, high MLSS and sludge age in membrane bioreactor systems, nitrification will take place at even lower dissolved oxygen levels. This will also increase denitrification efficiency in MBRs.

Pilot plant is designed to treat typical domestic sewage with ammonia concentrations up to 45 mg/l and hence the aeration system and blower capacity is selected

accordingly. However the influent COD (average:679 mg/l) and ammonia concentrations for Run II (average: 77mg/l) were well over the values taken into account for the pilot design. As this was the case, there was residual oxygen of 1.5-3 mg/l in the bulk liquid throughout the study where it should have been expected to be much lower with values less than 1 mg/l due to air feed deficiency and oxygen uptake by the bacteria. This clearly explains and verifies the fact that major portion of the supplied oxygen is unable to pass into the floc due to mass transfer limitation which is explained by increased half saturation constant of oxygen.

Manser et al. (2005) drew the same conclusion in terms of nitrification and denitrification from a different perspective. By the detailed analysis of the bacterial floc size and morphology grown in a membrane bioreactor system, they concluded that floc size affected oxygen supplies to the bacteria in the floc interior and hence also nitrification performance in a membrane bioreactor, 90% of the maximum nitrification rate is already attained at an oxygen concentration of 1 g/m³ (Figure 5.25). It is furthermore stated that due to lower oxygen concentration denitrification is improved because in overall less oxygen is passed from the aerobic into the anoxic denitrification zone.

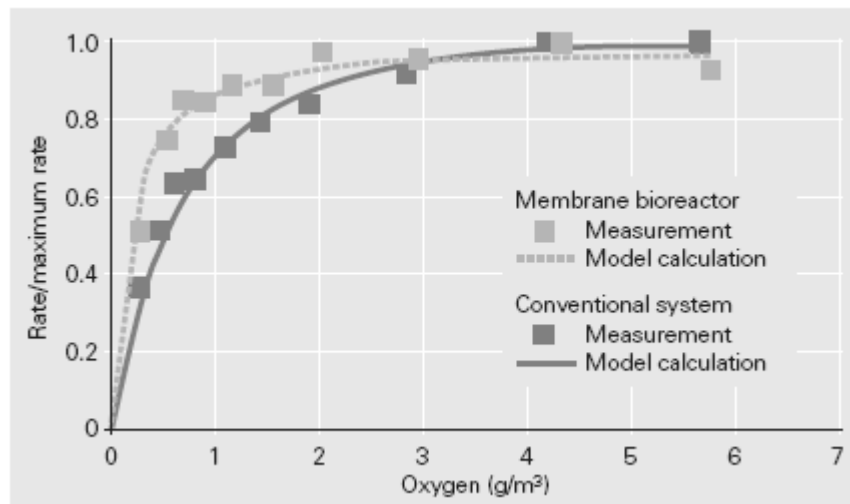


Figure 5.25: Measured and calculated nitrification rates as a function of oxygen concentration under excess substrate conditions (Manser et al., 2005)

The above graph explains the high rate of nitrification occurring in a membrane bioreactor operated under low dissolved oxygen concentrations in terms of population dynamics of nitrifiers under mass transfer limiting conditions.

5.6 Calibration Results

The summary of the calibrated model parameters for the MBR systems is given in Table 5.9.

Table 5.9: Summary of calibrated model parameter for MBR

Model Parameter	Units	ASMI (Henze et al., 1987)		This Study	
		Parameter (20°C)	Arrhenius , θ	Parameter (20°C)	Arrhenius , θ
<i>Stoichiometric</i>					
Heterotrophic Yield, Y_H	gcellCOD gCOD ⁻¹	0.67	-	0.66	-
Autotrophic Yield, Y_A	gcellCOD gN ⁻¹	0.24	-	0.24	-
Fraction of biomass leading to particulate products, f_p (f_{EX})	-	0.08	-	0.20	-
Fraction of biomass leading to soluble products, f_{ES}	-	-	-	0.05	-
Mass of nitrogen per mass of COD in biomass, i_{XB}	gN gCOD ⁻¹ in biomass	0.086	-	0.086	-
Mass of nitrogen per mass of COD in products from biomass, i_{XE}	gN gCOD ⁻¹ in end.mass	0.06	-	0.06	-
<i>Kinetic</i>					
Max specific growth rate for heterotrophic biomass, μ_{Hmax}	d ⁻¹	6	1.029	6	1.103
Half saturation constant for heterotrophic biomass, K_S	g m ⁻³	20	-	20	-
Decay rate for heterotrophic biomass, b_H	d ₁	0.62	1.029	0.24	1.119
Max specific growth rate for autotrophic biomass, μ_{Amax}	d ⁻¹	0.80	1.072	1	1.123
Decay rate for autotrophic biomass, b_A	d ⁻¹	0.05-0.15	1.029	0.06	1.119
Anoxic Correction factor for heterotrophs, η_g	dimensionless	0.80	-	0.80	-
Correction factor for hydrolysis under anoxic conditions, η_h	dimensionless	0.40	-	0.6	-
Correction factor decay under anoxic conditions, η_D	dimensionless	-	-	0.90	-
Max specific hydrolysis rate, K_h	gX _S (gcell COD.d) ⁻¹	3	1.050	3	1.116
Half saturation constant for hydrolysis of slowly biodeg. subs., K_X	gX _S gcell COD ⁻¹	0.03	1.029	0.03	1.116
Ammonification rate, k_a	m ³ COD (g .d) ⁻¹	0.08	1.050	0.08	1.071

5.7 Operation of the MBR without the Anoxic Tank- Results of Run III

The findings and results of the first two runs had the major question mark on the role of the anoxic tank within a membrane bioreactor system. Through simultaneous nitrification and denitrification (SNdN), the measured nitrate levels were unexpectedly low within the MBR tank with respect to the dissolved oxygen level maintained in the membrane reactor. This was previously explained by the mass transfer limitation and the diffusion limitation of oxygen from the bulk liquid into the bacterial cell resulting in an increased anoxic mass fraction within the floc. The results revealed that the nitrates recycled back to the anoxic tank were not so much further degraded to N_2 in a sense that it would be expected from an anoxic tank. The returned nitrate levels from the MBR were already low and the further reduction of nitrate within the anoxic tank was negligible. Based on these findings, it was also previously postulated that total nitrogen removal can be achieved in membrane bioreactor systems with a lower anoxic volume or no anoxic volume at all due to the increased denitrification potential and hence SNdN occurring in the membrane reactor itself. In order to justify this postulate, the anoxic tank was taken out of operation and the system was operated with only the membrane reactor for total nitrogen removal at various DO levels. The same set of analysis were conducted as done in the previous runs. The operation of the MBR system without the anoxic tank was also modelled using BioWin and the previously calibrated MBR model. Model results were compared with the laboratory measurements to check the models responsiveness and to mechanistically justify the total nitrogen removal in a membrane bioreactor system without an anoxic tank. The BioWin model setup for the operation of the MBR without the anoxic tank can be seen in Figure 5.26.

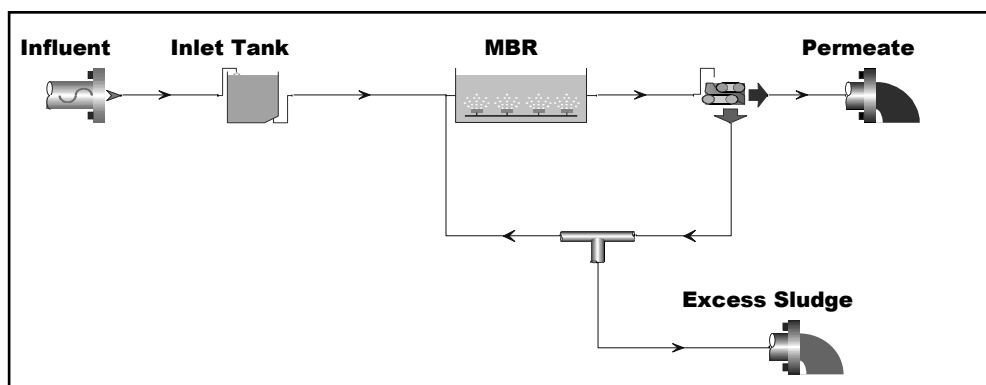


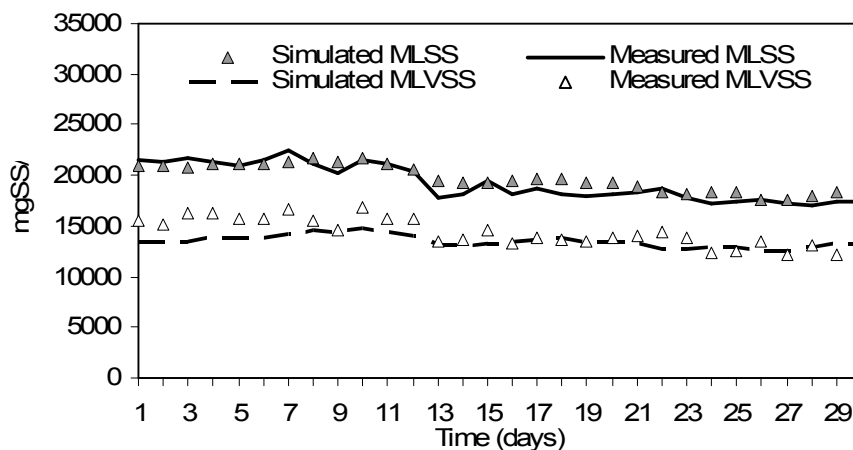
Figure 5.26: BioWin® 2.2 modelling setup for Run III

As it can be seen from the above figure the anoxic tank has been taken out of the modelling layout and the recirculation is eliminated. As stated previously, the circulation seen back to the MBR tank is to illustrate the complete solids retention of the solids within this reactor. This recirculation stream having a very high flow ($>50Q_{in}$) is designated as an internal recirculation stream representing the total solids entrapment within the MBR tank in terms of modelling purposes in the simulator. This very high flowrate of the internal recirculation becomes irrelevant and does not affect the amount of solids entrapment within the MBR tank above five times in the inlet flow. The overall influent wastewater characterization for Run III is given in Table 5.10.

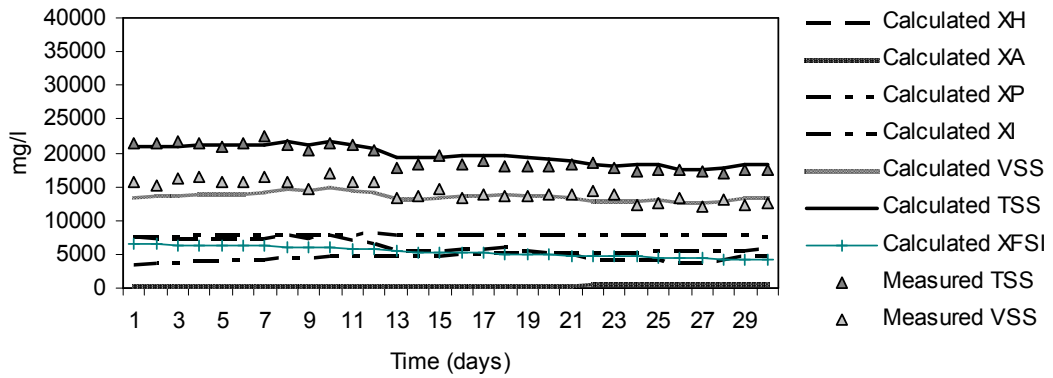
Table 5.10: Influent wastewater characterization (Run III)

<i>Parameter</i>	<i>Unit</i>	<i>Min</i>	<i>Max</i>	<i>Average</i>	<i>%70'ile</i>	<i>%90'ile</i>
COD	mg/l	302	926	586	630	713
TSS	mg/l	127	270	193	228	251
VSS	mg/l	89	110	149	172	183
TKN	mg/l	84,6	247,5	156,3	174,5	200,12
NH ₄ -N	mg/l	68	198	124,5	140	160

The system reached steady state conditions in terms of solids balance after 30 days of operation (Figure 5.27). The graphs presented below show the solids balance following the reach of steady state conditions.



(a)



(b)

Figure 5.27: Solids balance of MBR in Run III in terms of (a) VSS,TSS (b) all the particulate components

The system was balanced at 17,500-21,000 mg/l of TSS and 12,500-16,000 mg/l of VSS concentrations in which the ranges are related to varying influent conditions. Multiple steady state conditions can be defined in Run III as done in Run I. The sludge age was 36,5 days based on an excess sludge removal of 32 l/day. The model was run with the calibrated kinetic and stoichiometric parameters in Run I. The model results showed a good match against the measured values for the solids balance.

The average COD removal efficiency of the system was %94 where it went up to a maximum of 97%. The minimum observed COD removal efficiency was %89 (Figure 5.28).

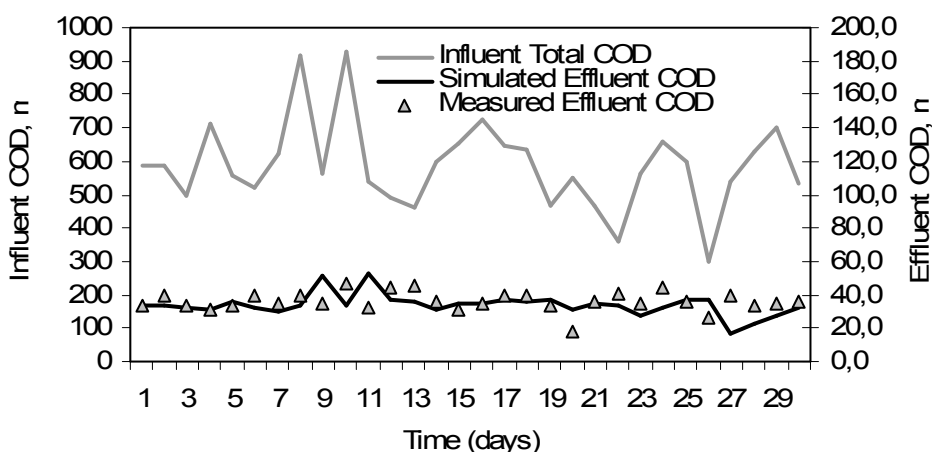


Figure 5.28: Influent, effluent COD and removal efficiencies

The raw sewage had a maximum COD of 926 mg/l where it can be considered as a very strong domestic sewage. However the MBR produced very low effluent COD

values regardless of the fluctuations encountered in the influent. The model mimicked the effluent COD values perfectly with respect to the measured values.

The air supplied to the MBR system was recorded on a daily basis where afterwards the oxygen utilization rate of the bacteria was modelled using BioWin. The modelling was based on coarse bubble aeration of the MBR reactor both for biodegradation of the carbonaceous and nitrogenous material and scouring of the membrane surface. Figure 5.29 shows the oxygen modelling results with respect to the calculated dissolved oxygen concentrations against the amount of air introduced into the reactor. The results are compared with the field recorded DO concentrations within the MBR tank.

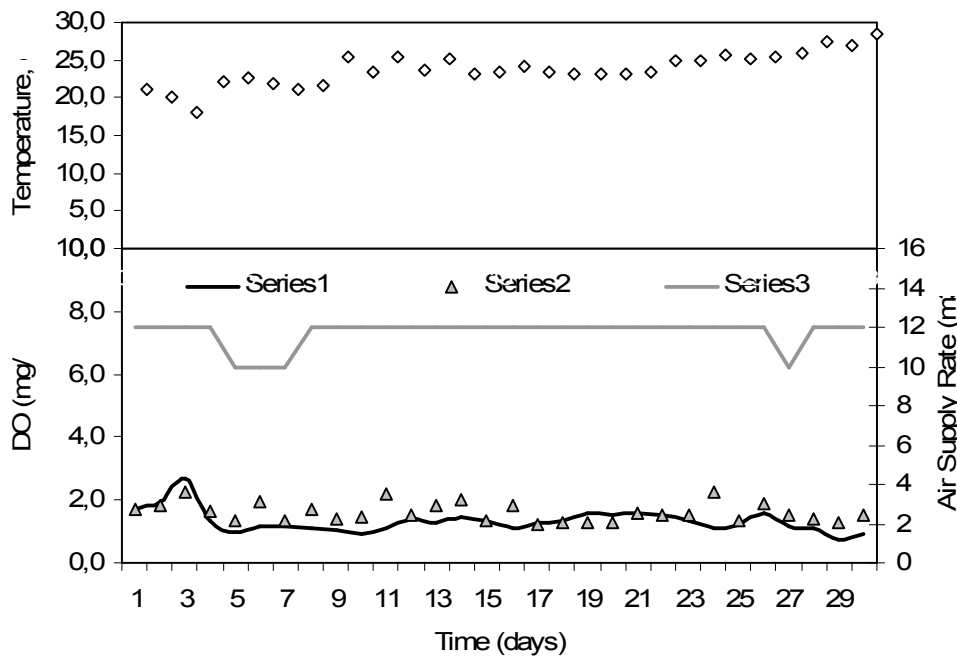
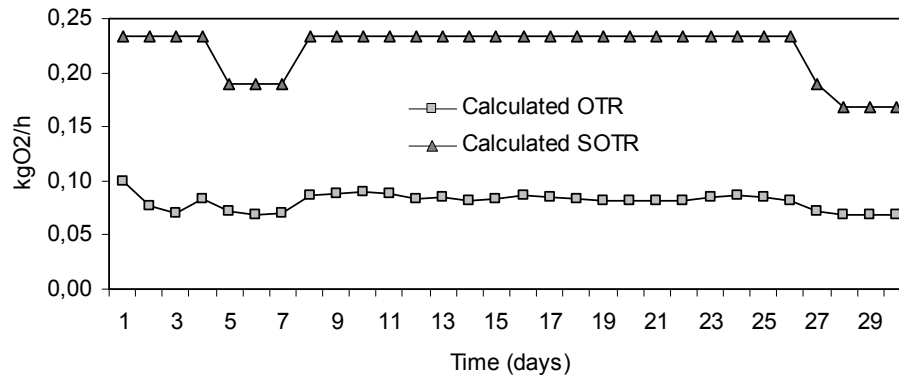
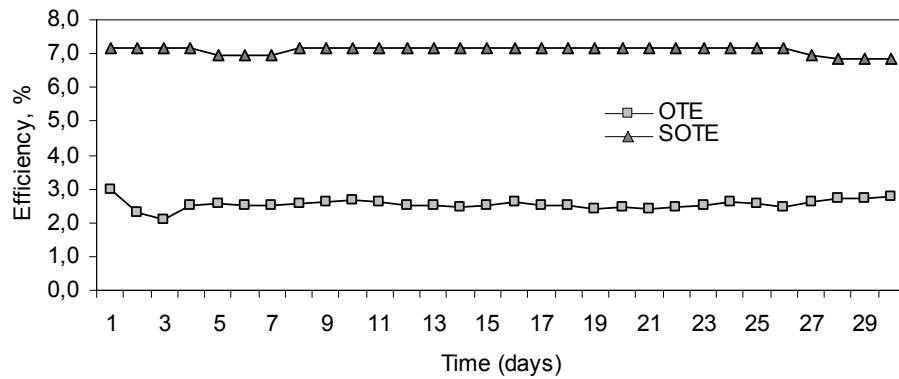


Figure 5.29: Oxygen modelling results

The calculated dissolved oxygen concentrations in relation to the amount of air introduced into the tank shows a fairly good match with the recorded DO levels in the MBR reactor. The dissolved oxygen levels maintained in the MBR reactor were in the range of 1-3 mg/l with an average of 1.7 mg/l. The level of oxygen in the membrane tank was very important because of its impact on simultaneous nitrification and denitrification (SNdN). The oxygen modelling in Run III was again calibrated at an alpha (α) factor of 0.4 as calibrated in Run I. The corresponding oxygen transfer rate and efficiencies are illustrated in Figure 5.30.



(a)



(b)

Figure 5.30: (a) Oxygen transfer rates, (b) Oxygen transfer efficiencies

The coarse bubble aeration system produced an average standard oxygen transfer efficiency of %7. The SOTR/OTR ratio was in the range of 2-2.5.

Nitrification and denitrification efficiency of the MBR system operated without the anoxic tank was the major focus in Run III, for the justification of the lesser need for an anoxic tank due to simultaneous nitrification and denitrification (SNdN). The influent TKN and ammonia levels were unexpectedly very high resembling a strong industrial waste. These influent conditions were dominant throughout Run III resulting in a very high nitrogenous load to the plant. The average influent TKN and ammonia nitrogen concentrations were 200 and 127 mg/l respectively with a resultant average S_{NH}/TKN ratio of 0.63 which is also low when compared to a typical domestic sewage. The peak influent TKN and ammonia nitrogen concentrations encountered were 279 and 198 mg/l respectively. As a result of the non-domestic nitrogenous material in the raw sewerage partial nitrification was encountered throughout the run. Full nitrification was never been achieved even though the sludge age and temperature were quite high. Four major causes can be

defined for the partial nitrification that has been observed; i.) *Nitrification is a substrate inhibitive process*, ii.) *the volume for nitrification and the amount of air introduced were not sufficient to achieve full oxidation of the incoming S_{NH}* , iii.) *the excessive diffusion limitation of oxygen at very high MLSS*, iv.) *Industrial discharge*

Modelwise, the combination of the above three aspects were explained by a lower max autotrophic growth rate defined in the model. The max autotrophic growth rate of the nitrifiers were calibrated to be 0.16 d^{-1} in Run III which is very less compared the growth rate in Run I. The ammonia nitrogen profile with respect to dissolved oxygen and temperature are illustrated in Figure 5.31.

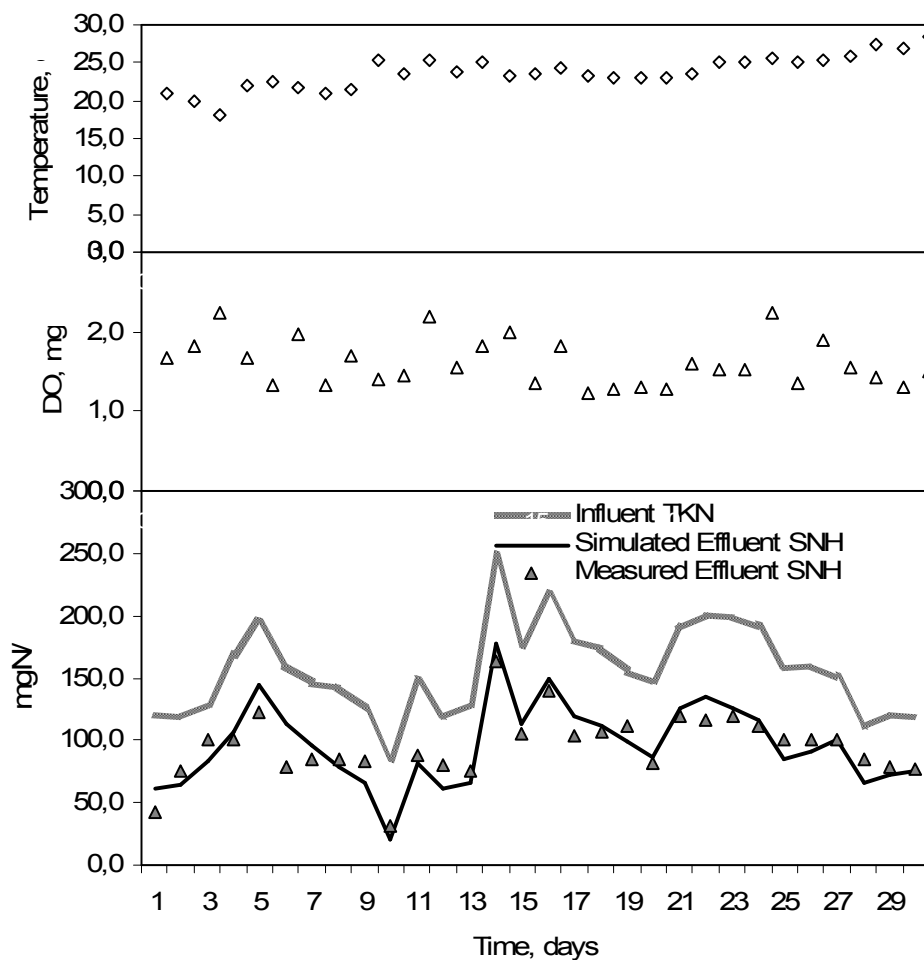


Figure 5.31: Ammonia nitrogen profile with respect to dissolved oxygen and temperature

As it can be seen from the above figures, partial nitrification was dominant even at high temperatures and moderate DO levels. The average oxidized ammonia nitrogen (N_{ox}) was 31 mg/l whilst the max measured figure was 103 mg/l . The latter figure corresponds to a typical nitrate concentration to be denitrified in a domestic sewage.

This means that it would be able to accomplish total nitrogen removal without an anoxic tank in a membrane bioreactor system as it was seen that the 30-40 mg/l of nitrate was simultaneously removed in the membrane reactor itself.

Since full nitrification could not be achieved, the efficiency of denitrification was assessed based on the oxidized ammonia nitrogen which is equal to the available nitrate nitrogen for reduction. The nitrate profile for Run III is illustrated in Figure 5.32.

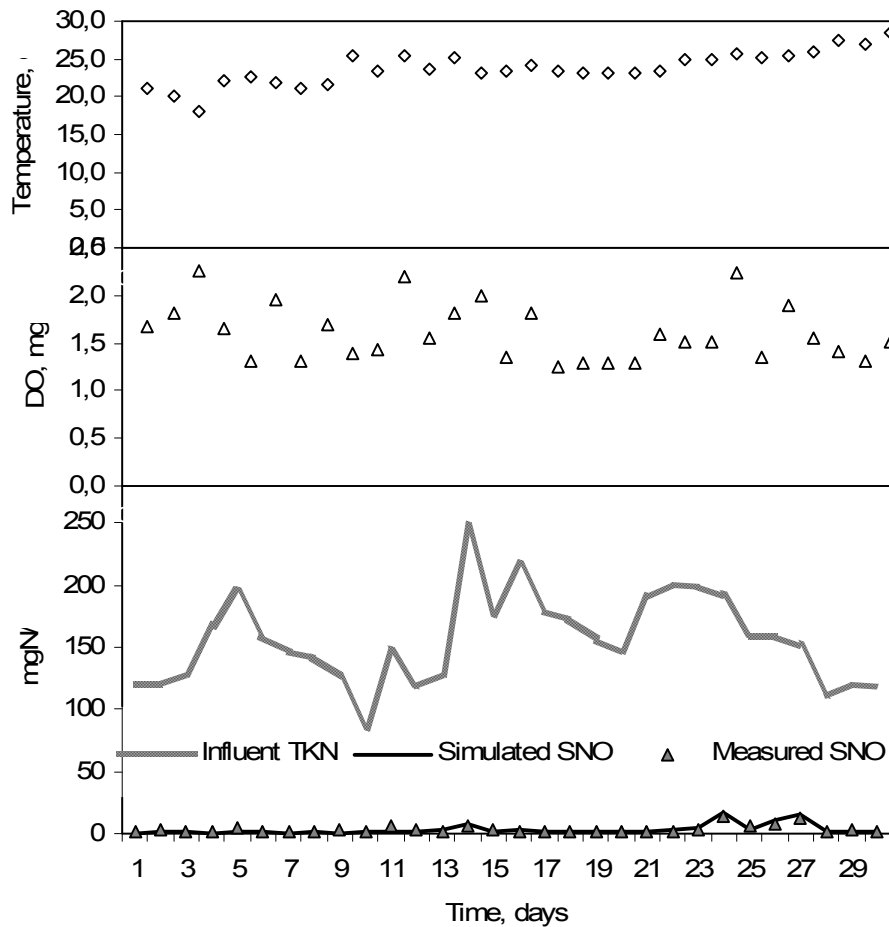


Figure 5.32: Nitrate profile

The nitrate levels were very low throughout the study which implies that nearly all of the nitrate formed within the MBR tank by nitrification was completely converted to N_2 through simultaneous nitrification and denitrification (SNdN). The average denitrification efficiency was observed to be %97. Checks were also conducted to observe any possible nitrite (NO_2^-) build up that may mislead the results, however no nitrite build up was seen throughout Run III. Due to the very high MLSS concentrations leading to a massive oxygen diffusion limitation, the SNdN was stable at all DO concentrations.

The half saturation constants for Run III were dynamically calibrated due to the fact that the MLSS levels were higher than Run I and lower than Run III. The oxygen half saturation constants for heterotrophs and autotrophs were calibrated to be $K_{OH}=1.75$ mg/l and $K_{OA}=2.0$ mg/l respectively (Table 5.11.). As previously stated, the correct assessment of nitrate reduction taking place in the membrane reactor is related to the amount of ammonia nitrogen oxidized (N_{OX}). Figure 5.33 shows the amount of ammonia nitrogen oxidized and the effluent nitrate nitrogen with respect to dissolved oxygen and COD/TKN ratio.

Table 5.11: Calibrated half saturation constants for MBR (Run III)

Half Saturation Parameter	Unit	This Study (Run III)	Reference (Henze et al.,1987;1995; Gujer et al.,1999)		
			ASM1	ASM2(d)	ASM3
K_{OH}	mgO ₂ /l	1.75	0.2	0.2	0.2
K_{OA}	mgO ₂ /l	2.0	0.4	0.5	0.5
K_{NH}	mgN/l	2.0	1.0	1.0	1.0
K_{NO}	mgN/l	2.0	0.5	0.5	0.5

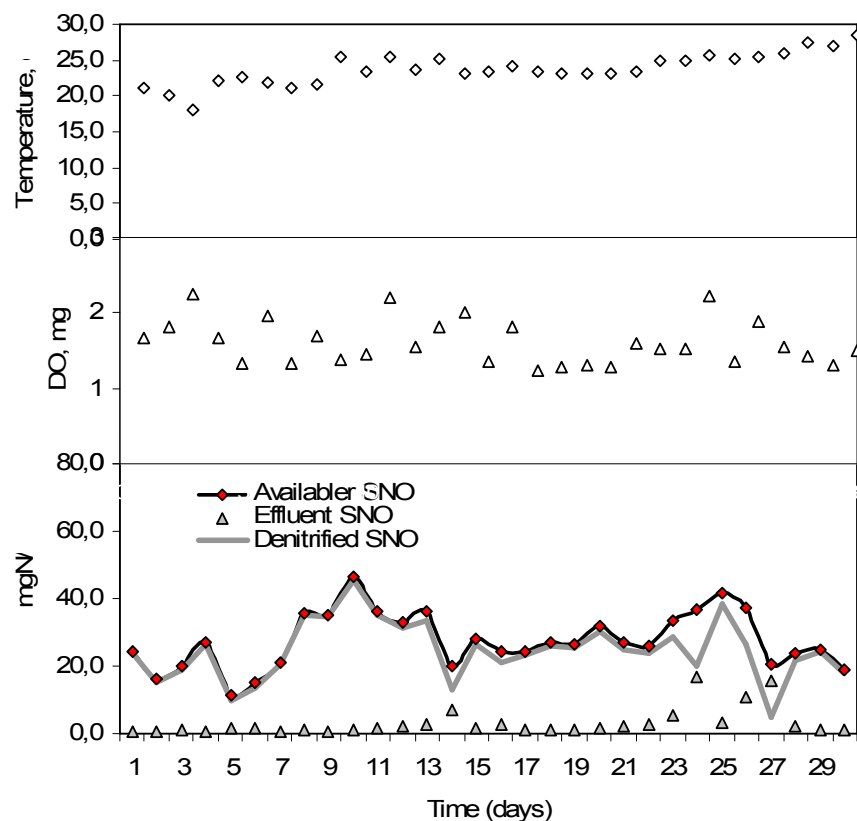


Figure 5.33: N_{OX} vs S_{NO} with respect to dissolved oxygen and COD/TKN ratio

Effect of DO on denitrification and SNdN is more pronounced at DO levels higher than 4 mg/l. Increase in nitrification is also encountered above these levels.

The nitrate formed during nitrification within the MBR tank was completely reduced to N_2 again within the same tank by SNdN. Two important factors should be looked upon for this mechanism, *i.) denitrification was sustained at all DO levels, ii.) reduction of nitrate to N_2 was occurring at COD/TKN levels below 10.* The denitrification occurring at high DO levels can be attributed to the increased oxygen diffusion limitation of autotrophs at higher MLSS, whilst the lesser carbon need for denitrification can be explained by the increased denitrification potential by SNdN as explained previously. Under these circumstances the nitrified S_{NH} converted to S_{NO} was completely denitrified, efficiencies reaching upto %99 (Figure 5.34 and 5.35).

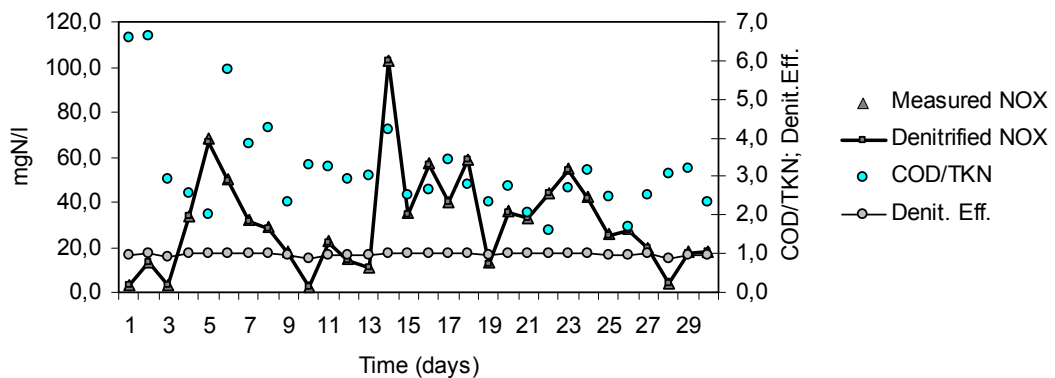


Figure 5.34: Oxidized S_{NH} and denitrified S_{NO}

As it can be seen from the above figure the measured N_{OX} values coincide with the denitrified N_{OX} values meaning the complete reduction of nitrate nitrogenous gas.

Recommended MLSS concentrations for MBRs operated without an anoxic tank to reach the desired effluent TN regulations must be in the range of 15.000-20.000mg/l. Two factors are governing when giving this range, *i.) the MLSS levels that will not inhibit nitrification through mass transfer limitation and provide sufficient ammonia oxidation, ii.) the MLSS levels that will provide the necessary mass transfer limitation for enhanced SNdN for nitrate reduction without the need for a dedicated volume for denitrification.*

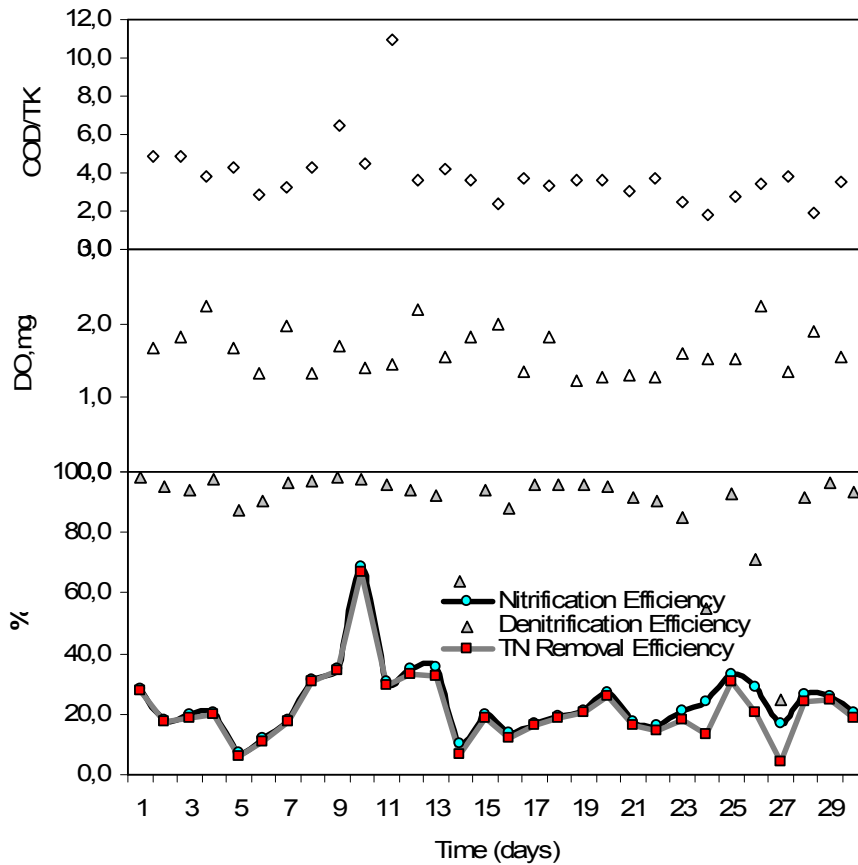


Figure 5.35: Nitrification and denitrification efficiencies

The major finding of Run III was that it would be possible to operate a membrane bioreactor system for total nitrogen removal with a decreased anoxic tank volume (lower V_D/V_T ratio) or no anoxic tank at all. The supporting phenomena behind this postulate is the oxygen diffusion limitation and hence mass transfer limitation caused by high MLSS. This causes changes in the inside morphology of the flocs forming anoxic zones which gets dominant and increases during lower DO levels which in turn increases the denitrification potential with respect to varying DO levels. In other words, in membrane bioreactor systems the simultaneous nitrification-denitrification process enables the use of overall N_{DP} for nitrogen removal. The controlling parameter is S_O rather than V_D/V_T in conventional activated sludge systems. Consequently, for a domestic sewage carrying typical amount of nitrogenous material it would be able to achieve an effluent TN limitation of 10-15 mg/l (dependant on the incoming raw TKN) by a membrane bioreactor system with low V_D/V_T or no anoxic volume at all. All in all, Run III serves as a justification for the phenomena of achieving total nitrogen removal in a membrane bioreactor system without an anoxic tank.

5.8 Physical Modelling Results

The pilot membrane bioreactor had a troublefree operation throughout the study in terms of physical operational parameters. The in-situ chemical cleaning was carried out only once after 287 days of continuous operation where the membrane supplier recommends chemical cleaning 6 months after startup and to be carried out twice a year. However there was an initial membrane fouling on the 43rd day of the operation due to a breakage in the air pipe that provided the necessary air scouring. The breakage was detected after the membrane was fouled and the tank was emptied, therefore this membrane fouling incident was logged to be a result of mechanical failure. The cleaning process occurred in-situ without removal of the membrane module with approximately %10-12 sodium hypochloride solution with a contact time of 2 hours with the modules. The operation was interrupted for the cleaning process and the cleaning agent was filled by gravity through the permeate side of the module. After a reaction time of three hours the switched to regular operation again. The plate modules were not cleaned mechanically from the outside.

The pilot membrane bioreactor was operated in a “constant flux” mode where the transmembrane pressure increased with time upto a point where membrane fouling occurred. No backwashing nor backpulsing were conducted throughout the study on a daily basis. The flux rate set for the entire duration of the study was $0.5\text{m}^3/\text{m}^2\text{-day}$ ($20.8\text{lt}/\text{m}^2\text{-h}$). The most important aspect to be pointed out is that the operational sequence of the membrane module was different from the recommended or previously done studies for flatsheet membranes. Howell et.al (2004) employed intermittent permeation to control fouling by periodically interrupting the permeate flow between 15 sec and 4 min for every 10 min. Gnder (2001) operated plate membranes with 8min filtration and 2 min relaxation mode where no permeate was extracted.

The pilot plant in this study was operated on a constant 12 h permeation and 10min relaxation with air scouring in a 24 h period. No considerable TMP increase nor irreversible fouling were observed between these relaxation periods. Permeate flow was extracted from the membrane module by hydrostatic pressure of 1m above the top level of the module. Suction pump was not used for this purpose. The level above the membrane module was kept constant by automatic level controlling and the hydrostatic pressure was continuously monitored.

Churchouse (2002) reported that it was possible to operate membrane plants with low biomass concentration for periods of 2 h with no observable increase in TMP where fluxes were low and aeration rates were adequate. The crossflow velocity and the air scouring rate are the two major parameters that have direct effect on the operational mode and membrane fouling. The necessary air to create the crossflow velocity was introduced into the membrane bioreactor through a coarse bubble diffuser system rather than a fine bubble system. It can be stated that a high and prolonged operation may be achieved by using a high aeration rate to generate a high crossflow velocity to minimize fouling. It must be noted that the specific crossflow aeration for the pilot plant was $1 \text{ m}^3 \text{air/m}^2 \text{ membrane-h}$ where Gnder (2001) reported crossflow aeration rates in the range of $0.5\text{-}0.75 \text{ m}^3/\text{m}^2 \text{ membrane-h}$ for submerged plate modules. The 10 min relaxation with high air scouring had a considerable effect on removing the cake layer formed on the surface of the membrane where uncontrollable build up of this cake layer results in fouling. The phenomena of fouling and cake layer formation are illustrated in Figure 5.36 (Wintgens et al., 2003).

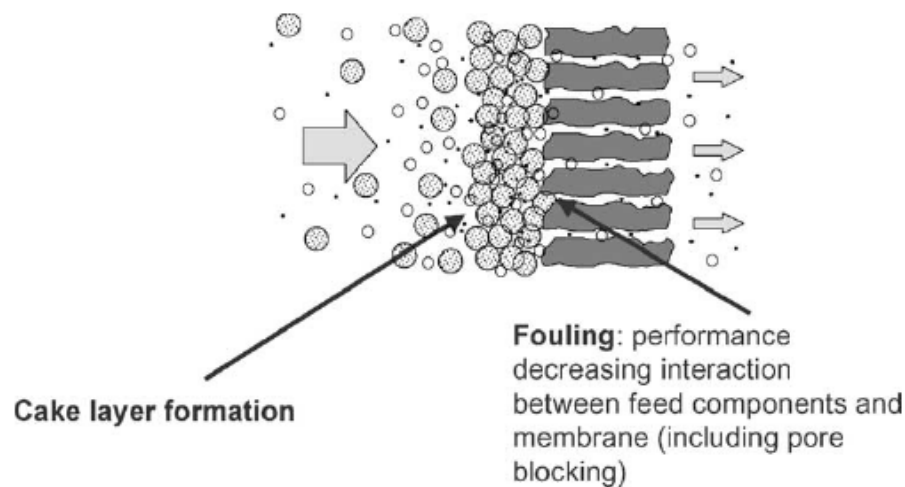


Figure 5.36: Phenomena limiting flux performance in membrane filtration (Wintgens et al., 2003)

The variation of longterm transmembrane pressure and flux values for the pilot membrane bioreactor are given in Figure 5.37.

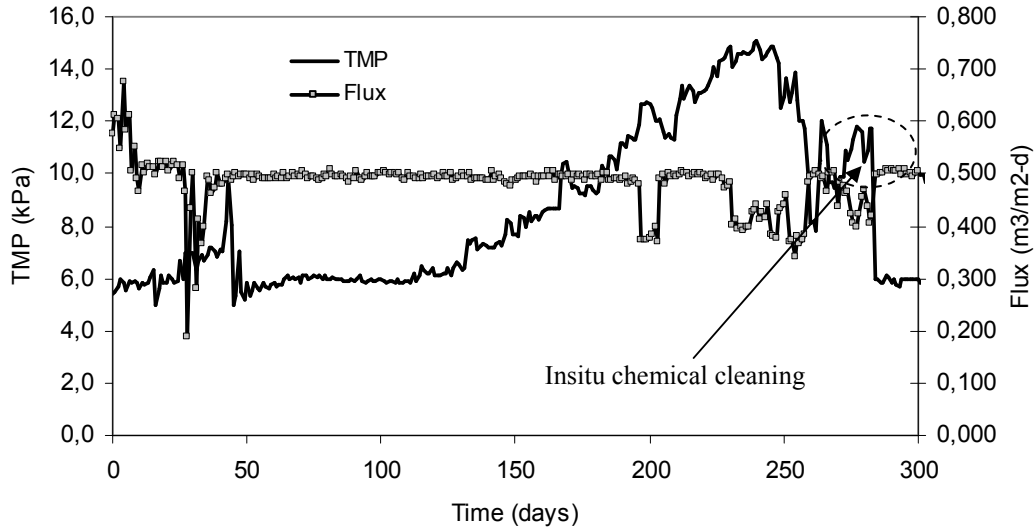


Figure 5.37: Variation of longterm TMP and flux values

Due to the operation mode the flux was constant throughout the study except for the 43rd day and the 250th day where the TMP increase caused the permeation flow to decrease and the membranes had to be chemically cleaned. As explained above, the first incident was due to a mechanical failure. The TMP had a mild linear increase between days 0-43 and 50-240 where the increase was very steep. This was linked to the increase of the cake layer on the surface of the membrane due to the constant decrease in temperature. The pilot plant was dynamically modelled and simulated for the longterm operation according to the resistance model. The model was used to calibrate the physical properties of the membrane to match the measured values of flux, TMP and hydraulic permeability. The model simulated flux mimicked the measured data which is illustrated in Figure 5.38.

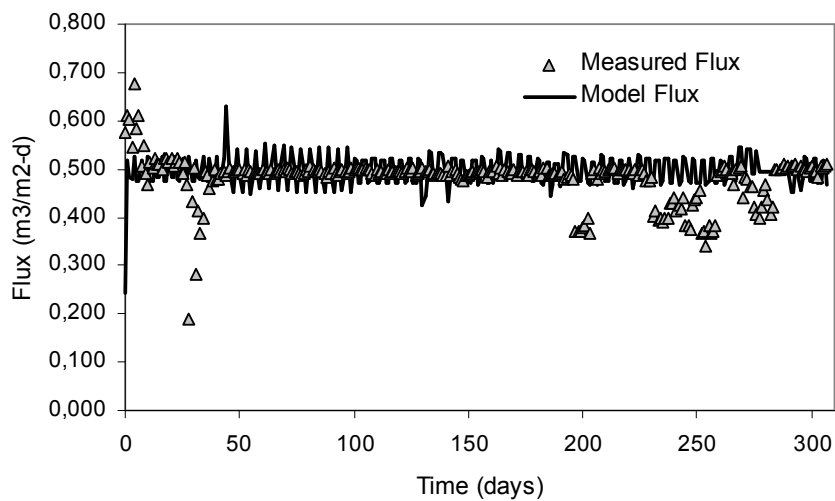


Figure 5.38: Longterm simulated vs measured flux values

The membrane model used in GPS-X enabled two different types of membrane operation; *i.) Constant flux, varying TMP, ii.) Constant TMP, varying permeate* and hence flux. The pilot plant was configured and modelled according to the latter operation mode and it characterized the physical parameters efficiently. As it can be seen from Figure 5.38, the model could not characterize the decrease in flux for the membrane fouling caused by mechanical failure on the 43rd day of operation. The spikes for the flux values for model results is related to the 12 hour filtration and 10 min relaxation over a 24 hour period whereas the measured flux values are based on daily averages derived from two readings a day.

The system had a varying hydraulic permeability throughout the study in relation to the transmembrane pressure. The highest permeability recorded was 0.1 m³/m²-d-kPA, where on the other hand the lowest was 0.0344 m³/m²-d-kPa before the chemical cleaning that was conducted on the 250th day (Figure 5.39). There was a mild decrease in the hydraulic permeability between days 50-140 where afterwards the decrease was severe until the 250th day where membrane fouling was reversed with insitu chemical cleaning.

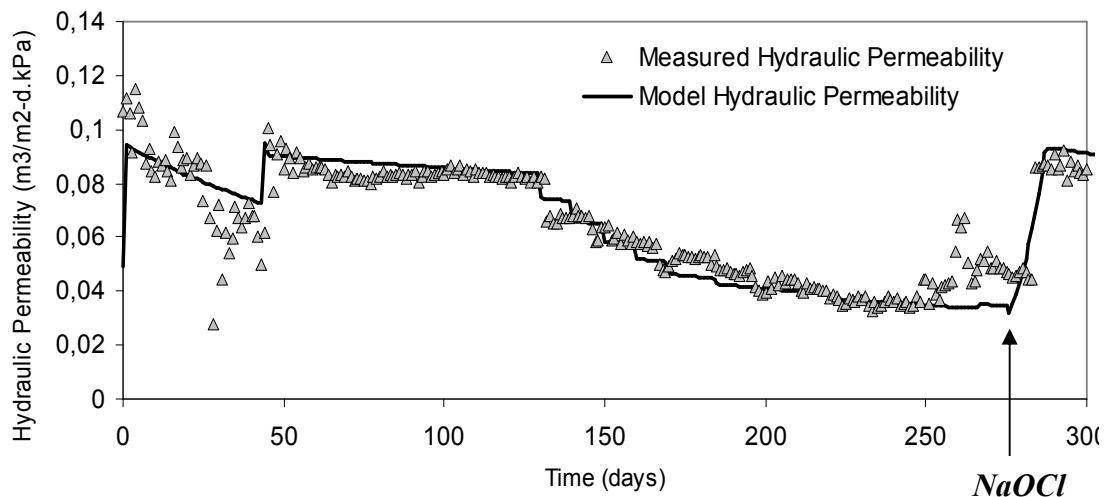


Figure 5.39: Longterm simulated vs measured hydraulic permeability values

Since the permeate flow and flux are constant, hydraulic permeability is inversely proportional to the transmembrane pressure. The buildup of cake layer on the membrane surface in time causes the transmembrane pressure to increase and the hydraulic permeability to decrease. However temperature is an important factor in the fluctuation of these two parameters due to the fact that it was also varying throughout the study. Modelwise it is not possible to distinguish the extent of the impact of

temperature on the TMP and hydraulic permeability. However when the recorded temperature values are superposed into Figure 5.40, it is obvious that temperature has a considerable effect on these two governing parameters.

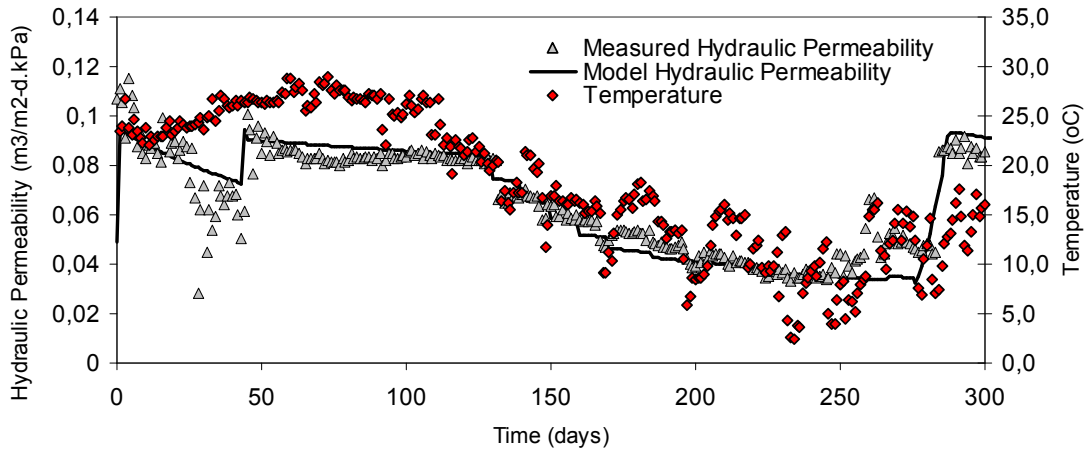


Figure 5.40: Temperature effect on the hydraulic permeability

As it can be seen in Figure 5.40. the decrease in temperature has a direct linear impact on the decrease of hydraulic permability. The impact of temperature is also noticeable for the transmembrane pressure. (Figure 5.41)

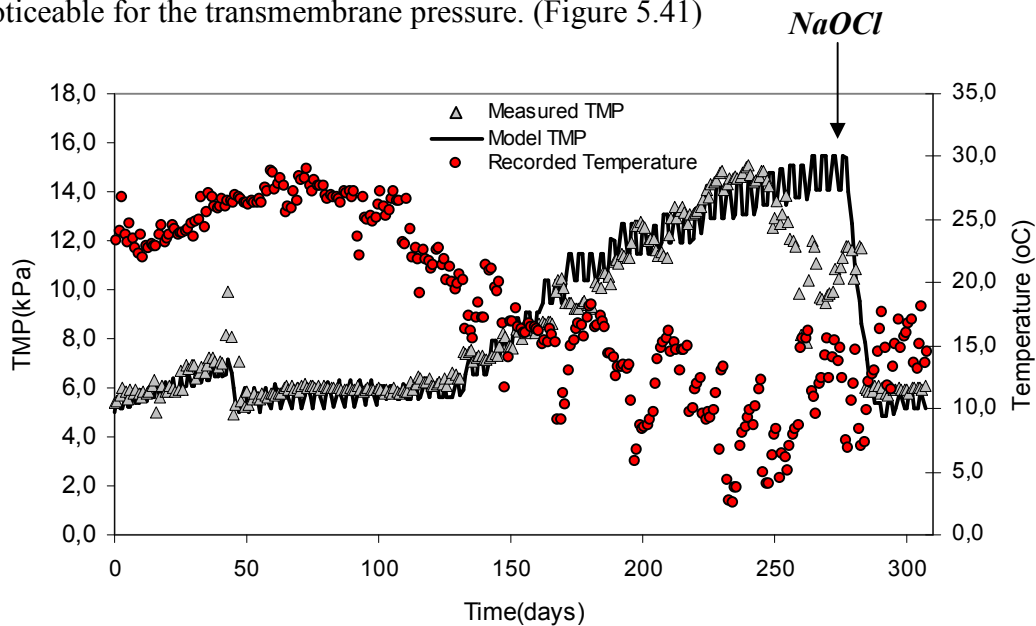


Figure 5.41: Longterm simulated vs measured TMP results with the effect of temperature

The model characterized the TMP of the system very efficiently against recorded data. However it is noteworthy to point out that if the conditions prevailed the same throughout the study and especially for temperature there would have been a linear

increase in the TMP of membranes. However as it can be seen from Figure 5.37, after the 150th day the increase in the TMP is linear, however the slope is linear for small time increments. This can be linked to the impact of temperature on the TMP. Chiemchaisri and Yamamoto (1994) reported an increase of transmembrane pressure from 40 to 85 kPa during a reduction of the temperature from 25 to 5°C. They concluded that a temperature decrease affected the permeate flux not only by increasing the viscosity of the mixed liquor but also by changing the total membrane resistance. It was also noted that less contribution of total membrane resistance was observed at higher temperatures.

Günder (2001) reported that a decrease in temperature from 20 to 10°C causes an increase of viscosity from 1.0 to 1.3 mPa.s and correspondingly a decrease by factor 1/3 in the flux. It was further pointed out that the temperature influence on the membrane surface and cake layer resistance cannot be calculated according to a model. A connection between the temperature dependant behaviour and the membrane resistance cannot be achieved due to the fact that the thickness and composition of the cake layer is dependant on the deposited particles.

The resistance model used and simulated for the pilot plant MBR did not include a varying temperature affect on the flux and TMP and hence the membrane resistance. The model was calibrated to fit the field measured TMP over a period of 310 days by changing the i.) membrane fouling resistance (R_m) and ii.) the fouling rate constant (α) which were the major parameters that played an important role in the cake layer formation and hence fouling.

The simulated cake resistance of the membrane module according to the resistance model is illustrated in Figure 5.42. The cake resistance of the membranes was steady until the 250th day where the membranes were fouled and insitu chemical cleaning had to be done. Following the chemical regeneration there was a sudden decrease in the cake resistance. The membrane resistance (R_m) or in other words called the intrinsic membrane resistance was $9e+11$ 1/m for the membranes used in this study (Figure 5.42).

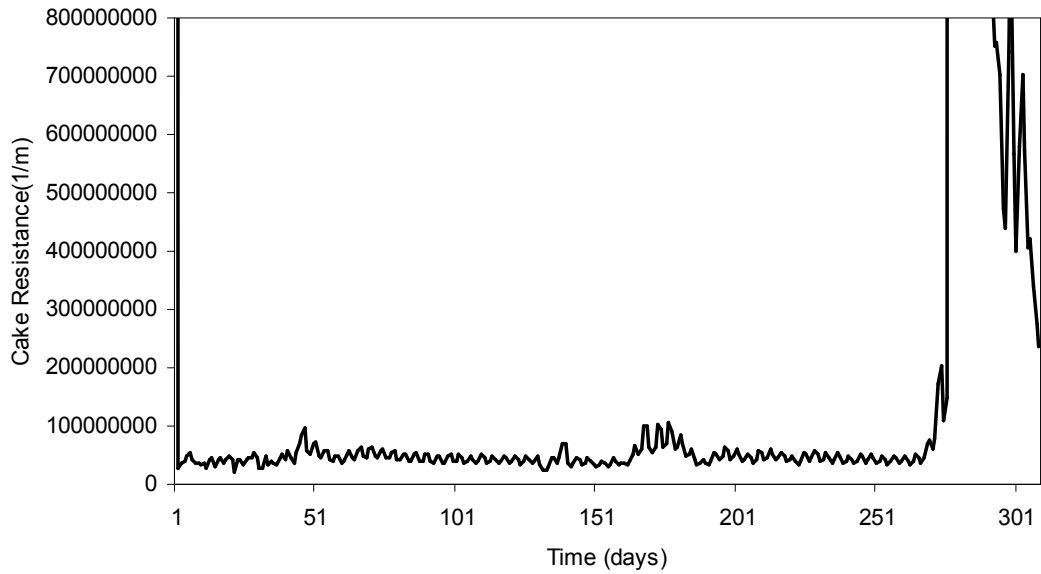


Figure 5.42: Simulated cake resistance

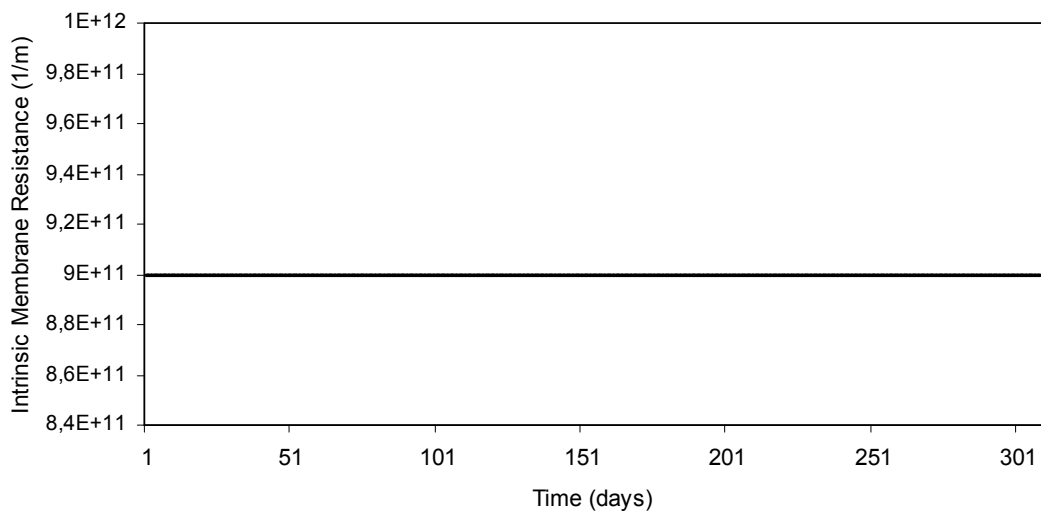


Figure 5.43: Intrinsic membrane resistance

The final factor that contributed to the total resistance was the fouling resistance of the membrane which was the governing and most important resistance parameter in flatsheet membrane bioreactors. The determination of fouling resistance is based on conditions where the cake layer has effectively been removed. The fouling and total membrane resistance of the membrane bioreactor for the longterm dynamic operation are illustrated in Figure 5.44 and 5.45 respectively.

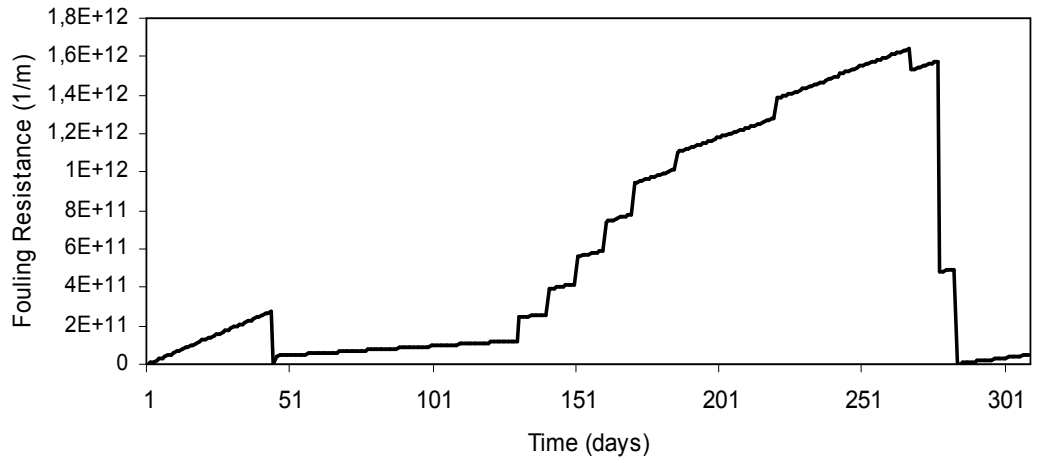


Figure 5.44: Fouling resistance of the membrane bioreactor

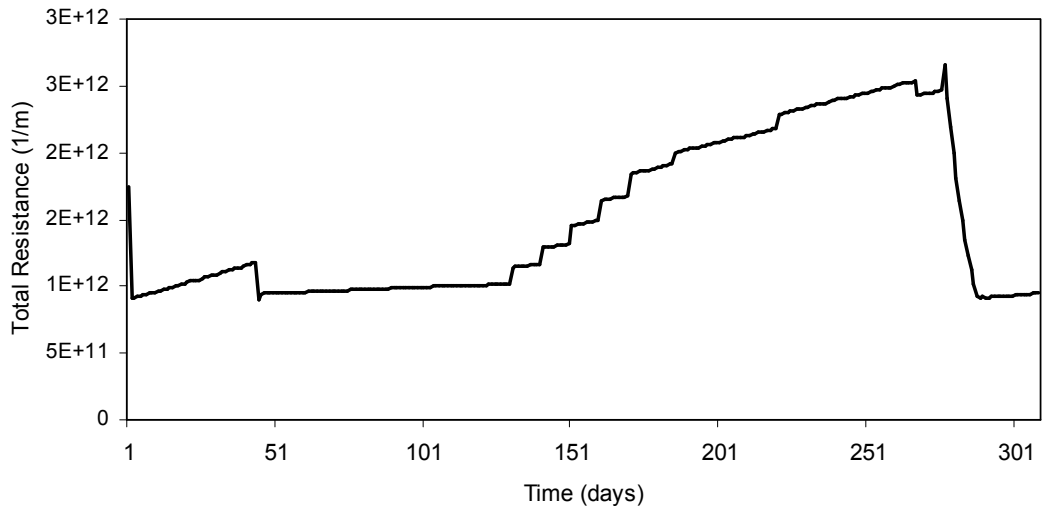


Figure 5.45: Total membrane resistance of the membrane bioreactor

In order to see the affect of each resistance parameter on total resistance, all of the resistance parameters have been superposed in one figure (Figure 5.46).

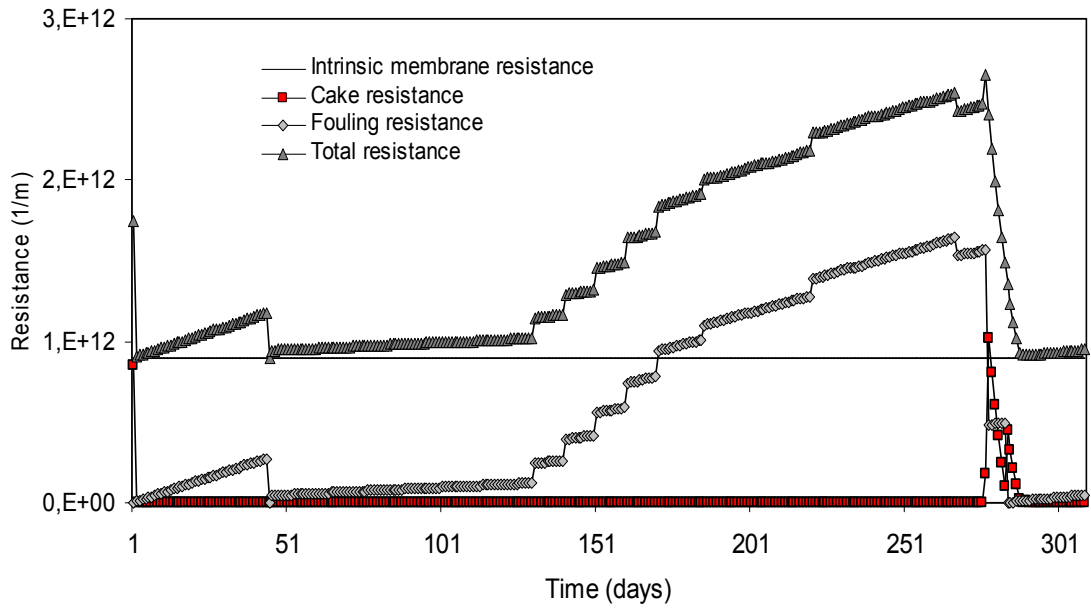


Figure 5.46: Superposed resistance parameters

The calibrated physical parameters of the membrane are given in Table 5.12.

Table 5.12: Summary of calibrated physical model parameters for flatsheet membranes

<i>Parameter</i>	<i>Symbol</i>	<i>Unit</i>	<i>Calibrated Value</i>
Intrinsic Membrane Resistance	R_m	1/m	9e+12
Maximum Fouling Resistance	R_t		
Day 0-45		1/m	6.5e+12
Day 45-130		1/m	7.5e+12
Day 130-283		1/m	9.9e+12
Day 283-310		1/m	3e+12
Fouling rate constant	α	-	
Day 0-45			0.001
Day 45-130			0.00015
Day 130-283			0.0015
Day 283-310			0.0004
Porosity of cake layer	ε	-	0.36
Effective cake particle diameter	d_p	m	0.000001

Due to the effect of temperature on the membrane pores, the maximum fouling resistance and the fouling rate constant had to be calibrated in four time segments.

These segments correspond to especially in parts where there were temperature fluctuations. As seen in Table 5.9 and in Figure 5.46 the peak fouling rate constant and the max fouling resistance were encountered during the third interval between days 130-283. This segments correspond to severe temperature decrease in the wastewater temperature which increases the viscosity and even causes the membrane pores to shrink. The increased fouling resistance in this segment is clearly visible in the steep slope of TMP in Figure 5.41.

The intrinsic membrane resistance was calibrated at $9e+12$ 1/m. This figure is high when compared to the intrinsic membrane resistance of a hollow fiber membrane ($1e+11$ 1/m). Further more the porosity (ϵ) of the cake layer was calibrated at 0.36 where the porosity for the hollow fiber membrane range between 0.14-0.18.

5.9 Microbiological Findings

As part of the research program, the identification and quantification of the nitrifying bacteria present in a pilot-scale membrane bioreactor treating municipal wastewater has been done by using fluorescence in situ hybridization (FISH) as a graduation project. The FISH results given in this study were obtained from the graduation project carried out by Pala (2006).

In the study fluorescent oligonucleotide probes for bacteria and nitrifiers were used to characterize and determine the microbial population diversity of the activated sludge in the MBR pilot plant. Average cell counts were calculated based on 10 random fields of view based on each sample where triplicate sampling was conducted within the membrane bioreactor. Table 5.13. summarizes the cell counts obtained from the FISH technique while Table 5.14 illustrates the relative abundances of phylogenetically defined groups of microorganisms in the eubacterial community.

Table 5.13: Average count of cells per field of view (Pala, 2006)

<i>Probe Name</i>	<i>Non-Filamentous</i>	<i>Filamentous</i>	<i>Total Count</i>
EUBMIX	568 ± 65	111 ± 15	679 ± 63
ALF968	165 ± 4	25 ± 4	190 ± 1
BET42a	165 ± 25	18 ± 3	182 ± 21
GAM42a	176 ± 8	25 ± 2	202 ± 10
HGC69a	299 ± 30	50 ± 4	349 ± 33
NB1000	46 ± 3	6 ± 0	52 ± 3
NEU	57 ± 9	8 ± 1	65 ± 10
NSV443	52 ± 3	7 ± 1	59 ± 2
NON338 ^a	26 ± 3	4 ± 2	30 ± 1
NSM156	111 ± 4	23 ± 1	134 ± 5
NON338 ^b	84	17	101

Table 5.14: Relative abundances of phylogenetically defined groups of microorganisms in the eubacterial community (Pala, 2006)

<i>Target Organism</i>	<i>Relative Abundance of Filamentous Morphology</i>	<i>Relative Abundance of the Microbial Population</i>
Ammonia - oxidizing Alpha-proteobacteria, except Rickettsiales	2.6 ± 0.5 %	19.8 ± 0.1 %
Ammonia - oxidizing Beta-proteobacteria	1.5 ± 0.4 %	18.7 ± 2.6 %
Ammonia - oxidizing Gamma-proteobacteria	2.6 ± 0.3 %	21.5 ± 1.3 %
Actinobacteria (high G+C Gram-positive bacteria)	6.3 ± 0.5 %	43.2 ± 4.4 %
Ammonia - oxidizers Nitrosomonas cluster	-	2.3 ± 0.18 %
Ammonia - oxidizing Halophilic and halotolerant members of the genus Nitrosomonas	-	4.46 ± 0.83 %
Ammonia - oxidizers Nitrospira cluster	-	3.58 ± 0.18 %
Nitrite oxidizing bacteria Nitrobacter spp.	-	2.53 ± 0.2 %

Hiraiwa (2002) compared the microbial community structures of a conventional activated sludge plant with the ones from four different membranes bioreactors. Alpha- and beta-proteobacteria were found to be dominant in the membrane

bioreactor community. On the other hand, in this study, it was reported that G+C gram positive bacteria dominated the membrane bioreactor microbial population. Pala (2006) reported that the members alpha-, beta- and gamma-proteobacterial groups also dominated the microorganisms of the eubacterial community.

Bulking is a very serious problem encountered in conventional activated sludge systems especially in biological nutrient removal plants. Van der Waarde et al. (2002) reported the major cause of bulking to be the excessive growth of filamentous type microorganisms which leads to poor settling and even non-settlement of the activated sludge flocs in conventional systems. Filamentous bulking is not a problem in the membrane bioreactor systems as the solid-liquid phase separation relies on the physical filtration through membrane pores. However, pin-point floc formation is a threat to blockage of the membranes pores which occurs in the absence of filamentous bacteria. This makes the amount of filamentous bacteria somewhat important in membrane bioreactor systems. On the other hand Meng et al. (2005) reported that, excessive growth of filamentous bacteria can be a cause for membrane fouling decreasing the efficiency of membrane filtration. Rosenberger et al. (2000) found that the filamentous microorganisms dominated the bacterial community where they have detected the filamentous colonies through FISH technique. It was found that the detected filamentous microorganisms in the bacterial community belonged to the alpha-, beta-, gamma-proteobacteria and high G+C gram-positive bacteria where the largest fraction of the filamentous microorganisms however belonged to the high G+C gram positive bacteria. Actinobacteria, which is a high G+C gram positive filamentous type bacteria were also reported to be found in large amounts in membrane bioreactors (Hiraiwa, 2002).

The total relative abundance of the bacteria belonging to genus *Nitrosomonas* was found to be 7% of the total bacterial community among the ammonia oxidizing microorganisms. Luxmy et al. (2000) found the relative abundance of the genus *Nitrosomonas* to be 6 % of the total community which coincides with the findings in this study. It can be concluded that, ammonia oxidation is related to the members of the genus *Nitrosomonas* rather than the members of *Nitrospira* due to the relative high abundance in the total bacterial community within the membrane bioreactor system. The relative abundance of the specific microbial populations and filamentous morphotypes are shown in Figure 5.47.

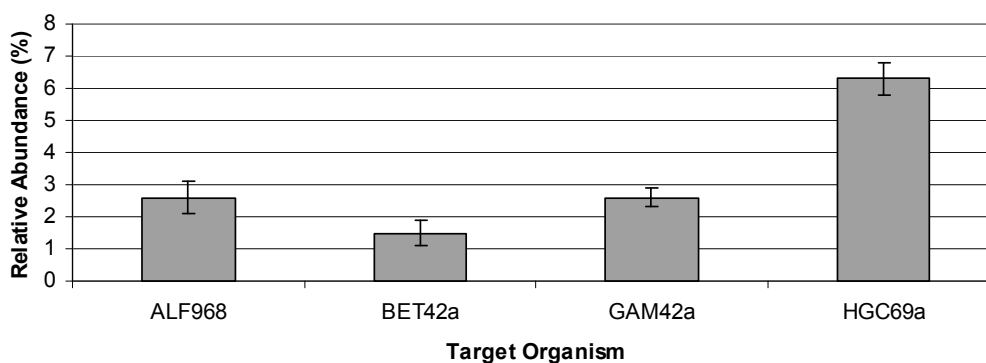


Figure 5.47: Relative abundance of filamentous morphotypes (Pala, 2006)

It was reported that, extremely high sludge ages in the range of 135 to 413 days brings out the difficulty of maintaining a nitrifier dominant population in the membrane bioreactor as the relative abundance of the total nitrifying community decreases with increasing sludge age. However in this study, the total sludge age was 38 days and the relative of the nitrifying bacteria in the total bacterial community was 13%. Li et al. (2005) reported that it would be possible to maintain high amounts of nitrifying bacteria in the membrane bioreactor since the sludge age was not so high. Characteristics of the incoming raw sewage may also be a factor on the high relative abundance of nitrifying bacteria in the total bacterial population. Growth of floc formers and hence heterotrophic bacteria may have been limited by the low strength influent stream and the high sludge residence time. Nitrifying bacteria can be abundant due to the high endogenous decay rates of the heterotrophic microorganisms in membranes bioreactors which relatively operate at higher sludge ages with respect to conventional activated sludge systems (Pala, 2006).

Bright signals can be received during *in situ* hybridization from the nitrifying bacteria which are not active because of their ability to preserve their rRNA content in the cell (Wagner et al., 2003). It has also been reported that some portion of the high abundant nitrifying microorganisms in the membrane bioreactor bacterial community are inactive.

Relative abundances of specific microbial populations are shown in Figure 5.48.

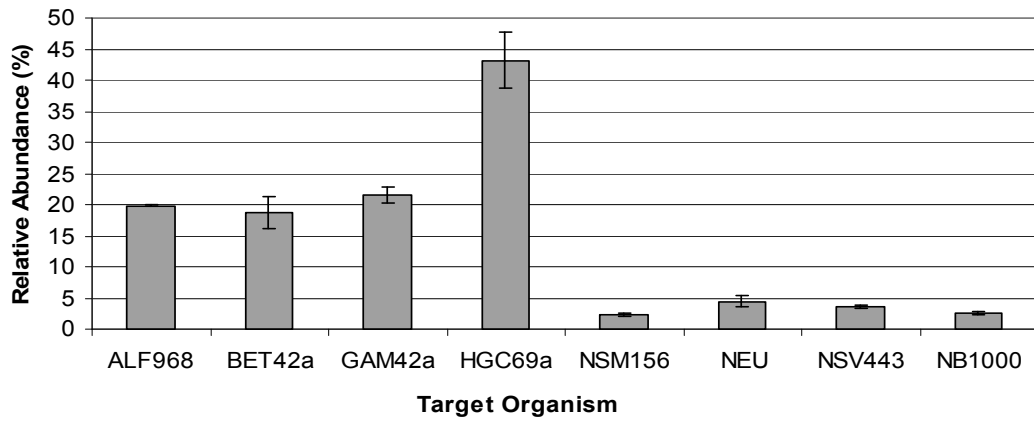


Figure 5.48: Relative abundance of the microbial population (Pala, 2006)

Figures 5.49 through 5.53 show epifluorescence examples of the hybridized MBR sludge samples.

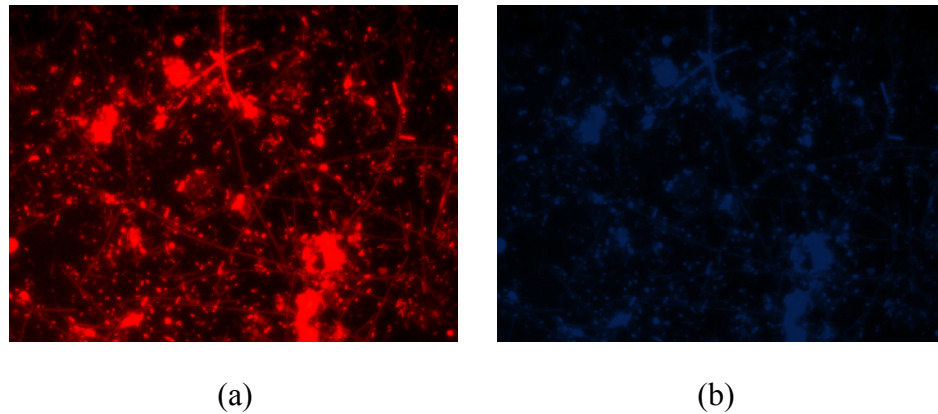


Figure 5.49: Cells detected with EUBMIX probe (a) Hybridized cells (b) DAPI-stained cells (Pala, 2006)

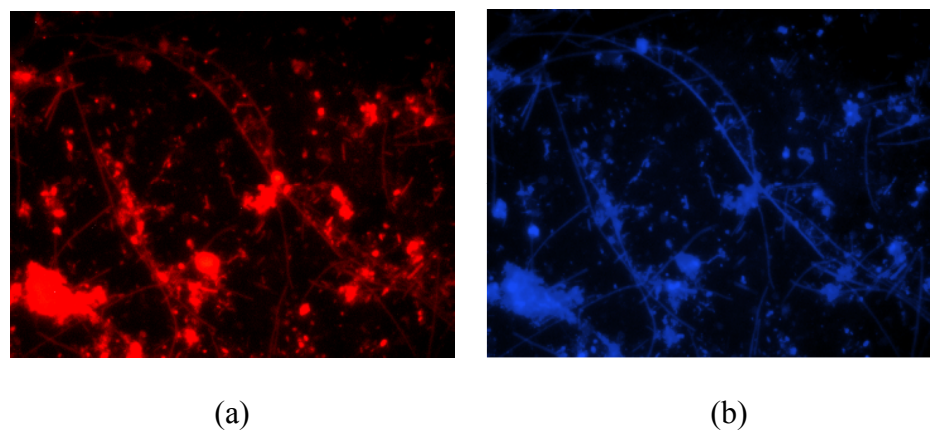


Figure 5.50: Cells detected with ALF968 probe (a) Hybridized cells (b) DAPI-stained cells (Pala, 2006)

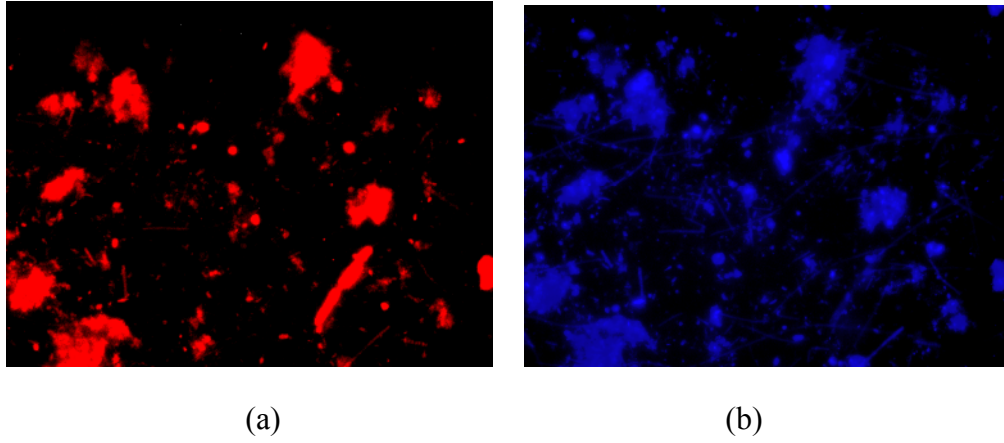


Figure 5.51: Cells detected with NB1000 probe (a) Hybridized cells (b) DAPI-stained cells (Pala, 2006)

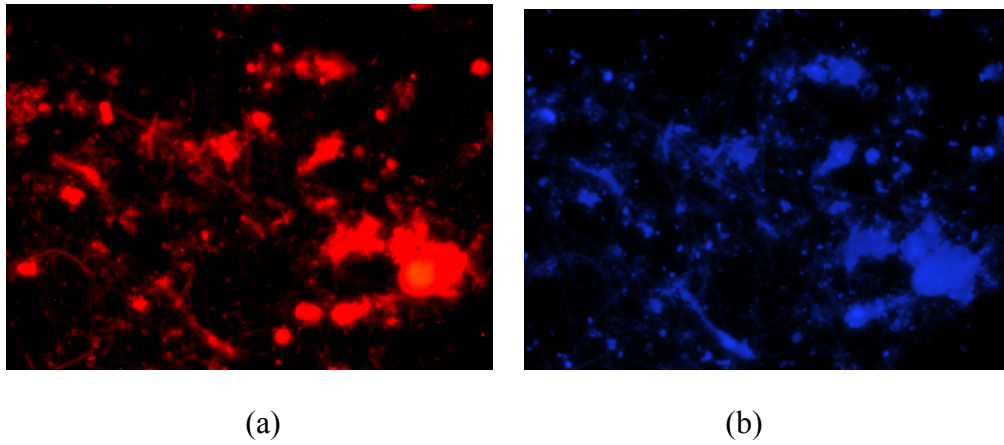


Figure 5.52: Cells detected with BET42a probe (a) Hybridized cells (b) DAPI-stained cells (Pala, 2006)

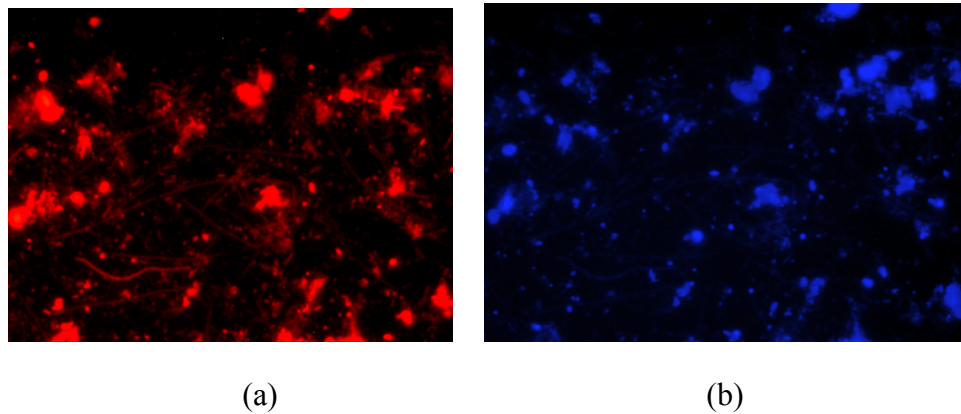


Figure 5.53: Cells detected with GAM42a probe (a) Hybridized cells (b) DAPI-stained cells (Pala, 2006)

6 DISCUSSION AND CONCLUSIONS

6.1 Evaluation of Results

The conclusions of the study can be summarized in three groups. *i.) Biological modelling, ii.) Physical modelling and iii.) Microbiological findings and conclusions.*

6.1.1 Biological modelling and validation

Based on this research it was concluded that the stoichiometric basis of the new adopted model for the MBR based on endogenous decay is reliable. The high accuracy of the nitrification and denitrification kinetics and stoichiometry were largely owed to the adopted modelling approach which included two additional processes and the concept of oxygen diffusion limitation. The impact of diffusion through biomass which obviously exerts a significant effect on system performance and denitrification is evaluated with success using the adopted model by means of switch functions that regulate nitrification-denitrification with respect to dissolved oxygen concentration in the bulk liquid. It is concluded that the high concentration of biomass results in a shift from an aerobic floc to an anoxic/aerobic floc where the substantial anoxic mass fraction exists in the center of the biomass flocs resulting in an oxygen diffusion limitation into the cell from the bulk liquid. In previous researches the diffusivity was explained by biofilm kinetics with diffusive links in the boundary layer. However these were lacking in the explanation of the biological reactions taking place in the bulk liquid. Rather, the main focus was on the biofilm formed on the surface of the membrane. Semmens and Shannan (2005) proposed a biofilm model focusing only on the biological conversions taking place in the film layer and assuming that no reaction is taking place in the bulk liquid.

In this study, the half saturation constant of oxygen for heterotrophs and autotrophs and the half saturation constant for ammonia nitrogen and nitrate nitrogen were successfully calibrated in explaining the level of simultaneous nitrification and denitrification occurring in the bulk liquid of a pilot scale membrane bioreactor. The

resultant half saturation constants were much higher than the ones used for the conventional activated sludge models. Higher half saturation constants correspond to lower diffusivity. The level of SNdN occurring in the membrane bioreactor suggests that this level of diffusion limitation is so high that it is even causing the anoxic fraction of biomass inside the floc to be dominant during high dissolved oxygen levels. During high dissolved oxygen levels, this fraction of biomass shifts from being anoxic to aerobic decreasing the level of SNdN.

It can be concluded that the factors and parameters triggering SNdN in MBR can be listed as *i.) dissolved oxygen concentration, ii.) floc size, iii.) MLSS concentration of the bulk liquid* which the latter two severely affects diffusion limitation of oxygen from the bulk liquid into the floc. MLSS concentration of the bulk liquid is interrelated with the sludge age of the system which is thought to have a direct effect on the culture and morphology of the bacteria in a membrane bioreactor system and thus SNdN.

The evaluation of simulations and measured data reveal that diffusion limitation of substrate and oxygen from the bulk liquid into the bacterial floc is the key for a better understanding of the processes in a MBR. The highly concentrated MLSS, enriched with medium to large sized flocs decrease the diffusion of oxygen into the cell thereby resulting in an anoxic mass fraction triggering simultaneous nitrification and denitrification. The level of SNdN occurring in the aerated MBR reactor fluctuates according to the oxygen level within the bulk liquid where low DO levels in the range of 0.3-0.6 mg/l increases the denitrification potential dramatically triggering up to more than 30 mg/l of nitrate uptake within the MBR, whilst DO levels in the range of 1.5-3.5 mg/l reduces the nitrate uptake to levels in between 10-20 mg/l. It can be concluded that a minimum of 10-15 mg/l of nitrate will be removed simultaneously in a MBR with DO levels in the range of 1.5-2.5 mg/l. In light of the stoichiometry of denitrification, it can be also concluded that anoxic decay of heterotrophs and autotrophs significantly contribute to the SNdN occurring in the MBR verifying that these systems are decay dominant. Cyclic anoxic/aerobic sequences are not necessary to achieve SNdN in MBRs.

There exists a balance point between the level of nitrification and denitrification with respect to the level of oxygen in the MBR reactor, when if controlled, effluent TN limits less than 15 mg/l can easily be achieved by operating a MBR continuously at

DO levels in the range of 0.3-0.8 mg/l and V_D/V_T ratios as low as 0.10. The MBR systems can be designed on having low anoxic volumes or no anoxic reactor at all dependant on the level of effluent nitrogen limits required. This would mean economical savings on the investment of MBR systems by avoiding tanks, equipments and instruments making these systems more competitive against conventional activated sludge systems. Further research has to be conducted for simultaneous nitrification-denitrification performance of MBR systems without an anoxic tank.

A stepwise long term dynamic calibration methodology was developed by initial introduction of three iterative steps in the order of VSS, TSS, $\text{NH}_4^+\text{-N}$, O_2 and $\text{NO}_3^-\text{-N}$ profiles respectively. The calibration parameters were chosen from the processes that had a considerable impact on the solids balance and simultaneous nitrification-denitrification. Following the successful calibration for the longterm dynamic conditions, the calibrated model was compared to the results of the mass balance derived stoichiometric equations for pseudo-steady state conditions. The results of the model and the stoichiometric equations validated and verified the correctness of the calibrated parameters for the pseudo-steady state conditions. This resulted in a better definition of the model certainty which in turn increased the model applicability and thereby reliability. It can be concluded that the switch functions which regulated the diffusivity of oxygen and other substrates cannot set apart in mass balances for the derivation of stoichiometric equations which is normally done in the activated sludge models for conventional systems. In conventional activated sludge systems the biological reactor's operational parameter set the reactions occurring in the system. For example, denitrification will be occurring only in a reactor where no oxygen is supplied and it will cease in an aerobic reactor in which the switch functions are often neglected. However such discrimination can never be made in pilot or even a full scale membrane bioreactor system due to the impact of diffusion and hence dissolved oxygen and temperature. Therefore special care must be given when conducting mass balance in a MBR.

The model sensitivity results revealed that every parameter had its impact on the relevant process. For example the half saturation constant of heterotrophs for oxygen had a considerable affect on denitrification whereas the decay coefficients had an impact on the solids balance sensitivity of the model. Naturally the influent and

operational parameters also had a high impact on the sensitivity of the model. In practice however, these data often contain errors. After a proper data evaluation and error correction the models can be simulated for full scale MBRs even without further calibration. It is therefore concluded that evaluation of operational data is very important and if it cannot be properly determined, calibration of these data for full scale MBRs should be considered in favor of calibration of the model parameters. The simultaneous nitrification and denitrification was also very sensitive to the η_D factor which governed the degree of denitrification occurring during anoxic decay of heterotrophs and autotrophs.

The average COD removal efficiency of the pilot scale membrane bioreactor was 95% reaching up to a max of 99% and the effluent COD did not get effected by the fluctuations encountered in the influent. Biodegradable COD was completely oxidized leaving only the inert COD of influent origin and soluble inert microbial products in the effluent. Slowly biodegradable COD of particulate and colloidal nature did not account to the effluent COD as these two fractions were also completely oxidized. The major advantage of the MBRs was that there was no COD contribution to the effluent related to the effluent suspended solids. The suspended solids in the effluent was not detectable throughout the study. The model mimicked the effluent COD efficiently against the measured data. The effluent BOD concentration was in the range of 1-5 mg/l sometimes being not detectable.

The performance of the MBR plants in municipal wastewater treatment can be defined as secure and reliable. The MLSS in the MBR tank can be adjusted to almost every desired value. However with very high MLSS values exceeding 25,000 mg/l, severe reduced oxygen transfer must be taken into account. Previous researches recommended α factors of less than 0.5 with MLSS of 10g/l and 0.2 for MLSS values of 20 gr/l. This oxygen transfer model used in this study was calibrated at α factor of 0.4 with MLSS values in the range of 14-16 gr/l. Connections between oxygen transfer to the activated sludge and MLSS can be shown on the basis of rheological qualities of the sludge at high solids concentration. It can be concluded that the oxygen transfer will considerably decrease in a MBR system with increasing MLSS values. However further research has to be conducted for the affect of α on oxygen transfer and energy consumption for increased MLSS values. It was found

this study that the design and operational MLSS should be limited to a maximum of 15-17 gr/lit in membrane bioreactor systems.

The practical conversion to the membrane bioreactor process in domestic sewage treatment depends on a variety of limiting conditions. Because of the high performance of the membrane bioreactor systems by membrane filtration, the application is suitable for where high requirements of effluent quality are needed. One of the major advantages of MBRs is that, running with long sludge ages lead to endogenous respiration within the biomass and therefore result reduced sludge production. Long SRTs also lead to the growth of specialized bacteria e.g. nitrifiers and enhance breakdown of large macromolecules. Organic loading rates are restricted by the flux but are always considerably higher than conventional activated sludge plants with higher carbon and nitrogen removal rates. Significant bacteria and virus rejection is accomplished with MF and UF membranes. Rejection with microfiltration membranes is enhanced by the build-up of a dynamic layer as well as high turbidity.

The mass transfer limitation hence substrate and oxygen diffusion limitation are severely affected by the concentration of microorganisms within the membrane bioreactor system. As mentioned above, this limitation is successfully explained through assignment of the specifically calibrated and validated oxygen and substrate half saturation concentrations within the switching functions. However it was also found that the oxygen half saturation constant for heterotrophs and autotrophs can only be validated for a certain MLSS concentration and as the biomass concentration increases the half saturation concentration of oxygen for both species also increase. The oxygen diffusion limitation for autotrophs are much more prone to increasing biomass concentration within the system. There exists an exponential relation between the biomass concentration and the K_{OA} , K_{OH} which can be fitted to show the trend however an exact equation for this relation cannot be given due to the reason that it was not possible to operate the MBR pilot plant with MLSS concentrations over 30,000 mg/lit to obtain the data and perform the model calibration at these levels.

Due to the excessive and abundant population of filamentous type microorganisms in MBRs, further focus and research should be given to filamentous growth kinetics.

As previously stated, the role of the anoxic tank within the MBR system was disputed in terms of its impact on denitrification. According to the results obtained in Run I, anoxic tank had minor effect on the overall denitrification of the system which led to the result of that MBR systems can be operated with lower V_D/V_T ratios or no anoxic volume at all for total nitrogen removal. In order to prove this Run III was conducted without the anoxic tank being in operation. It was found that 30-40 mg/l oxidized ammonia nitrogen which is equal to nitrate nitrogen was reduced to nitrogen gas through simultaneous nitrification and denitrification (SNdN) in a single MBR tank where nitrification also took place. This was explained by the increased denitrification potential of the system due to the oxygen diffusion limitation of the autotrophs at high MLSS concentrations. The increased denitrification potential was capable of denitrifying the produced nitrates of 30-40 mg/l even at lower COD/TKN ratios (<10) and relatively high DO levels for SNdN to take place. It can be concluded that for a domestic sewage carrying typical amount of nitrogenous material it would be able to achieve an effluent TN limitation of 10-15 mg/l (dependant on the incoming raw TKN) by a membrane bioreactor system with low V_D/V_T or no anoxic volume at all. The actual size of the anoxic tank or the ratio can be found by applying the new stoichiometric denitrification potential equation given in the previous chapters which is dependant on the operating DO.

6.1.2 Physical modelling

The pilot scale membrane bioreactor system was operated in a different membrane operational mode when compared to previous studies and the recommendation of the supplier. Furthermore no suction was conducted for the permeate. Continuous membrane filtration for 12 h and a 10 min relaxation with air scouring (no filtration) was the conducted operational sequence throughout the study. The physical model Previous studies implemented 8 min filtration and 2 min relaxation in a 10min period which was totally different compared to this study. The physical model setup using the in series resistance model was also done according to this sequence. According to the field and modelling results it can be concluded that the system was successfully operated with the adopted operational sequence without any fouling for 285 days of continuous operation. This is linked to the type of aeration system (coarse bubble) used to create the necessary crossflow velocity to remove the cake layer from the membrane surface.

It is very well known that coarse bubble aeration system gives more turbulence and it can be stated it is less dependant of the α value and MLSS when compared to fine bubble diffuser systems. This verifies the fact that the model has been calibrated at a higher α value for MLSS in the range of 14-16 mg/l when compared to Gnder (2001) findings. The less dependancy of this type of aeration system on α and MLSS is most probably caused by the lower viscosity as a result of much higher turbulence. The effect of 10 min relaxation with increased air scouring had a severe affect on the removal of the cake layer with high turbulence and this even continued during the continuous 12 h filtration period. This can be verified by the non-existence of sudden or linear increase in the TMP and hence decrease in the hydraulic permeability.

The major disadvantage of coarse bubble aeration used for crossflow velocity is the high energy demand. The specific air flow rate for the crossflow aeration used in this study was 6.6 m³/m³-h where in previous studies 3 m³/m³-h of specific air flow has been reported for fine bubble diffused air systems. However according to the findings in this study, it can be stated it will not be possible to operate flatsheet membrane bioreactos with a prolonged filtration mode because the fine bubble diffused aeration system will not be able to create the necessary turbulence and decrease the viscosity. Irreversible fouling will be inevitable and linear increase in TMP will be observed. Temperature increase has also a negative affect of oxygen transfer efficiency due to decreased oxygen solubility. Therefore, necessary provisions should be included when designing MBRs with coarse bubble aeration especially during summer times. It has been experienced that during summer times, the air introduced to create crossflow velocity for air scouring is not sufficient to provide the oxygen for biochemical reactions.

It can be concluded that temperature has a detrimental affect on the physical properties of the membrane and hence filtration. Temperature decrease increase viscosity and probably has a shrinkage affect on the membrane pores which immediately and severely increases the TMP and decreases the hydraulic permeability. Modelwise this cannot be explained by a modification to be implemented in the in series resistance model. The explanation cannot go further beyond the derivation of an empirical formula taking into consideration the specific physical characteristics of the membrane in question. Therefore it is recommended

that further research be conducted on the affect of temperature on membrane filtration.

The effect of temperature on TMP and hydraulic permeability in this study were explained by calibrating the maximum fouling resistance (R_t) and fouling rate constant (α) parameters to fit the measured data. Without the affect of temperature the increase in TMP would have been linear, however the TMP increase was exponential during low temperatures. It was found that fouling and intrinsic membrane resistance were the major parameters contributing to total resistance whereas cake resistance had minor affect.

Membrane material needs to be hydrophilic to some degree to reduce fouling especially by proteins and bacteria. Hydrophobic materials lead to increases in TMP or decreases in flux and hydraulic permeability which in turn lead to increases in energy and cleaning costs to overcome membrane fouling.

Fouling is inevitable in a membrane bioreactor system whether it is based on hollow fiber technology or flatsheet membrane technology. Irreversible fouling requires chemical cleaning. At this point flatsheet membranes offers the advantage of in situ chemical cleaning without the need for emptying the basin or taking out the modules and dipping them into a chemical tank and hence without interrupting the operation of the plant. 10-12% sodium hypochloride solution along with 0.5-1.0% oxalic acid solution must be used. However if the membrane surface is occupied with Ca deposits citric acid must be used rather than oxalic acid.

Furthermore, a very well and efficient operating primary treatment is a must upstream of the membrane bioreactor system. 0.75-1 mm screening along with grit and grease removal will have a positive affect in the reduction of the irreversible fouling casued by inorganic solids and grease. Therefore special care must be given when designing primary treatment for a membrane bioreactor system. The physical properties of the membrane to be used must be very well known. A buffer tank in front of the membrane bioreactor system will be helpful in avoiding the raw wastewater not to get in direct contact with the membranes.

6.1.3 Microbiological findings

Nitrification can be sustained by the maintenance of nitrifying bacteria within the activated sludge which is very important in terms of nutrient removal. Membrane bioreactors enable high sludge retention times with respect to conventional activated sludge systems through the incorporation of membranes into the activated sludge systems. Consequently, high ammonia removal efficiencies can be achieved by the high number of nitrifying bacteria kept within the total bacteria community. High biomass concentration as a result of high sludge ages in a membrane bioreactor also enhances the carbon removal efficiency.

The existence and excessive growth of filamentous microorganisms may cause settling, foaming, bulking and EPS problems in conventional activated sludge systems. However membrane bioreactor systems are free of such settling problems mentioned above due to the physical separation technique by membranes. On the other hand excessive growth of filamentous microorganisms can also result in poor filtration that increases the transmembrane pressure and deteriorates the effluent quality. It was seen that the high amount of filamentous microorganisms in the pilot membrane bioreactor operated at a sludge age of 38 days and MLSS concentration of 13,000-16,000 mg/l did not have any adverse effect on the filterability of the activated sludge and the transmembrane pressure, hence no irreversible fouling incident linked with these type of organisms has occurred.

Nitrification has found to be very robust and more efficient with respect to external factors such as temperature, DO, alkalinity and pH in membrane bioreactors when compared to the conventional activated sludge systems. Complete nitrification was achieved in this study with an average of 96% COD removal.

Different populations in natural and engineered systems can be determined using the FISH technique without cultivation from the natural environment, hence quantitative data can be obtained as a result of homogenization. Quantification of nitrifying bacteria in the pilot membrane bioreactor was achieved as part of the research. It was found that the relative abundance of the nitrifying bacteria in the total bacterial population was 13%. Previous researches have reported lower relative abundance values due to the very high sludge ages of the membrane bioreactors studied.

6.2 Conclusions and Recommendations

The conclusions and recommendations of this research can be summarized as;

1. Total nitrogen removal can be achieved with lower V_D/V_T ratios or no anoxic volume at all when compared to conventional activated sludge systems.
2. Full nitrification is sustainable at temperatures as low as 8°C due to the very high sludge age.
3. The controlling parameter for the denitrification in a membrane bioreactor system is dissolved oxygen rather than V_D/V_T .
4. Effluent TN regulations of 15 mg/lit can be achieved with MBRs operated without an anoxic tank for domestic sewage provided that MLSS levels and SNdN performance are kept under control through instrumental observation.
5. For efficient and desired level of TN removal performance in MBRs operated without an anoxic tank MLSS values should be in the range of 15.000-20000 mg/lit. MLSS values higher than 20.000 mg/lit will have adverse effect on nitrification thereby reducing the TN removal efficiency.
6. Mass transfer limitation and hence oxygen diffusion limitation is the governing factor in denitrification which regulates the transport of oxygen from the bulk liquid into the floc. Sludge age and hence MLSS, floc morphology and size are believed to have direct affect on SNdN.
7. Oxygen half saturation constants of both heterotrophs and autotrophs are much higher than in a conventional activated sludge system.
8. Denitrification potential in membrane bioreactor systems is higher than in a conventional activated sludge system with respect to available carbon in the raw sewage.
9. Denitrification potential (N_{DP}) is significantly dissolved oxygen dependant rather than COD/TKN. Real time DO control and automation should be implemented to control SNdN.
10. Prolonged filtration scheme can be applied without any problems thereby avoiding the necessity for short sequential relaxation periods in a day.

11. Excessive growth of filamentous microorganisms is inevitable in a membrane bioreactor system.
12. The floc morphology and internal structure of a floc shifts from being dominantly aerobic to anoxic in a membrane bioreactor culture with respect to the dissolved oxygen in the bulk liquid.
13. It is recommended that further research be made on filamentous bacteria kinetics especially in membrane bioreactor systems. Also, further research has to be conducted focusing on floc morphology and its internal structure.
14. Quantitative and qualitative analysis of the filamentous bacterial community present in a membrane bioreactor system is a must for a better understanding of the fouling mechanism in this technology. Furthermore, the operational conditions of membrane bioreactor systems in relation to the maintenance of high amount of nitrifying microorganisms is also a crucial matter that must be investigated for the occurrence of robust nitrification regardless of the environmental factors.

REFERENCES

- AbwV**, 1999. Verordnung über Anforderungen an das Einleiten von Abwasser in Gewässer Bundesgesetzblatt, ATV, Berlin
- Amann, R.I., Ludwig, W., Schleifer, K.H.**, 1995. Phylogenetic Identification and in situ detection of individual microbial cells without cultivation. *Microb.Rev.*, **59**, 143-169.
- APHA, AWWA, WEF.**, 1995. Standard Methods for the Examination of Water and Wastewater, 19th Edition, American Public Health Association, Washington, DC.
- Ardenn, E. and Lockett W.T.**, 1914. Experiment on the oxidation of sewage without the aid of filters, *J.Soc.Chem.Ind.*, **33**:523.
- Belfort, G., Davis, R.H., and Zydney, A.D.**, 1994. The behavior of suspensions and macromolecular solutions in crossflow microfiltration, *Journal of Membrane Science*, **96**, 1-58.
- Brindle, K. and Stephenson, T.**, 1996. The application of membrane biological reactors for the treatment of wastewaters, *Biotechnology Bioeng.*, **49**, 601-610.
- Chaize, S. and Huyard, A.**, 1991. Membrane bioreactor on domestic wastewater treatment sludge production and modelling approach, *Water Science and Technology*, **23(7-9)**, 1591-1600.
- Chang, I.S and Lee, C.H.**, 1998. Membrane filtration characteristics in membrane coupled activated sludge system: the effect of physiological states of activated sludge on membrane fouling, *Desalination*, **120(3)**, 221-233.
- Chiemchaisri, C. and Yamamoto K.**, 1993b. Performance of membrane separation bioreactor at various temperatures for domestic wastewater treatment, *Journal of Membrane Science*, **87**, 119-129.
- Chiemchaisri, C., Wong, Y.K., Urase, T., Yamamoto, K.**, 1992. Organic stabilization and nitrogen removal in membrane separation bioreactor for domestic wastewater treatment, *Water Science and Technology*, **25(10)**, 231-240.
- Chiemchaisri, C., Yamamoto, K.**, 1993a. Biological nitrogen removal under low temperature in a membrane separation bioreactor, *Water Science and Technology*, **28(10)**, 325-333.

- Cho, J., Ahn, K.-H., Seo, Y., Lee, Y.,** 2003. Modification of ASM No.1 for a submerged membrane bioreactor system: including the effects of soluble microbial products on membrane fouling, *Water Science and Technology*, **47(12)**, 177-181.
- Choi, S.W., Yoon, J., Haam, S., Kung, J.K., Kim, J.H., Kim, W.S.,** 2000. Modelling of permeate Flux during microfiltration of BSA absorbed microspheres in a stirred cell, *Journal of Coll. and Interface Sci.*, **228**, 270-278.
- Choo,K.H. and Stensel, H.D.,** 2000. Sequencing batch membrane reactor treatment: nitrogen removal and membrane fouling evaluation, *Water Environment Research*, **72**, 490-498.
- Churchouse, S.,** 2002. Membrane bioreactors: going from laboratory to large scale – problems to clear solutions, *Membranes and the Environment Conference*, University of Oxford, UK, July 14-17.
- Cote P., Bussion, H. and Pradrie M.,** 1998. Immersed membrane activated sludge process applied to the treatment of municipal wastewater, *Water Science and Technology*, **38(4-5)**, 437-442.
- Davis, R.H.,** 1992. In membrane handbook, Van Nostrad Reinhold, New York, 483-505.
- Dold,P.L. and Marais, G.v.R.,**1986.Evaluation of the general activated sludge model proposed by the IAWPRC task group, *Water Science and Technology*, **18(6)**, 63-89.
- Dold,P.L., Jones, R.M., Bye, C.M., Takacs,I., Stensel,H.D., Wilson,A.W., Sun,P. and Burry, S.** 2003. Methods for wastewater characterization in activated sludge modelling, *Water Environment Research Foundation*, IWA Publishing, London.
- Fane, A.G.,** 1986. Ultrafiltration factors influencing flux and rejection progress, *Filtration and Separation*, **4**, 101-109.
- Fernandez,A., Lozier, J., Daigger,G.,** 2000. Investigating membrane bioreactor operation for domestic wastewater treatment: A case study, Municipal wastewater treatment symposium, *Membrane treatment systems Proceedings, 73d Annual Conference, Water Environment Federation*, Anaheim,CA., USA.
- Flemming, H.C.,** 1995. Biofouling bei membranprozessen springer verlag, Berlin Heidelberg, Germany.
- Gander,M., Jefferson, B., Judd,S.J.,** 2000. Aerobic MBRs for domestic wastewater treatment : a review with cost considerations, *Separation and Purification Technology*, **18**, 119-130.

- Gander, M.A., Jefferson, B., Judd, S.J.**, 2000. Membrane bioreactors for use in small wastewater treatment plants: membrane materials and effluent quality, *Water Science and Technology*, **41(1)**, 205-211.
- German Association for Water,Wastewater and Reuse**, 2000. Dimensioning of single stage activated sludge plants, ATV DVWK 131-E, Germany.
- Ghyoot, W., Vandaele,S., Verstraete,W.** 1999. Nitrogen removal from reject water with a membrane assisted bioreactor, *Water Research*, **33(1)**, 23-32.
- Gujer, W., Henze, M., Mino, M., Loosdrecht, M.**, 1999. Activated Sludge Model No.3 ,*Water Science and Technology*, **39(1)**, 183-193.
- Günder B.**, 2001. The membrane coupled activated sludge process in municipal wastewater treatment, Technomic Publishing Inc., Lancaster, Pennsylvania.
- Hardt, F.W., Clesceri, L.S., Nemerow, N.L., Washington, D.R.**, 1970. Solid separation by ultrafiltration for concentrated activated sludge, *Journal WPCF*, **42(125)**, 2135-2148.
- Henze,M.**, 1992. Characterization of wastewater for modelling of activated sludge processes, *Water Science and Technology*, **25(6)**, 1-15.
- Henze, M., Gujer, W., Mino, T., Matsuo, T., Wentzel, M.C. and Marais, G.v.R.**,1995. Activated Sludge Model No.2., IAWQ, London,UK.
- Henze, M., Grady, C.P.L., Gujer, W., Marais, G.v.R. and Matsuo, T.**, 1987. A general model for single sludge wastewater treatment systems, *Water Research*, **21(5)**, 505-515.
- Hiraiwa M.N.**, 2002. Microbial community analysis in membrane bioreactors treating municipal wastewater, *M.Sc Thesis*, Department of Environmental Engineering, Hokkaido University, Japan.
- Howell, J.A.**, 1995. Subcritical flux operation of microfiltration., *Journal of Membrane Science*, **107**, 165-171.
- Howell, J.A., Chua, H.C., Arnot, T.C.**, 2004. In situ manipulation of critical flux in a submerged membrane bioreactor using variable aeration rates and effects of membrane history, *Journal of Membrane Science*, **242**, 13-19.
- Howell, J.A., Chua, H.C., Arnot, T.C.**, 2004. Insitu manipulation of critical flux in a submerged membrane bioreactor using variable aeration rates and effects of membrane history, *Journal of Membrane Science*, **242**, 13-19.

- Insel, G., Sin, G., Lee, D.S., Nopens, I., Vanrolleghem, P.A.,** 2006. A calibration methodology and model-based systems analysis for SBRs removing nutrients under limited aeration conditions, *Journal of Chemical Tech. and Biotech.*, **81**, 679-687.
- Ishida, H., Yamada, Y., Matsumura, S.,** 1993. Submerged membrane process, it's application into activated sludge process with high concentration of MLSS, *Proceedings 2nd International Conference Advances in Water and Effluent Treatment*, Cranfield UK, 321-330.
- Judd, S. and Jefferson B.,** 2003. Membranes for Industrial Wastewater Recovery Reuse, Elsevier Science Inc., New York, USA.
- Judd, S.,** 2005. Fouling control in submerged membrane bioreactors, *Water Science and Technology*, **51(6-7)**, 27-34.
- Judd, S.J. and Till, S.W.,** 2000. Bacteria breakthrough in crossflow microfiltration of sewage, *Desalination*, **127(3)**, 251-260.
- Katehis, D., Fillos, J. and Carrio, L.A.,** 2002. Comparison of bench scale testing methods for nitrifier growth rate measurement, *Water Science and Technology*, **46(1-2)**, 289-295.
- Kelly, S.T., Opang, W.S. and Fell C.J.D.,** 1993. Modelling fouling mechanisms in protein ultrafiltration, *Journal of Membrane Science*, **68**, 79-91.
- Kim, S. and Park, H.,** 1999. Prediction of critical flux conditions in crossflow microfiltration using a concentration polarisation model, *Proceedings Membrane Technology in Environmental Management Conference*, Tokyo, Japan, November 1-4, 186-192.
- Knowles, G.A., Downing, A.L. and Barrett, M.J.,** 1965. Determination of kinetic constants for nitrifying bacteria in mixed culture with the aid of an electronic computer, *Jour. Gen. Microbiol.*, **38**:263.
- Krauth, K.H., Staab, K.F.,** 1980. Schlussbericht zum forschungsvorhaben verfahren zur biologischen abwasserveinigug bei drucken zwischen 1 und 5 bar mit nitrification und denitrification, Institut für siedlungwasserbau, wassrgüte und abfallwirtschaft der Universitat Stuttgart, Germany.
- Lesjean, B., Rosenberger, S., Schrotter, J-C., Recherche, A.,** 2004. Membrane aided biological wastewater treatment- an overview of applied systems, *Membrane Techology*, **8**.
- Li H., Yang M., Zhang Y., Yu Ti Kamagata Y.,** 2005. Nitrification performance and microbial community dynamics in a submerged membrane bioreactor with complete sludge retention, *Journal of Biotechnology*, **123(1)**, 60 – 70.

- Lojkine, M.H., Field, R.W. and Howell, J.A.,** 1992. Crossflow microfiltration of cell suspensions; a review of models with emphasis on particle size effects, *Trans. I. Chm. E.*, **70**, 149-164.
- Lu, S.G., Imai, T., Ukita, M., Sekine, M., Higuchi, T., Fukagawa, M.,** 2000. A model for membrane bioreactor process based on the concept of formation and degradation of soluble microbial products, *Water Research*, **35(8)**, 2038-2048.
- Lu, S.G., Imai, T., Ukita, M., Sekine, M., Higuchi.,** 2002. Model prediction of membrane bioreactor process with the concept of soluble microbial product, *Water Science and Technology*, **46(11-12)**, 63-70.
- Luxmy B.S., Nakajima F., Yamamoto K.,** 2000. Analysis of bacterial community in membrane-separation bioreactors by fluorescent *in situ* hybridization (FISH) and denaturing gradient gel electrophoresis (DGGE) techniques, *Water Science and Technology*, **41(10-11)**, 259 – 268.
- Manser, R., Gujer, W., Siegrist, H.** 2005 Membrane bioreactor versus conventional activated sludge system: population dynamic of nitrifiers, *Water Science and Technology*, **52(10-11)**, 417-425.
- Marais, G.v.R. and Ekama, G.A.,**1976. The activated sludge process: part I- steady state behaviour, *Water SA*, **2**, 162-200.
- Marshall, A.D., Munro, P.A. and Tegardh, G.,** 1992. The effect of protein fouling in microfiltration on permeate flux, protein retention and selectivity, a literature review, *Desalination*, **91**, 65-82.
- Meng, F.H., Zhang, F., Yang, Y., Li, J., Xiao, X., Zhang, X.,** 2005. Effect of filamentous bacteria on membrane fouling in submerged membrane bioreactor, *Journal of Membrane Science*, **272(1-2)**, 161 – 168.
- Meng, F., Zhang, H., Yang, F., Zhang, S., Li, Y., Zhang, X.,** 2006. Identification of activated sludge properties affecting membrane fouling in submerged membrane bioreactors, *Separation and Purification Technology*, **51(1)**, 95-103.
- Meng., F., Zhang, H., Yang., F., Li, Y., Xiao, J., Zhang, X.,** 2005. Effect of filamentous bacteria on membrane fouling in submerged membrane bioreactor, *Journal of Membrane Science*, **272(1-2)**, 161-168.
- Mobarry B., Wagner M., Urbain V., Rittmann B.E., Stahl D.A.,** 1996. Phylogenetic Probes for Analyzing Abundance and Spatial Organization of Nitrifying Bacteria, *Applied Environmental Microbiology*, **62(6)**, 2156 – 2162.

- Murakami, T., Usui, T., Takamura, K. and Yushiwaika, T.**, 1999. Application of immersed type membrane separation, *Proceedings IWA Conference Membrane technology in environmental management*, Tokyo 256-262.
- Murat, S., Insel, G., Artan, N. and Orhon, D.**,2004. Effect of temperature on the nitrogen removal performance of a sequencing batch reactor treating tannery wastewater, *Water Science and Technology*, **48(11)**, 319-326.
- Münsch, E.V., Lant, P. and Keller, J.**, 1996. Simultaneous Nitrification and Denitrification in bench scale sequencing batch reactors, *Water Research*, **30(2)**, 277-284.
- Nagaoka, H.**, 1999. Nitrogen removal by submerged membrane separation activated sludge process, *Water Science and Technology*, **39(8)**,107-114.
- Nah, Y.M., Ahn, K.H. and Yeom, I.T.**, 2000. Nitrogen removal in household wastewater treatment using an intermittently aerated membrane bioreactor, *Environmental Technology*, **21**, 107-114.
- Napouka, H., Kono S., Yamanishi, S., and Miya, A.**, 1999. Modelling of biofouling by extracellular polymers in a membrane separation activated sludge system, *Water Science Technology*, **38(4-5)**, 497-504.
- Ognier, S., Wisniewski, C., Grasmick, A.**, 2002. Membrane fouling during constant flux filtration in membrane bioreactors, *Membrane Technology*, **7**.
- Orhon, D., Artan, N., Buyukmurat, S. and Gorgun, E.** 1992. The effect of residual COD on the biological treatability of textile wastewaters, *Water Science and Technology*, **26(3-4)**, 815-825.
- Orhon, D., Ateş E, Sözen, S., and Ubay Çokgör E.**, 1997. Characterization and COD fractionation of domestic wastewater, *Environmental Pollution*, **95(2)**, 191-204.
- Orhon, D. And Artan, N.**, 1994. Modelling of Activated Sludge Systems, Technomic Publishing Co.Inc., Lancaster, Pennsylvania, USA.
- Pala, İ.**, 2006. Fluorescence in situ Hybridization (FISH) for the Assessment of Nitrifying Bacteria in a Pilot-Scale Membrane Bioreactor, *Masters Thesis*, Department of Molecular Biology and Genetics, Istanbul Technical University, Institute of Science and Technology, İstanbul.
- Palacek, S.P. and Zydney, A.L.**, 1994. Intermolecular electrostatic attractions and their effect on flux and protein deposition during protein filtration. *Biotechnol. Prog.*, **10**, 207-213.
- Pochana, K. And Keller, J.**, 1999. Study of factors affecting simultaneous nitrification and denitrification (SND), *Water Science Technology*, **39(6)**, 61-68.

- Psoch, O., Schiewer, S.,** 2006. Resistance analysis for enhanced wastewater membrane filtration, *Journal of Membrane Science*, **280(1-2)**, 284-297.
- Rautenback, R.,** 1996. Membranverfahren grundloggen der modul und anlagenauslegung verlog, Berlin,Germany.
- Ripperger, S.,** 1992. Berechnungsansatze zur crossflow filtration, *Chem. Ing. Tech.*, **65(5)**, 533-540.
- Roeleveld, P.J. and Van Loosdrecht, M.C.M.,** 2002. Experience with guidelines for wastewater characterization in The Netherlands, *Water Science Technology*, **45(6)**, 77-87.
- Rosenberger, S., Krilger, U., Witzig, R., Manz, W., Szewzyk, U., Kraume, M.,** 2002. Performance of a bioreactor with submerged membranes for aerobic treatment of municipal wastewater, *Water Research*, **36**, 413 – 420.
- Rosenberger, S., Witzig, R., Manz, W., Szewzyk, U., Kraume, M.,** 2000. Operation of different membrane bioreactors: experimental results and physiological state of the micro-organisms, *Water Science Technology*, **41(10-11)**, 269-277.
- Semmens, M.J. and Shanahan, J.,** 2005. *Membrane Technology : Pilot Studies of Membrane Aerated Bioreactors, Final Report.*, Water Environment Research Foundation, Virginia, USA
- Semmens, M.J., Dahm, K., Shanahan, J. and Christianson, A.,** 2003. COD and nitrogen removal by biofilms growing on gas permeable membranes. *Water Research*, **37(18)**, 4343-4350.
- Seo, G.T., Lee, T.S., Moon, B.H., Lim J.H., Lee, K.S.,** 2000. Two stage intermittent aeration membrane bioreactor for simultaneous organic, nitrogen and phosphorus removal, *Water Science Technology*, **41(10-11)**, 217-225.
- Sezgin, M., Jenkins, D., Parker D.S.,** 1978. A unified theory of filamentous activated sludge bulking, *J.WPCF*, **50**, 362-381.
- Siegrist, H., Brunner, I., Koch, G., Phan, L.C. and Le, V.C.,** 1999. Reduction of biomass decay rate under anoxic and anaerobic conditions, *Water Science and Technology*, **39(1)**, 129-137.
- Smith, C.V., Gregorio, D., Talcott, R.M.,** 1969. The use of ultrafiltration membranes for activated sludge separation, *Proceedings of the 24th Purdue Industrial Waste Conference Purdue University, Lafayette Indiana USA* 1300-1310.

- Smith, S., Judd, S., Stephenson, T., Jefferson, B.,** 2003. Membrane bioreactors-hybrid activated sludge or a new process, *Membrane Technology*, **12**.
- Staudé, E.** 1992. Membranen und Membranprozesse, VCH Verlagsgesellschaft, Weinheim, Germany.
- Stephenson, T., Judd S., Jefferson B., Brindle K.,** 2000. Membrane Bioreactors for Wastewater Treatment, IWA Publishing London, UK.
- Stiefel, C.R., Washington, D.R.,** 1966. Aeration of activated sludge, *Biotechnology and Bioengineering*, **3**, 379-388.
- Ueda, T. and Hata, K.,** 1999. Domestic wastewater treatment by a submerged membrane bioreactor with gravitational filtration, *Water Research*, **33**, 2888-2892.
- Ujang, Z., Salim, M.R., Khor, S.L.,** 2002. The effect of aeration and non-aeration time on simultaneous organic, nitrogen and phosphorus removal using an intermittent aeration membrane bioreactor, *Water Science and Technology*, **46(9)**, 193-200.
- Van der Roest, H.F., Lawrence, D.P., Van Bentem, A.G.N.,** 2002. Membrane Bioreactors for Municipal Wastewater Treatment, IWA Publishing, London, UK.
- Van der Waarde J., Krooneman J., Geurkink B., van der Werf A., Eikelboom D., Beimfohr C., Snaidr J., Levantesi C., and Tandoi V.,** 2002. Molecular monitoring of bulking sludge in industrial wastewater treatment plants, *Water Science Technology*, **46(1 – 2)**, 551 – 558.
- Wagner M., Horn M., Daims H.,** 2003. Fluorescence *in situ* hybridisation for the identification and characterization of prokaryotes, *Curr. Opin. Microbiol.*, **6(3)**, 302 – 309.
- Wintgens, T., Rosen, J., Melin, T., Brepols, C., Drensla, K., Engelhardt, N.,** 2003. Modelling of a membrane bioreactor system for municipal wastewater treatment, *Journal of Membrane Science*, **216**, 55-65.
- Wuhrmann, K.,** 1964. Nitrogen removal in sewage treatment processes, *Verb. Internat. Verein. Limno.*, **15**, 580.
- Yamamoto, K., Hiosa, M., Mahmood, T., Matsuo, T.,** 1989. Direct solid liquid separation using hollow fiber membrane in an activated sludge aeration tank, *Water Science Technology*, **21**, 43-54.
- Yang, W., Cicek, N., Ilg, J.,** 2005. State of the art membrane bioreactors : Worldwide research and commercial applications in North America, *Journal of Membrane Science*, **270(1-2)**, 201-211.

Zhang, H-M., Xiao,J-N., Cheng, Y-J.,Liu L-F.,Zhang,X-W., Yang,F-L., 2005.
Comparison between a sequencing batch membrane bioreactor and a
conventional membrane bioreactor, *Process Biochemistry*, **41(1)**, 87-
95.

ANNEX

KINETIC CHARACTERIZATION OF THE ACTIVATED SLUDGE IN THE PILOT MEMBRANE BIOREACTOR

An experimental characterization study using two different methods has been conducted for the activated sludge in the membrane bioreactor with an average TSS and VSS concentrations of 19,000 mg/l and 14,500 mg/l respectively. The objective of the study was to determine the decay rate coefficient (b_H) of the activated sludge in the membrane bioreactor which was believed to be of primary importance in MBRs. The first experimental method was based on determining the decay coefficient by classical means whereas the second experimental study used respirometric procedures to calculate the the decay rate coefficient.

Determination of the Decay Rate Coefficient by Classical Methods

The experimental study conducted was based on determination of the decay rate coefficient using a lab scale batch reactor setup. According to the procedure, activated sludge samples taken from the membrane bioreactor were aerated in the batch reactor for 14 days. At the beginning and during the duration of the experiment, TSS and VSS analysis were done within 2-3 days intervals for the determination of the decay rate coefficient. The results of these analysis are given in Table A1.

Table A1: Batch experiment results

<i>Experiment Duration (days)</i>	<i>Solids Concentration in the Reactor</i>	
	<i>TSS (mg/l)</i>	<i>VSS (mg/l)</i>
0	13480	9630
2	12510	8950
4	11780	8380
10	9620	6890
12	9260	6800
13	9180	6460

According to the endogenous respiration process the change in the active biomass can be expressed as;

$$X_{H(t)} = X_{H(t_0)} \cdot e^{-k \cdot t}$$

In this case, the change in the active biomass with respect to time can be defined with a logarithmic equation and the slope of the line drawn according to this expression will yield the decay rate coefficient ;

$$\ln\left(\frac{X_{H(t)}}{X_{H(t_0)}}\right) = -b_H \cdot t$$

Assessment of the results of the experimental study conducted according to the above equation yields the line shown in Figure A1. As it can be seen from this figure , the decay rate coefficient is found to be $b_H=0.31$ 1/day.

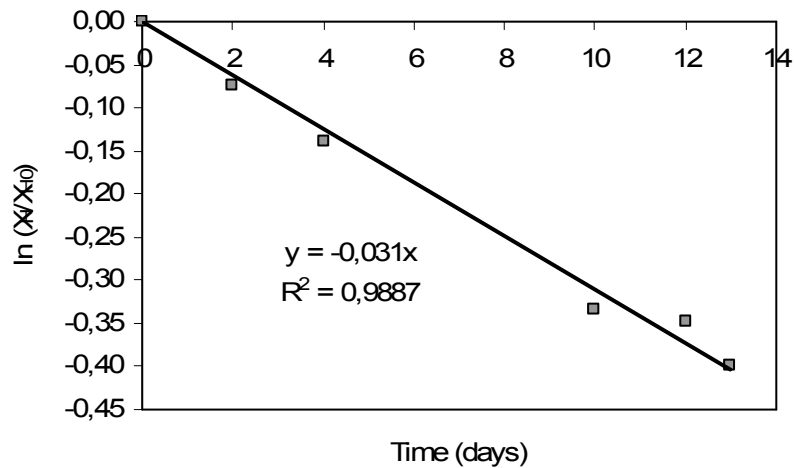


Figure A1: Change of active biomass with respect to time

The VSS results analyzed during the experimental study with respect to time show a good fit against the calculated change of the active biomass within the bioreactor using the determined b_H value in the first equation written above. Comparison of the experimental results with the calculated values is given in Figure A2.

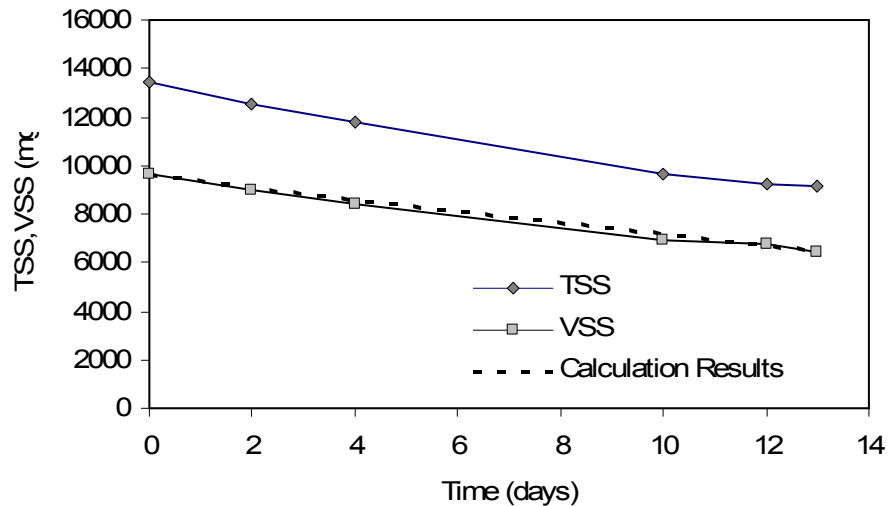


Figure A2: Comparison of the experimental results with the calculation results

Determination of the Decay Rate Coefficient by Respirometric Methods

The determination of the decay rate coefficient of the active biomass by respirometric methods has been done using the computer linked RA 1000 device. 1.5 l of activated sludge sample was fed and aerated continuously in the main reactor which is connected to the respirometry machine. Activated sludge samples were continuously pumped to the metering chamber of the respirometry device having a volume of 785ml. The oxygen uptake rate (OUR) and the dissolved oxygen concentrations (DO_{in} , DO_{out}) were continuously online recorded at the inlet and outlet of the DO metering chamber and the results were transferred to the computer every 60 seconds.

In order to test the viability of the activated sludge during the experimental study, 25 ml of acetic acid solution with 85 mg of COD content was fed to the aerated biomass in the main feeding reactor at the beginning of the study. The results obtained during the respirometric analysis are given in Figure A3.

The data interval that was related to the linear decrease in the OUR graph was used for the determination of the decay rate coefficient following the completion of the growth phase after the addition of the acetic acid solution. The oxygen uptake rate in the endogenous decay rate can be expressed with the following equation;

$$OUR = b_H \cdot X_H$$

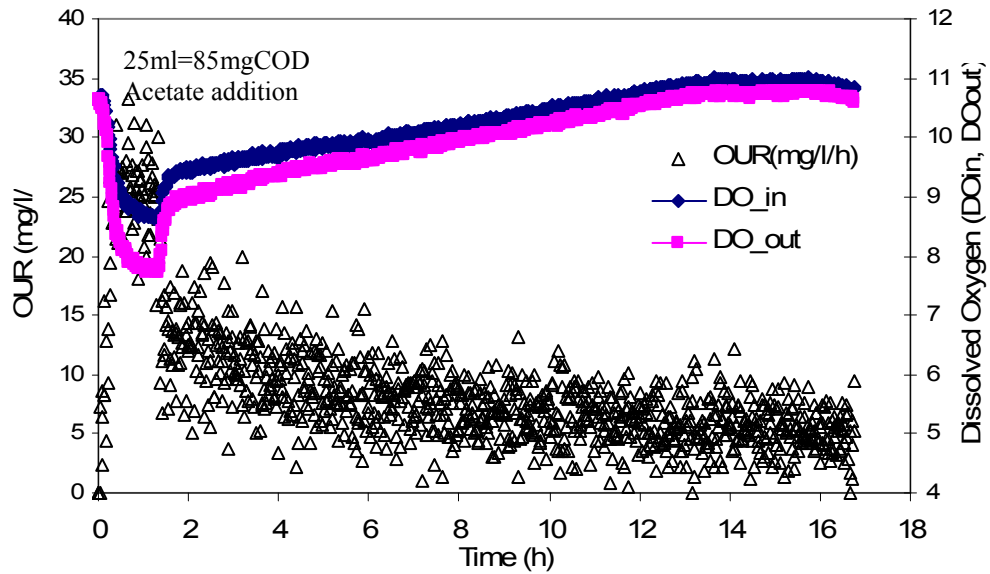


Figure A3: Results of the respirometric analysis

The slope of the line that is derived by taking the natural logarithm of the OUR values can be used in the calculation of the decay rate coefficient b_H as it can be seen in the following expression;

$$\ln OUR = -b_H \cdot t$$

Following the assessment of the data the resultant variation of $\ln OUR$ with respect to time is shown in Figure A4. As it can be seen from the figure, the decay rate coefficient, b_H was found to be 0.0149 1t/h or 0.36 1t/day.

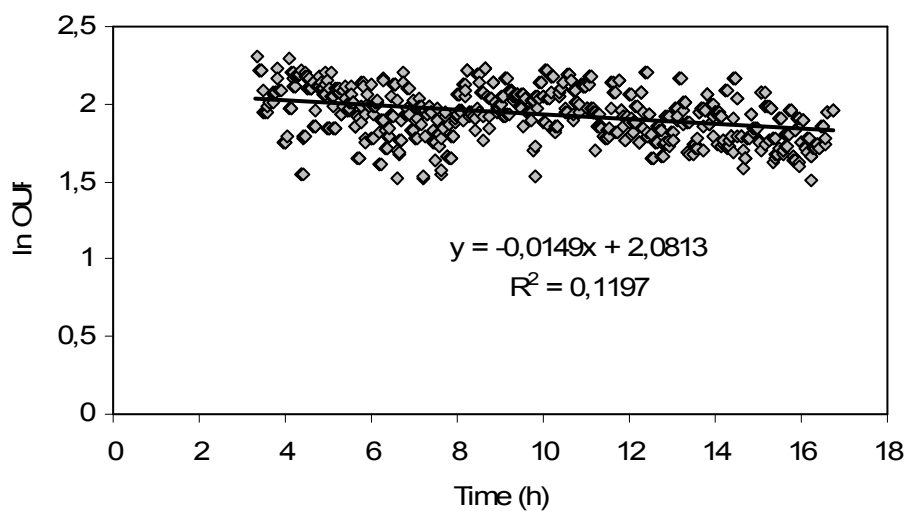


Figure A4: Determination of the decay rate coefficient (b_H) with OUR values

The decay rate coefficients of the activated sludge were found to be 0.31 1/day and 0.36 1/day using two different methods. However the determined rates are very high

with respect to the values given in the literature for conventional activated sludge systems. The derived results are limited in terms of accuracy with respect to the sensitivity of the methods used. The activated sludge samples taken from the membrane bioreactor was so viscous, sticky and gelly in form that detrimental difficulties have been faced during both the VSS, TSS analysis and as well as respirometric analysis methods. Most of all, the activated sludge samples were smothered to the oxygen probe in the respirometric device resulting in false readings. Afterwards the meterings were done manually using a separate oxygen meter. Due to the difficulties faced and explained above the accuracy and dependability of the results obtained are disputable. This is also visible when the calibrated decay rate coefficient is compared with the determined rates. The calibration of the adopted model was a failure using the decay rates obtained from the experimental studies. The model was calibrated at a decay rate coefficient of 0.24 l/day which is lower than the derived values from experiments. This discrepancy also verifies the question marks on the accuracy and dependability of the determined rates through experimental studies.

The experimental studies initiated and conducted to determine COD fractionation of the influent wastewater were also a failure due to the same reasons and difficulties explained above. Influent wastewater characterization experiments and studies could not be conducted because of the physical and structural properties of the activated sludge from the pilot membrane bioreactor resulting in experimental difficulties and problems.

CURRICULUM VITAE



M. Murat Sarioğlu was born in İstanbul, Turkey on February 1st, 1972. He completed elementary school at Nurettin Teksan Elementary School, junior high school at Göztepe Junior High and high school at Semiha Şakir High school. In 1995, he graduated as an Environmental Engineer from the Environmental Engineering Department of Istanbul Technical University (İ.T.Ü) with honors as being the top student in the department and in the faculty. He received his Master of Science degree from the same department in

1998. He started his PhD study in 1998. He has 13 years of experience in process, hydraulic design, startup and commissioning of domestic and industrial wastewater and potable water treatment plants. Majority of his work included detailed process and hydraulic design of water/wastewater treatment plants for both domestic and industrial effluents to meet stringent effluent regulations. The designs conducted for the domestic/industrial wastewater treatment plants also included the design of sludge streams to meet the desired sludge stabilization and dryness regulations. He has solid background in the conceptual and detailed process and hydraulic design of water and wastewater treatment systems with strong emphasis in biological nutrient removal. He is also experienced in the treatment of domestic and industrial sewage with membrane bioreactors for carbon and nutrient removal. He is skilled in the hydraulic and process modelling of water and sewage treatment plants with the ability to use ARA-BER 5.11, BioWin 2.2, GPS-X 5.0, AQUASIM and HYDKA 4.04 softwares. He has been working as the technical manager at Mass Treatment systems, Inc. since 1997.

PUBLICATION LIST

Sarioglu, M., Orhon, D., Gorgun, E., Artan, N., 2003. Design Procedure for Carbon Removal in Contact Stabilization Activated Sludge Process, *Water Science and Technology*, **48** (11-12), 285-292.

Sarioglu, M., Insel, G., Artan, N., Orhon, D., 2007. Modelling of Longterm Simultaneous Nitrification and Denitrification (SNdN) Performance of a Pilot Scale Membrane Bioreactor, *The 4th IWA International Membrane Conference*, Harrogate, UK. 15-17 May 2007.

- Sarioglu,M., Insel, G., Artan, N., Orhon, D., 2007.** Design procedure for Biological Nutrient Removal in Membrane Bioreactors -state of the art. (in preparation)
- Sarioglu,M.,2007.** Dynamic calibration and validation of prolonged filtration in a flatsheet membrane bioreactor using the in series resistance model. (in preparation)
- Sarioglu,M., Insel G.,2007.** Modelling and validation of the oxidation ditch technology with tapered aeration for a full scale BNR plant using SNdN. (in preparation)